Global Translational Medicine

ACCSCIENCE PUBLISHING

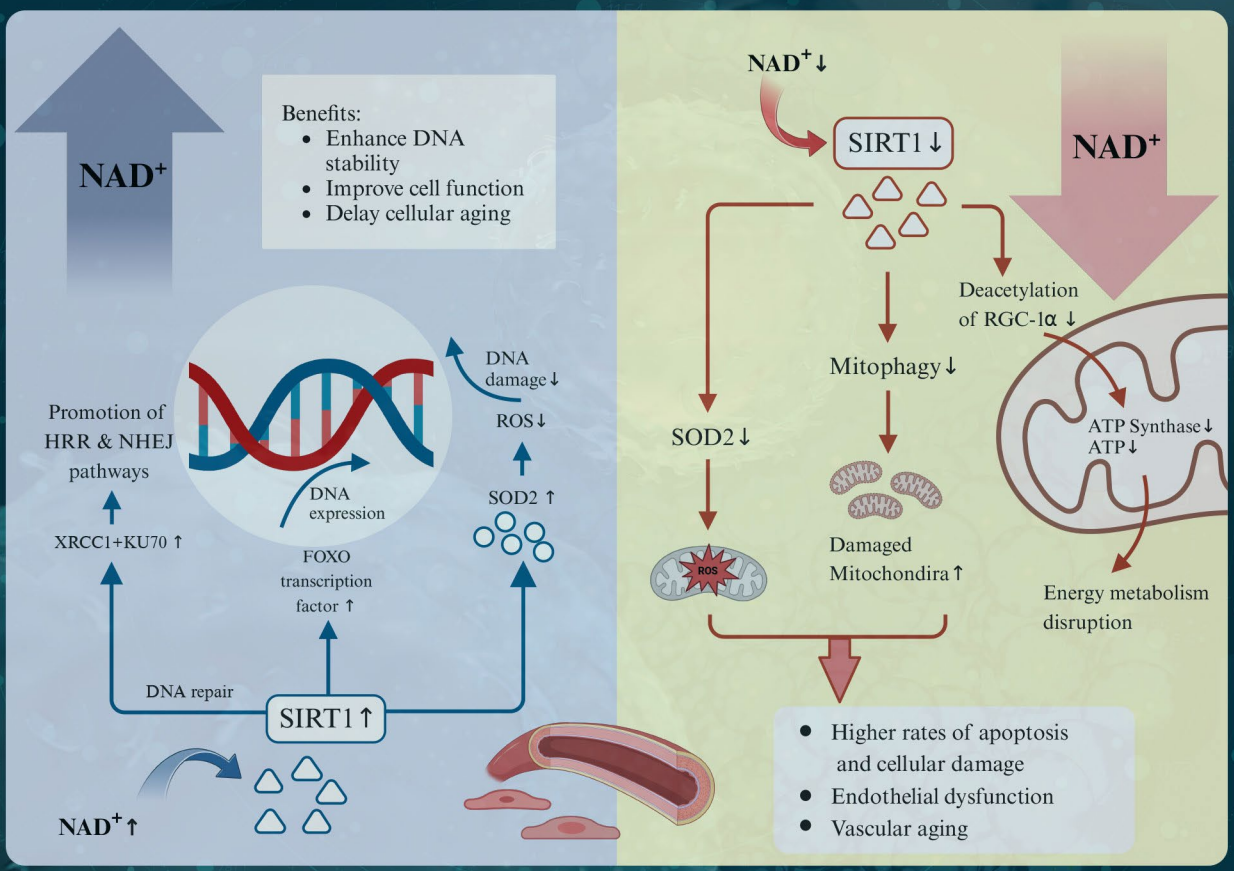

Senescence in cardiovascular diseases: Insights into metabolic dysfunction in vascular cells

ISSN: 3060-8600 (Print)
ISSN: 2811-0021 (Online)
Volume 3 · Issue 4
December 2024

Global Translational Medicine

Print ISSN: 3060-8600
Online ISSN: 2811-0021

Global Translational Medicine is a quarterly journal that focuses on medicine, biological sciences, and biomaterials engineering. *Global Translational Medicine* provides a platform to fill the gaps in preclinical and inter-disciplinary research, to promote clinical translation of scientific research results, and to contribute to the conception of new and improved preventive measures as well as diagnostic and therapeutic techniques of diseases.

About the Publisher

AccScience Publishing is a publishing company based in Singapore. We publish a range of high-quality, open-access, peer-reviewed journals and books from a broad spectrum of disciplines.

Contact Us

Managing Editor
gtm.office@accscience.sg

AccScience Publishing
8 Burn Road, #15-03 Trivex, Singapore 369977.

Volume 3 • Issue 4 • December 2024
ISSN 3060-8600 (print) ISSN 2811-0021 (online)

GLOBAL TRANSLATIONAL MEDICINE

ACCSCIENCE PUBLISHING

Access Science Without Barriers

GLOBAL TRANSLATIONAL MEDICINE

ISSN: 3060-8600 (print)
ISSN: 2811-0021 (online)

Editorial and Production Credits

Publisher: AccScience Publishing
Managing Editor: Alice Liu
Production Editor: Sharmila Velapasamy
Article Layout and Typeset: Sinjore Technologies (India)

For all advertising queries, contact gtm.office@accscience.sg.

Supplementary file

Supplementary files of articles can be obtained at https://accscience.com/journal/GTM/3/4.

About the Cover

An abstract illustration of human brain

Disclaimer

AccScience Publishing is not liable to the statements, perspectives, and opinions contained in the publications. The appearance of advertisements in the journal shall not be construed as a warranty, endorsement, or approval of the products or services advertised and/or the safety thereof. AccScience Publishing disclaims responsibility for any injury to persons or property resulting from any ideas or products referred to in the publications or advertisements. AccScience Publishing remains neutral with regard to jurisdictional claims in published maps and institutional affiliations.

Global Translational Medicine

Editorial Board

ACCSCIENCE PUBLISHING

Volume 3 | Issue 4 | December 2024 |

Global Translational Medicine

https://accscience.com/journal/gtm

CONTENTS

ACCSCIENCE PUBLISHING

Global Translational Medicine

REVIEW ARTICLE

Pathogenesis and current therapeutic approaches for Parkinson's disease

Raxida Umar[1] and Hao Lyu[2]*

[1]Department of Clinical Medicine, School of Medicine, Shenzhen University, Shenzhen, Guangdong, People's Republic of China

[2]Department of Neurosurgery, Shenzhen Second People's Hospital, Shenzhen, Guangdong, People's Republic of China

Abstract

Parkinson's disease (PD) is a common neurodegenerative disorder among the elderly, characterized by a spectrum of motor and non-motor symptoms. Motor symptoms, including resting tremor, bradykinesia, rigidity, and postural instability, typically emerge as the predominant clinical features in advanced stages, signifying irreversible neurodegenerative changes. Early detection, accurate diagnosis, and timely intervention are crucial for improving prognosis and quality of life in patients with PD. Treatment options for PD remain a hot topic within the medical community. Pharmacotherapeutic approaches have expanded beyond traditional agents such as levodopa, monoamine oxidase inhibitors, and dopamine agonists to include novel drugs, including α-synuclein misfolding inhibitors and glucagon-like peptide 1 receptor agonists, which have demonstrated promising efficacy. Surgical interventions, particularly deep brain stimulation, continue to play a pivotal role in symptom management and are widely applied in clinical practice. Recent advancements in understanding the pathogenesis of PD have catalyzed the development of innovative treatment strategies. Emerging therapies, including gene therapy and stem cell therapy, offer transformative potential by addressing the underlying disease mechanisms. These therapies hold distinct advantages, such as controlling the pathological progression of PD, restoring damaged brain function, and minimizing treatment-associated adverse effects, positioning them as promising candidates for future standard-of-care approaches. This review summarizes the latest research progress in the understanding of PD pathogenesis and treatment, aiming to provide guidance for the clinical management of PD.

Keywords: Parkinson's disease; Pathogenesis; Deep brain stimulation; Gene therapy; Stem cell therapy

Corresponding author:
Hao Lyu
(louielyu@link.cuhk.edu.hk)

Citation: Umar R, Lyu H. Pathogenesis and current therapeutic approaches for Parkinson's disease. *Global Transl Med*. 2024:3(4):5082. doi: 10.36922/gtm.5082

Received: October 8, 2024
Accepted: December 2, 2024
Published Online: December 27, 2024

1. Introduction

With the global population aging at an accelerating pace, Parkinson's disease (PD), the second most common neurodegenerative disease, has shown a steady rise in incidence. Between 2000 and 2023, the global prevalence of PD increased from 1.18% to 3.81%.[1] Pathologically, PD is characterized by the degeneration of dopaminergic neurons in the substantia nigra, the abnormal aggregation of α-synuclein (α-syn) in the form of Lewy bodies, neurofibrillary

tangles, mitochondrial dysfunction, and inflammatory responses.[2,3] Clinically, PD manifests as a spectrum of motor symptoms, including tremors, bradykinesia, and rigidity, as well as non-motor symptoms, such as cognitive impairment, emotional disturbances, sleep disorders, and autonomic dysfunction.[4] PD not only significantly impairs patients' daily functioning and quality of life but also imposes significant psychological and economic burdens on patients and their families. Current treatment options for PD encompass pharmacotherapy, surgical interventions, gene therapy, stem cell therapy, and traditional Chinese medicine, among others. In clinical practice, a comprehensive treatment approach is commonly adopted to slow disease progression and alleviate symptoms. Given the growing prevalence and complexity of PD, its pathogenesis and treatment strategies remain a hot topic in the medical field.

2. The pathogenesis of PD

2.1. Dysfunction and loss of dopaminergic neurons

The dysfunction and loss of dopaminergic neurons in the substantia nigra pars compacta (SNpc) plays a significant role in the pathogenesis of PD. Their progressive degeneration leads to motor impairments such as bradykinesia, resting tremors, and muscle rigidity, which are hallmark features of PD. Although numerous studies have established a correlation between dopaminergic neuronal loss and PD, the underlying mechanisms remain unclear. SIRT2, a nicotinamide adenine dinucleotide-dependent protein deacetylase primarily localized in the cytoplasm, regulates various cellular pathways through the deacetylation of multiple substrates. Research in cellular and animal models of PD has shown that SIRT2 translocates from the cytoplasm to the nucleus, a process that promotes dopaminergic neuronal death. This nuclear translocation is facilitated by phosphorylation at Ser331 and Ser335, mediated by cyclin-dependent kinase 5, which is essential for this process.[5] The myeloid cell-specific triggering receptor 1 (TREM-1), expressed on the surface of microglia and neutrophils, has been implicated in PD. Elevated levels of serum soluble TREM-1 in PD patients positively correlate with disease severity and motor impairment intensity. In a subacute PD mouse model, microglial TREM-1 levels significantly increased after 1-methyl-4-phenyl-1,2,3,6-tetrahydropyridine (MPTP) injection. *TREM1* knockout (KO) in these models provided neuroprotection and prevented MPTP-induced dopaminergic neuronal death, likely through the inhibition of neutrophil infiltration and suppression of pro-inflammatory cytokines. TREM-1 can further exacerbate neuroinflammation by activating downstream spleen tyrosine kinase, and TREM-1 activation in neutrophils mediates apoptosis of dopaminergic neurons.[6]

In addition, studies have identified a specific cleavage of UNC5C at positions N467 and N547 by asparagine endopeptidase (AEP) in the substantia nigra of PD patients, as well as in human α-syn transgenic mice, neurotoxin-induced PD mouse models, and neurons derived from pluripotent stem cells. This cleavage exhibits an age-dependent increasing trend and negatively correlates with netrin-1 levels. Blocking netrin-1 induces the activation of AEP and caspase-3, leading to the cleavage of the UNC5C protein into pro-apoptotic fragments, which promotes apoptosis of dopaminergic neurons.[7]

In summary, these studies highlight diverse mechanisms contributing to dopaminergic neuronal degeneration in PD, including the nuclear translocation of SIRT2, TREM-1-mediated interactions between microglia and neutrophils, and the proteolytic cleavage of the UNC5C receptor. These findings offer new perspectives for understanding the pathophysiology of PD and suggest potential targets for the development of new therapeutic strategies.

2.2. Neuroinflammation

Neuroinflammation, involving a variety of cells and molecules such as microglia, astrocytes, T cells, and various inflammatory mediators, plays a decisive role in the progression of PD. Both pre-clinical experiments and clinical studies have provided substantial evidence supporting the involvement of neuroinflammation in PD. The development of PD is mediated by multiple inflammatory signaling pathways.

The nuclear factor kappa B (NF-κB) pathway, a critical nuclear transcription factor, is involved in diverse pathophysiological processes, such as immune responses, inflammatory reactions, and cell growth and death. NF-κB is expressed in all cells of the nervous system and regulates neuroinflammation by controlling the expression of tumor necrosis factor (TNF), interleukin 1, and monocyte chemoattractant protein-1.[8,9] Research using *in vivo* CRISPR-Cas9 screening has identified apoptosis induced by p53 activation, mediated through the TNF-α–NF-κB pathway, as a primary cause of dopaminergic neuronal loss. Furthermore, the TNF-α inhibitor adalimumab has demonstrated significant neuroprotective effects, increasing the survival of dopaminergic neurons and promoting functional recovery in PD mouse models.[10]

Toll-like receptors (TLRs), as pattern recognition receptors, serve as key triggers of innate immune inflammatory responses. Literature indicates that TLR4-mediated immune inflammatory responses play a crucial role in PD, as well as other neurological diseases such as stroke and Alzheimer's disease.[11] The NLRP3

inflammasome is also implicated in PD pathogenesis and progression, with the TLR4/TAK1/IRF7 pathway regulating NLRP3 expression and activity, influencing dopaminergic neuronal apoptosis.[12]

Emerging studies highlight the cyclic guanosine monophosphate-adenosine monophosphate synthase–Stimulator of Interferon Genes (cGAS-STING) signaling pathway as an essential component of the innate immune system involved in PD. The cGAS-STING signaling pathway regulates numerous cellular processes, such as autophagy, protein synthesis, glycolipid metabolism, DNA damage repair, cellular senescence, and various forms of cell death.[13]

PRKN and *PINK1*, two genes associated with early-onset PD, play essential roles in mitophagy, the clearance of damaged mitochondria. Research shows that exhaustive exercise in *Prkn*- and *Pink1*-KO (*Prkn*$^{-/-}$ and *Pink1*$^{-/-}$) mice induces a pronounced inflammatory phenotype. With aging, *Prkn*$^{-/-}$; mutator mice accumulate mitochondrial DNA mutations, leading to an inflammatory response. Interestingly, the absence of STING mitigates this inflammatory response and rescues dopaminergic neuronal loss and motor deficits in aged *Prkn*$^{-/-}$; mutator mice.[14]

Withaferin A, a naturally occurring compound with neuroprotective effects, has shown potential in PD treatment. Whole-genome deep sequencing has linked withaferin A's neuroprotective effects to the DJ1-NRF2-STING pathway in the SNpc. Studies using transgenic mice (*Dj1*-KO, *Nrf2*-KO, STINGgt/gt, and STING-KO) and immunostaining techniques have confirmed the significant role of STING in PD pathogenesis.[15]

Mechanistically, the cGAS-STING pathway is activated in response to pathogen invasion, mitochondrial damage, or genomic instability, which leads to the accumulation of cytoplasmic double-stranded (ds) DNA. The DNA receptor cGAS recognizes this dsDNA and catalyzes the formation of the secondary messenger 2'3'-cGAMP from GTP and ATP. cGAMP subsequently binds to the receptor protein STING homodimer located on the endoplasmic reticulum membrane, initiating a conformational change that activates STING. The synthesis of cGAMP is considered the critical first step in activating the cGAS-STING pathway.

In mammals, the catalytic activity of cGAS is triggered by its interaction with dsDNA, a process that has been extensively studied and is now well understood through structural and biochemical research.[13] It has been found that PD is associated with aging and the senescence of astrocytes. Further investigations have revealed that the cGAS-STING-YY1 axis promotes astrocyte aging by upregulating the expression of LCN2, thereby facilitating the progression of PD.[16]

In summary, various inflammatory pathways, including NF-κB, TLR signaling, and the cGAS-STING pathway, are closely interconnected and contribute to the occurrence and progression of PD.

2.3. α-Synuclein aggregation

α-Synuclein is the main component of Lewy bodies, a pathological hallmark of neuronal degeneration in PD. The abnormal aggregation and propagation of α-syn are closely related to the onset and progression of PD. Enriched at pre-synaptic sites, α-syn associates with vesicles and membranes. In its pathological form, it exerts detrimental effects at the synapse during early disease stages, disrupting vesicle clustering and altering the post-synaptic response to neurotransmitters, ultimately impairing synaptic plasticity.

A recent finding in PD research highlights the self-restrictive oligomerization of α-syn on membranes. This process may be associated with the pathological functions of α-syn, affecting its roles both pre- and post-synaptically.[17] Breakthroughs in imaging techniques have significantly improved the visualization of α-syn pathology in animal models and PD patients. Researchers have developed a small molecule ligand, C05-05, for *in vivo* visualization of α-syn deposits in the brain. Using optical and positron emission tomography (PET) imaging techniques, C05-05 enables the tracking of fibril formation along neural pathways and the subsequent destruction of these structures. *In vitro* experiments have demonstrated the high-affinity binding of 18F-C05-05 to α-syn aggregates in human brain tissue. Notably, compared to healthy controls, an enhanced PET-detectable 18F-C05-05 signal has been observed in the midbrain of PD and dementia with Lewy bodies patients, marking the first *in vivo* visualization of α-syn pathology in these diseases.[18]

α-Syn not only accumulates intracellularly but also spreads to other cells through intercellular interactions. This spread extends from the brain to the gut and other peripheral tissues through the vagus nerve. Such transcellular and trans-tissue propagation increases α-syn accumulation across multiple brain regions, exacerbating PD symptoms. Furthermore, α-syn interacts with tau protein, co-localizing within Lewy bodies and affecting α-syn pathology in PD.

Researchers have developed gut PD mouse models expressing α-syn N103 or tau N368 with a red fluorescent protein in the enteric nervous system, but not in the brain. These models simulate the spread of α-syn and tau co-pathology from the gut to the brain, accompanied

by related behavioral impairments. Findings from these models revealed that α-syn and tau co-pathology initially manifest in the gut, followed by propagation to the dorsal motor nucleus of the vagus or the nucleus of the solitary tract, and subsequently to other brain regions. This progression was associated with behavioral deficits in $SYN103^{+/-}$ and/or $TAU368^{+/-}$ transgenic mouse models.[19]

In summary, α-syn plays a central role in the pathophysiological processes of PD. It serves not only as a biomarker for disease diagnosis but is also intricately connected to the disease's pathogenesis and therapeutic strategies.

2.4. Oxidative stress

Oxidative stress refers to a state of cellular damage resulting from an imbalance between the generation of reactive oxygen species (ROS) and the body's antioxidant defenses. The brain, due to its high metabolic activity, is particularly vulnerable to oxidative stress. Numerous central nervous system diseases, such as PD, Alzheimer's disease, Huntington's disease, and ischemic diseases, are associated with oxidative stress.[20]

Oxidative stress is considered a critical factor in the development of PD, with key sources including mitochondrial dysfunction, dopamine metabolism, and neuroinflammation. Mitochondrial abnormalities lead to ROS production and disrupt calcium homeostasis, ultimately leading to neuronal apoptosis. Pathogenic gene products associated with PD, such as DJ-1, PINK1, Parkin, α-syn, and LRRK2, affect mitochondrial function in complex ways, leading to increased ROS production and increased susceptibility to oxidative stress. Dysfunctions in these gene products impair mitochondrial clearance, further exacerbating oxidative stress.[21]

In addition, oxidative stress is closely linked to neuroinflammation. By affecting the ubiquitin-proteasome system and mitophagy, oxidative stress promotes the accumulation of ROS, forming a vicious cycle that intensifies neuronal damage.[21,22] Studies have also pointed out that oxidative stress contributes to PD through the MHC-I pathway. In SH-SY5Y cells treated with 1-methyl-4-phenylpyridinium, silencing PINK1 via specific small interfering RNA resulted in increased MHC-I expression, indicating that oxidative stress may regulate MHC-I expression through the PINK1 pathway, thereby contributing to PD onset.[23]

Moreover, ROS production in cells is regulated by LRRK2 kinase,[24] further underscoring its role in oxidative stress-related processes. Despite the central role of oxidative stress in PD pathogenesis and its involvement in various cellular processes and molecular pathways, treatment strategies targeting oxidative stress have yet to achieve success in clinical trials. However, a deeper understanding of PD-related gene products and oxidative stress response mechanisms offers potential avenues for novel treatment strategies. Future research should focus on further elucidating these mechanisms to develop more effective neuroprotective strategies for PD.

2.5. Mitochondrial dysfunction

Mitochondria, as the center of cellular energy metabolism, play a critical role in maintaining neuronal health, and their dysfunction can severely impact the nervous system. Studies have pointed out that mitochondrial damage is associated with various neurological diseases, including PD, Alzheimer's disease, Huntington's disease, and amyotrophic lateral sclerosis.[25] The abnormal aggregation of α-syn, a hallmark pathological feature of PD, impairs the dynamic balance of mitochondria. When α-Syn aggregates abnormally, it impairs mitochondrial motility and alters axonal transport. This disruption in mitochondrial transport can result in energy deficits and increased oxidative stress, further exacerbating neuronal damage.[26,27] Furthermore, a decline in the clearance capacity of the autophagy-lysosome system can contribute to the abnormal aggregation of α-syn.[28]

Proteins encoded by PD-related genes, such as PARKIN, PINK1, and DJ-1, are involved in mitochondrial metabolic pathways.[29] These genes play a role in mitophagy, the selective degradation of damaged mitochondria. Impaired mitophagy leads to increased ROS generation, which exacerbates neuronal damage.[26]

Mitochondrial dysfunction is a key factor in the pathogenesis of PD and holds significant potential for the development of new therapeutic strategies. Further research is needed to elucidate the complex interactions between mitochondrial dynamics, oxidative stress, and neuroinflammation in PD. Understanding these mechanisms is crucial for designing targeted therapies aimed at preventing or reversing the progression of this debilitating disease.

2.6. Environmental and genetic factors

Approximately 5 – 10% of PD cases are monogenic inherited diseases, highlighting the significant role of genetic susceptibility in the pathogenesis of PD.[30] Researchers have developed methods to enrich and perform transcriptomic analysis of dopaminergic neurons from PD patients and control groups, identifying 10 distinct dopaminergic neuron subpopulations. Using the Slide-seq technology, the spatial localization of these subpopulations within the SNpc was determined, revealing that the SOX6_AGTR1

group was most enriched in the ventral tier of the SNpc. The finding suggests that genetic risk factors for PD may selectively affect these susceptible neuron populations.[31]

In genetic forms of PD, genes such as *SNCA*, *LRRK2*, and *VPS35* are inherited in an autosomal dominant manner, while *PRKN*, *PINK1*, *DJ1*, and other genes follow autosomal recessive inheritance. In addition, variations in genes such as *ATP13A2*, *DCTN1*, *DNAJC6*, *FBXO7*, *PLA2G6*, and *SYNJ1* are associated with X-linked inheritance and atypical PD phenotypes.[30]

Environmental factors such as occupational exposure and lifestyle also contribute to the occurrence and progression of PD.

3. Treatment for PD

3.1. Pharmacological treatment

Pharmacological treatment is essential for controlling symptoms, slowing disease progression, and improving the quality of life for PD patients. Advances in research on PD pathogenesis have driven the development of novel pharmacological therapies, offering new hope for patients. Ongoing studies continue to expand the range of drug options, offering promising avenues for more effective symptom management and disease modification.

3.2. Conventional medication

3.2.1. Levodopa

Levodopa, a precursor of dopamine, is converted into dopamine in the central nervous system and plays an irreplaceable role in the treatment of PD. The half-life of levodopa in the blood is approximately 1 – 3 h, and its efficacy tends to decline with age and disease progression.[32] In addition, long-term use of levodopa is associated with side effects such as the wearing-off phenomenon, on-off phenomenon, and dyskinesia, which can significantly impact patients' quality of life.[33] To address these challenges, the development of new levodopa formulations aimed at extending its half-life and mitigating side effects has become a research hotspot. New formulations, such as levodopa/carbidopa intestinal gel and sustained-release levodopa preparations, have successfully extended levodopa's half-life in the bloodstream.[34] Levodopa inhalant (CVT-301) is rapidly absorbed through the lungs, reaching the brain within about 10 min, and provides rapid relief of PD symptoms during off periods.[35]

3.2.2. Monoamine oxidase-B inhibitors

Monoamine oxidase-B inhibitors (MAO-B) reduce dopamine degradation by inhibiting monoamine oxidase activity. MAO-B inhibitors not only alleviate motor and non-motor symptoms in patients but also delay disease progression. Over time, MAO-B inhibitors have evolved from non-selective, irreversible inhibitors to highly selective, reversible inhibitors.

The first generation of MAO-B inhibitors had significant side effects, such as the "cheese effect," which limited their clinical application. The second generation, represented by selegiline and rasagiline, addressed selectivity issues to some extent but formed irreversible covalent bonds with the enzyme through an N-propylamine group. The third generation, such as safinamide, features reversible and highly selective inhibitors, further improving safety and efficacy.[36-38]

3.2.3. Catechol-O-methyltransferase (COMT) inhibitors

COMT is an enzyme responsible for the metabolism of dopamine and other catechol compounds. COMT inhibitors are recommended as first-line adjunctive therapy to levodopa, effectively improving motor fluctuations in PD patients by increasing "on" time while reducing "off" time.

The main COMT inhibitors currently used in clinical practice include entacapone, tolcapone, and opicapone. Entacapone and opicapone are peripheral COMT inhibitors, while tolcapone crosses the blood–brain barrier and inhibits COMT activity within the brain. Opicapone, a newer COMT inhibitor, overcomes some limitations of earlier generations by offering sustained enzyme inhibition without the toxicity observed with previous agents.[39-41]

3.2.4. Dopamine agonists

Dopamine agonists stimulate dopamine receptors on the post-synaptic side of dopaminergic neurons, enhancing the body's response to dopamine stimulation. These drugs are effective in controlling both motor and certain non-motor symptoms of PD.

Commonly used dopamine receptor agonists include non-ergoline agonists (such as pramipexole, ropinirole, and rotigotine) and ergoline agonists (such as bromocriptine and cabergoline). Dopamine agonists can be used as an initial treatment for early-stage PD or as adjunctive treatment for advanced-stage PD.[42,43]

Studies suggest that, compared with levodopa, dopamine agonists may reduce the risk of motor complications during the initial years of treatment. However, their long-term effects and tolerability require further investigation. Non-ergoline dopamine agonists show promise in treating both motor and non-motor symptoms, but side effects and limited bioavailability restrict their broader application.[44]

3.3. New drug development

New drug development in PD pharmacotherapy remains a major area of research focus. α-Syn, a protein encoded by the *SNCA* gene and composed of 140 amino acids, plays a role in cellular DNA repair.[45] However, under pathological conditions, its abnormal aggregation forms Lewy bodies, showing certain neuronal toxicity. Therefore, α-syn misfolding inhibitors have demonstrated promising results in clinical trials for PD treatment.[46] In addition, research has highlighted the neuroprotective potential of glucagon-like peptide 1 receptor agonists, c-Abl inhibitors, and ceftriaxone in animal models of PD with dementia.[34] As our understanding of the pathogenesis of PD advances, the development of more targeted drugs in PD pharmacotherapy is anticipated, offering improvements in long-term prognosis and quality of life for patients.

3.4. Surgical treatment

With advancements in medical technology, surgical treatment has become increasingly important in managing PD. Initially, surgical interventions primarily focused on symptom relief, such as through deep brain stimulation (DBS). Over time, surgical approaches have evolved from simple stimulation therapies to nerve nucleus destruction and, more recently, cell transplantation, providing PD patients with a broader range of treatment options.

3.4.1. DBS

DBS is a procedure that alleviates symptoms in PD patients by implanting electrodes to stimulate specific brain areas, such as the subthalamic nucleus (STN) or the globus pallidus internus (GPi). The STN is the preferred target for stimulation, effectively controlling tremors, bradykinesia, rigidity, and dyskinesia, while also enabling a reduction in medication dosage.[47] In a clinical trial investigating DBS, PD patients were randomly assigned to two groups: The experimental group received bilateral STN DBS in addition to optimal drug treatment (ODT), whereas the control group received ODT alone. Subjects were followed for 2 years, mainly through outpatient visits over the past 5 years. Compared with the control group, the experimental group required less daily levodopa, and the probability of needing additional drug treatment within 5 years was reduced to 0.06 times that of the control group. Furthermore, the incidence of worsening clinical symptoms, such as resting tremor, was reduced to 0.21 times that of the control group.[48] These findings indicate that early STN DBS reduces medication dependency and improves motor symptoms in PD patients.

A meta-analysis examined the long-term (1 – 3 years) effects of STN or GPi DBS on cognitive functions in PD patients, primarily focusing on cognitive domains such as memory, executive function, language, and mood. Results indicated that post-DBS, PD patients experienced slight improvements in anxiety and depressive symptoms compared to pre-operative levels; however, declines were observed in long-term memory, language fluency, and task-specific performance. The study also pointed out that these cognitive impacts may improve over time.[49] While DBS significantly improves motor symptoms in PD patients, its long-term effects on certain cognitive functions warrant further research to balance its therapeutic effects and cognitive side effects.

2.4.2. Focused ultrasound ablation (FUSA)

FUSA is a non-invasive treatment that uses focused ultrasound waves to disrupt specific brain areas. In a randomized controlled trial, 94 PD patients were divided into two groups: the experimental group received FUSA treatment (69 patients), whereas the control group underwent sham surgery (25 patients). All patients exhibited motor disabilities during the "off" period (off-medication state, defined as discontinuing anti-Parkinson's medication for at least 12 h) and motor complications, such as motor fluctuations and dyskinesias, during the "on" period (on-medication state, after taking anti-Parkinson's medication).

A positive outcome was defined as at least a 3-point decrease in the motor disability score during the "off" period or the dyskinesia score during the "on" period. After a 3-month follow-up, the positive outcome rate in the experimental group was 69%, compared to 32% in the control group. Furthermore, the experimental group showed significant improvements in both MDS-UPDRS III (Motor Disability Score) and UDysRS (Dyskinesia Score) compared to the control group.[50] FUSA offers new hope for PD patients due to its high safety profile, ease of operation, minimal side effects, and significant therapeutic effects. However, technological challenges remain, such as ensuring precise targeting and evaluating therapeutic outcomes. Further research and exploration are needed to optimize FUSA's application in PD treatment.

In addition to FUSA, surgical treatments for PD include neuroablative surgery, neural implantable prosthetic devices, and cell transplantation. Surgical treatment for PD is a complex process that requires individualized assessment by health-care professionals. Close monitoring of the patient's condition and active collaboration between patients and clinicians is essential to achieve optimal therapeutic outcomes.

3.5. Stem cell therapy

Advances in technology and medicine have positioned stem cell therapy as a promising and innovative treatment

method that has garnered increasing attention in clinical settings. It is currently used in the clinical treatment of diseases across 11 major human systems. Stem cell therapy offers a novel treatment approach, with its core concept centered on replacing lost dopaminergic neurons through stem cell transplantation to rebuild neural function. Stem cells, characterized by self-renewal and multi-lineage differentiation, primarily include mesenchymal stem cells (MSCs), embryonic stem cells (ESCs), neural stem cells (NSCs), and induced pluripotent stem cells (iPSCs).[51]

First, MSCs, which belong to adult stem cells, are currently the most widely used in clinical practice. In one study, researchers recruited 23 PD patients, with 12 patients in the experimental group receiving MSC transplantation and 11 patients in the control group undergoing drug therapy without placebo injection. The researchers assessed motor and non-motor symptoms using the MDS-UPDRS score (Section III), the Hamilton Depression Scale, the Pittsburgh Sleep Quality Index, the Epworth Sleepiness Scale, the Non-Motor Symptoms Scale, and the 39-Item PD Questionnaire. Assessments were conducted before transplantation and 1 and 3 months after transplantation. The results indicated that motor and non-motor symptoms in the experimental group significantly improved compared to the control group after MSC transplantation.[52] A meta-analysis of the clinical effects of MSC treatment for PD revealed that MSCs could improve motor and memory function in pre-clinical PD models and offered certain protective effects on dopaminergic neuronal function. The study further noted that transplanting MSCs containing neurotrophic factors into the brain's striatum had the strongest impact on improving motor function and protecting dopaminergic neuronal function.[53]

Second, ESCs, isolated from early embryos, can differentiate into mature dopaminergic neurons. Researchers induced the differentiation of human ESCs into midbrain dopaminergic neurons, named TED-A9. After transplanting midbrain dopaminergic neurons into the right brain of a rat PD model, measurements taken 16 weeks later showed a significant improvement in dopamine secretion in the experimental group compared to the control group. At 11 months post-transplantation, DNA content analysis confirmed the presence of human cells in the rat brain without affecting survival rates or causing tumor formation.[54]

Third, NSCs, capable of differentiating into neurons, oligodendrocytes, and astrocytes, have been explored in PD treatment. In one study, researchers transplanted human NSCs (ANGE-S003) into PD patients through the nasal mucosa. Patients were divided into three groups based on transplant doses: 1.5 million, 5 million, and 15 million units. They were followed for 12 months, with assessments conducted using the MDS-UPDRS score. Results indicated that from the 3rd month of follow-up, MDS-UPDRS scores continued to improve compared to baseline, with the most significant improvement observed at 6 months, averaging a decrease of 19.9 points across the three treatment groups. Notably, the degree of clinical symptom improvement was not correlated with the transplant dose.[55]

Finally, iPSCs, with the potential to differentiate into cells or tissues of all three germ layers, are increasingly being applied in clinical applications. Researchers induced human iPSCs into midbrain organoids (hMOs) resembling fetal ventral mesencephalon tissue and transplanted them into a PD mouse model. Observations conducted over 12 weeks following transplantation revealed surviving A9 midbrain dopaminergic neurons in the striatum. The study indicated that the axons of hMO-derived neurons extended and integrated into the mature central nervous system, thereby alleviating motor dysfunction in PD mice.[56]

Stem cell therapy for PD represents a cutting-edge field of medical research with positive results from laboratory studies and preliminary clinical trials. However, further clinical data are needed to verify its long-term efficacy and safety.

3.6. Gene therapy

Gene therapy involves introducing normal or therapeutic exogenous genes into target cells through specific mechanisms, influencing their gene expression and thereby altering the biological characteristics of the target cells to achieve therapeutic purposes. Gene therapy, with its precision, safety, and effectiveness, is gradually transitioning from laboratory research to clinical applications. As research on PD advances, the role of genetic abnormalities in PD pathogenesis is becoming increasingly evident. High-penetrance genes associated with PD include *SNCA*, *VPS35*, *PINK1*, *PARK7*, and *PLA2G6*; variable-penetrance genes include *LRRK2* and *GBA*; and genes related to PD but potentially unrelated to pathogenicity include *HTRA2*, *UCHL1*, *GIGYF2*, and *EIF4G1*.[57,58]

At present, adeno-associated virus (AAV)-based gene therapy has shown tremendous potential in the treatment of central nervous system diseases. A review highlighted that clinical studies suggest AAV gene therapy has certain therapeutic effects on neurodegenerative diseases such as PD and Alzheimer's disease, neuromuscular diseases such as spinal muscular atrophy and amyotrophic lateral sclerosis, and lysosomal storage diseases such as mucopolysaccharidosis and Pompe disease.[59] In addition, gene therapies targeting the expression of glial cell line-derived neurotrophic factor, cerebral dopamine

neurotrophic factor, aromatic L-amino acid decarboxylase, and glutamate decarboxylase have shown promising results in PD animal models, though further clinical research is required to clarify their efficacy and safety.[60]

Dopamine transporter deficiency syndrome (DTDS) is a progressive and life-threatening neurodegenerative disease. As children with DTDS age, they exhibit "Parkinsonian symptoms," such as bradykinesia and rigidity, which resemble those seen in PD. Researchers first pointed out that the activity of the dopamine transporter (DAT) in DTDS patients is significantly reduced. This low DAT activity not only leads to reduced expression of key enzymes involved in dopamine synthesis but also induces apoptosis of midbrain dopaminergic neurons. Introducing the normal human *SLC6A3* gene into the midbrain dopaminergic neurons of DTDS patients significantly increased DAT activity. Subsequently, researchers constructed a recombinant AAV2 vector expressing human *SLC6A3*. When this AAV recombinant virus was injected into a mouse model of DAT dysfunction, it was found that DAT expression improved significantly, accompanied by enhanced survival rates and reduced motor impairments.[59]

Recent advancements in gene therapy have enabled the selective regulation of neural circuits affected by PD, improving symptoms in PD animal models. D1-MSN and D2-MSN are medium spiny neurons in the striatum that express dopamine receptor 1 or 2, respectively. D1-MSN promotes movement, whereas D2-MSN inhibits it, both receiving signals from the substantia nigra. Researchers modified AAV to construct a novel vector, AAV8R12, incorporating a promoter highly expressed in D1-MSN and a chemogenetic manipulation effector. To test this vector's effectiveness and specificity, researchers injected AAV8R12-G88P3-HA-hM3Dq, which expresses the designed receptor (DREADD) effector hM3Dq activated by a specifically designed drug, into the substantia nigra of mice. Behavioral analysis revealed that activation of D1-MSN in the mouse brain improved motor function. In addition, the research results suggest that this gene therapy can regulate signal pathways related to D1-MSN. Subsequently, researchers used a PD model in non-human primates (macaque monkeys) for further investigation. Using the same AAV8R12 therapy, they observed significant improvements in PD-related motor symptoms of the macaques: tremor symptoms disappeared completely, bradykinesia improved markedly, and motor abilities showed varying degrees of recovery.[61] Although there is currently no cure for PD, gene therapy has emerged as a promising treatment approach, showing tremendous potential in slowing disease progression and improving the quality of life for patients. However, most gene therapies remain in the clinical trial phase, and their long-term safety and efficacy must be verified through extensive clinical research.

3.7. Traditional Chinese medicine treatment

Acupuncture, a major component of traditional Chinese medicine, involves the stimulation of specific acupoints on the human body through needling or moxibustion to regulate the flow of Qi and blood, as well as the meridians, thereby alleviating clinical symptoms and treating diseases. As an important part of the traditional Chinese medical treatment system, acupuncture, and moxibustion therapy have been increasingly applied in clinical practice in recent years. A substantial number of clinical studies have indicated that acupuncture and moxibustion therapy can alleviate both motor and non-motor symptoms in patients with PD.

In addressing emotional disorders such as anxiety and depression, an 8-week acupuncture and moxibustion therapy intervention resulted in a 0.22-point difference in Hamilton Anxiety Scale (HAM-A) scores between the observation group (PD patients) and the control group. Compared to pre-treatment levels, the HAM-A scores in the observation group decreased by 7.03 points.[62] Sleep disorders, which are common among some PD patients and can exacerbate the condition, have also been shown to improve with acupuncture. Researchers divided PD patients with sleep disorders into a treatment group receiving real acupuncture (RA) and a control group receiving sham acupuncture (SA). Parkinson's disease sleep scale (PDSS) scores were recorded at 4 and 8 weeks of follow-up. Results indicated that both the RA and SA groups showed improvements in PDSS scores compared to baseline, with increases of 29.65 and 10.47 points, respectively. Furthermore, the RA group exhibited significantly greater improvements in PDSS scores than the SA group at both 4 and 8 weeks, with increases of 19.75 and 20.24 points, respectively.[63]

Acupuncture therapy has also demonstrated certain therapeutic effects on the motor symptoms of PD patients. After 4 weeks of combined acupuncture therapy and traditional PD treatment (traditional treatment refers to the standard medical treatment, which includes levodopa, carbidopa-levodopa, dopamine agonists, anticholinergics, amantadine, etc.), the acupuncture group exhibited significant improvements compared to the traditional treatment group. Specifically, gait rhythm was significantly reduced, whereas stride amplitude, single support time, and swing amplitude were significantly increased. Moreover, the UPDRS scores (related to walking and

balance) were markedly decreased. These results suggest that acupuncture therapy can improve gait stability and postural balance in PD patients.[64]

The clinical effectiveness of acupuncture for PD has been confirmed to some extent, although its mechanism of action requires further in-depth study. Research in PD mouse models has shown that acupuncture stimulation affects melanin-concentrating hormone (MCH)-mediated reactive gliosis, providing a protective effect on dopaminergic neurons in the SNpc. Furthermore, acupuncture enhances glutamatergic synaptic plasticity in the hippocampus. These changes collectively improve motor disorders and memory deficits in PD. Projections from MCH neurons, specifically $MCH^{LH/ZI \rightarrow SNpc}$ and $MCH^{LH \rightarrow HPC}$, play major roles in alleviating motor disorders and memory deficits, respectively.[65] Acupuncture treatment shows promising potential in managing PD. Future research should focus on elucidating the mechanisms of acupuncture in PD therapy and developing personalized treatment strategies to enhance therapeutic outcomes.

4. Conclusion

As science and technology continue to advance across generations, the treatment of PD is poised to explore new possibilities. With an increasing understanding of the pathogenesis of PD, future research is expected to focus more on individualized treatment and precision medicine, aiming to develop personalized therapeutic strategies tailored to the specific conditions of individual patients. In addition, advancements in gene-editing technologies and stem cell therapies will likely expand the range of treatment options for PD.

In recent years, significant progress has been made in the treatment of PD. A variety of approaches, including pharmacotherapy, surgical interventions, gene therapy, and stem cell therapy, as well as rehabilitation and psychological support, have provided patients with a broader spectrum of options. However, further in-depth research is essential to achieve the goals of personalized treatment and precision medicine, ultimately improving therapeutic outcomes and enhancing the quality of life for patients with PD.

Acknowledgments

None.

Funding

None.

Conflict of interest

The authors declare that they have no competing interests.

Author contributions

Conceptualization: All authors
Writing – original draft: Raxida Umar
Writing – review & editing: Hao Lyu

Ethics approval and consent to participate

Not applicable.

Consent for publication

Not applicable.

Availability of data

Not applicable.

References

1. Zhu J, Cui Y, Zhang J, *et al*. Temporal trends in the prevalence of Parkinson's disease from 1980 to 2023: A systematic review and meta-analysis. *Lancet Healthy Longev*. 2024;5(7):e464-e479.

   doi: 10.1016/S2666-7568(24)00094-1

2. Simon DK, Tanner CM, Brundin P. Parkinson disease epidemiology, pathology, genetics, and pathophysiology. *Clin Geriatr Med*. 2020;36(1):1-12.

   doi: 10.1016/J.CGER.2019.08.002

3. Dextera DT, Jenner P. Parkinson disease: From pathology to molecular disease mechanisms. *Free Radic Biol Med*. 2013;62:132-144.

   doi: 10.1016/J.FREERADBIOMED.2013.01.018

4. McGregor MM, Nelson AB. Circuit mechanisms of Parkinson's disease. *Neuron*. 2019;101(6):1042-1056.

   doi: 10.1016/J.NEURON.2019.03.004

5. Yan J, Zhang P, Tan J, *et al*. Cdk_5 phosphorylation-induced $SIRT_2$ nuclear translocation promotes the death of dopaminergic neurons in Parkinson's disease. *NPJ Parkinsons Dis*. 2022;8(1):46.

   doi: 10.1038/S41531-022-00311-0

6. Shen T, Cui G, Chen H, *et al*. TREM-1 mediates interaction between substantia nigra microglia and peripheral neutrophils. *Neural Regen Res.* 2024;19(6):1375-1384.

   doi: 10.4103/1673-5374.385843

7. Chen G, Ahn EH, Kang SS, *et al*. UNC5C receptor proteolytic cleavage by active AEP promotes dopaminergic neuronal degeneration in Parkinson's disease. *Adv Sci* (*Weinh*). 2022;9(7):e2103396.

   doi: 10.1002/ADVS.202103396

8. Singh SS, Rai SN, Birla H, Zahra W, Rathore AS, Singh SP. NF-κB-mediated neuroinflammation in Parkinson's disease and potential therapeutic effect of polyphenols. *Neurotox*

Res. 2020;37(3):491-507.

doi: 10.1007/s12640-019-00147-2

9. Mattson MP, Camandola S. NF-kappaB in neuronal plasticity and neurodegenerative disorders. *J Clin Invest*. 2001;107(3):247-254.

doi: 10.1172/JCI11916

10. Kim TW, Koo SY, Riessland M, *et al*. TNF-NF-κB-p53 axis restricts *in vivo* survival of hPSC-derived dopamine neurons. *Cell*. 2024;187(14):3671-3689.e23.

doi: 10.1016/J.CELL.2024.05.030

11. Kim HJ, Kim H, Lee JH, Hwangbo C. Toll-like receptor 4 (TLR_4): New insight immune and aging. *Immun Ageing*. 2023;20(1):67.

doi: 10.1186/s12979-023-00383-3

12. Quan W, Liu Y, Li J, *et al*. Investigating the TLR_4/TAK_1/IRF_7 axis in $NLRP_3$-mediated pyroptosis in Parkinson's disease. *Inflammation*. 2024;47(1):404-420.

doi: 10.1007/S10753-023-01918-Y

13. Decout A, Katz JD, Venkatraman S, Ablasser A. The cGAS-STING pathway as a therapeutic target in inflammatory diseases. *Nat Rev Immunol*. 2021;21(9):548-569.

doi: 10.1038/S41577-021-00524-Z

14. Sliter DA, Martinez J, Hao L, *et al*. Parkin and $PINK_1$ mitigate STING-induced inflammation. *Nature*. 2018; 561(7722):258-262.

doi: 10.1038/S41586-018-0448-9

15. Zhao M, Wang B, Zhang C, *et al*. The DJ_1-Nrf_2-STING axis mediates the neuroprotective effects of Withaferin A in Parkinson's disease. *Cell Death Differ*. 2021;28(8):2517-2535.

doi: 10.1038/S41418-021-00767-2

16. Jiang SY, Tian T, Yao H, *et al*. The cGAS-STING-YY_1 axis accelerates progression of neurodegeneration in a mouse model of Parkinson's disease via LCN_2-dependent astrocyte senescence. *Cell Death Differ*. 2023;30(10):2280-2292.

doi: 10.1038/S41418-023-01216-Y

17. Calabresi P, Di Lazzaro G, Marino G, Campanelli F, Ghiglieri V. Advances in understanding the function of alpha-synuclein: Implications for Parkinson's disease. *Brain*. 2023;146(9):3587-3597.

doi: 10.1093/brain/awad150

18. Endo H, Ono M, Takado Y, *et al*. Imaging α-synuclein pathologies in animal models and patients with Parkinson's and related diseases. *Neuron*. 2024;112(15):2540-2557.e8.

doi: 10.1016/J.NEURON.2024.05.006

19. Xiang J, Tang J, Kang F, *et al*. Gut-induced alpha-Synuclein and Tau propagation initiate Parkinson's and Alzheimer's disease co-pathology and behavior impairments. *Neuron*. 2024;112:3585-3601.e5.

doi: 10.1016/J.NEURON.2024.08.003

20. Alqahtani T, Deore SL, Kide AA, *et al*. Mitochondrial dysfunction and oxidative stress in Alzheimer's disease, and Parkinson's disease, Huntington's disease and Amyotrophic Lateral Sclerosis - An updated review. *Mitochondrion*. 2023;71:83-92.

doi: 10.1016/J.MITO.2023.05.007

21. Dias V, Junn E, Mouradian MM. The role of oxidative stress in Parkinson's disease. *J Parkinsons Dis*. 2013;3(4):461-491.

doi: 10.3233/JPD-130230

22. Jenner P. Oxidative stress in Parkinson's disease. *Ann Neurol*. 2003;53(Suppl 3):S26-S36; discussion S36-S38.

doi: 10.1002/ANA.10483

23. Wang BY, Ye YY, Qian C, *et al*. Stress increases MHC-I expression in dopaminergic neurons and induces autoimmune activation in Parkinson's disease. *Neural Regen Res*. 2021;16(12):2521-2527.

doi: 10.4103/1673-5374.313057

24. Keeney MT, Rocha EM, Hoffman EK, *et al*. LRRK2 regulates production of reactive oxygen species in cell and animal models of Parkinson's disease. *Sci Transl Med*. 2024;16(767):17-20.

doi: 10.1126/SCITRANSLMED.ADL3438

25. Klemmensen MM, Borrowman SH, Pearce C, Pyles B, Chandra B. Mitochondrial dysfunction in neurodegenerative disorders. *Neurotherapeutics*. 2024;21(1):e00292.

doi: 10.1016/j.neurot.2023.10.002

26. Li HY, Liu DS, Zhang YB, Rong H, Zhang XJ. The interaction between alpha-synuclein and mitochondrial dysfunction in Parkinson's disease. *Biophys Chem*. 2023;303:107122.

doi: 10.1016/J.BPC.2023.107122

27. Geibl FF, Henrich MT, Xie Z, *et al*. α-Synuclein pathology disrupts mitochondrial function in dopaminergic and cholinergic neurons at-risk in Parkinson's disease. bioRxiv [Preprint]. 2023.

doi: 10.1101/2023.12.11.571045

28. Nguyen M, Wong YC, Ysselstein D, Severino A, Krainc D. Synaptic, mitochondrial, and lysosomal dysfunction in Parkinson's disease. *Trends Neurosci*. 2019;42(2):140-149.

doi: 10.1016/J.TINS.2018.11.001

29. Borsche M, Pereira SL, Klein C, Grünewald A. Mitochondria and Parkinson's disease: Clinical, molecular, and translational aspects. *J Parkinsons Dis*. 2021;1(1):45-60.

doi: 10.3233/JPD-201981

30. Jia F, Fellner A, Kumar KR. Monogenic Parkinson's disease: Genotype, phenotype, pathophysiology, and genetic testing.

Genes (*Basel*). 2022;13(3):471.

doi: 10.3390/GENES13030471

31. Kamath T, Abdulraouf A, Burris SJ, *et al*. Single-cell genomic profiling of human dopamine neurons identifies a population that selectively degenerates in Parkinson's disease. *Nat Neurosci*. 2022;25(5):588-595.

doi: 10.1038/S41593-022-01061-1

32. Demailly A, Moreau C, Devos D. Effectiveness of continuous dopaminergic therapies in Parkinson's disease: A review of L-DOPA pharmacokinetics/pharmacodynamics. *J Parkinsons Dis*. 2024;14:925-939.

doi: 10.3233/jpd-230372

33. Farzanehfar P, Woodrow H, Horne M. Assessment of wearing off in Parkinson's disease using objective measurement. *J Neurol*. 2021;268(3):914-922.

doi: 10.1007/s00415-020-10222-w

34. Murakami H, Shiraishi T, Umehara T, Omoto S, Iguchi Y. Recent advances in drug therapy for Parkinson's disease. *Intern Med*. 2023;62(1):33-42.

doi: 10.2169/internalmedicine.8940-21

35. LeWitt PA, Hauser RA, Pahwa R, *et al*. Safety and efficacy of CVT-301 (levodopa inhalation powder) on motor function during off periods in patients with Parkinson's disease: A randomised, double-blind, placebo-controlled phase 3 trial. *Lancet Neurol*. 2019;18(2):145-154.

doi: 10.1016/S1474-4422(18)30405-8

36. Zou D, Liu R, Lv Y, Guo J, Zhang C, Xie Y. Latest advances in dual inhibitors of acetylcholinesterase and monoamine oxidase B against Alzheimer's disease. *J Enzyme Inhib Med Chem*. 2023;38(1):2270781.

doi: 10.1080/14756366.2023.2270781

37. Lv Y, Zheng Z, Liu R, Guo J, Zhang C, Xie Y. Monoamine oxidase B inhibitors based on natural privileged scaffolds: A review of systematically structural modification. *Int J Biol Macromol*. 2023;251:126158.

doi: 10.1016/J.IJBIOMAC.2023.126158

38. Tan YY, Jenner P, Di Chen S. Monoamine oxidase-B inhibitors for the treatment of Parkinson's disease: Past, present, and future. *J Parkinsons Dis*. 2022;12(2):477-493.

doi: 10.3233/JPD-212976

39. Jenner P, Rocha JF, Ferreira JJ, Rascol O, Soares-da-Silva P. Redefining the strategy for the use of COMT inhibitors in Parkinson's disease: The role of opicapone. *Expert Rev Neurother*. 2021;21(9):1019-1033.

doi: 10.1080/14737175.2021.1968298

40. Moschovou K, Melagraki G, Mavromoustakos T, Zacharia LC, Afantitis A. Cheminformatics and virtual screening studies of COMT inhibitors as potential Parkinson's disease therapeutics. *Expert Opin Drug Discov*. 2020;15(1):53-62.

doi: 10.1080/17460441.2020.1691165

41. Fabbri M, Ferreira JJ, Rascol O. COMT Inhibitors in the management of Parkinson's disease. *CNS Drugs*. 2022;36(3):261-282.

doi: 10.1007/S40263-021-00888-9

42. Woitalla D, Buhmann C, Hilker-Roggendorf R, *et al*. Role of dopamine agonists in Parkinson's disease therapy. *J Neural Transm* (*Vienna*). 2023;130(6):863-873.

doi: 10.1007/S00702-023-02647-0

43. Jing XZ, Yang HJ, Taximaimaiti R, Wang XP. Advances in the therapeutic use of non-ergot dopamine agonists in the treatment of motor and non-motor symptoms of Parkinson's disease. *Curr Neuropharmacol*. 2023;21(5):1224-1240.

doi: 10.2174/1570159X20666220915091022

44. Gray R, Ives N, Rick C, *et al*. Long-term effectiveness of dopamine agonists and monoamine oxidase B inhibitors compared with levodopa as initial treatment for Parkinson's disease (PD MED): A large, open-label, pragmatic randomised trial. *Lancet*. 2014;384(9949):1196-1205.

doi: 10.1016/S0140-6736(14)60683-8

45. Rose EP, Osterberg VR, Gorbunova V, Unni VK. Alpha-synuclein modulates the repair of genomic *DNA* double-strand breaks in a *DNA-PK*$_{cs}$-regulated manner. *Neurobiol Dis*. 2024;201:106675

doi: 10.1016/j.nbd.2024.106675

46. Price DL, Khan A, Angers R, *et al*. *In vivo* effects of the alpha-synuclein misfolding inhibitor minzasolmin supports clinical development in Parkinson's disease. *NPJ Parkinsons Dis*. 2023;9(1):114.

doi: 10.1038/S41531-023-00552-7

47. Hariz M, Blomstedt P. Deep brain stimulation for Parkinson's disease. *J Intern Med*. 2022;292(5):764-778.

doi: 10.1111/JOIM.13541

48. Hacker ML, Turchan M, Heusinkveld LE, *et al*. Deep brain stimulation in early-stage Parkinson disease: Five-year outcomes. *Neurology*. 2020;95(4):E393-E401.

doi: 10.1212/WNL.0000000000009946

49. Kremer NI, van Laar T, Lange SF, *et al*. STN-DBS electrode placement accuracy and motor improvement in Parkinson's disease: Systematic review and individual patient meta-analysis. *J Neurol Neurosurg Psychiatry*. 2023;94(3):236-244.

doi: 10.1136/JNNP-2022-329192

50. Krishna V, Fishman PS, Eisenberg HM, *et al*. Trial of globus pallidus focused ultrasound ablation in Parkinson's disease. *N Engl J Med*. 2023;388(8):683-693.

doi: 10.1056/NEJMOA2202721

51. Cui Z, Wei H, Goding C, Cui R. Stem cell heterogeneity, plasticity, and regulation. *Life Sci.* 2023;334:122240.

doi: 10.1016/j.lfs.2023.122240

52. Boika A, Aleinikava N, Chyzhyk V, Zafranskaya M, Nizheharodava D, Ponomarev V. Mesenchymal stem cells in Parkinson's disease: Motor and nonmotor symptoms in the early posttransplant period. *Surg Neurol Int*. 2020;11:380.

doi: 10.25259/SNI_233_2020

53. Park JM, Rahmati M, Lee SC, Shin JI, Kim YW. Effects of mesenchymal stem cell on dopaminergic neurons, motor and memory functions in animal models of Parkinson's disease: A systematic review and meta-analysis. *Neural Regen Res*. 2024;19(7):1584-1592.

doi: 10.4103/1673-5374.387976

54. Park S, Park CW, Eom JH, *et al*. Preclinical and dose-ranging assessment of hESC-derived dopaminergic progenitors for a clinical trial on Parkinson's disease. *Cell Stem Cell*. 2024;31(1):25-38.e8.

doi: 10.1016/J.STEM.2023.11.009

55. Jiang S, Wang H, Yang C, *et al*. Phase 1 study of safety and preliminary efficacy of intranasal transplantation of human neural stem cells (ANGE-S00$_3$) in Parkinson's disease. *J Neurol Neurosurg Psychiatry.* 2024;95:1102-1111.

doi: 10.1136/JNNP-2023-332921

56. Zheng X, Han D, Liu W, *et al*. Human iPSC-derived midbrain organoids functionally integrate into striatum circuits and restore motor function in a mouse model of Parkinson's disease. *Theranostics*. 2023;13(8):2673-2692.

doi: 10.7150/THNO.80271

57. Nalls MA, Blauwendraat C, Vallerga CL, *et al*. Identification of novel risk loci, causal insights, and heritable risk for Parkinson's disease: A meta-analysis of genome-wide association studies. *Lancet Neurol*. 2019;18(12):1091-1102.

doi: 10.1016/S1474-4422(19)30320-5

58. Day JO, Mullin S. The genetics of parkinson's disease and implications for clinical practice. *Genes* (*Basel*). 2021;12(7):1006.

doi: 10.3390/genes12071006

59. Kang L, Jin S, Wang J, *et al*. AAV vectors applied to the treatment of CNS disorders: Clinical status and challenges. *J Control Release*. 2023;355:458-473.

doi: 10.1016/J.JCONREL.2023.01.067

60. Grote J, Patel N, Bates C, Parmar MS. From lab bench to hope: A review of gene therapies in clinical trials for Parkinson's disease and challenges. *Neurol Sci.* 2024;45:4699-4710.

doi: 10.1007/S10072-024-07599-1

61. Chen Y, Hong Z, Wang J, *et al*. Circuit-specific gene therapy reverses core symptoms in a primate Parkinson's disease model. *Cell*. 2023;186(24):5394-5410.e18.

doi: 10.1016/J.CELL.2023.10.004

62. Fan JQ, Lu WJ, Tan WQ, *et al*. Effectiveness of acupuncture for anxiety among patients with parkinson disease: A randomized clinical trial. *JAMA Netw Open*. 2022;5(9):e2232133.

doi: 10.1001/jamanetworkopen.2022.32133

63. Yan M, Fan J, Liu X, *et al*. Acupuncture and sleep quality among patients with Parkinson disease: A randomized clinical trial. *JAMA Netw Open*. 2024;7(6):e2417862.

doi: 10.1001/jamanetworkopen.2024.17862

64. Jang JH, Park S, An J, *et al*. Gait disturbance improvement and cerebral cortex rearrangement by acupuncture in Parkinson's disease: A pilot assessor-blinded, randomized, controlled, parallel-group trial. *Neurorehabil Neural Repair*. 2020;34(12):1111-1123.

doi: 10.1177/1545968320969942

65. Oh JY, Lee H, Jang SY, *et al*. Central role of hypothalamic circuits for acupuncture's anti-parkinsonian effects. *Adv Sci* (*Weinh*). 2024;11:e2403245.

doi: 10.1002/ADVS.202403245

ACCSCIENCE PUBLISHING

Global Translational Medicine

REVIEW ARTICLE

Senescence in cardiovascular diseases: Insights into metabolic dysfunction in vascular cells

Ying Qu[1,2,3], Anan Wang[4], Caihua Long[4], Qiuyue Gao[1,2,3], and Baoqi Yu[1,2,3]*

[1]Department of Physiology and Pathophysiology, School of Basic Medical Sciences, Capital Medical University, Beijing, China

[2]The Key Laboratory of Cardiovascular Remodeling-Related Diseases, Ministry of Education, Beijing, China

[3]Beijing Key Laboratory of Metabolic Disorder-Related Cardiovascular Diseases, Beijing, China

[4]Department of Basic Medical Sciences, Capital Medical University, Beijing, China

Abstract

Senescence is an independent risk factor and plays a critical role in altering vascular structure and functions. Reportedly, senescence accelerates pathological processes and notably increases the risk of cardiovascular diseases, such as atherosclerosis, which are the leading causes of mortality worldwide. Therefore, understanding vascular senescence mechanisms is essential for controlling the increasing incidence and mortality of cardiovascular diseases. This review highlights the progress in research on the various mechanisms underlying the senescence of endothelial cells, smooth muscle cells, and macrophages – such as stem cell senescence, metabolic dysregulation, mitochondrial autophagy (mitophagy) impairment, and ferroptosis – and summarizes various antisenescence strategies to target these mechanisms. Key interventions include restoration of the nicotinamide adenine dinucleotide/reduced nicotinamide adenine dinucleotide (NAD^+/NADH) ratio and administration of metformin and acarbose to regulate blood glucose levels, which balances the cellular energy and redox. Further, stem cell therapies, rapamycin administration, and melatonin supplementation demonstrate substantial potential. In addition, exercise, dietary modification, and caloric restriction support senescence mitigation. These strategies illustrate the multifaceted nature of senescence and highlight the potential of integrated therapeutic approaches to extend the health span and delay age-related diseases. This review provides a comprehensive summary of age-related metabolic pathways and explores promising antisenescence therapeutic strategies, thereby providing valuable insights into the prevention, diagnosis, and treatment of senescence-related vascular diseases.

Keywords: Senescence; Cardiovascular disease; Vascular disease; Metabolism; Stem cells

***Corresponding author:**
Baoqi Yu
(baoqiyu@ccmu.edu.cn)

Citation: Qu Y, Wang A, Long C, Gao Q, Yu B. Senescence in cardiovascular diseases: Insights into metabolic dysfunction in vascular cells. *Global Transl Med*. 2024:3(4):4619.
doi: 10.36922/gtm.4619

Received: August 21, 2024

Accepted: October 14, 2024

Published Online: November 21, 2024

1. Introduction

Senescence represents a state of cell cycle arrest exhibited in all cells, tissues, organs, and the entire organism. It constitutes an inevitable, time-dependent process that ultimately disrupts cellular homeostasis and limits the reparative capacity of cells for repairing, further leading to a generalized decrease in physiological functions throughout the body.

Senescence can be classified into two types: physiological and pathological. Physiological senescence refers to the natural degeneration that occurs in organisms with age, whereas pathological senescence refers to age-related changes that manifest in young organisms because of various factors, such as obesity, inflammation, and metabolic disorders. Vascular senescence is crucial for the development of several vascular diseases, including atherosclerosis, vascular calcification (VC), hypertension, arterial aneurysm, arterial dissection, and peripheral vascular diseases. Therefore, understanding the fundamental mechanisms underlying vascular senescence to develop effective strategies for preventing and treating age-related vascular diseases is imperative.

1.1. Overview of senescence

Although not a disease, senescence increases an organism's vulnerability and triggers various pathological conditions. There are 12 senescence biomarkers (Table 1): genomic instability, telomere attrition, epigenetic alterations, loss of proteostasis, disabled macroautophagy, deregulated nutrient sensing, mitochondrial dysfunction, cellular senescence, stem cell exhaustion, altered intercellular communication, chronic inflammation, and dysbiosis.[1]

2. Types of senescence

2.1. Vascular senescence

Blood vessels serve as crucial conduits that transport blood and nutrients throughout the body, maintaining vital life activities.[2] In humans, senescence typically starts with vascular senescence, leading to alterations in blood vessel morphology and functions. Vascular senescence is an intrinsic physiological and pathological process regulated by various risk factors, such as genetics, the environment, and lifestyle. Reportedly, an individual's genetic background considerably influences blood vessel elasticity and wall thickness. Specific genes are closely associated with vascular senescence, and as individuals age, alterations in these gene expressions contribute to arterial stiffness and diminished elasticity. Moreover, environmental factors, such as prolonged exposure to smoking and environmental pollution, as well as an unhealthy lifestyle characterized by a high-fat, high-sugar diet, augment oxidative stress, and endothelial cell damage and result in severe vascular senescence and inflammatory responses, accelerating the progression of atherosclerosis.[2,3] This process is characterized by notable alterations, such as lumen enlargement, intima-media thickening, elastic fiber disruption and fracturing, increased collagen fiber deposition, and augmented vascular stiffness. In addition, prominent features of vascular senescence include VC, remodeling, intravascular plaque formation, decreased sensitivity to vasoactive factors, and reduced neovascularization capacity.[4]

2.2. Cellular senescence

Cellular senescence refers to the irreversible cessation of proliferation in normal cells, characterized by their withdrawal from the cell cycle.[5] The accumulation of senescent cells in various tissues primarily drives senescence.[6] Cellular senescence involves the gradual loss of cellular ability to withstand stress and damage over time, further declining the cellular function and survival rate. This manifests as systemic functional decline throughout the body, slowed metabolism, and the emergence of aging characteristics. Naturally, cellular senescence is an intrinsic clock-driven process in which cells undergo aging over time, even in the absence of important external stress. Reportedly, cells in the senescent stage often show cell cycle arrest in the G1 or G2 phase due to the activation of specific pathways – such as the tumor protein

Table 1. Senescence biomarkers

Level	Phenotype	Clinical indicators	References
Vascular level	Vascular stiffening	PWV, ABI, PP, and ePWV	77,78
	Calcification	CACS	79
Cellular level	Endothelial dysfunction	$CD8^+CD28^-$T-cells	72
	Cell cycle arrest	$p15^{INK4B}$, $p16^{INKA}$, $p21^{CIP1}$, p53, and pRb	80
	DNA damage	P-γH2AX, ATM, and ATR	81
Molecular level	Plasma proteins	IGF1	82
	Metabolic changes	SA-β-gal	6
	SASP	IL-6 and IL-8	8

Abbreviations: PWV: Pulse wave velocity; ABI: Ankle brachial index; PP: Pulse pressure; ePWV: Estimated pulse wave velocity; CACS: Coronary artery calcium score; $p15^{INK4B}$: Cyclin-dependent kinase inhibitor 2B (CDKN2B); $p16^{INKA}$: Cyclin-dependent kinase inhibitor 2A (CDKN2A); $p21^{CIP1}$: Cyclin-dependent kinase inhibitor 1 (CDKN1A); p53: Tumor protein p53; pRb: Retinoblastoma protein; P-γH2AX: Anti-phosphorylated histone H2AX antibody; ATM: Ataxia-telangiectasia mutated; ATR: ATM and Rad3 related; IGF1: Insulin-like growth factor 1; SA-β-gal: Senescence-associated β-galactosidase; SASP: Senescence-associated secretory phenotype; IL-6: Interleukin-6; IL-8: Interleukin-8.

p53 (p53)/p21 and cyclin-dependent kinase inhibitor 2A ($p16^{INK4a}$)/retinoblastoma pathways. These pathways act as critical checkpoints that prevent the cells from continuing to divide at specific thresholds related to time-dependent or intrinsic signals.[7] Thus, senescence is a response to external damage and an intrinsic physiological mechanism evolving because of the accumulation of cell cycle arrest signals over time or senescence is not exclusively a response to external damage; it is an intrinsic physiological mechanism that evolves because of the accumulation of cell cycle arrest signals over time. Typical features of senescent cells include cell cycle arrest and the development of a senescence-associated secretory phenotype (SASP), characterized by the secretion of proinflammatory chemokines (e.g., chemokine [C–X–C motif] ligand [CXCL]1 and CXCL8), cytokines (e.g., interleukin [IL]-6, IL-1α, IL-8, and tumor necrosis factor-alpha [TNF-α]), growth factors, and reactive oxygen species (ROS).[8] Cellular senescence underlies and triggers the development of various diseases, particularly age-related ones, and cellular senescence is reportedly involved in cardiac remodeling, atherosclerosis, and heart failure.[5] Next, we will focus on the mechanisms underlying endothelial cells, smooth muscle cells, macrophages, and stem cell senescence (Figure 1).

2.2.1. Endothelial cell senescence

Vascular endothelial cells are located in the intima of blood vessels, exerting regulatory effects over vasodilation, vasoconstriction, maintenance of blood vessel wall integrity, and blood pressure regulation. Endothelial cell senescence remarkably contributes to vascular senescence by inducing heightened secretory and proinflammatory cytokine activities, as well as exhibiting an enlarged and flattened appearance, which is a characteristic of cellular senescence. Consequently, the presence of senescent endothelial cells impairs endothelial function and reduces vasodilation ability, resulting in ischemia across multiple organs. In addition, these cells display increased polyploidy levels, along with elevated senescence-associated β-galactosidase activity, and telomere shortening.[9] Moreover, the SASP in endothelial cells underscores age-related alterations that play a pivotal role in arterial dysfunction.[10]

Endothelial cell senescence is an important predisposing factor for various cardiovascular diseases.[11] For example, endothelial cell senescence can locally recruit macrophages to the subendothelium, in which they transform into foam cells owing to SASP alterations. In addition, senescent endothelial cells can modulate the phenotypic transformation of smooth muscle and inflammatory cells through exosome secretions, thereby promoting plaque formation and increasing atherosclerosis susceptibility.[12] Senescent endothelial cells also upregulate pathways associated with arterial remodeling (e.g., transforming growth factor β and matrix metalloproteinase [MMP] pathways), which may promote atherosclerosis. As senescent markers, p53 and p21 usually increase in

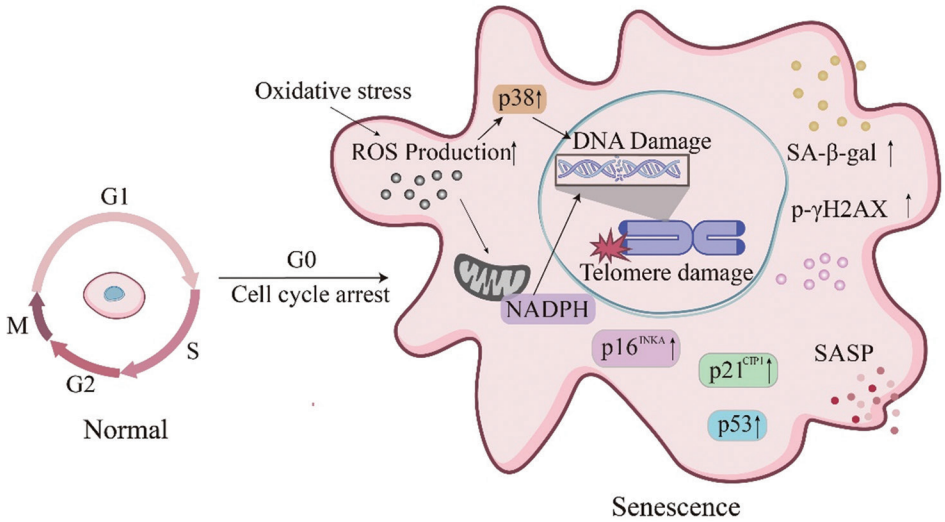

Figure 1. Mechanisms underlying senescence; senescent cells undergo cell cycle arrest at the G0 phase, a process regulated by diverse molecular mechanisms. Initially, ROS accumulation, DNA damage, telomere shortening, and oxidative stress contribute to cellular senescence. Various senescence markers, including $p16^{INK4A}$, $p21^{CIP1}$, p53, and p-γH2AX, are upregulated during this senescence process. Next, senescent cells exhibit elevated SA-β-gal activity, secretion of SASP factors, and alterations in metabolic pathways. Image created by the authors.
Abbreviations: ROS: Reactive oxygen species; $p16^{INKA}$: Cyclin-dependent kinase inhibitor 2A (CDKN2A); $p21^{CIP1}$: Cyclin-dependent kinase inhibitor 1 (CDKN1A); p53: Tumor protein p53; p-γH2AX: Anti-phosphorylated histone H2AX antibody; SA-β-gal: Senescence-associated β-galactosidase; SASP: Senescence-associated secretory phenotype.

senescent cells; p21 is a downstream cell cycle-dependent kinase (CDK) of phosphorylated p53 and functions as a cell cycle inhibitor by binding to and inhibiting CDK2, preventing the transition from the G1 to the S phase of the cell cycle.[13] For example, young mice with defective endothelial DNA repair exhibit elevated p21 expression in their endothelial cells, thereby developing atherosclerosis.[11]

2.2.2. Smooth muscle cell senescence

Vascular smooth muscle cells (VSMCs) exhibit remarkable plasticity and undergo phenotypic transformation owing to various pathological stimuli, such as proinflammatory cytokines and mechanical stretch.[14] VSMC senescence promotes atherosclerosis and arterial calcification, leading to decreased arterial compliance and impaired elastic reservoir function, which serves as the pathological basis of diseases, such as hypertension, and represents an independent risk factor for heart failure.[15]

VSMCs' phenotypic transformation plays a crucial role in vascular senescence. Cellular senescence promotes the transformation of VSMCs to SASP, and this phenotypic transition enhances the synergistic effects, accelerating arterial senescence.[16] A study on mouse models of senescence and hypertension demonstrated that levels of contractile markers (e.g., α-SM-actin and calponin) decreased and those of synthetic markers (e.g., osteopontin) increased in both models. Furthermore, this effect was pronounced in the senescence and hypertension combination, accompanied by a decrease and an increase in protein kinase B and mitogen-activated protein kinase signaling, respectively, indicating reciprocal regulation of VSMC phenotypic switching.[17] However, the phenotypic switch of VSMCs offers novel insights into the development of aneurysms.[16] A recent study demonstrated that age-related nuclear factor (erythroid-derived 2)-like 2 (NRF2) dysfunction acts as a contributing factor to VSMC senescence and VC in VSMC-specific Nrf2-knockdown mice. In addition, repressors of DNA-binding 2 (*Id2*) – a core downstream gene regulated by NRF2, along with Id2 overexpression – can alleviate VC induced by NRF2 silencing-induced VC and VSMC senescence. These findings highlight the protective role played by the NRF 2–ID2 axis against calcification by counteracting VSMC senescence.[18]

2.2.3. Macrophage senescence

Macrophages are immune cells that primarily respond to immune challenges through phagocytosis, removing damaged cells and cellular debris. In contrast, macrophage senescence is characterized by persistent cell cycle arrest and a secretory phenotype associated with chronic, low-grade inflammation-like senescence.

Lipopolysaccharides can upregulate the expression of bromodomain-containing protein 4, which is involved in inflammation-induced macrophage senescence, through nuclear factor kappa B (NF-κB) pathway activation. Senescent macrophages are characterized by morphological changes, SASP, DNA damage response, and promotion of lipid uptake associated with atherosclerosis.[19] Reportedly, extracellular signal-regulated kinase 5 (ERK5) promotes atherosclerotic plaque formation and senescence-associated phenotype secretions via aryl hydrocarbon receptor signaling in macrophages, particularly in the ERK5 S496A KI mouse model.[20] Moreover, at the onset of atherosclerosis, senescent foamy macrophages accumulate in the endothelium, inducing an atherosclerotic process with increased levels of inflammatory cytokines (e.g., IL-1α and TNF-α), chemokines, and metalloproteinase (e.g., Mmp3 and Mmp13). However, in advanced lesions, senescent cells contribute to plaque destabilization by enhancing metalloproteinase production, including elastic fiber degradation and fibrous cap thickness reduction.[21] These findings suggest that macrophage senescence promotes atherosclerosis development and maturation. In addition to other senescent cells, endothelial cells (marked by $p16^{Ink4a+}$), and VSMCs, senescent macrophages drive atherosclerotic plaque formation and create a conducive environment for further growth of lesions.[22]

2.2.4. Stem cell senescence

Stem cells possess the capacity for self-renewal and multilineage differentiation. Under normal conditions, adult stem cells exist in a quiescent state in many tissues. However, alterations in the tissue microenvironment activate these cells, which is essential for tissue homeostasis.[23]

When stem cells become senescent, the organism experiences a reduction of cells capable of participating in the renewal processes, resulting in senescence when homeostasis is disrupted. Therefore, stem cell senescence is considered a crucial characteristic and driving force of organismal senescence and various senescence-related diseases.[24] A comprehensive understanding of the mechanisms underlying stem cell senescence can identify strategies for preserving and promoting the regenerative capacity of stem cells to maintain tissue function during senescence. Multiple molecular mechanisms are involved in stem cell senescence, with key doctrines including

(1). oxidative stress damage: excessive ROS accumulation induces oxidative stress and cellular senescence – a hallmark of senescent stem cells.[25] In stem cells, oxidative stress damages proteins, lipids, and DNA and activates senescence-associated genes, such as *p53* and $p16^{INK4a}$, inducing stem cells into a senescent state[26]

(2). Telomeres and telomerase: telomeres play an essential role in maintaining chromosome integrity and regulating cell division, whereas telomere dysfunction drives the initiation and progression of cellular senescence, along with associated diseases.[27] With each cellular division, telomeres undergo gradual shortening. Once they reach a critically low length, cells stop dividing and enter a state known as replicative senescence.[28] Research shows that silent mating-type information regulation 2 homolog-1 (SIRT1 or sirtuin 1) protects mesenchymal stem cells (MSCs) from age-related DNA damage by inducing the expression of telomerase reverse transcriptase and enhancing telomerase activity while exerting no effect on telomere length. In addition, SIRT1 upregulates tripeptidyl peptidase 1 (TPP1) – a key component of the shelterin complex responsible for the protection of chromosome ends from DNA damage. Consequently, SIRT1 mitigates age-related MSC senescence through multiple mechanisms, including TPP1 upregulation, increased telomerase activity, and reduced DNA damage.[29] Conversely, SIRT1 overexpression reverses the senescence phenotype associated with MSC senescence[30]

(3). Protein homeostasis theory: impaired protein homeostasis results in aberrant protein folding and accumulation of damage within cells, leading to cellular dysfunction, tissue and organ impairment, and organismal senescence.[31] The mitochondrial unfolded protein response (UPR^{mt}) is indispensable for maintaining cellular homeostasis and proteostasis. In stem cells, UPR^{mt} activation is critical for sustaining mitochondrial function. However, the effectiveness of UPR^{mt} may diminish with senescence or prolonged stress, resulting in mitochondrial dysfunction and protein misfolding or aggregation. Consequently, this deterioration impairs the vitality and self-renewal capacity of stem cells, thereby accelerating their senescence[32]

(4). Epigenetic theory: this refers to alterations in the epigenetic landscape, including histone modifications, chromatin remodeling, and DNA methylation.[33] Reportedly, senescence in hematopoietic stem cells is associated with altered patterns of histone modifications, particularly a reduction in trimethylation of lysine 27 on histone H3 (H3K27me3), reducing the activity of hematopoietic stem cells and potentially contributing to their senescence and dysfunction.[25] When hematopoietic stem cells age, there is often a global decline in DNA methylation levels, predominantly characterized by reduced methylation within CpG island regions,[34] which contributes to genomic instability and abnormal gene expression, accelerates senescence, and contributes to the development of atherosclerosis.[27] Similarly, senescence and changes in DNA methylation affect VSMC functions, resulting in structural and functional abnormalities in blood vessel walls, further developing hypertension.[34]

3. Other senescence mechanisms

3.1. Dysregulation of cellular metabolism

Cellular metabolism is fundamentally essential for maintaining various physiological functions, including senescence. Recent studies have identified seven metabolites closely associated with senescence, exhibiting antisenescence effects across different species;[29] these metabolites include nicotinamide adenine dinucleotide (NAD^+), α-ketoglutarate, tryptophan, methionine, spermidine, triglycerides, and cholesterol, of which NAD^+ exerts a notable influence on senescence in various model organisms. NAD^+ serves as a critical coenzyme in the tricarboxylic acid cycle and actively participates in glucose metabolism, insulin secretion, and protein homeostasis while playing an indispensable role in preventing cellular senescence and age-related diseases.[30] As a group of NAD^+-dependent deacetylases, the SIRT family (including seven members, SIRT1–SIRT7) plays a pivotal role in senescence and age-related diseases in mammals.[35]

Under normal physiological conditions, the activity of NAD^+-dependent SIRT1 is enhanced in endothelial cells, which can directly deacetylate and activate DNA repair proteins or regulate DNA repair by activating the related transcription factors.[31,32] In addition, SIRT1 can reduce ROS production by upregulating the expression and activity of superoxide dismutase 2 (SOD2), further enhancing DNA stability, reducing DNA damage and mutations, maintaining normal endothelial cell and blood vessel functions, and decelerating senescence.[36]

The characteristic of age-related disorders includes a decrease in NAD^+ levels in tissues, potentially affecting SIRT activity and contributing to age-related metabolic disorders.[33] NAD^+ dysregulation is considered a substantial risk factor for vascular senescence. On the one hand, reduced NAD^+ can lead to DNA damage and mitochondrial dysfunction, promoting the development of senescence. On the other hand, low levels of NAD^+ during senescence alter metabolic activity in cells, affecting SASP development. This secretory phenotype and the progression of cellular senescence are linked to specific metabolic changes rather than simply being attributed to high metabolic demands.[37] Reportedly, SIRT1 activity is associated with mitochondrial function, and a decrease in SIRT activity can impair the deacetylation of peroxisome proliferator-activated receptor γ coactivator 1α, leading to dysfunctional electron transport chain complexes

and adenosine triphosphate (ATP) synthase, thereby inhibiting mitochondrial biogenesis and causing energy metabolism disorders (Figure 2).[31] Furthermore, reduced SIRT1 activity can inhibit mitochondrial autophagy (mitophagy), accumulating damaged mitochondria and decreasing antioxidant enzymes, such as SOD2, which results in increased oxidative stress, vascular stiffness, vascular senescence, and a higher risk of atherosclerosis.[38] Moreover, knocking out SIRT1 in MSCs in mice leads to fat tissue loss, indicating that SIRT1 coordinates antioxidant responses and inhibits cellular senescence to protect adipogenesis.[39] SIRT1 mitigates cellular senescence by deacetylating cell cycle-related proteins, such as p53. Furthermore, it inhibits inflammatory pathways, such as NF-κB, for reducing the release of SASP factors alleviating inflammation, and delays cellular senescence.[39] Research has also been conducted on other members of the SIRT family. For example, Sirt2 – as an epigenetic regulator – can regulate vascular senescence through the cytoplasm–mitochondrial shuttle mechanism.[40] Sirt3 maintains metabolic homeostasis and the redox balance through deacetylation, providing a new perspective for treating senescence.[41] Sirt6 has also been associated with the improvement of dyslipidemia, cellular senescence, and left ventricular hypertrophy.[42]

3.2. Mitochondrial autophagy disorder

Mitochondria are essential organelles for ATP production and play a critical role in maintaining cellular energy homeostasis.[43] Mitochondrial dysfunction can expedite senescence by disrupting the cytoplasmic NAD^+/reduced nicotinamide adenine dinucleotide (NADH) ratio and increasing ROS production ROS. Impaired mitophagy, which is crucial for removing damaged mitochondria, accumulates dysfunctional mitochondria, which further exacerbates oxidative stress and accelerates the senescence process.[44]

Mitophagy can be broadly categorized into ubiquitin-dependent and non-ubiquitin-dependent pathways. The ubiquitin-dependent pathway, which is the most extensively studied, primarily relies on the ubiquitination of mitochondrial surface proteins to facilitate mitophagy.[45] The key proteins in the ubiquitin-dependent pathway are

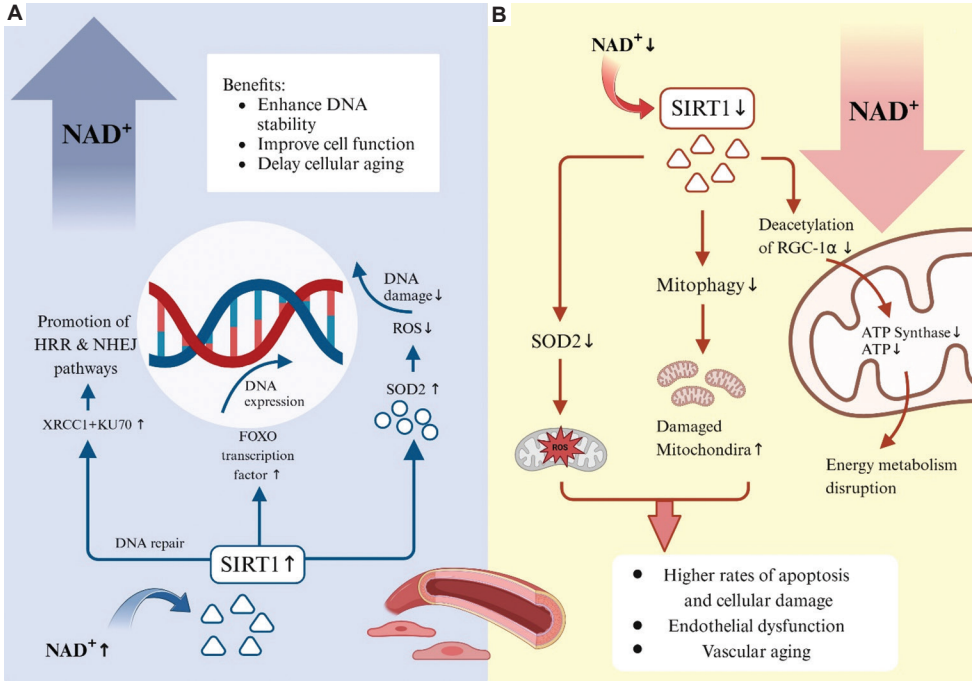

Figure 2. Mechanism of senescence induced by NAD^+ and the SIRT family; (A) NAD^+ levels in endothelial cells increase, leading to upregulation of SIRT1 activity. (1) SIRT1 deacetylates and activates DNA repair proteins (e.g., Ku70 and XRCC1), promoting HRR and NHEJ. (2) SIRT1 deacetylates and activates FOXO, regulating multiple gene expressions involved in DNA repair and antioxidation. (3) SIRT1 regulates the expression and activity of SOD2, thereby reducing ROS production. (B) NAD^+ levels in endothelial cells decrease. Because NAD^+ is a cofactor of SIRT1, decreased NAD^+ levels decrease SIRT1 activity. (1) Decreased SIRT1 activity hampers PGC-1α deacetylation, inhibiting mitochondrial biogenesis. (2) Decreased SIRT1 activity impairs mitophagy, accumulating damaged mitochondria. (3) Decreased SIRT1 activity results in decreased expression of antioxidant enzymes (e.g., SOD2), increased ROS production, and oxidative stress. Image created by the authors.

Abbreviations: NAD^+: Nicotinamide adenine dinucleotide; SIRT1: Silent mating–type information regulation 2 homolog-1; HRR: Homologous recombination repair; NHEJ: Non-homologous end joining; FOXO: Forkhead box transcription factor; SOD2: Superoxide dismutase 2; ROS: Reactive oxygen species; PGC-1α: Alpha subunit of peroxisome proliferator–activated receptor-γ coactivator-1.

phosphatase and tensin homolog-induced putative kinase 1 (PINK1) and ubiquitin ligase (Parkin RBR E3 ubiquitin-protein ligase [Parkin]). Under normal conditions, PINK1 is guided to the mitochondrial inner membrane by a mitochondrial targeting sequence, in which it is cleaved and hydrolyzed. However, when the mitochondria are damaged, their membrane potential decreases, further accumulating PINK1 on the outer membrane of the mitochondria. In addition, Parkin, as an E3 ubiquitin ligase, is recruited to the damaged mitochondria, in which it undergoes phosphorylation and activation by PINK1.[46] Mitophagy within atherosclerotic plaques plays a crucial role in decomposing and eliminating excessive or impaired mitochondria.[47] Therefore, mitophagy represents a potential therapeutic target for stabilizing atherosclerotic plaques, preventing plaque rupture, and slowing atherosclerosis progression.[48] PINK1 can also recruit autophagy receptor proteins (e.g., optineurin and nuclear dot protein 52) to linear granules through ubiquitin phosphorylation. These receptors facilitate the aggregation of microtubule-associated protein 1 light chain 3 (LC3), enabling engulfment of damaged mitochondria by autophagosomes. In addition, dysregulation of PINK1-mediated mitophagy may contribute to the progression of cardiovascular diseases. Mitochondrial dysfunction is closely linked to the development of conditions such as atherosclerosis, hypertension, and heart failure. Modulating PINK1 function could enhance mitophagy, potentially alleviating these vascular disorders.[49] Non-ubiquitin-dependent pathways involve mitophagy receptors rather than surface proteins. In the PINK1–Parkin-independent pathway for mitophagy, PINK1 directly recruits autophagy receptor proteins (e.g., NIX, BNIP3, and FUNDC1) through ubiquitin phosphorylation. These receptors can facilitate the recruitment of LC3 and Parkin, promoting the formation of mitochondrial phagosomes, independent of PINK1's direct influence.[50] Similarly, mitophagy is also affected by external stimuli, such as excess ROS, nutrient deprivation, and cellular senescence, leading to pathological states such as neurodegenerative diseases, metabolic disorders, and senescence (Figure 3).

3.3. Ferroptosis

Ferroptosis is a novel form of regulated cell death that differs from other known cell death types, such as apoptosis and necrosis. It is characterized by the accumulation of ferrous iron (Fe^{2+}) and oxidative attack on cellular and mitochondrial membranes by polyunsaturated fatty acids.[51]

Recent studies have demonstrated that pro-ferroptosis signaling contributes to vascular NAD^+ loss, cellular senescence, remodeling, and stiffness by promoting ferritin autophagy mediated by nuclear receptor coactivator 4. Conversely, the inhibition of ferroptosis signaling or the activation of peroxisome proliferator-activated receptor gamma delays vascular senescence,[52] indicating that targeting pro-ferroptosis signals may offer a promising strategy for treating senescence or age-related cardiovascular diseases.

4. Antisenescence strategies

4.1. Metabolic intervention

Metabolism is fundamental to cellular and tissue functions, encompassing energy production, nutrient use, and waste elimination, and is essential for maintaining cellular homeostasis. Metabolism dysregulation can disturb the cellular energy balance, redox state, and overall functionality, subsequently impacting general health and senescence.[44] Metabolic regulation involves several critical processes, including modulation of the NAD^+/NADH ratio, blood glucose control, and caloric restriction. The NAD^+/NADH ratio plays a crucial role in maintaining the cellular redox balance and energy metabolism, consequently influencing the overall metabolic efficiency. Effective blood glucose regulation is essential for sustaining metabolic homeostasis and preventing metabolic disorders. In addition, caloric restriction enhances mitochondrial function and reduces oxidative stress, which contributes to improved metabolic health and an extended lifespan.[53] These interconnected factors collectively facilitate metabolic regulation and overall well-being.

4.1.1. NAD^+/NADH ratio

In redox equilibrium, ROS plays diverse roles in various pathophysiological reactions, which are closely associated with an increased NAD^+/NADH ratio and L-2-hydroxylglutaric acid accumulation. Increased circulating α-hydroxy-butyric acid levels are associated with an increased NAD^+/NADH ratio and impaired glucose metabolism.[54] Restoring NAD^+ levels through precursor supplementation reestablishes the NAD^+/NADH ratio, delaying cellular senescence and reducing vascular damage. Three main strategies have been explored for increasing NAD+ levels: (1) supplementing a synthetic precursor of NAD (dietary supplement), such as β-nicotinamide mononucleotide and nicotinamide ribose, both of which can be obtained through one's diet and are predominantly used in clinical practice;[55] (2) activating key enzymes involved in NAD biosynthesis, including α-amino-β-carboxylicmuconate-ε-semialdehyde decarboxylase and the rate-limiting enzyme of the remedial pathway amino phosphoribosyl transferase;[56] and (3) regulating enzymes related to NAD^+ degradation to maintain cell health and homeostasis.[57] Increasing NAD^+ levels can enhance endothelial cell function, improve vascular relaxation, and

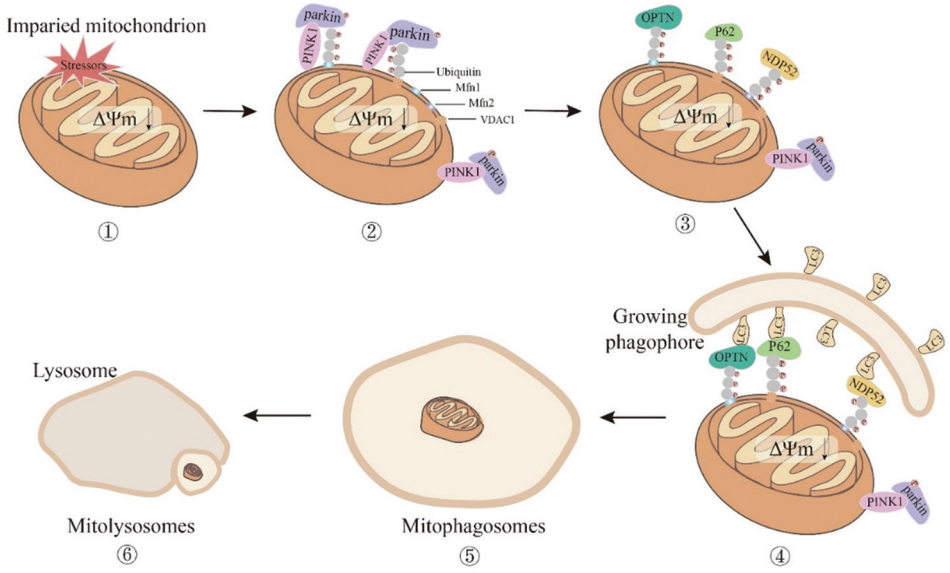

Figure 3. Mitophagy PINK1–Parkin signaling pathway; (1) external stresses, such as increased ROS, mitochondrial DNA mutations, toxic chemicals, and nutritional deficiencies, induce mitochondrial damage and depolarization, leading to the loss of mitochondrial membrane potential. (2) The decreased mitochondrial membrane potential (ΔΨm) impedes the translocation of PINK1 into the inner mitochondrial membrane, causing its accumulation on the outer mitochondrial membrane, in which it recruits and activates Parkin. (3) Upon phosphorylation and activation by PINK1, Parkin catalyzes the transfer of ubiquitin molecules (p62, OPTN, and NDP52) onto specific substrates within the mitochondria for subsequent degradation. (4) Following ubiquitination, autophagy receptor proteins accumulate on the outer membrane of the mitochondria and facilitate binding with autophagosomes through LC3. (5) The ubiquitinated mitochondrial substrates are recognized and engulfed by autophagosomes to form autophagolysosomes. (6) Eventually the autophagolysosomes containing mitochondria undergo degradation. Image created by authors Abbreviations: PINK1: PTEN-induced putative kinase 1; Parkin: Parkin RBR E3 ubiquitin-protein ligase; ROS: Reactive oxygen species; p62: Ubiquitin-binding protein p62; OPTN: Optineurin; NDP52: Nuclear dot protein 52; LC3: Microtubule-associated protein 1 light chain 3.

improve blood flow, further preventing and alleviating atherosclerosis.

4.1.2. Blood glucose levels

Metformin can regulate the insulin/insulin-like growth factor-1 (IGF1) signaling pathway to reduce blood glucose levels and slow down senescence.[58] Simultaneously, it can activate the 5' adenosine monophosphate-activated protein kinase (AMPK) pathway, thereby participating in the enzyme activity of ATP synthesis and decomposition and reducing energy consumption. Reportedly, metformin can modulate vascular senescence by activating the AMPK–SIRT1/SIRT6 axis, which delays age-related atherosclerosis.[59] At present, clinical studies conduct randomized controlled trials to investigate the potential antisenescence properties of metformin and explore how the baseline metabolic health status affects treatment efficacy. Such studies suggest that baseline metabolic health is key to determining the efficiency of metformin in retarding senescence, claiming that metabolic pathways may be essential for antisenescence therapies.[60]

Acarbose (ACA) – an α-glucosidase inhibitor – is clinically used as a hypoglycemic agent because of its ability to reduce the intestinal absorption of simple sugars.[61] The current understanding is that ACA may potentially extend the lifespan through mechanisms akin to caloric restriction[61] and that carbohydrates contribute to senescence, leading to widespread concern about the impact of hyperglycemia on age-related diseases. Considerably, there is widespread interest in exploring ACA's potential as an antisenescence agent.[62]

4.1.3. Caloric restriction

Caloric restriction diets lead to alterations in the gut microbiota of mice, reducing the levels of effector memory T and B cells in the gut and delaying immune cell senescence, specifically within the colon.[63] These findings suggest that modifications in the gut microbiota may underlie the observed attenuation of immune senescence across multiple organs because of caloric restriction.

4.2. Stem cell intervention

Stem cell antisenescence replenishes the stem cells in the body.[64] Clinical trials have shown that stem cell therapy is a promising treatment for cardiovascular diseases. For personalized stem cell therapy, individual disease parameters play a crucial role in determining the optimal choice of cell type, dosage, and delivery method.[65] At present, several pharmacological interventions targeting stem cell senescence are being explored.

4.2.1. Rapamycin

The mammalian target of rapamycin protein (mTOR) is a vital regulatory factor involved in cellular growth and proliferation.[66] By inhibiting mTORC1, rapamycin reduces cellular growth, proliferation, and metabolic rate, while enhancing autophagy. These effects highlight the potential of rapamycin and its analogs, such as everolimus and sirolimus, in the research and treatment of cancer, senescence, and various metabolic disorders. Rapamycin can reportedly improve health conditions associated with senescence, extend the lifespan of model organisms, and reduce the incidence of age-related diseases.[67] mTOR inhibition delays stem cell senescence and prolongs the lifespan of eukaryotes. Further, rapamycin can delay the senescence of dental pulp stem cells by inhibiting protein homeostasis and impaired intercellular signal transduction and regulating mitochondrial dysfunction.[68] The results of clinical trials conducted on the skin have also shown that rapamycin administration reduces $p16^{INK4A}$ expression, which is consistent with cellular senescence and suggests that rapamycin therapy is a potential antisenescence treatment.[69]

4.2.2. Melatonin

MSCs are a commonly used source for various stem cell-based therapies. Melatonin is a highly effective antioxidant predominantly used for treating insomnia, jet lag, depression, anxiety, pre-menstrual syndrome, and menopausal symptoms and supporting immune system functions. Although initially recognized for its role in regulating sleep and circadian rhythms, melatonin possesses substantial antioxidant properties. It effectively neutralizes free radicals and mitigates oxidative stress through several mechanisms – direct free-radical scavenging, enhancement of endogenous antioxidant enzyme activity, and improvement of the cellular antioxidant defense system.[70] These actions position melatonin as a remarkably effective agent in combating senescence, inflammation, and cellular damage, exceeding initial expectations. Research demonstrates that melatonin enhances the expression of heat shock protein family A (Hsp70) member 1-like, which subsequently promotes mitophagy and facilitates the removal of damaged mitochondria.[71] In addition, melatonin exhibits antioxidant properties that alleviate age-related oxidative stress, protecting the functionality of MSCs and ultimately delaying MSC senescence.[71]

4.3. Other interventions

4.3.1. Exercise

Chronic endurance exercise training (≥8 weeks) can improve age-induced SIRT3 inhibition regardless of age. Therefore, long-term regular exercise serves as an effective intervention for enhancing SIRT3 expression and mitigating age-related diseases.[41] Regular physical activity and exercise play a pivotal role in the primary and secondary prevention of cardiovascular diseases.[72]

4.3.2. Dietary regulation

Reducing the content of branched-chain amino acids in the diet can simulate starvation and extend the lifespan of fruit flies.[73] In addition, mTORC1 modulates growth factor signaling by regulating cell anabolism and nutrient sensing through the RagGTPase signaling pathway. Reduced intracellular nutrition levels inhibit the RagGTPase signaling pathway, which suppresses the mTORC1 signaling pathway. Therefore, manipulation of the diet composition, such as caloric restriction, fasting, or dietary protein content increase, can inhibit the mTORC1 signaling pathway and delay senescence progression.[74]

5. Conclusion

Senescence is a complex physiological process that intensifies with advancing age and leads to structural and functional changes in tissues and organs. Cardiovascular diseases are the leading cause of mortality worldwide and are attracting broad research attention. In recent years, senescence has been identified as a significant risk factor for cardiovascular diseases, highlighting the importance of understanding its impact on the vascular system. Notably, investigations into cellular senescence mechanisms have focused on endothelial cells, smooth muscle cells, macrophages, and stem cells because of their direct influence on vascular function and contribution to the development and progression of cardiovascular diseases. Senescence involves multifaceted mechanisms, such as stem cell senescence, cellular metabolic dysregulation, mitophagy, and ferroptosis.

This review aimed to comprehensively summarize the mechanisms underlying senescence, while proposing potential strategies to counteract them, with the goal of offering new therapeutic insights into diseases related to vascular senescence. Strategies targeting stem cell senescence may involve interventions in the stem cell microenvironment, aimed at delaying senescence. Cellular metabolic dysregulation might be achieved through optimizing metabolic pathways and enhancing metabolic regulation. Mitochondrial function protection and optimization might be achieved by applying antioxidants, whereas intervention in ferroptosis requires the regulation of iron metabolism and related pathways.

When cardiovascular diseases coexist with other systemic conditions, such as diabetes, metabolic syndrome,

or neurodegenerative diseases, treatment complexity substantially increases. For instance, patients with diabetes may experience reduced effectiveness of standard antihypertensive treatments because of endothelial dysfunction and chronic inflammation. Furthermore, the accumulation of advanced glycation end products triggers oxidative stress.[75] When cardiovascular diseases coexist with neurodegenerative diseases (e.g., Alzheimer's disease), there is a synergistic exacerbation of vascular damage and acceleration of vascular senescence. Vascular lesions contribute to diminishing cerebral perfusion, whereas neuroinflammation compromises the integrity of vascular walls, culminating in blood–brain barrier dysfunction, further deteriorating cognitive function.[76]

Despite the systematic review and analysis of these mechanisms, there are some shortcomings in clinical application. For example, the safety and efficacy of certain medicines in clinical settings need further exploration. In addition, mechanisms and treatment strategies specific to certain senescence-related vascular diseases require a profound discussion and could focus on validating the clinical relevance of these mechanisms and exploring effective treatment methods for addressing the challenges posed by vascular senescence-related diseases.

Acknowledgments

None.

Funding

This work was supported by a grant from the National Key Research and Development Program of China (2023YFC3606500) and the National Natural Science Foundation of China (32271231).

Conflict of interest

Baoqi Yu is an Editorial Board Member of this journal but was not in any way involved in the editorial and peer-review process conducted for this paper, directly or indirectly. Separately, other authors declared that they have no known competing financial interests or personal relationships that could have influenced the work reported in this paper.

Author contributions

Conceptualization: Ying Qu, Baoqi Yu
Visualization: Anan Wang, Caihua Long
Writing – original draft: Ying Qu, Baoqi Yu
Writing – review & editing: Ying Qu, Qiuyue Gao, Baoqi Yu

Ethics approval and consent to participate

Not applicable.

Consent for publication

Not applicable.

Availability of data

Not applicable.

References

1. López-Otín C, Blasco MA, Partridge L, Serrano M, Kroemer G. Hallmarks of aging: An expanding universe. *Cell*. 2023;186(2):243-278.

   doi: 10.1016/j.cell.2022.11.001

2. Lakatta EG, Levy D. Arterial and cardiac aging: Major shareholders in cardiovascular disease enterprises: Part I: Aging arteries: A "set up" for vascular disease. *Circulation*. 2003;107(1):139-146.

   doi: 10.1161/01.cir.0000048892.83521.58

3. Donato AJ, Black AD, Jablonski KL, Gano LB, Seals DR. Aging is associated with greater nuclear NF Kappa B, reduced I Kappa B Alpha, and increased expression of proinflammatory cytokines in vascular endothelial cells of healthy humans. *Aging Cell*. 2008;7(6):805-812.

   doi: 10.1111/j.1474-9726.2008.00438.x

4. Consortium AB, Zhang L, Guo J, *et al*. A framework of biomarkers for vascular aging: A consensus statement by the Aging Biomarker Consortium. *Life Med*. 2023;2(4):lnad033.

   doi: 10.1093/lifemedi/lnad033

5. Roger L, Tomas F, Gire V. Mechanisms and regulation of cellular senescence. *Int J Mol Sci*. 2021;22(23):13173.

   doi: 10.3390/ijms222313173

6. Lee BY, Han JA, Im JS, *et al*. Senescence-associated beta-galactosidase is lysosomal beta-galactosidase. *Aging Cell*. 2006;5(2):187-195.

   doi: 10.1111/j.1474-9726.2006.00199.x

7. Campisi J. Cellular senescence: Putting the paradoxes in perspective. *Curr Opin Genet Dev*. 2011;21(1):107-112.

   doi: 10.1016/j.gde.2010.10.005

8. Li X, Li C, Zhang W, Wang Y, Qian P, Huang H. Inflammation and aging: Signaling pathways and intervention therapies. *Signal Transduct Target Ther*. 2023;8(1):239.

   doi: 10.1038/s41392-023-01502-8

9. Erusalimsky JD, Kurz DJ. Endothelial cell senescence. *Handb Exp Pharmacol*. 2006;(176 Pt 2):213-248.

   doi: 10.1007/3-540-36028-x_7

10. Ritschka B, Storer M, Mas A, *et al*. The senescence-associated secretory phenotype induces cellular plasticity and tissue regeneration. *Genes Dev*. 2017;31(2):172-183.

    doi: 10.1101/gad.290635.116

11. Bloom SI, Islam MT, Lesniewski LA, Donato AJ. Mechanisms and consequences of endothelial cell senescence. *Nat Rev Cardiol*. 2023;20(1):38-51.

doi: 10.1038/s41569-022-00739-0

12. Libby P, Buring JE, Badimon L, *et al*. Atherosclerosis. *Nat Rev Dis Primers*. 2019;5(1):56.

doi: 10.1038/s41572-019-0106-z

13. Hernandez-Segura A, Nehme J, Demaria M. Hallmarks of cellular senescence. *Trends Cell Biol*. 2018;28(6):436-453.

doi: 10.1016/j.tcb.2018.02.001

14. Liu M, Gomez D. Smooth muscle cell phenotypic diversity. *Arterioscler Thromb Vasc Biol*. 2019;39(9):1715-1723.

doi: 10.1161/atvbaha.119.312131

15. Durham AL, Speer MY, Scatena M, Giachelli CM, Shanahan CM. Role of smooth muscle cells in vascular calcification: Implications in atherosclerosis and arterial stiffness. *Cardiovasc Res*. 2018;114(4):590-600.

doi: 10.1093/cvr/cvy010

16. Cao G, Xuan X, Hu J, Zhang R, Jin H, Dong H. How vascular smooth muscle cell phenotype switching contributes to vascular disease. *Cell Commun Signal*. 2022;20(1):180.

doi: 10.1186/s12964-022-00993-2

17. Zhang L, Xu Z, Wu Y, Liao J, Zeng F, Shi L. Akt/eNOS and MAPK signaling pathways mediated the phenotypic switching of thoracic aorta vascular smooth muscle cells in aging/hypertensive rats. *Physiol Res*. 2018;67(4):543-553.

doi: 10.33549/physiolres.933779

18. Xu M, Wei X, Wang J, *et al*. The NRF2/ID2 axis in vascular smooth muscle cells: Novel insights into the interplay between vascular calcification and aging. *Aging Dis*. 2024.

doi: 10.14336/ad.2024.0075

19. Wang H, Fu H, Zhu R, *et al*. BRD4 contributes to LPS-induced macrophage senescence and promotes progression of atherosclerosis-associated lipid uptake. *Aging* (*Albany NY*). 2020;12(10):9240-9259.

doi: 10.18632/aging.103200

20. Abe JI, Imanishi M, Li S, *et al*. An ERK5-NRF2 axis mediates senescence-associated stemness and atherosclerosis. *Circ Res*. 2023;133(1):25-44.

doi: 10.1161/circresaha.122.322017

21. Childs BG, Baker DJ, Wijshake T, Conover CA, Campisi J, van Deursen JM. Senescent intimal foam cells are deleterious at all stages of atherosclerosis. *Science*. 2016;354(6311):472-477.

doi: 10.1126/science.aaf6659

22. Wang L, Hong W, Zhu H, *et al*. Macrophage senescence in health and diseases. *Acta Pharm Sin B*. 2024;14(4):1508-1524.

doi: 10.1016/j.apsb.2024.01.008

23. Morrison SJ, Spradling AC. Stem cells and niches: Mechanisms that promote stem cell maintenance throughout life. *Cell*. 2008;132(4):598-611.

doi: 10.1016/j.cell.2008.01.038

24. Neves J, Sousa-Victor P, Jasper H. Rejuvenating strategies for stem cell-based therapies in aging. *Cell Stem Cell*. 2017;20(2):161-175.

doi: 10.1016/j.stem.2017.01.008

25. Sen P, Shah PP, Nativio R, Berger SL. Epigenetic mechanisms of longevity and aging. *Cell*. 2016;166(4):822-839.

doi: 10.1016/j.cell.2016.07.050

26. Bigarella CL, Liang R, Ghaffari S. Stem cells and the impact of ROS signaling. *Development*. 2014;141(22):4206-4218.

doi: 10.1242/dev.107086

27. Lourida KG, Louridas GE. Epigenetic perspective on atherosclerotic cardiovascular diseases: The holistic principle of systems biology and epigenetic reasoning. *Glob Transl Med*. 2023;2(4):1868.

doi: 10.36922/gtm.1868

28. Chakravarti D, LaBella KA, DePinho RA. Telomeres: History, health, and hallmarks of aging. *Cell*. 2021;184(2):306-322.

doi: 10.1016/j.cell.2020.12.028

29. Bao H, Cao J, Chen M, *et al*. Biomarkers of aging. *Sci China Life Sci*. 2023;66(5):893-1066.

doi: 10.1007/s11427-023-2305-0

30. O'Callaghan C, Vassilopoulos A. Sirtuins at the crossroads of stemness, aging, and cancer. *Aging Cell*. 2017;16(6):1208-1218.

doi: 10.1111/acel.12685

31. Zhang HN, Dai Y, Zhang CH, *et al*. Sirtuins family as a target in endothelial cell dysfunction: Implications for vascular ageing. *Biogerontology*. 2020;21(5):495-516.

doi: 10.1007/s10522-020-09873-z

32. Luna A, Aladjem MI, Kohn KW. SIRT1/PARP1 crosstalk: Connecting DNA damage and metabolism. *Genome Integr*. 2013;4(1):6.

doi: 10.1186/2041-9414-4-6

33. McReynolds MR, Chellappa K, Baur JA. Age-related NAD^+ decline. *Exp Gerontol*. 2020;134:110888.

doi: 10.1016/j.exger.2020.110888

34. Vaidya H, Jeong HS, Keith K, *et al*. DNA methylation entropy as a measure of stem cell replication and aging. *Genome Biol*. 2023;24(1):27.

doi: 10.1186/s13059-023-02866-4

35. Bi S, Jiang X, Ji Q, *et al*. The sirtuin-associated human senescence program converges on the activation of placenta-specific gene PAPPA. *Dev Cell*. 2024;59(8):991-1009.e12.

doi: 10.1016/j.devcel.2024.02.008

36. Li H. Sirtuin 1 (SIRT1) and oxidative stress. In: Laher I, editior. *Systems Biology of Free Radicals and Antioxidants*. Berlin: Springer Berlin Heidelberg; 2014. p. 417-435.

37. Chini CCS, Cordeiro HS, Tran NLK, Chini EN. NAD metabolism: Role in senescence regulation and aging. *Aging Cell*. 2024;23(1):e13920.

doi: 10.1111/acel.13920

38. Zha S, Li Z, Cao Q, Wang F, Liu F. PARP1 inhibitor (PJ34) improves the function of aging-induced endothelial progenitor cells by preserving intracellular NAD^+ levels and increasing SIRT1 activity. *Stem Cell Res Ther*. 2018;9(1):224.

doi: 10.1186/s13287-018-0961-7

39. Yu A, Yu R, Liu H, Ge C, Dang W. SIRT1 safeguards adipogenic differentiation by orchestrating anti-oxidative responses and suppressing cellular senescence. *Geroscience*. 2024;46(1):1107-1127.

doi: 10.1007/s11357-023-00863-w

40. Zhang Y, Wang X, Li XK, *et al*. Sirtuin 2 deficiency aggravates ageing-induced vascular remodelling in humans and mice. *Eur Heart J*. 2023;44(29):2746-2759.

doi: 10.1093/eurheartj/ehad381

41. Zhou L, Pinho R, Gu Y, Radak Z. The role of SIRT3 in exercise and aging. *Cells*. 2022;11(16):2596.

doi: 10.3390/cells11162596

42. Winnik S, Auwerx J, Sinclair DA, Matter CM. Protective effects of sirtuins in cardiovascular diseases: From bench to bedside. *Eur Heart J*. 2015;36(48):3404-3412.

doi: 10.1093/eurheartj/ehv290

43. Sarvari P, Sarvari P. Mitochondria: The master regulator of aging. *Innosc Theranostics Pharm Sci*. 2024;7(2):1726.

doi: 10.36922/itps.1726

44. Wiley CD, Campisi J. The metabolic roots of senescence: Mechanisms and opportunities for intervention. *Nat Metab*. 2021;3(10):1290-1301.

doi: 10.1038/s42255-021-00483-8

45. Lu Y, Li Z, Zhang S, Zhang T, Liu Y, Zhang L. Cellular mitophagy: Mechanism, roles in diseases and small molecule pharmacological regulation. *Theranostics*. 2023;13(2):736-766.

doi: 10.7150/thno.79876

46. Jin SM, Youle RJ. The accumulation of misfolded proteins in the mitochondrial matrix is sensed by PINK1 to induce PARK2/Parkin-mediated mitophagy of polarized mitochondria. *Autophagy*. 2013;9(11):1750-1757.

doi: 10.4161/auto.26122

47. Wenzel DM, Lissounov A, Brzovic PS, Klevit RE. UBCH7 reactivity profile reveals parkin and HHARI to be RING/HECT hybrids. *Nature*. 2011;474(7349):105-108.

doi: 10.1038/nature09966

48. Wu Y, Jiang T, Hua J, *et al*. PINK1/Parkin-mediated mitophagy in cardiovascular disease: From pathogenesis to novel therapy. *Int J Cardiol*. 2022;361:61-69.

doi: 10.1016/j.ijcard.2022.05.025

49. Sekine S, Youle RJ. PINK1 import regulation; A fine system to convey mitochondrial stress to the cytosol. *BMC Biol*. 2018;16(1):2.

doi: 10.1186/s12915-017-0470-7

50. Lampert MA, Orogo AM, Najor RH, *et al*. BNIP3L/NIX and FUNDC1-mediated mitophagy is required for mitochondrial network remodeling during cardiac progenitor cell differentiation. *Autophagy*. 2019;15(7):1182-1198.

doi: 10.1080/15548627.2019.1580095

51. Muñoz-Espín D, Serrano M. Cellular senescence: From physiology to pathology. *Nat Rev Mol Cell Biol*. 2014;15(7):482-496.

doi: 10.1038/nrm3823

52. Sun DY, Wu WB, Wu JJ, *et al*. Pro-ferroptotic signaling promotes arterial aging via vascular smooth muscle cell senescence. *Nat Commun*. 2024;15(1):1429.

doi: 10.1038/s41467-024-45823-w

53. Merry BJ. Oxidative stress and mitochondrial function with aging--the effects of calorie restriction. *Aging Cell*. 2004;3(1):7-12.

doi: 10.1046/j.1474-9728.2003.00074.x

54. Patgiri A, Skinner OS, Miyazaki Y, *et al*. An engineered enzyme that targets circulating lactate to alleviate intracellular NADH: NAD^+ imbalance. *Nat Biotechnol*. 2020;38(3):309-313.

doi: 10.1038/s41587-019-0377-7

55. Alegre GFS, Pastore GM. NAD^+ Precursors Nicotinamide Mononucleotide (NMN) and Nicotinamide Riboside (NR): Potential dietary contribution to health. *Curr Nutr Rep*. 2023;12(3):445-464.

doi: 10.1007/s13668-023-00475-y

56. Covarrubias AJ, Perrone R, Grozio A, Verdin E. NAD^+ metabolism and its roles in cellular processes during ageing. *Nat Rev Mol Cell Biol*. 2021;22(2):119-141.

doi: 10.1038/s41580-020-00313-x

57. Li F, Wu C, Wang G. Targeting NAD metabolism for the therapy of age-related neurodegenerative diseases. *Neurosci Bull*. 2024;40(2):218-240.

doi: 10.1007/s12264-023-01072-3

58. Khan J, Pernicova I, Nisar K, Korbonits M. Mechanisms of ageing: Growth hormone, dietary restriction, and

metformin. *Lancet Diabetes Endocrinol*. 2023;11(4):261-281.

doi: 10.1016/s2213-8587(23)00001-3

59. Pulipaka S, Singuru G, Sahoo S, Shaikh A, Thennati R, Kotamraju S. Therapeutic efficacies of mitochondria-targeted esculetin and metformin in the improvement of age-associated atherosclerosis via regulating AMPK activation. *Geroscience*. 2024;46(2):2391-2408.

doi: 10.1007/s11357-023-01015-w

60. Kumari S, Bubak MT, Schoenberg HM, *et al*. Antecedent Metabolic Health and Metformin (ANTHEM) aging study: Rationale and study design for a randomized controlled trial. *J Gerontol A Biol Sci Med Sci*. 2022;77(12):2373-2377.

doi: 10.1093/gerona/glab358

61. Smith DL, Jr., Orlandella RM, Allison DB, Norian LA. Diabetes medications as potential calorie restriction mimetics-a focus on the alpha-glucosidase inhibitor acarbose. *Geroscience*. 2021;43(3):1123-1133.

doi: 10.1007/s11357-020-00278-x

62. Du N, Yang R, Jiang S, *et al*. Anti-aging drugs and the related signal pathways. *Biomedicines*. 2024;12(1):127.

doi: 10.3390/biomedicines12010127

63. Sbierski-Kind J, Grenkowitz S, Schlickeiser S, *et al*. Effects of caloric restriction on the gut microbiome are linked with immune senescence. *Microbiome*. 2022;10(1):57.

doi: 10.1186/s40168-022-01249-4

64. Liu B, Qu J, Zhang W, Izpisua Belmonte JC, Liu GH. A stem cell aging framework, from mechanisms to interventions. *Cell Rep.* 2022;41(3):111451.

doi: 10.1016/j.celrep.2022.111451

65. Müller P, Lemcke H, David R. Stem cell therapy in heart diseases - cell types, mechanisms and improvement strategies. *Cell Physiol Biochem*. 2018;48(6):2607-2655.

doi: 10.1159/000492704

66. Heitman J, Movva NR, Hall MN. Targets for cell cycle arrest by the immunosuppressant rapamycin in yeast. *Science*. 1991;253(5022):905-909.

doi: 10.1126/science.1715094

67. Blagosklonny MV. Cell senescence, rapamycin and hyperfunction theory of aging. *Cell Cycle*. 2022;21(14):1456-1467.

doi: 10.1080/15384101.2022.2054636

68. Zhang S, Zhang R, Qiao P, *et al*. Metformin-induced microrna-34a-3p downregulation alleviates senescence in human dental pulp stem cells by targeting CAB39 through the AMPK/mTOR signaling pathway. *Stem Cells Int*. 2021;2021:6616240.

doi: 10.1155/2021/6616240

69. Chung CL, Lawrence I, Hoffman M, *et al*. Topical rapamycin reduces markers of senescence and aging in human skin: An exploratory, prospective, randomized trial. *Geroscience*. 2019;41(6):861-869.

doi: 10.1007/s11357-019-00113-y

70. Reiter RJ, Mayo JC, Tan DX, Sainz RM, Alatorre-Jimenez M, Qin L. Melatonin as an antioxidant: Under promises but over delivers. *J Pineal Res*. 2016;61(3):253-278.

doi: 10.1111/jpi.12360

71. Lee JH, Yoon YM, Song KH, Noh H, Lee SH. Melatonin suppresses senescence-derived mitochondrial dysfunction in mesenchymal stem cells via the HSPA1L-mitophagy pathway. *Aging Cell*. 2020;19(3):e13111.

doi: 10.1111/acel.13111

72. Carrasco E, Gómez de las Heras MM, Gabandé-Rodríguez E, Desdín-Micó G, Aranda JF, Mittelbrunn M. The role of T cells in age-related diseases. *Nat Rev Immunol*. 2022;22(2):97-111.

doi: 10.1038/s41577-021-00557-4

73. Weaver KJ, Holt RA, Henry E, Lyu Y, Pletcher SD. Effects of hunger on neuronal histone modifications slow aging in *Drosophila*. *Science*. 2023;380(6645):625-632.

doi: 10.1126/science.ade1662

74. Ortega-Molina A, Lebrero-Fernández C, Sanz A, *et al*. A mild increase in nutrient signaling to mTORC1 in mice leads to parenchymal damage, myeloid inflammation and shortened lifespan. *Nat Aging*. 2024;4:1102-1120.

doi: 10.1038/s43587-024-00635-x

75. Ferrucci L, Fabbri E. Inflammageing: Chronic inflammation in ageing, cardiovascular disease, and frailty. *Nat Rev Cardiol*. 2018;15(9):505-522.

doi: 10.1038/s41569-018-0064-2

76. Kapasi A, DeCarli C, Schneider JA. Impact of multiple pathologies on the threshold for clinically overt dementia. *Acta Neuropathol*. 2017;134(2):171-186.

doi: 10.1007/s00401-017-1717-7

77. Zhu ZQ, Chen LS, Wang H, *et al*. Carotid stiffness and atherosclerotic risk: Non-invasive quantification with ultrafast ultrasound pulse wave velocity. *European Radiol*. 2019;29(3):1507-1517.

doi: 10.1007/s00330-018-5705-7

78. Matsushima H, Hosomi N, Hara N, *et al*. Ability of the ankle brachial index and brachial-ankle pulse wave velocity to predict the 3-month outcome in patients with non-cardioembolic stroke. *J Atheroscler Thromb*. 2017;24(11):1167-1173.

doi: 10.5551/jat.38901

79. Miname MH, Bittencourt MS, Pereira AC, *et al*. Vascular age derived from coronary artery calcium score on the

risk stratification of individuals with heterozygous familial hypercholesterolaemia. *Eur Heart J Cardiovasc Imaging*. 2019;21(3):251-257.

doi: 10.1093/ehjci/jez280

80. Medzhitov R. The spectrum of inflammatory responses. *Science*. 2021;374(6571):1070-1075.

doi: 10.1126/science.abi5200

81. Blackford AN, Jackson SP. ATM, ATR, and DNA-PK: The trinity at the heart of the DNA damage response. *Mol Cell*. 2017;66(6):801-817.

doi: 10.1016/j.molcel.2017.05.015

82. Fulop GA, Ramirez-Perez FI, Kiss T, *et al*. IGF-1 deficiency promotes pathological remodeling of cerebral arteries: A potential mechanism contributing to the pathogenesis of intracerebral hemorrhages in aging. *J Gerontol A Biol Sci Med Sci*. 2019;74(4):446-454.

doi: 10.1093/gerona/gly144

ACCSCIENCE PUBLISHING

Global Translational Medicine

REVIEW ARTICLE

Post-traumatic stress disorder: Cerebral and extracerebral processing of traumatic memories and treatment strategies

Adonis Sfera[1,2,3], Jacob J. Anton[4], Jasper H. C. Luong[5], and Zisis Kozlakidis[6]*

[1]Patton State Hospital, Patton, CA, United States of America

[2]Department of Psychiatry, University of California Riverside, Riverside, CA, United States of America

[3]Department of Psychiatry, Loma Linda University, Loma Linda, CA, United States of America

[4]Department of Health Sciences, California Baptist University, Riverside, CA, United States of America

[5]Smoke-Free and Healthy Life Association of Macau, Macau SAR, China

[6]International Agency for Research on Cancer, World Health Organization, Lyon, Rhone Alpes, France

Abstract

Post-traumatic stress disorder (PTSD) is a severe neuropsychiatric condition characterized by anxiety-related symptoms, including intrusive memories. However, the exact anatomic location of traumatic memories remains unclear. Traumatic imagery may involve the amygdala and posterior cingulate cortex, rather than the hippocampus. Besides the central nervous system, cells and even proteins can process information and store memories. For instance, >36% of cardiac transplant recipients inherit donor personality traits, emphasizing that tissues can store and recall memories. Moreover, physical therapists mention "musculofascial memories," *that is*, the ability of muscles and fascia to retain the memory of past injuries and adapt their function accordingly. Immune cells record previous infections, demonstrating the broader perspective of memory storage in the body. At the cellular level, psychological stress induces premature cellular senescence, a survival program characterized by proliferation arrest; resistance to apoptosis; and a toxic secretome known as the senescence-associated secretory phenotype (SASP). SASP contains brain-derived neurotropic factor (BDNF), a neurotrophin linked to fear memory that is frequently elevated in the peripheral blood of patients with PTSD. Endothelial cells (ECs), the tiles paving the lumen of large and small vessels, age earlier than other cells in patients with severe mental illness, including PTSD. Senescent ECs release SASP directly into the systemic circulation, spreading senescence throughout the body. In this narrative review, we hypothesize that ECs store traumatic memories and SASP-associated BDNF activates traumatic imagery. We also discuss membrane lipid replacement, mitochondrial transplantation and transfer, and several natural and synthetic compounds that may counteract endothelial senescence and SASP.

Keywords: PTSD; Psychological trauma; Traumatic amnesia; Traumatic hypermnesia; Cellular senescence

***Corresponding author:**
Zisis Kozlakidis
(kozlakidisz@who.int)

Citation: Sfera A, Anton JJ, Luong JHC, Kozlakidis Z. Post-traumatic stress disorder: Cerebral and extracerebral processing of traumatic memories and treatment strategies. *Global Transl Med*. 2024:3(4):3974.
doi: 10.36922/gtm.3974

Received: June 19, 2024

Accepted: September 18, 2024

Published Online: November 22, 2024

1. Introduction

Post-traumatic stress disorder (PTSD) is characterized by numerous memory-related symptoms, including traumatic amnesia, hypermnesia, and intrusive thoughts related to the traumatic event.[1]

Cerebral endothelial cells (CECs) are an important source of brain-derived neurotrophic factor (BDNF), producing 50 times more BDNF levels than neurons, suggesting that these cells play a substantial role in PTSD.[2-4] In fact, BDNF regulates stress hormones and the vulnerability to stress-related disorders.[2] BDNF level is elevated in the peripheral blood of patients with PTSD and is believed to be a biomarker of this pathology.

The BDNF receptor tropomyosin receptor kinase B (Trk-B) is crucial for neuronal plasticity, survival, and growth as well as for long-term potentiation (LTP).[5] In contrast, the receptor for pro-BDNF, the p75 neurotrophin receptor (p75NTR), which mediates the apoptosis of hippocampal and amygdalar neurons, probably accounts for the brain volume reduction in patients with PTSD.[6] In fact, a study in neuroimaging has associated PTSD with brain volume loss, involving the hippocampus, amygdala, insular cortex, and anterior cingulate cortex, suggesting that these areas suppress traumatic memories.[7]

CECs express abundant monocarboxylate transporter (MCT), a lactate-transporting molecule because these cells utilize lactate as their primary energy source.[8,9] A recent study linked lactate to spatial memory enhancement, suggesting a beneficial effect of glycolysis on the brain. Conversely, lactylation, a post-translational modification of histone protein lysine residues (Kla), is associated with neuropsychiatric disorders, including PTSD.[10] Moreover, our research group reported an association between lactylation and the pathogenesis of traumatic memories in patients with PTSD.[11]

CECs regulate blood flow to the brain and interact with the surrounding parenchyma, playing a significant role in the pathogenesis of dementia and further linking memory to endothelia.[12] Senescent CECs represent a significant burden of senescent cells in the body. Excessive lactate production links these senescent ECs to PTSD and cardiovascular disease (CVD).[13-16]

The proprotein convertase subtilisin/kexin family member 3 (FURIN), a newly identified player in neuropsychiatric illness, is highly expressed in CECs and plays a vital role in cellular senescence by interfering with BDNF maturation.[17-19] Furin is a proprotein convertase that transforms precursor proteins into biologically active forms, including pro-BDNF into BDNF. Its ability to activate toxins or pathogens, such as anthrax, by proteolytic cleavage brought furin to the forefront of bioweapon research, where it remains up to the present day.[20-23]

In lipid metabolism, furin activates lipoprotein lipase (LPL), an enzyme that regulates the plasma levels of triglycerides and high-density lipoproteins (HDL). Both triglycerides and HDLs have been implicated in stress-related disorders, including PTSD.[24]

Interest in furin resurfaced during the COVID-19 pandemic, as the virus exploits this protein to increase infectivity. Nevertheless, the viral exploitation of furin disrupts plasmin and BDNF, potentially predisposing individuals to PTSD.[25] Hence, COVID-19 was associated with a higher prevalence of PTSD, as this condition was promoted by excessive isolation and lockdown as well as furin disruption and altered BDNF levels.[26] Furthermore, because BDNF is a part of the SASP, its elevated levels in the peripheral blood of patients with PTSD may be explained.[27] We suggest that non-cerebral BDNF is detrimental and likely induces cellular senescence, including cognitive deficit.

Psychological stress is associated with premature cellular aging, a phenotype characteristic of several mental illnesses, including schizophrenia (SCZ) and PTSD. Psychological stress triggers sterile inflammation, activation of the NOD-like receptor family pyrin domain-containing 3 (NLRP3) inflammasome, and generation of interleukin (IL)-1) and IL-18, a family of cytokines associated with neuroinflammation, anxiety, or psychosis.[28]

In this narrative review, we explore the existing knowledge regarding senescent ECs in PTSD and discuss several natural and synthetic compounds that may counteract endothelial senescence, SASP, and mitochondrial transplant or transfer.

2. Traumatic memories are decentralized

Unlike conventional memories, traumatic imprinting is believed to occur in the right amygdala and posterior cingulate cortex.[29,30] Here, emotionally charged memories are processed without the involvement of the hippocampus and are experienced as though they occur in the present moment.[31] Recent studies have demonstrated that dysfunctional peripheral blood mononuclear cells could cause or exacerbate PTSD, suggesting that extracerebral cells and tissues are detrimental to traumatic recall.[32,33] This raises the question, can cognition generally "dwell" in peripheral tissues? In fact, early studies have found that single cells or unicellular life forms can process and recall information.[34,35]

2.1. What is decentralized cognition?

Cognition and memory are precious human assets that make us unique and distinct from other species. Therefore,

cognitive functions may be distributed throughout the body to reduce the risk of memory loss due to brain injuries or pathology. They are probably encoded in the molecular networks of all cells. For instance, the cellular cytoskeleton communicates with the proteins of the extracellular matrix through integrins and lipid rafts (membrane windows that unite intracellular and extracellular molecular networks), generating global assemblies.[36]

The proteins in molecular networks are believed to encode memory in a quantum manner by altering the conformational dynamics of various molecules. Proteins have unique properties that facilitate information processing and storage. Proteins fold along specific lines such as in origami, connect instantly with each other in a Lego-like manner, and, such as transformers, build new structures from the old components. Proteins can also exist as two-state systems, engendering logic gates, the building blocks of quantum circuits.[37]

The molecular network-mediated memory allows storing information in neurons and most body cells, engendering a decentralized "blockchain" cognition. Conditions such as phantom limb, pseudocyesis, psychogenic blindness, or cardiac transplant recipients adopting the donor's personality traits demonstrate that cells and molecules can harbor memories and behavioral patterns.[38,39]

In severe mental illness (SMI), including PTSD, cells throughout the body undergo premature cellular senescence, a phenotype triggered by dysfunctional tight junctions.[40,41] At the level of the gut and blood–brain barrier (BBB), senescent cells increase permeability further, enabling microbial migration into the host circulation and eventually reaching the brain. Senescent glial cells and multipotent stem cells stop replicating or replicate sporadically. In contrast, the opposite phenomenon occurs in cancer, with the occurrence of uncontrolled proliferation, suggesting that senescence and tumorigenesis act like the two faces of Janus.

Ancient viruses inherited from our predecessors, *namely*, human endogenous retroviruses (HERVs), dwell in our DNA, comprising approximately 8% of the genome.[42]

HERVs are activated by different pathologies, including cancer, SMI, and contemporary viruses, including SARS-CoV-2, the etiologic agent of the COVID-19 pandemic.[43] Some HERVs have become "domesticated" and "work" for the human host. For instance, HERV-W ENV encodes a placental protein that, under pathological conditions, may cause infertility.[44] Another example is the activity-regulated cytoskeleton-associated (Arc) protein derived from an ancestral virus, which is expressed primarily in the brain, promoting synaptic plasticity, learning, and LTP.[45,46]

Anecdotally, we recall a patient with cysticercosis who was treated years earlier. He behaved, walked, and generally talked. The only complaints were mild forgetfulness and word-finding difficulties. The resident physician performed a dementia work-up, including an MRI of the brain. We observed surprising results and wondered how this patient could be alive. He had very little brain parenchyma left. Although numerous cysts were detected throughout his CNS, he appeared to be minimally impaired. This individual and others like him are proof that information and memories are stored not only in the brain but also in cells throughout the body. This may explain the patient's normal functioning despite the loss of cerebral volume. In fact, the amount of information in the DNA, which is present in every single cell of the body, ensures that the genetic information is not lost or altered. Moreover, our muscles and tendons "remember" the old postures we have long abandoned. Immune cells recall previous infections, as shown by studies that 36% of patients with heart transplants inherit bits and pieces of the donor's personality.[38,47]

2.2. Cellular senescence

In 1961, Leonard Hayflick found that human somatic cells do not replicate indefinitely but exit the cell cycle after 40 – 60 divisions, the so-called Hayflick's limit.[48] These cells enter a state of replicative senescence marked by proliferative arrest in which they remain alive, have an active metabolism, and release toxic molecules known as the SASP.

A few decades later, it was discovered that in addition to replicative senescence, human cells can activate the senescence program in response to various insults, including damaged DNA or plasma membranes, suggesting that senescence is a default state responsible for averting cell/neuronal loss.

Over the past few years, it became clear that SMI also triggers cellular, including neuronal and CEC, senescence, thereby disrupting the BBB, a characteristic of several neuropsychiatric disorders.

At present, the exact mechanism of how mental illness, including PTSD, triggers senescence remains unclear. Nevertheless, it may involve viruses because virus-mediated lipid peroxidation may activate senescence. For instance, under normal circumstances, cholesterol negatively regulates cellular senescence, whereas oxidized cholesterol triggers this phenotype.[49] Furthermore, in neuropsychiatric illnesses, including PTSD, cells become senescent before reaching Hayflick's limit, whereas cancer cells never undergo senescence and continue to replicate indefinitely.[50] An anticancer therapeutic strategy involves

inducing senescence in malignant cells by infecting them with viruses to block their replication.[51] Moreover, people with SMI show a lesser increase in the number of human hippocampal progenitor neurons compared with that in the general population, linking the cognitive deficit to the cell cycle of these undifferentiated cells. It remains unclear why some undifferentiated cells proliferate incessantly, such as HeLa cells, whereas others do not. Pursuing this line of research may bring progress in both cancer and mental illness.

3. Cellular immortality against human mortality

In contrast to SMI, cancer cells replicate and increase in number for several decades, as observed in HeLa cells.

The term HeLa is derived from Henrietta Lacks, an African American woman from Baltimore who had cervical cancer and died in the early 1950s at the age of 31 years. Cells taken from her body (without her knowledge or consent) were developed into the HeLa cell line, which has been used for research and has contributed to several innovations, including the human papillomavirus (HPV) vaccine, HIV medications, and more recently, COVID-19 vaccines.

HeLa cells, which endogenously express furin, and Trk-B, the BDNF receptor, may be suitable for investigating PTSD.[52,53] For instance, gravity can decelerate the cell cycle of HeLa cells, suggesting that biophysical strategies, such as whole-body vibration, play a role in treating cancer and mental illness.[54]

The HeLa case sparked legal and ethical debates, which are still ongoing, over an individual's rights to his/her genetic material and tissues.

The HeLa cell line was kept alive for more than 70 years, emphasizing that cancer cells are immortal and not subject to Hayflick's limit. There were exciting developments and anecdotes regarding HeLa cells during the Cold War, which led to the discernment of the role of gravity in cancer. For instance, in the 1960s, scientists in the Soviet Union became interested in HeLa cells as they intended to explore cancer behavior at zero gravity.[55] Therefore, HeLa cells, obtained from the Johns Hopkins University, were sent on the first orbit flight around the earth in 1961 with Yuri Gagarin, the first Soviet astronaut. HeLa cells were sent again with other Soviet missions, including Vostok 4 in 1962, Vostok 5 and 6 in 1963, Voskhod 1 in 1964, and Zond 5 in 1968.[56] These space experiments concluded that compared with normal cells, which maintained average growth at zero gravity, HeLa cells became more aggressive, dividing faster with each trip, suggesting that zero or low gravity accelerates cancer growth.

In 1971, Richard Nixon signed the National Cancer Act, known as the "War on Cancer." As part of this legislature, the US and USSR began cooperating in cancer research. Nevertheless, due to bilateral mistrust, the exchanged HeLa cells were contaminated, sabotaging several research projects by infecting other cell cultures in both countries and ultimately exacerbating Cold War tensions.

The COVID-19 pandemic has placed a new emphasis on cellular proliferation and cancer, reviving the interest in forcing cellular senescence on cancer cells to stop proliferation.[57,58]

Altogether, both cancer and mental illness ignore Hayflick's limit, with the former driving uncontrolled proliferation and immortality, whereas the latter by deficient proliferation and premature mortality.

4. Role of furin in the human stress response

Furin is rapidly becoming a significant player in the pathogenesis of neurodegenerative and neuropsychiatric diseases, opening a potential avenue for new interventions.[9] For instance, furin inhibitors prevent N-methyl-d-aspartate (NMDA)-mediated neuronal injury; therefore, targeting furin may exert procognitive and possibly antipsychotic effects. For instance, a previous study found that furin can improve dendritic morphogenesis, memory, and learning.[59]

Both psychological and biological stressors alter organismal homeostasis, forcing the system to adopt behavioral or physiological changes to restore the functional balance.[60] The immediate response to stressors consists of sympathetic–adreno–medullar activation, whereas the hypothalamus–pituitary–adrenal axis responds later.[61,62]

PTSD is frequently comorbid with CVD, and the amygdala processes both psychological and biological stressors.[63,64] For instance, the basolateral amygdala (BLA) processes aversive stimuli, whereas the central nucleus of the amygdala (CeA) responds to stress-associated changes in vital signs, such as blood pressure and redox alterations.[65-68]

Dysfunction of two opposite systems, angiotensin II (ANG II) and oxytocin (OXT), has been implicated in both PTSD and CVD.[69,70] Consistent with this, human CECs express abundant OXT receptors, which are believed to protect against stroke.[71] BDNF, expressed in the amygdala, opposes OXT, thereby promoting fear learning.[72,73] Interestingly, furin acts as a common denominator for stroke and myocardial infarction, suggesting its involvement in reducing OXT levels by upregulating BDNF levels.[74]

4.1. Like good and bad cholesterol, there is good and bad BDNF

BDNF can positively and negatively affect human health.[52] We hypothesize that there are two sources of BDNF: cerebral cells and extracerebral cells. With senescence, each group of cells produces even more BDNF.

Normal BDNF promotes LTP, learning, memory, and euthymic mood. The "good" BDNF is neuroprotective, preventing neurodegenerative diseases, and is upregulated by exercise. In contrast, the "bad" BDNF, an SASP component, promotes long-term depression (LTD), dysthymic mood, premature senescence, and learning difficulties.

Both the "good" and "bad" BDNF forms are probably tumorigenic. Therefore, cancer cells, including HeLa cells, overexpress BDNF-associated furin.[52]

4.2. Psychological stress and vascular aging

Cellular senescence, the building block of organismal aging, is a default program of replicative arrest in which cells permanently exit the cell cycle, rewire their metabolism, and secrete SASP. When DNA damage is substantial, the cell activates the senescence program, and repairing the genome requires replicative arrest.[75] Senescence affects ECs first, probably to increase the levels of BDNF, an angiogenesis-promoting neurotrophin that facilitates the sprouting of new vessels to replace the damaged ones.[25,76-78] In fact, senescent cells upregulate BDNF because this growth factor is a component of the SASP and is spread locally in a paracrine/exocrine manner.[20] In PTSD, a condition marked by premature cellular senescence, BDNF levels are probably elevated due to cellular senescence.[79]

BDNF is derived from pro-BDNF, an inactive precursor protein that requires proteolytic cleavage by furin or plasmin to be converted into the biologically active form. Furin protein, encoded by *FURIN*, is a calcium (Ca^{2+})-dependent serine protease that plays a vital role in the activation of numerous endogenous and exogenous proteins into functional molecules. Furin and plasmin activate BDNF, whereas plasminogen activator inhibitor-1 (PAI-1) inhibits plasmin and suppresses the proteolytic activity of furin.[80]

Over the past few decades, furin has attracted the attention of researchers and clinicians for two reasons; first, the weaponization of anthrax by the Soviet Union in the 1950s and 1960s, and second, its vital role in COVID-19 infectivity. The former triggered an intensive biological arms race, which stopped only after the "Sverdlovsk anthrax outbreak of 1979" that killed 64 people.[81] The collective memories of anthrax weaponization programs and the discovery of *FURIN* in 1990 raised the question of whether other pathogens, especially viruses, could be manipulated to increase infectivity (gain of function).

Nonetheless, despite the pandemic and reemergent worldwide concerns regarding the weaponization of this virus, COVID-19 contributed to a better understanding of furin, the convertase usurped by the SARS-CoV-2 to cleave the S (spike) protein into S1 and S2, thereby increasing infectivity. An arginine-rich sequence, PRRAR (proline–arginine–arginine–alanine–arginine), which hijacks human furin, facilitates the viral morbidity of SARS-CoV-2.

In neuropsychiatric illness, the levels of furin, previously implicated in SMI, decrease in patients with SCZ, dementias, and PTSD and increase in patients with epilepsy, suggesting a novel neuropsychiatric target.[82-84] Furthermore, as furin is intertwined with the serotonergic system, increased BDNF levels can contribute to the spread of fear-mediated behavior.[85] Furthermore, several cancers upregulate BDNF, probably due to its angiogenetic properties, which may facilitate metastatic dissemination.[86] In fact, because ECs release large amounts of BDNF, their exploitation can result in the total control of this growth factor.[26]

Pro-BDNF acts on p75NTR, whereas BDNF interacts with Trk-B. The former induces LTD, whereas the latter induces LTP, learning, and memory. LTP promotes the growth of neurites and dendritic spines, increasing the gray matter volume and lowering aggressive behavior.[87,88]

We shall next focus on PTSD and the most recent molecular and clinical insights.

4.3. Do microtubules encode traumatic memories?

Upregulated BDNF interacts with Trk-B, inhibiting glycogen synthase kinase-3 (GSK-3), an enzyme implicated in cellular senescence that is overactive in patients with SCZ, PTSD, bipolar disorder, and dementias (approximately 10% of patients with frontotemporal dementia behavioral variant exhibit dysfunctional GSK-3β). In fact, GSK-3β (also termed tau kinase) promotes the hyperphosphorylation of tau (p-tau), a marker of tauopathies, including Alzheimer's disease (AD). In patients with PTSD, GSK-3β and p-tau levels are elevated; however, in patients with SCZ, both tau and p-tau levels are decreased.[89]

Under physiological circumstances, tau is a microtubular stabilizer believed to participate in tubulin memory storage and retrieval. Microtubules (MTs) are cytoskeletal components formed by tubulin polymerization and held together by tau. It was hypothesized that the MT lattices

encode memories in a quantum manner through calcium–calmodulin-dependent protein kinase II (CaMKII).[90]

Recent pre-clinical studies showed that social stress disrupts memory by impairing tubulin polymerization, thereby linking traumatic amnesia and hypermnesia, documented in PTSD, to microtubular pathology.[91,92] PTSD-related intrusive memories may depend on the degree of tau phosphorylation.

Under physiological conditions, GSK-3β phosphorylates tau protein, stabilizing the conformation of MTs. Nevertheless, excessive tau phosphorylation destabilizes MTs, altering not only recall but also behavior.[38,93] MT-destabilizing agents, including chemotherapeutics, colchicine, and fluorides, are associated with defective recall and behavioral disturbances.[94,95] Because the same agents activate microglia, it is not surprising that these cells have been implicated in behavioral disturbances.[96]

Recent research has demonstrated that the tau protein engages in brain oscillatory activity, contributing to the rapid oscillations implicated in higher cognitive functions.[97]

Altogether, under pathological conditions, GSK-3β may engage in the hyperphosphorylation of tau protein, thereby maintaining traumatic memories and fear.

5. Therapeutic strategies

We had previously discussed potential novel therapies for PTSD.[26,98] Here, we describe a unique strategy, membrane lipid replacement (MLR) augmented with kaempferol and berberine. This combination of natural compounds suppresses GSK-3β activity through three distinct mechanisms, thus averting tau hyperphosphorylation.

5.1. Membrane lipid replacement

MLR is a technique that utilizes healthy, natural glycerophospholipids to substitute the oxidized components of the plasma membrane lipid bilayer, thus restoring the physiological fluidity of the cell and mitochondrial membranes. The membrane lipid bilayer comprises phospholipids, cholesterol, and ceramide, which disrupt neurotransmission when oxidized. Oxidized lipids, including oxysterols, phospholipids, and toxic ceramide, are gradually replaced with natural glycerophospholipids, restoring membrane homeostasis.

A subclass of glycerophospholipids are plasmalogens, lipids containing a vinyl-ether bond that comprises up to 20% of the total membrane lipid.[99] Plasmalogen levels may decrease in the brain tissue of patients with AD, suggesting that plasmalogen supplementation is beneficial.[100]

Studies have demonstrated that MLR, an oral supplementation with natural phospholipids and antioxidants, halts the dissemination of cellular senescence to neighboring healthy cells by inhibiting SASP.[101-103] (Figure 1). Furthermore, MLR facilitates not only cell membranes but also the damaged mitochondrial inner and outer membranes with natural lipid species. In fact, the loss of lysophosphatidylethanolamine (LPE), phosphatidylglycerol (PG), and phosphatidylinositol (PI) in senescent mitochondria causes organelle death. Conversely, replacement with healthy lipids may promote mitochondrial homeostasis.[26]

5.2. Phosphoinositide-dependent kinase 1 (PDK-1) inhibitors

In contrast to the long-held belief that cellular senescence and proliferation arrest are irreversible, groundbreaking data now suggest a promising avenue for intervention. PDK-1 inhibitors, particularly kaempferol, can potentially reverse the senescent phenotype.[104] This discovery opens up new possibilities for research and treatment in biochemistry, pharmacology, and neurology. Furthermore, combining PDK-1 inhibitors with MLR and berberine may offer a novel approach to antipsychotic treatment that avoids the typical adverse effects associated with conventional antipsychotics.

5.3. Kaempferol

Kaempferol is a flavonoid that reduces lipid peroxidation and directly inhibits GSK-3β.[106] It also exhibits antimicrobial, anti-inflammatory, antioxidant, antitumor, cardioprotective, neuroprotective, and antidiabetic activities.[107] Due to GSK-3β inhibition, the effects of kaempferol are similar to those of lithium and several antipsychotics, indicating its probable efficacy against psychosis and mood instability without the side effects of conventional psychotropic drugs (Figure 1).

Kaempferol possesses antioxidant properties and scavenges reactive oxygen species. It also deactivates the nuclear factor kappa-light-chain-enhancer of activated B cell (NF-κB) signaling, indicating anti-inflammatory properties and the ability to reduce neuroinflammation[108] as shown in Table 1.

5.4. Berberine

Berberine is a plant alkaloid extracted from *Hydrastis canadensis*, *Phellodendron chinense*, *Coptis chinensis*, and *Berberis aquifolium*. It has been used in Asia for centuries due to its antimicrobial and antihelminthic properties. Berberine has been used to treat CVD, hyperlipidemia, diabetes, and hypertension as it reduces toxic levels of ceramide, lowering the insulin resistance caused by this toxin. Furthermore, berberine recently received attention as a potential anticancer agent, a property

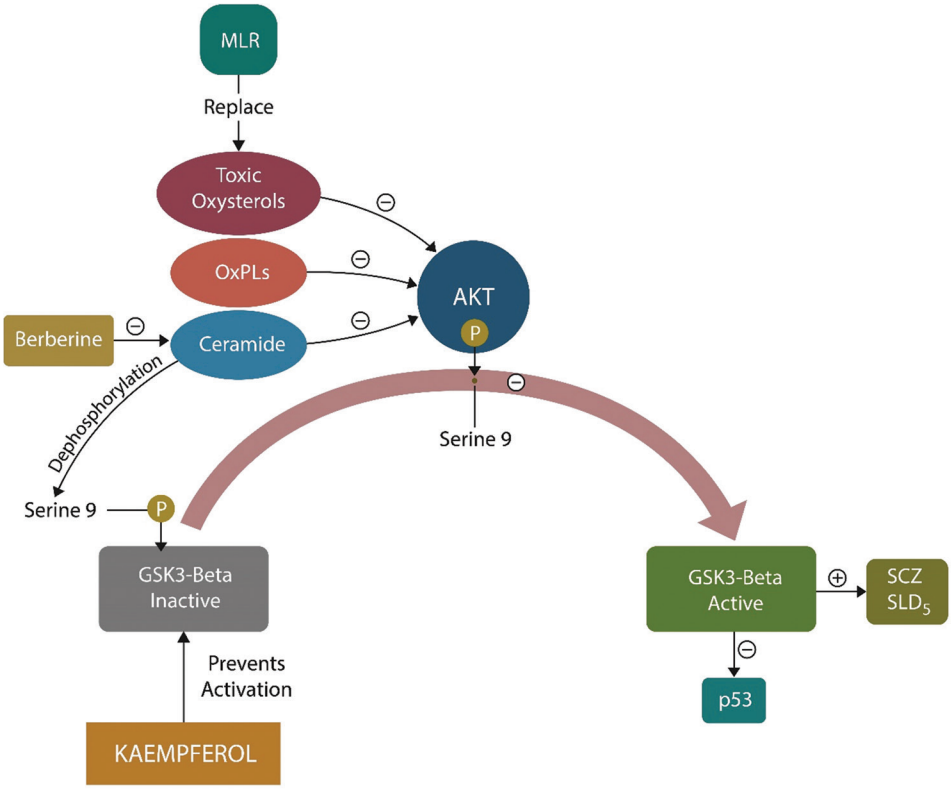

Figure 1. MLR supplies natural glycerophospholipids to replace the oxidized phospholipids, cholesterol, and ceramide. Under normal circumstances, lipids from the membrane bilayer activate Akt, inhibiting GSK-3β by phosphorylation at serine 9. Without lipidomic input, GSK-3β suppresses p53, disrupting genomic repair. Kaempferol prevents GSK-3β activation, whereas berberine inhibits ceramide, preventing serine 9 phosphorylation.[105] Image created by the authors Abbreviations: MLR: Membrane lipid replacement; SCZ: Schizophrenia; SLD_5: Schizophrenia-like disorders.

related to altering the cell cycle dynamics, autophagy, and cellular senescence.[109] In fact, berberine ameliorates cellular senescence by inhibiting cyclins and p16.[110] It also inhibits oxidized ceramide and, indirectly, GSK-3β *through* serine 9. Moreover, berberine alleviates anxiety, suggesting its beneficial effects in patients with PTSD.[111] In ECs, berberine inhibits proliferation, suggesting its antimetastatic effects.[112]

More studies are required on the potential use of these natural compounds as antipsychotic drugs because current clinical data are sporadic.

6. Mitochondrial transfer and transplantation

Mitochondria are intracellular organelles that were previously bacteria, became "domesticated," and currently function in symbiosis with human cells. Mitochondria generate energy in the form of ATP and play a significant role in preventing neuropathology, including depression, marked by several symptoms, including low power.[121] Nevertheless, their role does not end here; these organelles also regulate life and health span.[122] Studies of people in the Blue Zones, areas with the highest number of centenarians, have identified socialization and interconnectedness as the primary keys to longevity.[123] As mitochondria power the social brain, they probably increase the lifespan.[124]

Mitochondria are now known to leave the cell and function in the extracellular compartment, playing a role in regulating metabolism and immunity. Cell-free mitochondrial DNA (cf-mtDNA) is a marker of inflammatory disease whose levels increase due to psychological stress and social isolation.[125] Cf-mtDNA is a measure of psychological stress that can be used as a PTSD biomarker.[126] For instance, loneliness and socialization deficits are associated with increased cf-mtDNA-toll-like receptor 9 (TLR9) signaling. Reducing cf-mtDNA signaling with deoxyribonuclease I (DNase I) attenuates stress associated with impaired social behavior.[127] Furthermore, isolation-upregulated cf-mtDNA acts as a damage-associated molecular pattern (DAMP), activating inflammation. Inflammation without pathogens, known as "sterile," is implicated in psychological stress.[128,129] Therefore, measuring cf-mtDNA levels may explain why

Table 1. A summary of the natural inhibitors of PDK-1 and foods that contain these active ingredients

PDK1 inhibitor	Mechanism of action	Plant	References
Kaempferol	GSK-3β inhibitor	Fruits, vegetables, and herbs	113
Quercetin	Reduces lipid peroxidation	Onions, kale, and broccoli	114
Myricetin	Anticancer, antidiabetic, and antiobesity and cardiovascular protection	Oranges, berries, tomatoes, nuts, and tea	115
Epigallocatechin-3 gallate	Immunoregulation and neuroprotection	Green tea	116
Lupiwighteone isoflavone	Cell cycle arrest and apoptosis and activates the Nrf2/ARE pathway	*Glycyrrhiza glabra; Lotus pedunculatus*	117
Delphinidin	Antiangiogenic activities	Citrus fruits	118
Honokiol	Antidepressant and antitumorigenic	Cherries, berries, and grapes	119
Rutin	Reduces the formation of reactive oxygen species	Oranges, lemons, grapes, peaches, limes, and buckwheat	120

some individuals develop PTSD while others do not (vulnerability quantification). A recent study strictly explored this aspect in veterans with war-related and unrelated stressors and demonstrated that cf-mtDNA levels reflect glucocorticoid sensitivity in individuals with PTSD, a measure of susceptibility.[130]

Altogether, mitochondria serve as more than just energy-producing batteries; their involvement in stress places them at the interface of biological and psychological stressors.

As a former bacterium, the mitochondrion has retained the ability to communicate with intestinal microbes, contributing to the gut–brain axis. For instance, metabolites produced by gut microbes interact directly with mitochondria in the brain, regulating their function. In this regard, short-chain fatty acids by the gut microbiota cross the BBB, influencing the mitochondria and alleviating the symptoms of depression.[131]

Mitochondria contain GSK-3β, a kinase implicated in SMI, including PTSD. Lithium, berberine, and kaempferol inhibit the activity of GSK-3 β, thereby decreasing the risk of death of the organelle. Furthermore, the transfer of mitochondria from astrocytes to neurons ensures energy availability in the CNS.

6.1. Mitochondrial transplantation

Mitochondrial transplantation experiments started in the 1980s when naked organelles were coincubated with various cell types to facilitate internalization.[132] Using originally HeLa cells and mesenchymal stem cells as mitochondrial sources, this transplantation technique took 1 – 2 h to supply organelles to the target, mitochondria-depleted cells.[133,134] Successful mitochondrial transplantation is currently possible on several cell types, and for instance, on cardiomyocytes, which can be confirmed by the presence of mitochondrial DNA (mtDNA) in the cardiac circulation.[135]

Mitochondrial transplantation for rescuing neurons from apoptosis or ferroptosis is now possible and was performed successfully in both animals and humans. Nevertheless, to the best of our knowledge, it has not been attempted as a treatment for mental illness.[136]

Rescuing the mitochondrion using MLR, kaempferol, and berberine is a strategy to prevent GSK-3β overactivation by toxic ceramides, oxysterols, or oxidized phospholipids. Moreover, serotonin reuptake inhibitors (SSRIs) facilitate mitochondrial transfer, emphasizing potential strategies for restoring neurometabolic homeostasis in SMI and neurodegeneration.

6.2. Mitochondrial transfer

Under physiological or pathological conditions, intercellular mitochondrial transfer can occur via tunneling nanotubes (TNTs) or extracellular vesicles (EVs).

Non-canonical mitochondrial transfer can occur through cell–cell fusion, synaptosomes, or dendritic networks. Cell–cell fusion can occur in senescent neurons that reenter the cell cycle but cannot complete replication, remaining indefinitely in a fused state.

Besides its role in the intracellular compartment, a growing body of evidence indicates that under physiological or pathological conditions, mitochondria can be secreted into the extracellular space, where they play a vital role in regulating metabolism or immunity.[137]

Pre-clinical research has shown that mitochondrial transplantation decreases LPS-induced depression, indicating its possible therapeutic application for PTSD or major depressive disorder (MDD).[138] Antidepressant drugs belonging to the SSRI category improve mitochondrial

transfer from astrocytes to neurons, suggesting a non-synaptic antidepressant mechanism.

6.3. Mitochondrial transfer or transplantation for premature cellular senescence

Novel studies have reported that the addition of healthy mitochondria to the system can reverse cellular senescence markers, including β-galactosidase, p21, and p16.[139] Interestingly, the "bad" BDNF was shown to halt mitochondrial transfer from astrocytes to neurons, whereas SSRIs facilitated this process.[137,140]

7. Conclusion

Similar to other neuropsychiatric conditions, PTSD is associated with premature senescence in ECs, including CECs. The levels of BDNF, a component of the detrimental senescent secretome, increase in patients with PTSD and may represent a biomarker. In addition to the "bad" BDNF in SASP, the "good" BDNF promotes brain plasticity, learning, and LTP.

Although there is extensive research on protein alterations in various pathologies, cell membrane lipids remain less scrutinized. The COVID-19 pandemic, with its hijacking of furin and subsequent LPL dysfunction, has completely changed this perspective.

We hypothesize that extracerebral BDNF, released as part of the SASP by ECs, exerts detrimental effects such as LTD, impaired plasticity, and cognitive impairment by interfering with mitochondrial transfer from astrocytes to neurons.

The pandemic has also shed light on cellular proliferation and cancer, reviving interest in inducing malignant cells to activate the senescence program to inhibit cell growth.

Acknowledgments

None.

Funding

None.

Conflict of interest

The authors declare that they have no competing interests.

Author contributions

Conceptualization: Adonis Sfera
Visualization: All authors
Writing – original draft: Jacob J. Anton, Jasper H.C. Luong
Writing – review & editing: Adonis Sfera, Zisis Kozlakidis

Ethics approval and consent to participate

Not applicable.

Consent for publication

Not applicable.

Availability of data

Not applicable.

Further disclosure

Zisis Kozlakidis is identified as a personnel of the International Agency for Research on Cancer/WHO and is responsible for the views expressed in this article, which do not necessarily represent the decisions, policies, or views of the International Agency for Research on Cancer/WHO.

References

1. van der Hart O, Piedfort-Marin O. Amnesia and hypermnesia as a paradigm of non-realization in trauma-related dissociation: Pierre Janet's case of Irène. *Eur J Trauma Dissoc*. 2023;7(4):100357.

   doi: 10.1016/j.ejtd.2023.100357

2. Notaras M, van den Buuse M. Neurobiology of BDNF in fear memory, sensitivity to stress, and stress-related disorders. *Mol Psychiatry*. 2020;25(10):2251-2274.

   doi: 10.1038/s41380-019-0639-2

3. Guo S, Kim WJ, Lok J, *et al*. Neuroprotection via matrix-trophic coupling between cerebral endothelial cells and neurons. *Proc Natl Acad Sci U S A*. 2008;105(21):7582-7587.

   doi: 10.1073/pnas.0801105105

4. El Hayek L, Khalifeh M, Zibara V, *et al*. Lactate mediates the effects of exercise on learning and memory through SIRT1-dependent activation of hippocampal brain-derived neurotrophic factor (BDNF). *J Neurosci*. 2019;39(13):2369-2382.

   doi: 10.1523/JNEUROSCI.1661-18.2019

5. Green CR, Corsi-Travali S, Neumeister A. The role of BDNF-TrkB signaling in the pathogenesis of PTSD. *J Depress Anxiety*. 2013;2013(S4):006.

   doi: 10.4172/2167-1044.S4-006

6. Teng KK, Hempstead BL. Neurotrophins and their receptors: Signaling trios in complex biological systems. *Cell Mol Life Sci*. 2004;61:35-48.

   doi: 10.1007/s00018-003-3099-3

7. Hughes KC, Shin LM. Functional neuroimaging studies of post-traumatic stress disorder. *Expert Rev Neurother*. 2011;11(2):275-285.

   doi: 10.1586/ern.10.198

8. Wang J, Cui Y, Yu Z, *et al*. Brain endothelial cells maintain lactate homeostasis and control adult hippocampal neurogenesis. *Cell Stem Cell*. 2019;25(6):754-767.e9.

doi: 10.1016/j.stem.2019.09.009

9. Zhang Y, Chen K, Sloan SA, *et al*. An RNA-sequencing transcriptome and splicing database of glia, neurons, and vascular cells of the cerebral cortex. *J Neurosci*. 2014;34:11929-11947.

doi: 10.1523/jneurosci.1860-14.2014

10. Wu Y, Hu H, Liu W, *et al*. Hippocampal lactate-infusion enhances spatial memory correlated with monocarboxylate transporter 2 and lactylation. *Brain Sci*. 2024;14:327.

doi: 10.3390/brainsci14040327

11. Kozlakidis Z, Shi P, Abarbanel G, Klein C, Sfera A. Recent developments in protein lactylation in PTSD and CVD: Novel strategies and targets. *BioTech* (*Basel*). 2023;12(2):38.

doi: 10.3390/biotech12020038

12. Quick S, Moss J, Rajani RM, Williams A. A vessel for change: Endothelial dysfunction in cerebral small vessel disease. *Trends Neurosci*. 2021;44(4):289-305.

doi: 10.1016/j.tins.2020.11.003

13. Yousefzadeh MJ, Zhao J, Bukata C, *et al*. Tissue specificity of senescent cell accumulation during physiologic and accelerated aging of mice. *Aging Cell*. 2020;19:e13094.

doi: 10.1111/acel.13094

14. Lehmann ML, Poffenberger CN, Elkahloun AG, Herkenham M. Analysis of cerebrovascular dysfunction caused by chronic social defeat in mice. *Brain Behav Immun*. 2020;88:735-747.

doi: 10.1016/j.bbi.2020.05.030

15. Beristianos MH, Yaffe K, Cohen B, Byers AL. PTSD and risk of incident cardiovascular disease in aging veterans. *Am J Geriatr Psychiatry*. 2016;24(3):192-200.

doi: 10.1016/j.jagp.2014.12.003

16. Rentschler C. From danger to trauma. In: Frosh P, Pinchevski A, editors. *Media Witnessing*. London: Palgrave Macmillan; 2009.

doi: 10.1057/9780230235762_8

17. Zhao Y, Gao X, Bai X, Yao S, Chang YZ, Gao G. The emerging role of furin in neurodegenerative and neuropsychiatric diseases. *Transl Neurodegener*. 2022;11(1):39.

doi: 10.1186/s40035-022-00313-1

18. Yang X, Yang W, McVey DG, *et al*. FURIN expression in vascular endothelial cells is modulated by a coronary artery disease-associated genetic variant and influences monocyte transendothelial migration. *J Am Heart Assoc*. 2020;9(4):e014333.

doi: 10.1161/JAHA.119.014333

19. AbdelMassih AF, Ye J, Kamel A, *et al*. A multicenter consensus: A role of furin in the endothelial tropism in obese patients with COVID-19 infection. *Obes Med*. 2020;19:100281.

doi: 10.1016/j.obmed.2020.100281

20. Anerillas C, Herman AB, Munk R, *et al*. A BDNF-TrkB autocrine loop enhances senescent cell viability. *Nat Commun*. 2022;13(1):6228.

doi: 10.1038/s41467-022-33709-8. Erratum in: *Nat Commun*. 2022;13(1):7540.

21. Farkas CB, Dudás G, Babinszky GC, Földi L. Analysis of the virus SARS-CoV-2 as a potential bioweapon in light of international literature. *Mil Med*. 2023;188(3-4):531-540.

doi: 10.1093/milmed/usac123

22. Thomas, G. Furin at the cutting edge: From protein traffic to embryogenesis and disease. *Nat Rev Mol Cell Biol*. 2002;3:753-766.

doi: 10.1038/nrm934

23. Braun E, Sauter D. Furin-mediated protein processing in infectious diseases and cancer. *Clin Transl Immunology*. 2019;8(8):e1073.

doi: 10.1002/cti2.1073

24. Chourpiliadis C, Zeng Y, Lovik A, *et al*. Metabolic profile and long-term risk of depression, anxiety, and stress-related disorders. *JAMA Netw Open*. 2024;7(4):e244525.

doi: 10.1001/jamanetworkopen.2024.4525

25. Mojtabavi H, Saghazadeh A, van den Heuvel L, Bucker J, Rezaei N. Peripheral blood levels of brain-derived neurotrophic factor in patients with post-traumatic stress disorder (PTSD): A systematic review and meta-analysis. *PLoS One*. 2020;15(11):e0241928.

doi: 10.1371/journal.pone.0241928

26. Sfera A, Osorio C, Rahman L, *et al*. PTSD as an endothelial disease: Insights from COVID-19. *Front Cell Neurosci*. 2021;15:770387.

doi: 10.3389/fncel.2021.770387

27. Wu GWY, Wolkowitz OM, Reus VI, *et al*. Serum brain-derived neurotrophic factor remains elevated after long term follow-up of combat veterans with chronic post-traumatic stress disorder. *Psychoneuroendocrinology*. 2021;134:105360.

doi: 10.1016/j.psyneuen.2021.105360

28. Cho S, Ying F, Sweeney G. Sterile inflammation and the NLRP3 inflammasome in cardiometabolic disease. *Biomed J*. 2023;46(5):100624.

doi: 10.1016/j.bj.2023.100624

29. Perl O, Duek O, Kulkarni KR, *et al*. Neural patterns differentiate traumatic from sad autobiographical memories in PTSD. *Nat Neurosci*. 2023;26(12):2226-2236.

doi: 10.1038/s41593-023-01483-5

30. Iyadurai L, Visser RM, Lau-Zhu A, Porcheret K, Horsch A, Holmes EA, James EL. Intrusive memories of trauma: A target for research bridging cognitive science and

its clinical application. *Clin Psychol Rev*. 2019;69:67-82.

doi: 10.1016/j.cpr.2018.08.005

31. van der Kolk BA. The body keeps the score: Memory and the evolving psychobiology of posttraumatic stress. *Harv Rev Psychiatry*. 1994;1(5):253-265.

doi: 10.3109/10673229409017088

32. Andrews JA, Neises KD. Cells, biomarkers, and post-traumatic stress disorder: Evidence for peripheral involvement in a central disease. *J Neurochem*. 2012;120(1):26-36.

doi: 10.1111/j.1471-4159.2011.07545.x

33. Benedict TM, Keenan PG, Nitz AJ, Moeller-Bertram T. Post-traumatic stress disorder symptoms contribute to worse pain and health outcomes in veterans with PTSD compared to those without: A systematic review with meta-analysis. *Mil Med*. 2020;185(9-10):e1481-e1491.

doi: 10.1093/milmed/usaa052

34. Dussutour A. Learning in single cell organisms. *Biochem Biophys Res Commun*. 2021;564:92-102.

doi: 10.1016/j.bbrc.2021.02.018

35. Cheikhi A, Wallace C, St Croix C, *et al*. Mitochondria are a substrate of cellular memory. *Free Radic Biol Med*. 2019;130:528-541.

doi: 10.1016/j.freeradbiomed.2018.11.028

36. Agnati LF, Zunarelli E, Genedani S, Fuxe K. On the existence of a global molecular network enmeshing the whole central nervous system: Physiological and pathological implications. *Curr Protein Pept Sci*. 2006;7(1):3-15.

doi: 10.2174/138920306775474086

37. Miyamoto T, Razavi S, DeRose R, Inoue T. Synthesizing biomolecule-based Boolean logic gates. *ACS Synth Biol*. 2013;2(2):72-82.

doi: 10.1021/sb3001112

38. Al-Juhani A, Imran M, Aljaili ZK, *et al*. Beyond the pump: A narrative study exploring heart memory. *Cureus*. 2024;16(4):e59385.

doi: 10.7759/cureus.59385

39. Carter B, Khoshnaw L, Simmons M, Hines L, Wolfe B, Liester M. Personality changes associated with organ transplants. *Transplantology*. 2024;5:12-26.

doi: 10.3390/transplantology5010002

40. Feng Y, Shen J, He J, Lu M. Schizophrenia and cell senescence candidate genes screening, machine learning, diagnostic models, and drug prediction. *Front Psychiatry*. 2023;14:1105987.

doi: 10.3389/fpsyt.2023.1105987

41. Solana C, Pereira D, Tarazona R. Early senescence and leukocyte telomere shortening in SCHIZOPHRENIA: A role for cytomegalovirus infection? *Brain Sci*. 2018;8:188.

doi: 10.3390/brainsci8100188

42. Nelson PN, Carnegie PR, Martin J, *et al*. Demystified. Human endogenous retroviruses. *Mol Pathol*. 2003;56(1):11-18.

doi: 10.1136/mp.56.1.11

43. Charvet B, Brunel J, Pierquin J, *et al*. SARS-CoV-2 awakens ancient retroviral genes and the expression of proinflammatory HERV-W envelope protein in COVID-19 patients. *iScience*. 2023;26(5):106604.

doi: 10.1016/j.isci.2023.106604

44. Gholami Barzoki M, Shatizadeh Malekshahi S, Heydarifard Z, *et al*. The important biological roles of Syncytin-1 of human endogenous retrovirus W (HERV-W) and Syncytin-2 of HERV-FRD in the human placenta development. *Mol Biol Rep*. 2023;50:7901-7907.

doi: 10.1007/s11033-023-08658-0

45. Sibarov DA, Tsytsarev V, Volnova A, *et al*. Arc protein, a remnant of ancient retrovirus, forms virus-like particles, which are abundantly generated by neurons during epileptic seizures, and affects epileptic susceptibility in rodent models. *Front Neurol*. 2023;14:1201104.

doi: 10.3389/fneur.2023.1201104

46. Shepherd JD. Arc - An endogenous neuronal retrovirus? *Semin Cell Dev Biol*. 2018;77:73-78.

doi: 10.1016/j.semcdb.2017.09.029

47. Liester MB. Personality changes following heart transplantation: The role of cellular memory. *Med Hypotheses*. 2020;135:109468.

doi: 10.1016/j.mehy.2019.109468

48. Shay JW, Wright WE. Hayflick, his limit, and cellular ageing. *Nat Rev Mol Cell Biol*. 2000;1(1):72-76.

doi: 10.1038/35036093

49. Martín-Fernández M, Aller R, Heredia-Rodríguez M, *et al*. Lipid peroxidation as a hallmark of severity in COVID-19 patients. *Redox Biol*. 2021;48:102181.

doi: 10.1016/j.redox.2021.102181

50. Wertz J, Caspi A, Ambler A, *et al*. Association of history of psychopathology with accelerated aging at midlife. *JAMA Psychiatry*. 2021;78:530-539.

doi: 10.1001/jamapsychiatry.2020.4626

51. Qin S, Schulte BA, Wang GY. Role of senescence induction in cancer treatment. *World J Clin Oncol*. 2018;9(8):180-187.

doi: 10.5306/wjco.v9.i8.180

52. Essalmani R, Jain J, Susan-Resiga D, *et al*. Distinctive roles of Furin and TMPRSS2 in SARS-CoV-2 infectivity. *J Virol*. 2022;96(8):e0012822.

doi: 10.1128/jvi.00128-22. Erratum in: *J Virol.* 2022;96 (13):e0074522.

doi: 10.1128/jvi.00745-22

53. Yuan Y, Ye HQ, Ren QC. Proliferative role of BDNF/TrkB signaling is associated with anoikis resistance in cervical cancer. *Oncol Rep*. 2018;40(2):621-634.

doi: 10.3892/or.2018.6515

54. Pahl A, Wehrle A, Kneis S, Gollhofer A, Bertz H. Feasibility of whole body vibration during intensive chemotherapy in patients with hematological malignancies - a randomized controlled pilot study. *BMC Cancer*. 2018;18(1):920.

doi: 10.1186/s12885-018-4813-8

55. Furukawa S, Nagamatsu A, Nenoi M, *et al*. Space radiation biology for "living in space". *Biomed Res Int.* 2020;2020:4703286.

doi: 10.1155/2020/4703286

56. Antipov VV, Delone NL, Parfyonov GP, Vysotsky VG. Results of biological experiments carried out under conditions of "Vostok" flights with the participation of cosmonauts. *Life Sci Space Res*. 1965;3:215-229.

57. Hu X, Zhang H. Doxorubicin-induced cancer cell senescence shows a time delay effect and is inhibited by epithelial-mesenchymal transition (EMT). *Med Sci Monit*. 2019;25:3617-3623.

doi: 10.12659/MSM.914295

58. Petrova NV, Velichko AK, Razin SV, Kantidze OL. Small molecule compounds that induce cellular senescence. *Aging Cell*. 2016;15:999-1017.

doi: 10.1111/acel.12518

59. Zhu B, Zhao L, Luo D, *et al*. Furin promotes dendritic morphogenesis and learning and memory in transgenic mice. *Cell Mol Life Sci*. 2018;75(13):2473-2488.

doi: 10.1007/s00018-017-2742-3

60. Russell G, Lightman S. The human stress response. *Nat Rev Endocrinol*. 2019;15:525-534.

doi: 10.1038/s41574-019-0228-0

61. Godoy LD, Rossignoli MT, Delfino-Pereira P, Garcia-Cairasco N, de Lima Umeoka EH. A comprehensive overview on stress neurobiology: Basic concepts and clinical implications. *Front Behav Neurosci*. 2018;12:127.

doi: 10.3389/fnbeh.2018.00127

62. Schneiderman N, Ironson G, Siegel SD. Stress and health: Psychological, behavioral, and biological determinants. *Annu Rev Clin Psychol*. 2005;1:607-628.

doi: 10.1146/annurev.clinpsy.1.102803.144141

63. Muscatell KA, Merritt CC, Cohen JR, Chang L, Lindquist KA. The stressed brain: Neural underpinnings of social stress processing in humans. *Curr Top Behav Neurosci*. 2022;54:373-392.

doi: 10.1007/7854_2021_281

64. Bremner JD. Traumatic stress: Effects on the brain. *Dialogues Clin Neurosci*. 2006;8:445-461.

doi: 10.31887/DCNS.2006.8.4/jbremner

65. Hostinar CE, Sullivan RM, Gunnar MR. Psychobiological mechanisms underlying the social buffering of the hypothalamic-pituitary-adrenocortical axis: A review of animal models and human studies across development. *Psychol Bull*. 2014;140:256-282.

doi: 10.1037/a0032671

66. Saha S. Role of the central nucleus of the amygdala in the control of blood pressure: Descending pathways to medullary cardiovascular nuclei. *Clin Exp Pharmacol Physiol*. 2005;32:450-456.

doi: 10.1111/j.1440-1681.2005.04210.x

67. Wellman LL, Forcelli PA, Aguilar BL, Malkova L. Bidirectional control of social behavior by activity within basolateral and central amygdala of primates. *J Neurosci*. 2016;36:8746-8756.

68. Jackson KL, Palma-Rigo K, Nguyen-Huu TP, Davern PJ, Head GA. Major contribution of the medial amygdala to hypertension in BPH/2J genetically hypertensive mice. *Hypertension*. 2014;63:811-818.

doi: 10.1161/HYPERTENSIONAHA.113.02020

69. Jankowski M, Broderick TL, Gutkowska J. The role of oxytocin in cardiovascular protection. *Front Psychol*. 2020;11:2139.

doi: 10.3389/fpsyg.2020.02139

70. Panaro MA, Benameur T, Porro C. Hypothalamic neuropeptide brain protection: Focus on oxytocin. *J Clin Med*. 2020;9(5):1534.

doi: 10.3390/jcm9051534

71. McKay EC, Counts SE. Oxytocin receptor signaling in vascular function and stroke. *Front Neurosci*. 2020;14:574499.

doi: 10.3389/fnins.2020.574499

72. Lorenzetti V, Costafreda SG, Rimmer RM, Rasenick MM, Marangell LB, Fu CHY. Brain-derived neurotrophic factor association with amygdala response in major depressive disorder. *J Affect Disord*. 2020;267:103-106.

doi: 10.1016/j.jad.2020.01.159

73. Marazziti D, Baroni S, Mucci F, *et al*. Relationship between BDNF and oxytocin. *Compr Psychoneuroendocrinol.* 2023;16:100207.

doi: 10.1016/j.cpnec.2023.100207

74. Wichaiyo S, Koonyosying P, Morales NP. Functional roles of furin in cardio-cerebrovascular diseases. *ACS Pharmacol Transl Sci*. 2024;7(3):570-585.

doi: 10.1021/acsptsci.3c00325

75. d'Adda di Fagagna F. Living on a break: Cellular senescence as a DNA-damage response. *Nat Rev Cancer*. 2008;8:512-522.

doi: 10.1038/nrc2440

76. Xin M, Jin X, Cui X, *et al*. Dipeptidyl peptidase-4 inhibition prevents vascular aging in mice under chronic stress: Modulation of oxidative stress and inflammation. *Chem Biol Interact*. 2019;314:108842.

doi: 10.1016/j.cbi.2019.108842

77. Yao BC, Meng LB, Hao ML, Zhang YM, Gong T, Guo ZG. Chronic stress: A critical risk factor for atherosclerosis. *J Int Med Res*. 2019;47(4):1429-1440.

doi: 10.1177/0300060519826820

78. Su S, Xiao Z, Lin Z, Qiu Y, Jin Y, Wang Z. Plasma brain-derived neurotrophic factor levels in patients suffering from post-traumatic stress disorder. *Psychiatry Res*. 2015;229(1-2):365-369.

doi: 10.1016/j.psychres.2015.06.038

79. Lohr JB, Palmer BW, Eidt CA, *et al.* Is post-traumatic stress disorder associated with premature senescence? A review of the literature. *Am J Geriatr Psychiatry.* 2015;23(7):709-725.

doi: 10.1016/j.jagp.2015.04.001

80. Angelucci F, Veverova K, Katonová A, Vyhnalek M, Hort J. Plasminogen activator inhibitor-1 serum levels in frontotemporal lobar degeneration. *J Cell Mol Med*. 2024;28(5):e18013.

doi: 10.1111/jcmm.18013

81. Meselson M, Guillemin J, Hugh-Jones M, *et al*. The Sverdlovsk anthrax outbreak of 1979. *Science*. 1994;266:1202-1208.

doi: 10.1126/science.7973702

82. Fromer M, Roussos P, Sieberts SK, *et al*. Gene expression elucidates functional impact of polygenic risk for schizophrenia. *Nat Neurosci*. 2016;19(11):1442-1453.

doi: 10.1038/nn.4399

83. Yang Y, He M, Tian X, *et al*. Transgenic overexpression of furin increases epileptic susceptibility. *Cell Death Dis.* 2018;9(11):1058.

doi: 10.1038/s41419-018-1076-x

84. Lin L, Zhou XF, Bobrovskaya L. Blockage of p75NTR ameliorates depressive-like behaviours of mice under chronic unpredictable mild stress. *Behav Brain Res*. 2021;396:112905.

doi: 10.1016/j.bbr.2020.112905

85. Moskaliuk VS, Kozhemyakina RV, Khomenko TM, *et al*. On associations between fear-induced aggression, Bdnf transcripts, and serotonin receptors in the brains of Norway Rats: An influence of antiaggressive drug TC-2153. *Int J Mol Sci*. 2023;24(2):983.

doi: 10.3390/ijms24020983

86. Malekan M, Nezamabadi SS, Samami E, Mohebalizadeh M, Saghazadeh A, Rezaei N. BDNF and its signaling in cancer. *J Cancer Res Clin Oncol*. 2023;149(6):2621-2636.

doi: 10.1007/s00432-022-04365-8

87. Cefis M, Chaney R, Quirié A, *et al*. Endothelial cells are an important source of BDNF in rat skeletal muscle. *Sci Rep.* 2022;12:311.

doi: 10.1038/s41598-021-03740-8

88. Hofhansel L, Weidler C, Votinov M, *et al*. Morphology of the criminal brain: gray matter reductions are linked to antisocial behavior in offenders. *Brain Struct Funct*. 2020;225:2017-2028.

doi: 10.1007/s00429-020-02106-6

89. Wei Z, Mahaman YAR, Zhu F, *et al.* GSK-3β and ERK1/2 incongruously act in tau hyperphosphorylation in SPS-induced PTSD rats. *Aging* (*Albany NY*). 2019;11(18):7978-7995.

doi: 10.18632/aging.102303

90. Craddock TJ, Tuszynski JA, Hameroff S. Cytoskeletal signaling: is memory encoded in microtubule lattices by CaMKII phosphorylation? *PLoS Comput Biol*. 2012;8(3):e1002421.

doi: 10.1371/journal.pcbi.1002421

91. Le TH, Oh JM, Rami FZ, Li L, Chun SK, Chung YC. Effects of social defeat stress on microtubule regulating proteins and tubulin polymerization. *Clin Psychopharmacol Neurosci*. 2024;22(1):129-138.

doi: 10.9758/cpn.23.1077

92. Al Abed AS, Ducourneau EG, Bouarab C, Sellami A, Marighetto A, Desmedt A. Preventing and treating PTSD-like memory by trauma contextualization. *Nat Commun*. 2020;11(1):4220.

doi: 10.1038/s41467-020-18002-w

93. Guadagna S, Esiri MM, Williams RJ, Francis PT. Tau phosphorylation in human brain: relationship to behavioral disturbance in dementia. *Neurobiol Aging*. 2012;33(12):2798-806.

doi: 10.1016/j.neurobiolaging.2012.01.015

94. Grube M. Violent behavior in cancer patients--a rarely addressed phenomenon in oncological treatment. *J Interpers Violence*. 2012;27(11):2163-2182.

doi: 10.1177/0886260511431434

95. Niu R, Xue X, Zhao Y, *et al*. Effects of fluoride on microtubule ultrastructure and expression of Tubα1a and Tubβ2a in mouse hippocampus. *Chemosphere*. 2015;139:422-427.

doi: 10.1016/j.chemosphere.2015.07.011

96. Baharikhoob P, Kolla NJ. Microglial dysregulation and

suicidality: A stress-diathesis perspective. *Front Psychiatry*. 2020;11:781.

doi: 10.3389/fpsyt.2020.00781

97. Rodrigues FR, Papanikolaou A, Holeniewska J, Phillips KG, Saleem AB, Solomon SG. Altered low-frequency brain rhythms precede changes in gamma power during tauopathy. *iScience*. 2022;25(10):105232.

doi: 10.1016/j.isci.2022.105232

98. Sfera A, Anton JJ, Imran H, Kozlakidis Z, Klein C, Osorio C. Of soldiers and their ghosts: Are we ready for a review of PTSD evidence? *BioMed*. 2023;3:484-506.

doi: 10.3390/biomed3040039

99. Paul S, Lancaster GI, Meikle PJ. Plasmalogens: A potential therapeutic target for neurodegenerative and cardiometabolic disease. *Prog Lipid Res*. 2019;74:186-195.

doi: 10.1016/j.plipres.2019.04.003

100. Gu J, Chen L, Sun R, *et al*. Plasmalogens eliminate aging-associated synaptic defects and microglia-mediated neuroinflammation in mice. *Front Mol Biosci*. 2022;9:815320.

doi: 10.3389/fmolb.2022.815320

101. Yoon JH, Seo Y, Jo YS, *et al*. Brain lipidomics: From functional landscape to clinical significance. *Sci Adv*. 2022;8(37):eadc9317.

doi: 10.1126/sciadv.adc9317

102. Nicolson GL, Ash ME. Lipid replacement therapy: A natural medicine approach to replacing damaged lipids in cellularmembranes and organelles and restoring function. *Biochim Biophys Acta*. 2014;1838:1657-1679.

doi: 10.1016/j.bbamem.2013.11.010

103. Horn A, Jaiswal JK. Structural and signaling role of lipids in plasma membrane repair. *Curr Top Membr*. 2019;84:67-98.

doi: 10.1016/bs.ctm.2019.07.001

104. An S, Cho SY, Kang J, *et al*. Inhibition of 3-phosphoinositide-dependent protein kinase 1 (PDK1) can revert cellular senescence in human dermal fibroblasts. *Proc Natl Acad Sci U S A*. 2020;117(49):31535-31546.

doi: 10.1073/pnas.1920338117

105. Emamian ES. AKT/GSK3 signaling pathway and schizophrenia. *Front Mol Neurosci*. 2012;5:33.

doi: 10.3389/fnmol.2012.00033

106. Bangar SP, Chaudhary V, Sharma N, Bansal V, Ozogul F, Lorenzo JM. Kaempferol: A flavonoid with wider biological activities and its applications. *Crit Rev Food Sci Nutr*. 2023;63(28):9580-9604.

doi: 10.1080/10408398.2022.2067121

107. Imran M, Salehi B, Sharifi-Rad J, *et al*. Kaempferol: A key emphasis to its anticancer potential. *Molecules*. 2019;24(12):2277.

doi: 10.3390/molecules24122277

108. Calderón-Montaño JM, Burgos-Morón E, Pérez-Guerrero C, López-Lázaro M. A review on the dietary flavonoid kaempferol. *Mini Rev Med Chem*. 2011;11:298-344.

doi: 10.2174/138955711795305335

109. Agnarelli A, Natali M, Garcia-Gil M, *et al*. Cell-specific pattern of berberine pleiotropic effects on different human cell lines. *Sci Rep*. 2018;8:10599.

doi: 10.1038/s41598-018-28952-3

110. Dang Y, An Y, He J, *et al*. Berberine ameliorates cellular senescence and extends the lifespan of mice via regulating p16 and cyclin protein expression. *Aging Cell*. 2020;19(1):e13060.

doi: 10.1111/acel.13060

111. Lee B, Shim I, Lee H, Hahm DH. Berberine alleviates symptoms of anxiety by enhancing dopamine expression in rats with post-traumatic stress disorder. *Korean J Physiol Pharmacol*. 2018;22(2):183-192.

doi: 10.4196/kjpp.2018.22.2.183

112. Wen X, Zhou X, Guo L. Berberine inhibits endothelial cell proliferation via repressing ERK1/2 pathway. *Nat Prod Commun*. 2023;18(3).

doi: 10.1177/1934578X231152690

113. Qattan MY, Khan MI, Alharbi SH, *et al*. Therapeutic importance of kaempferol in the treatment of cancer through the modulation of cell signalling pathways. *Molecules*. 2022;27:8864.

doi: 10.3390/molecules27248864

114. Coskun O, Kanter M, Korkmaz A, Oter S. Quercetin, a flavonoid antioxidant, prevents and protects streptozotocin-induced oxidative stress and beta-cell damage in rat pancreas. *Pharmacol Res*. 2005;51:117-123.

doi: 10.1016/j.phrs.2004.06.002

115. Singh S, Srivastava P. Molecular docking studies of myricetin and its analogues against human PDK-1 kinase as candidate drugs for cancer. *Comput Mol Biosci*. 2015;5:20.

doi: 10.4236/cmb.2015.52004

116. Qin J, Fu M, Wang J, *et al*. PTEN/AKT/mTOR signaling mediates anticancer effects of epigallocatechin-3-gallate in ovarian cancer. *Oncol Rep*. 2020;43:1885-1896.

doi: 10.3892/or.2020.7571

117. Ren J, Yang J, Xu Y, Huang Q, Yang M, Hu K. Lupiwighteone induces cell cycle arrest and apoptosis and activates the Nrf2/ARE pathway in human neuroblastoma cells. *Biomed Pharmacother*. 2015;69:153-161.

doi: 10.1016/j.biopha.2014.11.016

118. Liu X, Yao Z. Chronic over-nutrition and dysregulation of GSK3 in diseases. *Nutr Metab.* 2016;13:49.

doi: 10.1186/s12986-016-0108-8

119. Issinger OG, Guerra B. Phytochemicals in cancer and their effect on the PI3K/AKT-mediated cellular signalling. *Biomed Pharmacother*. 2021;139:111650.

doi: 10.1016/j.biopha.2021.111650

120. Kreft S, Knapp M, Kreft I. Extraction of rutin from buckwheat (*Fagopyrum esculentum* Moench) seeds and determination by capillary electrophoresis. *J Agric Food Chem*. 1999;47:4649-4652.

doi: 10.1021/jf990186p

121. Khan M, Baussan Y, Hebert-Chatelain E. Connecting dots between mitochondrial dysfunction and depression. *Biomolecules.* 2023;13:695.

doi: 10.3390/biom13040695

122. Akbari M, Kirkwood TBL, Bohr VA. Mitochondria in the signaling pathways that control longevity and health span. *Ageing Res Rev*. 2019;54:100940.

doi: 10.1016/j.arr.2019.100940

123. Buettner D, Skemp S. Blue zones: Lessons from the world's longest lived. *Am J Lifestyle Med.* 2016;10(5):318-321.

doi: 10.1177/1559827616637066

124. Ülgen DH, Ruigrok SR, Sandi C. Powering the social brain: Mitochondria in social behaviour. *Curr Opin Neurobiol*. 2023;79:102675.

doi: 10.1016/j.conb.2022.102675

125. Möller M, Du Preez JL, Viljoen FP, Berk M, Emsley R, Harvey BH. Social isolation rearing induces mitochondrial, immunological, neurochemical and behavioural deficits in rats, and is reversed by clozapine or N-acetyl cysteine. *Brain Behav Immun*. 2013;30:156-167.

doi: 10.1016/j.bbi.2012.12.011

126. Trumpff C, Marsland AL, Basualto-Alarcón C, *et al*. Acute psychological stress increases serum circulating cell-free mitochondrial DNA. *Psychoneuroendocrinology*. 2019;106:268-276.

doi: 10.1016/j.psyneuen.2019.03.026

127. Tripathi A, Bartosh A, Whitehead C, *et al*. Activation of cell-free mtDNA-TLR9 signaling mediates chronic stress-induced social behavior deficits. *Mol Psychiatry*. 2023;28:3806-3815.

doi: 10.1038/s41380-023-02189-7

128. Fleshner M, Crane CR. Exosomes, DAMPs and miRNA: Features of stress physiology and immune homeostasis. *Trends Immunol*. 2017;38(10):768-776.

doi: 10.1016/j.it.2017.08.002

129. Hummel EM, Piovesan K, Berg F, *et al*. Mitochondrial DNA as a marker for treatment-response in post-traumatic stress disorder. *Psychoneuroendocrinology*. 2023;148:105993.

doi: 10.1016/j.psyneuen.2022.105993

130. Blalock ZN, Wu GWY, Lindqvist D, *et al*. Circulating cell-free mitochondrial DNA levels and glucocorticoid sensitivity in a cohort of male veterans with and without combat-related PTSD. *Transl Psychiatry*. 2024;14:22.

doi: 10.1038/s41398-023-02721-x

131. Luu M, Visekruna A. Short-chain fatty acids: Bacterial messengers modulating the immunometabolism of T cells. *Eur J Immunol*. 2019;49:842-848.

doi: 10.1002/eji.201848009

132. Clark MA, Shay JW. Mitochondrial transformation of mammalian cells. *Nature*, 1982;295(5850):605-607.

doi: 10.1038/295605a0

133. Gollihue JL, Rabchevsky AG. Prospects for therapeutic mitochondrial transplantation. *Mitochondrion*. 2017;35:70-79.

doi: 10.1016/j.mito.2017.05.007

134. Kubat GB, Ulger O, Akin S. Requirements for successful mitochondrial transplantation. *J Biochem Mol Toxicol*. 2021;35(11):e22898.

doi: 10.1002/jbt.22898

135. Pour PA, Hosseinian S, Kheradvar A. Mitochondrial transplantation in cardiomyocytes: Foundation, methods, and outcomes. *Am J Physiol Cell Physiol*. 2021;321:C489-C503.

doi: 10.1152/ajpcell.00152.2021

136. Chen T, Majerníková NA, Marmolejo-Garza A, *et al*. Mitochondrial transplantation rescues neuronal cells from ferroptosis. *Free Radical Biol Med*. 2023;208:62-72.

doi: 10.1016/j.freeradbiomed.2023.07.034

137. Suh J, Lee YS. Mitochondria as secretory organelles and therapeutic cargos. *Exp Mol Med*. 2024;56:66-85.

doi: 10.1038/s12276-023-01141-7

138. Wang Y, Ni J, Gao C, *et al*. Mitochondrial transplantation attenuates lipopolysaccharide- induced depression-like behaviors. *Prog Neuropsychopharmacol Biol Psychiatry*. 2019;93:240-249.

doi: 10.1016/j.pnpbp.2019.04.010

139. Borcherding N, Brestoff JR. The power and potential of mitochondria transfer. *Nature*. 2023;623(7986):283-291.

doi: 10.1038/s41586-023-06537-z

140. Noh SE, Lee SJ, Lee TG, Park KS, Kim JH. Inhibition of cellular senescence hallmarks by mitochondrial transplantation in senescence-induced ARPE-19 cells. *Neurobiol Aging*. 2023;121:157-165.

doi: 10.1016/j.neurobiolaging.2022.11.003

ACCSCIENCE PUBLISHING

Global Translational Medicine

REVIEW ARTICLE

Sustainable innovations in biomedical materials: A review of eco-friendly synthesis approaches

Narsimha Mamidi[1]* and Jesús Fernando Flores Otero[2]

[1]Wisconsin Center for NanoBiosystems, School of Pharmacy, Wisconsin University-Madison, Wisconsin, United States of America

[2]Department of Chemistry and Nanotechnology, The School of Engineering and Science, Tecnológico de Monterrey, Monterrey, Nuevo Leon, Mexico

Abstract

In recent years, the biomedical field has witnessed significant advancements at the intersection of technology and biology. Metallic, polymeric, and carbonaceous materials have emerged as crucial components in developing and enhancing cutting-edge technologies. The properties of these materials, such as particle size, stability, and surface chemistry, are determined by their synthesis methods, which, in turn, enable specific applications. These materials are primarily synthesized through top-down and bottom-up techniques, each characterized by distinct preparation conditions, precursor materials, and catalytic processes. However, conventional synthesis methods often require substantial energy consumption, hazardous solvents, and non-renewable precursors, leading to environmental concerns and long-term costs. This review aims to provide an overview of the primary approaches and recent efforts to optimize the production and preparation processes of nanomaterials for biomedical applications. It addresses the advantages and limitations of green synthesis methods compared to traditional chemical and physical methods, offering an objective overview of green synthesis. In addition, it provides insights into the pre-clinical and clinical statuses of various nanomaterials. These efforts aim to mitigate the environmental impact of biomedical material synthesis by adopting eco-friendly strategies, such as minimizing energy consumption, utilizing environmentally friendly precursors, and embracing environmentally benign catalytic methodologies, while still leveraging traditional techniques.

Keywords: Green synthesis; Biomedical applications; Nanomaterials; Eco-friendly materials; Carbonaceous materials

***Corresponding author:**
Narsimha Mamidi
(narsimhachem06@gmail.com)

Citation: Mamidi N, Otero JFF. Sustainable innovations in biomedical materials: A review of eco-friendly synthesis approaches. *Global Transl Med*. 2024:3(4):4698. doi: 10.36922/gtm.4698

Received: August 29, 2024

Accepted: October 30, 2024

Published Online: November 28, 2024

1. Introduction

Biomedicine is a multidisciplinary field in the medical realm, featuring biological and technological advances. It encompasses many applications such as drug delivery, tissue engineering, prosthetics, and biotechnology.[1] Metallic materials, ceramics, polymers, cells, and tissue are used in biomedical applications. However, the mechanical, chemical, and biological properties of these materials can be further improved or tuned by changing the size and structure of said materials. Because of this, nanotechnology has been proposed as an approach to control the previously mentioned properties.[2] Nanotechnology is defined as the development of particles, materials, or molecular

structures with dimensions in the nanometer scale (generally with at least one dimension between 1 and 100 nm).[3] Nanomaterials have been useful for applications in dentistry,[4,5] water treatment,[6] drug delivery,[7,8] and food science.[9] The characteristics of these materials such as shape and size can be controlled by changing the conditions in which they are synthesized. In addition, these parameters have an impact on the physical and chemical properties of the material. For instance, Suchomel *et al.*[10] proposed a size-controlled synthesis of Au nanoparticles and evaluated the effect of this characteristic on the catalytic activity of the material.[10] On the other hand, Zhang *et al.*[11] presented a size-tunable synthesis of rhodium nanostructures and subsequently studied their plasmonic properties.

Nanomaterials are generally synthesized through top-down (*e.g.*, milling, laser ablation, etching) and bottom-up (*e.g.*, chemical vapor deposition [CVD], hydrothermal method) approaches with varying conditions of temperature and pressure.[12] However, many of these approaches require the usage of excessive amounts of energy and temperature along with the usage of solvents that are harmful to the environment. Because of this, green synthesis of nanomaterials has been proposed as an alternative to reduce the impact of producing these materials. Green synthesis of materials and nanomaterials is defined as the usage of methods and procedures that intend to reduce or eliminate toxic waste, energy consumption, secondary products, and chemical accidents and, on the other hand, utilize catalysts, renewable resources, and more ecological solvents and precursors.[13-15] Nanomaterials synthesized through green methods exhibit improved antimicrobial activity and improved reducing and stabilizing properties. For instance, Saratale *et al.*[16] demonstrated that varying the amount of bio-reducing agents affects these characteristics in metallic nanoparticles.[16] The main advantages of green synthesis methods over traditional top-down and bottom-up approaches can be seen in the environmental impact they have as they generally do not require toxic solvents (or they can be replaced by less toxic alternatives), use lower synthesis temperatures and pressures (although some of them require specific equipment such as microwave-assisted and laser ablation methods, which require increased amounts of energy) and have a lower carbon footprint overall, as presented by the 12 principles of green chemistry.[17]

In this review, we examine nanomaterials employed for biomedical applications and investigate green approaches to their fabrication. These approaches offer the potential to create sustainable materials while simultaneously controlling biological, chemical, and physical properties by altering their morphology, shape, and size. Finally, we discuss future perspectives and summarize key conclusions.

2. Metallic nanomaterials

Metallic nanomaterial synthesis involves both top-down and bottom-up methods. Researchers more commonly use bottom-up chemical and biological techniques for biomedical applications.[18] These methods typically utilize a metal precursor and a stabilizing agent to prevent nanoparticle agglomeration in an aqueous medium.[19] However, bottom-up methods often require high temperatures or toxic solvents to produce the desired nanomaterial. To address this issue, researchers have proposed green approaches using bioactive components, such as fungi, microorganisms, and plant materials as precursors and natural substances or solvents as stabilizing agents.[20] Figure 1 illustrates the key aspects of these green approaches and some applications of the resulting nanomaterials. The most prominent examples of these nanomaterials for biomedical applications include silver, copper, titanium zinc, and gold nanoparticles (AuNPs).

2.1. Silver nanoparticles (AgNPs)

AgNPs have garnered significant attention in the biomedical field for their potent antibacterial and antimicrobial properties coupled with low toxicity. As depicted in Figure 2,[21] AgNPs find diverse applications in the biomedical realm, including cancer therapy, wound dressings, antibacterial scaffolds, and protective clothing.[22] Green synthesis of these nanomaterials involves the biological reduction of Ag^{+} to Ag^{0} using species or compounds derived from plants or organisms,

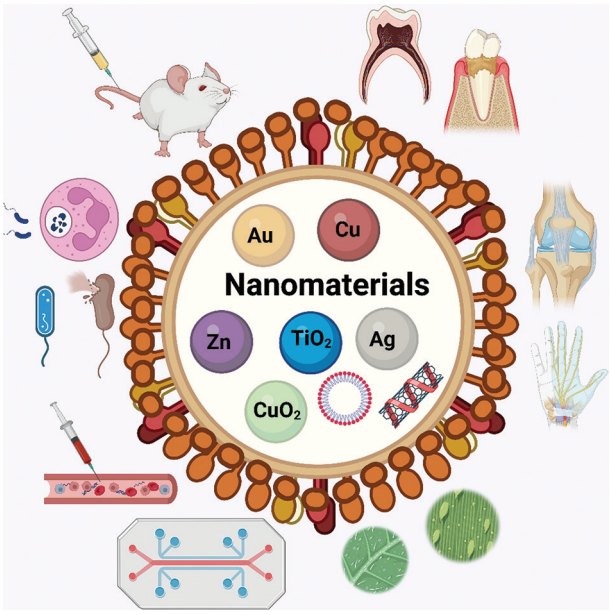

Figure 1. A schematic showing the list of metallic and metallic oxide nanomaterials and their wide range of applications. The figure was created using BioRender (https://www.biorender.com/).

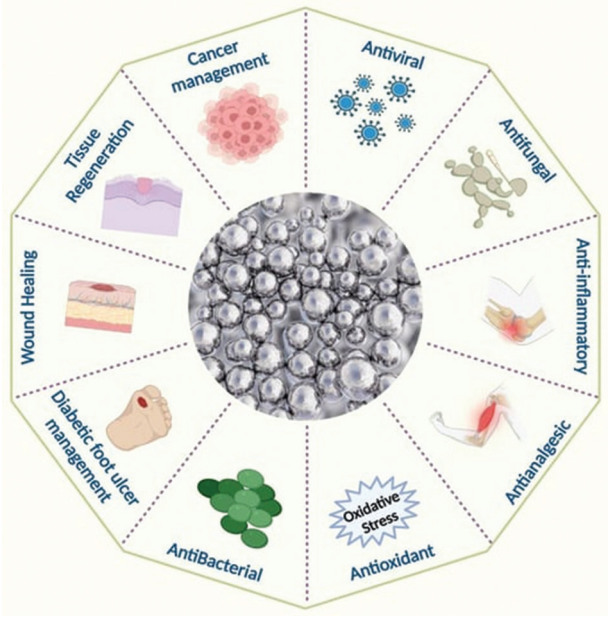

Figure 2. Main biomedical applications of AgNPs. Reproduced from Sabarees *et al.*[21] Copyright © 2022, The Author(s).
Abbreviation: AgNPs: Silver nanoparticles.

such as viruses, microalgae, fungi, yeast, and bacteria. Alternatively, physical methods, such as laser, microwave, and ionizing irradiation can facilitate AgNP synthesis, eliminating the need for chemical reagents.[23,24] However, this comes at the cost of increasing the energy input for a reduced preparation time needed to produce the material, with microwave irradiation requiring between 100 Wh and 400 Wh,[25] laser irradiation 400 – 1500 Wh depending on the laser type[26] and ionization irradiation requiring a comparable amount of energy.

The main parameters that control the antimicrobial activity of AgNPs are size, shape, and colloidal state.[27] Green approaches have been made to synthesize this material while at the same time controlling the previously mentioned properties. Rautela *et al.* proposed a one-step procedure utilizing *Tectona grandis* seed extract and silver nitrate ($AgNO_3$) as the silver precursor. The proposed synthesis produced spherical AgNPs with sizes of 10 – 30 nm.[28] Ashraf *et al.*[29] synthesized AgNPs utilizing $AgNO_3$ as the precursor with aloe vera leaf extract as the solvent and reducing agent. In addition, AgNPs were evaluated against advanced glycation end-products (AGEs), a substance present in diabetes complications, showing an inhibitory effect in said compounds.[29] Regarding physical methods, Seku *et al.*[30] synthesized AgNPs through a microwave-assisted procedure using *Cochlospermum gossypium* as the reducing agent, a naturally abundant polysaccharide component.[30] Although AgNPs are renowned for their antimicrobial activity against many pathogens and green synthesis does increase the biocompatibility of these materials, this activity can also negatively impact human cells and tissues in the long term as noted by Mao *et al.*[31] who presented how the production of reactive oxygen species, which are some of the substances responsible for the antimicrobial effect of AgNPs and can also cause apoptosis, DNA damage, and autophagy in human cells.[31] This also occurs with other types of metallic nanoparticles, such as Cu/CuO,[32] Au[33], and ZnO.[34]

2.2. Copper and copper-based nanoparticles (CuNPs)

CuNPs are common materials in biomedical applications due to their antimicrobial properties and low toxicity.[35] These properties are derived from the metallic ions formed during synthesis, which induce a decrease in the transmembrane electrochemical potential of the bacteria, which consequently causes an integrity loss of the cell membrane leading to oxidative stress and cellular death (Figure 3).[36] Due to this mechanism, CuNPs have been proposed for bone implants, photocatalytic activity,[37] cancer therapy, wound dressings, and oral applications.[38] For example, van Hengel *et al.*[39] implemented CuNPs on TiO_2 implants to prevent implant-associated infections, specifically the ones caused by *Staphylococcus aureus*.[39] In general, the chosen synthesis method may have a more significant impact on specific applications over others. For instance, CuNPs are preferred for wound dressing applications over other metallic nanomaterials as they promote skin regeneration more efficiently.[40] However, this is not the case for surface plasmon resonance (SPR) applications in which Au or AgNPs are preferred.[41] Although the proposal of CuNPs for these and other applications has been studied, the standardization of these is challenging as there is no regulatory framework for nanomaterials since these materials have a wide variety of shapes and sizes that affect their properties, especially their cytotoxicity.

The main approaches to synthesizing Cu and Cu-based nanomaterials consist of chemical methods such as thermal decomposition and chemical reduction methods. Betancourt-Galindo *et al.*[42] synthesized CuNPs using copper chloride, sodium oleate, and phenyl ether as solvent agents, using a temperature of 250°C.[42] Aguilar *et al.*[43] generated Cu NPs through a chemical reduction method at room temperature using sodium borohydride and polyvinylpyrrolidone as reducing and stabilizing agents, respectively.[43] Although the latter described method is generally considered a "greener" approach in contrast with the thermal decomposition method, the usage of a chemical reduction route may cause aggregation of the

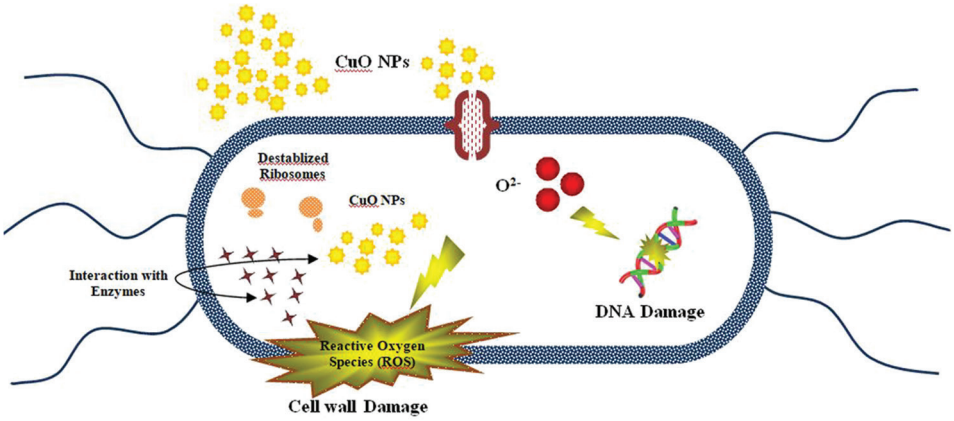

Figure 3. Graphical representation of antibacterial mechanism of copper nanoparticles (CuNPs). Reproduced from Mohsin Ali *et al.*[36] Copyright © 2021, The Author(s).
Abbreviation: CuNPs: Copper nanoparticles.

nanomaterial, which is why the selection of the stabilizing agent is as important as the temperature control in the thermal reduction route.[44]

Along with the usage of a stabilizing agent, the reducing agent is one of the components that determine the main characteristics of the synthesized nanomaterial. One of the most common approaches to making a green solvent consists of the usage of a plant extract. For instance, Mali *et al.*[45] synthesized CuNPs using a *Celastrus paniculatus* Wild. Leaf extract with a particle size of 2 – 10 nm.[45] However, green reducing and stabilizing agents are not limited to plant extracts. Jiménez-Rodríguez *et al.*[46] managed to synthesize Cu_2O nanocubes utilizing starch as a capping agent, which controlled the aggregation and particle size of the material.[46]

2.3. Titanium dioxide nanoparticles

Titanium dioxide is mainly utilized for drug delivery, cell imaging, and biosensors due to its catalytic, photocatalytic, and antibacterial properties, as shown in Figure 4.[47] TiO_2 exists in three forms depending on the crystallographic nature of the material: Anatase, brookite, and rutile.[48] TiO_2 is mainly applied in water purification, energy conversion, and agriculture. For instance, Horváth *et al.*[49] proved the decontamination of water by using a TiO_2 nanowires/carbon nanotubes (CNTs) nanocomposite photocatalytic filter.[49] Gohari *et al.*,[50] on the other hand, evaluated the effect of different concentrations of TiO_2 NPs (0, 50, 100, and 200 mg/L) on agronomic traits of Moldavian balm (*Dracocephalum moldavica* L.).[50]

TiO_2 nanomaterials are usually synthesized through routes such as sol-gel and hydrothermal methods. The sol-gel process usually consists of the transition of a material from a colloidal liquid (sol) into a solid phase (gel).[51] The hydrothermal method consists of the use of an aqueous solution in steel vessels (autoclaves) with controlled temperature and pressure parameters.[52] However, both procedures require the usage of high temperatures, which consequently involve the need for high electrical power input.

To reduce the impact of the production of TiO_2 nanomaterials synthesis, green routes have been proposed mainly utilizing green chemical reduction methods. For instance, Aravind *et al.*[53] used jasmine flower extract as a reducing agent and titanium tetra isopropoxide as a titanium precursor.[53] Sethy *et al.*[54] utilized *Syzygium cumini* extract as a capping agent to produce photocatalytic TiO_2 nanoparticles (TiO_2 NPs) for the removal of lead from water. In addition, the required temperature for synthesis (80°C) is considerably reduced compared to the traditional hydrothermal method (150°C).

2.4. Zinc oxide (ZnO) nanoparticles

Zinc is a trace element that is essential for many enzymes in the human body such as carbonic anhydrase and alcohol dehydrogenase.[55,56] ZnO nanomaterials are some of the most common ZnO materials used in electronic and optical applications due to their semiconducting, optical, and piezoelectric properties.[57] ZnO is also known for its antibacterial activity enabled through interference with the surface and/or core of bacteria.[58] Because of this property, ZnO has been used in ointments for the treatment of injuries throughout centuries, dating back to ancient Egypt.[59] In the current age, the biological and biomedical applications of ZnO include biosensing, anti-inflammatory activity, drug, and gene delivery.

Nanomaterials have attracted interest as platforms for the development of biosensors to detect various

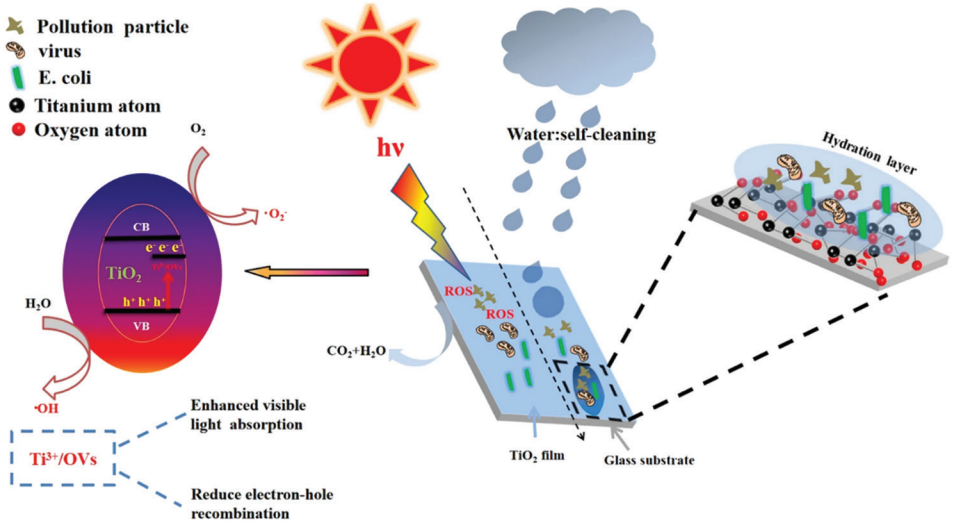

Figure 4. Main biomedical applications of titanium dioxide nanoparticles (TiO_2 NPs). Reproduced from Zhou *et al.*[47] Copyright © 2024, The Author(s). Abbreviations: hv: The function of sunlight represented in photochemical reactions; OVs: Oxygen vacancies.

biomolecules such as enzymes and proteins.[60] For instance, Paltusheva *et al.*[61] prepared a fiber optic-based biosensor coated with ZnO for the detection of the CD44 protein. The inclusion of ZnO nanoparticles (ZnO NPs) allowed for an increase in spectral amplitude and sensitivity to the changes in the refractive index of the analyzed environment.[61] The anti-inflammatory mechanism consists of the inhibition of the inducible nitric oxide synthase (iNOS) enzyme, as seen in Figure 5.[62] On drug and gene delivery, ZnO NPs are generally utilized for the treatment of cancer due to their cytotoxic properties against cancerous cells. Sharma *et al.*[63] prepared doxorubicin-loaded ZnO NPs to evaluate the therapeutic efficacy of the combination of said compound with ZnO, showing an increase in this parameter.[63]

The main green methodologies for the synthesis of ZnO NPs include the sol-gel method and chemical reduction from green extracts. The former consists of using a zinc precursor and sodium hydroxide as a reducing agent to form a suspension (usually in water or methanol) followed by precipitation of the nanoparticles.[64] The latter method generally involves the usage of a green plant extract to reduce a zinc precursor to form a suspension, following a similar principle to that of the sol-gel method.[65] For example, Jayachandran *et al.*[66] proposed a plant-mediated approach using *Cayratia pedata* leaf extract to reduce zinc nitrate hexahydrate, producing ZnO NPs with an average size of approximately 52 nm.[66]

2.5. AuNPs

AuNPs have analogous properties to other metallic nanoparticles such as size and shape-related optoelectronic properties, high surface-to-volume ratio, biocompatibility, and low toxicity.[67,68] However, the key property that allows the implementation of AuNPs in biomedical applications is SPR, a phenomenon where the electrons present on the surface of a metallic material are excited by photons of the incident light, which propagate parallel to the surface of the material.[69] This principle is mainly utilized for the fabrication of SPR sensors for the detection of biomarkers, as shown in Figure 6.[70] This property is determined by the shape of the nanoparticle, classified based on its dimensions as one-dimensional (nanorods, nanowires, nanotubes), two-dimensional (nanoplates), and three-dimensional (nanotadpoles, nanodumbbells). The degree of anisotropy in these structures determines their source of plasmon absorption in the visible and near-infrared regions.[71] The main biomedical applications of AuNPs include biosensing,[72] photothermal, and photodynamic therapy.[73]

The method proposed by Turkevich *et al.*[74] is the most widely used method for the preparation of AuNPs with the previously mentioned variety of shapes and sizes. This method consists of the treatment of hydrogen tetrachloroaurate ($HAuCl_4$) with citric acid in water at boiling temperature. The nucleation of the AuNPs can be controlled by varying the $HAuCl_4$–citric acid ratio, as shown in the study performed by Frens.[75] Green approaches to synthesize this nanomaterial, as with other metallic nanoparticles; aim to replace the reducing agent (citric acid) with a green extract from plants. However, an added advantage of this approach is the reduced preparation temperature, as seen in the work of Li *et al.*,[76] who used a *Mentha longifolia* leaf extract at room temperature with a wet chemistry method to prepare AuNPs

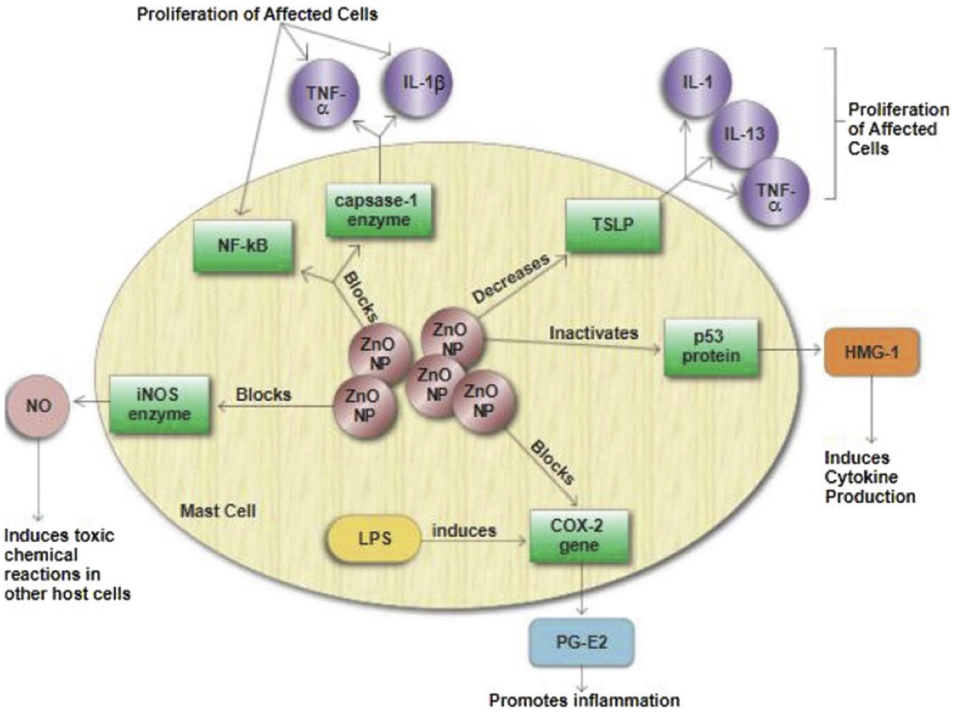

Figure 5. Anti-inflammatory mechanism of ZnO NPs. Reproduced from Agarwal *et al.*[62] Copyright © 2018, Agarwal *et al.*
Abbreviations: COX-2: Cyclooxygenase-2; HMG-1: High-mobility group protein 1; IL: Interleukin; iNOS: Inducible nitric oxide synthase; NO: Nitric oxide; LPS: Lipopolysaccharide; NF-κB: Nuclear factor kappa B; PG-E2: Prostaglandin E2; TNF-α: Tumor necrosis factor alpha; TSLP: Thymic stromal lymphopoietin, ZnO NPs: Zinc oxide nanoparticles.

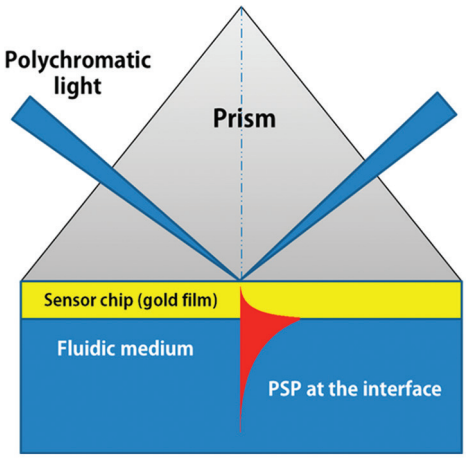

Figure 6. Representation of a Kretschmann-based surface plasmon resonance biosensor. Reproduced from Nguyen *et al.*[70] Copyright © 2015, The Author(s).
Abbreviation: PSP: Propagating surface plasmon.

with an average size of 36 nm. Although the green synthesis of AuNPs presents many environmental advantages, some limitations are present as the standardization of green reducing agents such as plants and bacteria are difficult due to variations in phytochemicals and metabolites, respectively.[77,78] Purification and further characterization of green reducing agents are needed for a method as robust as traditional wet chemistry methods.[79] However, the usage of these green-reducing agents circumvents the need for chemical-reducing agents and stabilizers, which may reduce costs in the production of green AuNPs.[80] In light of this, more studies aiming to standardize green synthesis should be prioritized to advance and promulgate these methods. In addition, novel synthesis methods such as supercritical fluid,[81] electrochemical[82], and ionic liquid-mediated[83] synthesis should be evaluated further to determine their advantages and disadvantages in comparison to both green and traditional synthesis methods. The standardization of innovative synthesis methods for AuNPs requires a multi-disciplinary approach. For example, in biomedical sensing applications, SPR behavior should remain consistent when employing green synthesis approaches, such as those using plant or bacterial extracts. In addition, thorough characterization is essential to define key attributes, such as crystal structure (through X-ray diffraction), size (measured by dynamic light scattering), and morphology (using scanning and transmission microscopy), as well as to assess how different conditions impact these properties. Finally,

while green methods provide a sustainable alternative, traditional synthesis methods remain valuable as their parameters and behaviors often parallel those of green approaches.[84]

2.6. Zeolitic imidazolate framework (ZIF)

Metal-organic frameworks (MOF) are materials formed by metallic ions and organic ligands that possess specific properties such as low density, high surface-to-volume ratio, and porosity. As with other nanomaterials, these properties are controlled by the size and shape of the material, specifically the length, structure, and coordination mode of the organic ligands.[85] ZIF is a subgroup of MOFs with additional physical and chemical properties such as chemical and thermal stability, pore control, and variety in their structure,[86,87] as noted by Park *et al.* who reported 12 types of ZIF materials, with two of them (ZIF-8 and ZIF-11) having high stability of up to 550°C and chemical resistance to boiling water and organic solvents.[88] As with other MOFs, ZIFs are formed by the reaction of transition metals (*e.g.*, Zn, Co, Fe) with organic ligands such as imidazole or imidazole derivatives (Figure 7).[89] For the previously mentioned reaction, the typical synthesis methods are solvothermal and hydrothermal synthesis with a wide range of reaction temperatures (from room temperature up to 200°C) and times (from hours to days). In this instance, solvents such as ethanol and *N, N*-dimethylformamide, or mixtures of organic solvents, which decompose in toxic components and consequently result in risks and pollution for the environment, are utilized.

The formation of ZIF materials can be adapted to follow the principles of green synthesis by the usage of greener solvents, reduced synthesis temperatures, and renewable materials as well as other synthesis methods such as microwave-assisted synthesis[91] and ultrasound-assisted synthesis.[92] Kenyotha *et al.* proposed a water-based synthesis of ZIF-8 with 2-methyl imidazole as a hydrogen bond donor and quaternary ammonium salts as a hydrogen bond acceptor, obtaining a ZIF-8 material with increased CO_2 uptake without the need for a toxic solvent.[93] On lower synthesis temperatures, ZIF-67 films were prepared by Lo *et al.* using ultralow temperature-CVD (ULT CVD) at 140°C under an argon atmosphere, providing a synthesis method suitable for direct application on electronic devices.[94] The main biomedical applications for ZIF materials include drug delivery, antimicrobial activity, biosensors, and imaging. Magnetic Fe_3O_4@ZIF-8 NPs were proposed by Cai *et al.*[95] for the release of norfloxacin through a pH-sensitive mechanism, along with antimicrobial activity against *Escherichia coli*.[95] Studies like this one are necessary to decide the release conditions by MOFs as one of the greatest challenges is the non-uniform drug release, compromising effective drug concentration. In addition, although antimicrobial activity is desirable, long-term damage can occur to human cells as well.[96] Limitations of MOFs can also be seen in biosensing and imaging applications.[97-99] Even though many studies have been conducted on *in vitro* samples, most of them did not report an evaluation of real samples such as urine, blood, or tissues.[100-102] MOFs have potential in the biomedical area but further studies must be carried out for more specific applications.

3. Carbon nanomaterials

3.1. Carbon nanotubes

The first successful synthesis of CNTs was conducted by Iijima[103] through an arc-discharge evaporation method. These nanotubes are classified by their structure as single-walled (SWCNTs), double-walled (DWCNTs), and multi-walled (MWCNTs) carbon nanotubes, as shown in Figure 8.[104] CNTs have been recently introduced in pharmacy and medicine for drugs, biomolecules and gene delivery, tissue regeneration, and biosensors.[105-107]

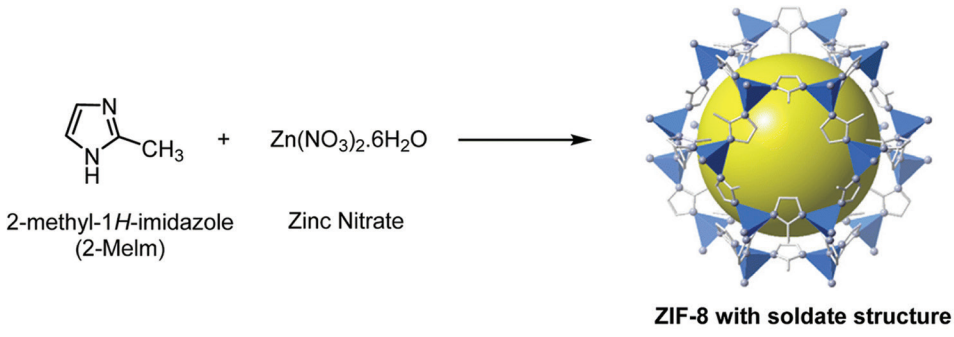

Figure 7. Structure of ZIF-8: Zn (polyhedral), N (sphere), and C (line) obtained from the reaction between 2-Melm and $Zn(NO_3)_2$. Reproduced from Kouhdareh *et al.*[90] Copyright © 2023, The Royal Society of Chemistry.
Abbreviation: ZIF: Zeolitic imidazolate framework.

Qian *et al.* synthesized a CNT gel scaffold for targeted drug delivery and *in vitro* osteogenesis, which resulted in beneficial effects on adipose-derived stem cell activity and osteogenic differentiation.[108] On biosensors, Gupta *et al.* fabricated an electrochemical non-enzymatic glucose sensor based on a set of CNTs microelectrodes. The sensor was evaluated by quantifying glucose in non-diabetic human blood and diabetic patient urine samples.[109]

Carbon nanotubes usually are synthesized by CVD. High-temperature techniques, such as laser ablation[110] or arc discharge,[111] were previously used but have been substituted by CVD methods since the geometric and morphological characteristics can be more accurately controlled at lower temperatures (below 800°C) while also having the option to synthesize other types of nanotubes at higher temperatures. For instance, Chan *et al.*[112] synthesized MWCNTs at 600 °C with a heating rate of 10 °C/min, while Ding *et al.* prepared semiconducting SWCNTs at 920°C.[113]

The main strategies for the green synthesis of CNTs include the usage of greener precursors and catalysts along with the optimization of methodologies to reduce the environmental impact. The Principles of Green Chemistry must be considered when defining the precursors, catalysts, purification, and gas emissions during synthesis.[17] Examples of this include the work of Adeniran and Mokaya who synthesized CNTs using carbon tetrachloride as a precursor and ferrocene/Ni as substrate/catalyst at 180°C, reducing the energy input required for CNTs formation.[114] Tripathi *et al.* used plant extracts as precursors for synthesis using a CVD process at 575°C.[115]

3.2. Graphene and graphene oxide (GO)

Graphene consists uniquely of carbon atoms bound together by sp^2 hybrid bonds to form a honeycomb structure. On the other hand, GO is a layered structure with =O, -OH, -O- and -COOH functional groups attached to the edges of the layer.[116] The oxygen content present in GO may be reduced through chemical or thermal methods to form reduced GO.[113-115] Drug delivery,[117] biosensing,[118,119], and implants[120] are the major applications of GO. Both top-down and bottom-up approaches are used for the preparation of these materials. Top-down approaches consist of separating graphite from graphene layers; however, these methods require high energy in the form of heat or electricity while at the same time offering a low yield.[121] Among the bottom-up approaches, CVD is considered one of the most efficient, offering high quality and yield. In addition, this method allows the formation of graphene directly on the desired surface, as shown in the work of Xu *et al.*, who deposited graphene on a thin metallic surface.[122] Graphene and its derivatives, such as GO and reduced GO (rGO), have gained significant research interest due to their exceptional properties and advancements in synthesis methods, making them readily available for various applications (Figure 9).[123]

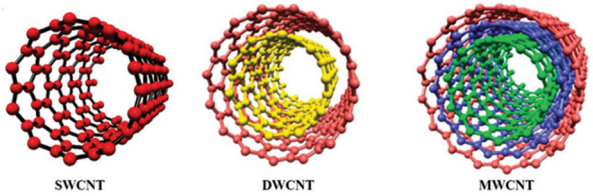

Figure 8. Schematic representation of single-walled (SWCNT), double-walled (DWCNT), and multi-walled carbon nanotube (MWCNT). Reproduced from Patil *et al.*[104] Copyright © 2021, The Author(s).

Pure graphene green synthesis is generally limited to the usage of relatively high temperatures (over 100°C) compared to its previously mentioned derivatives, as shown in the work of Gürünlü *et al.*,[124] who prepared graphene from flake graphite using salts at 500°C, and Bindumadhavan *et al.*, who prepared graphene from GO at 100°C using a wet chemistry approach.[125] As with graphene, the preparation of GO requires a high energy input and earlier preparation of pure graphene for oxidation. Greener methods are more common in the preparation of reduced GO from graphene. Similar to metallic nanomaterials, green extracts can be used to prepare rGO materials. For example, Meka Chufa *et al.* prepared rGO using a *Vernonia amygdalina* extract through a green wet chemistry approach requiring a relatively low temperature (50°C).[126]

4. Liposomes

Liposomes are lipid-based vesicles that have gained significant attention in biomedical research due to their unique properties and versatility in various applications. They consist of a lipid bilayer structure, such as cell membranes, enclosing an aqueous core. This composition allows liposomes to encapsulate hydrophilic substances within their core and incorporate hydrophobic compounds within the lipid bilayer.[127,128] Figure 10 shows the general structure of a liposome and its different biomedical applications.[129]

They have been extensively used in biomedical applications as follows:

a) *Drug delivery.* Liposomes have been extensively explored as drug-delivery vehicles. They can encapsulate drugs within their aqueous core or lipid bilayer and efficiently transport them to specific target sites in the body. Liposomes can improve the pharmacokinetics and biodistribution of drugs, enhance their stability, and enable controlled release, resulting in improved therapeutic efficacy and reduced side effects.

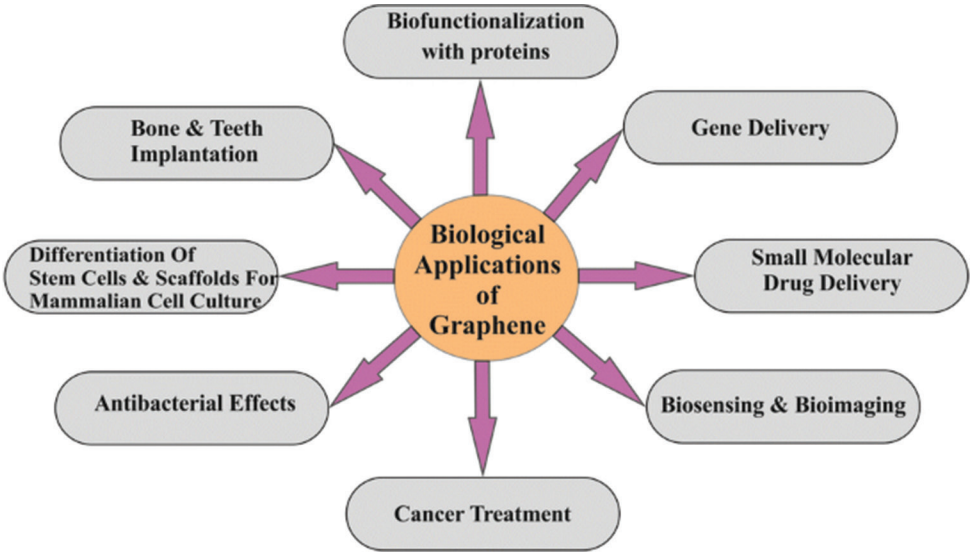

Figure 9. Schematic representation of biomedical applications of graphene. Reproduced from Priyadarsini *et al.*[123] Copyright © 2018, The Author(s).

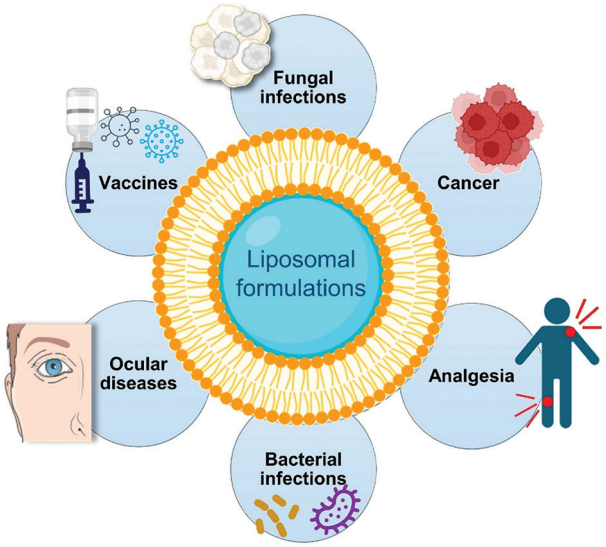

Figure 10. Different biomedical applications of liposomes. Reproduced from Luiz *et al.*[129] Copyright © 2023, The Author(s).

b) *Gene delivery.* Liposomes offer a promising approach for delivering genetic material, such as DNA or RNA, into cells for gene therapy or genetic research. Cationic liposomes can interact with negatively charged nucleic acids, forming lipoplexes that can be taken up by cells. Liposomes protect the genetic material from degradation and ease its intracellular delivery, allowing for potential gene editing or gene expression modulation.

c) *Vaccines.* Liposomes have been used in vaccine development to enhance immune responses. They can encapsulate antigens or adjuvants, mimicking pathogens and helping antigen presentation to immune cells. Liposomal vaccines can improve the stability and immunogenicity of antigens, leading to better immune system activation and potentially more effective protection against infectious diseases.

d) *Imaging.* Liposomes can be functionalized with imaging agents, such as fluorescent dyes or contrast agents, for various imaging techniques, including optical imaging, magnetic resonance imaging (MRI), and positron emission tomography (PET). These liposomal formulations can enable targeted imaging of specific tissues or cells, aiding in disease diagnosis and monitoring treatment response.

e) *Theranostics.* Liposomes can combine therapeutic and diagnostic functionalities, creating theranostic platforms. By incorporating both therapeutic agents and imaging agents within the same liposomal formulation, these systems can simultaneously deliver therapy to target sites while providing real-time imaging to monitor treatment efficacy. Thus, it is worth noting that liposome technology is continuously evolving, and ongoing research aims to enhance their stability, improve targeting strategies, and explore novel applications in areas such as cancer treatment, infectious diseases, and regenerative medicine. Liposome preparation methods follow the same concept: emulsification of lipids in an aqueous medium. These methods include the thin-film method, which consists of the formation of a thin film of lipids in a rotary evaporator flask followed by hydration and removal of layer;[130] the pro-liposome method

Table 1. List of nanomaterials utilized for pre-clinical and clinical applications

Material	Method	Studied application	Material size	References
TiO_2 NPs	Chemical reduction method with jasmine flower extract	Antibacterial, anti-inflammatory, anti-fungal and anti-microbial activities	32 – 48 nm	53
CuO NPs	Chemical reduction method with plant extract (*Achillea millefolium* leaf)	Antibacterial activity against *Staphylococcus aureus, Mycobacterium tuberculosis, Escherichia coli, Klebsiella pneumoniae, Proteus mirabili, Corynebacterium diphtheriae and Streptococcus pyogenes*, and antifungal activity against *Candida albicans, Aspergillus flavus, Microsporum canis* and *Candida glabrata*	28 nm	135
ZnO NPs	Chemical reduction method with fruit extract (*Myristica fragrans*)	Antibacterial activity against *K. pneumoniae*, *E. coli*, *etc.*; antidiabetic activity; cancer treatment	43.3 – 83.1 nm	136
Fe_2O_3 NPs	Chemical reduction method with Sageretia thea extract	Antimicrobial activity, enzyme inhibition, and antioxidant activity	29 nm	137
PU/GNp nanocomposite	*In situ* polymerization with poly(ε–caprolactone)diol and hexamethylene diisocyanate (HDI)	Biocompatibility study through MTT assay	35 – 56 nm (GNp)	138
AgNPs	Chemical reduction method with *Cucumis prophetarum* extract	Antibacterial activity against *S. aureus* (Gram-positive) and *Salmonella typhi* (Gram-negative) bacteria, and antiproliferative activity against cancer cells	90 nm	139
Carbon dots	Chemical oxidation of graphene oxide and carbon nanoonions	Fluorescent properties for biosensing and bioimaging applications	3.0 – 6.4 nm	140
SWCNTs	Purified SWCNTs with HNO_3 and purified water. Functionalized with curcumin through solvent evaporation	Curcumin delivery system and environmental applications	170.4 nm	141
ZIF-8@Fe_3O_4/NAD^+ENF MOF	Functionalization of Fe_3O_4 NPs with 4-carboxyphenylboronic acid	Enzymatic cascade biotransformations	~20 nm	142

Abbreviations: GNp: Graphene nanoplatelet; MOF: Metal-organic framework; NPs: Nanoparticles; PU: Polyurethane; SWCNTs: Single-walled carbon nanotubes; ZIF: Zeolitic imidazolate framework.

consists of dissolving lipids in water and ethanol at 60°C to create a lipid paste, which is then hydrated with water;[131] and injection methods performed by injecting the lipid suspension in water.[132]

The optimization of these methods through green approaches mainly focuses on reducing the formation temperature of liposomes and using green sources for the lipids utilized. For instance, Hou *et al.* managed to produce liposomes at a relatively low temperature (35°C) by using a vacuum-rotatory evaporation.[133] A similar technique was used by Siyadatpanah *et al.* by preparing liposomes at 45°C through a vacuum evaporation method.[134] However, both works use chloroform for liposome formation, a toxic non-green solvent.

5. Pre-clinical and clinical status of different nanomaterials

As mentioned in earlier sections of this review, nanomaterials are becoming more common in the biomedical field for clinical applications. Furthermore, in some instances, these materials can be prepared or synthesized through sustainable and green methodologies without sacrificing their physicochemical and biological properties. Table 1 presents a list of pre-clinical applications of different eco-friendly nanomaterials.[53,134-141]

In recent research, various nanoparticles have been synthesized using eco-friendly plant extracts and functionalized polymers for targeted applications in biomedicine and environmental science. TiO_2 NPs, produced through chemical reduction with jasmine flower extract, have demonstrated antibacterial, anti-inflammatory, antifungal, and antimicrobial activities, with particle sizes ranging from 32 to 48 nm.[53] Similarly, CuO NPs synthesized using *Achillea millefolium* leaf extract exhibits potent antibacterial effects against pathogens such as *S. aureus* and *M. tuberculosis*, along with antifungal properties, at an average size of 28 nm.[134] ZnO NPs, created with *Myristica fragrans* fruit extract, have shown promise in antibacterial and antidiabetic applications and even

cancer treatment, with sizes ranging between 43.3 and 83.1 nm.[135] Meanwhile, Fe_2O_3 NPs derived from *Sageretia thea* extract exhibit antimicrobial, enzyme inhibition, and antioxidant activities at a size of 29 nm.[136] Polyurethane/graphene nanoplatelet (PU/GNp) nanocomposites, synthesized by *in situ* polymerization, were tested for biocompatibility through MTT assays, with GNp sizes ranging from 35 to 56 nm.[137] Ag NPs from *Cucumis prophetarum* extract demonstrated antibacterial and antiproliferative activities against *S. aureus* and *Salmonella typhi*, with a size of 90 nm.[138] Carbon dots produced through the chemical oxidation of GO and carbon nano-onions offer fluorescent properties suitable for biosensing and bioimaging, sized between 3 and 6.4 nm.[139] SWCNTs functionalized with curcumin through solvent evaporation serve as a curcumin delivery system, with additional environmental applications and an approximate size of 170.4 nm.[140] Finally, ZIF-8@Fe_3O_4/NAD^+ENF MOF was used for enzymatic cascade biotransformations.[141]

6. Future perspectives

Green synthesis methods for nanomaterials often involve extracting the desired material from a precursor similar to traditional approaches. However, these green techniques typically yield lower outputs than conventional methods, and it remains challenging to fully optimize each methodological aspect to ensure a wholly sustainable approach. In addition, traditional wet chemistry methods employ a continuous production process that aligns well with scalable industrial applications, whereas green synthesis is usually conducted in batch processes, posing scalability limitations. Advancing green synthesis will require further research to develop methodologies that enhance efficiency and effectiveness, reduce environmental impact, and maintain high performance. This research should extend beyond the nanomaterials covered in this article to include ceramic nanoparticles, other MOFs, and lipid-based, and polymeric nanoparticles, which could also benefit from the methods discussed here.

7. Conclusions

The methods employed for the synthesis of nanomaterials have traditionally had negative impacts on the environment; however, they can be fine-tuned to produce comparable results while minimizing their environmental impact. The physical and chemical properties of the nanomaterials presented for biomedical applications, as well as their synthesis methods, can be manipulated to control their behavior and activity. Despite the potential benefits of green synthesis, it stays challenging with limitations such as low yield and difficulties in extracting raw materials from natural sources. To fully realize the potential of green synthesis methods, these challenges must be addressed, and efforts must be made to establish these methods as standard procedures.

Acknowledgments

The authors gratefully acknowledge Tecnologico de Monterrey, Consejo Nacional de Ciencia y Tecnología de México (CONACYT), and Sistema Nacional de Investigadores (SNI). Narsimha Mamidi acknowledges the University of Wisconisn-Madison, USA.

Funding

None.

Conflict of interest

Narsimha Mamidi is an Editorial Board Member of this journal but was not in any way involved in the editorial and peer-review process conducted for this paper, directly or indirectly. Separately, other authors declared that they have no known competing financial interests or personal relationships that could have influenced the work reported in this paper.

Author contributions

Conceptualization: Narsimha Mamidi
Writing – original draft: All authors
Writing – review & editing: Narsimha Mamidi

Ethics approval and consent to participate

Not applicable.

Consent for publication

Not applicable.

Availability of data

Not applicable.

References

1. Ghadi R, Jain A, Khan W, Domb AJ. In: Ågren MS, editor. *Microparticulate Polymers and Hydrogels for Wound Healing*. Ch. 10. United Kingdom: Woodhead Publishing; 2016. p. 203-25.

   doi: 10.1016/B978-1-78242-456-7.00010-6

2. McNamara K, Tofail SA. Nanoparticles in biomedical applications. *Adv Phys*. 2017;2(1):54-88.

   doi: 10.1080/23746149.2016.1254570

3. Hyman P. Bacteriophages and nanostructured materials. In: Laskin AI, Sariaslani S, Gadd GM, editors. In: *Advances in Applied Microbiology*. Ch. 3. United States: Academic Press; 2012. p. 55-73.

doi: 10.1016/B978-0-12-394805-2.00003-8

4. Mamidi N, Flores Otero JF. Metallic and carbonaceous nanoparticles for dentistry applications. *Curr Opin Biomed Eng*. 2023;25:100436.

doi: 10.1016/j.cobme.2022.100436

5. Mamidi N, García RG, Martínez JDH, *et al*. Recent advances in designing fibrous biomaterials for the domain of biomedical. Clinical, and environmental applications. *ACS Biomater Sci Eng*. 2022;8(9):3690-3716.

doi: 10.1021/acsbiomaterials.2c00786

6. Mamidi N, Delgadillo RMV, Sustaita AO, Lozano K, Yallapu MM. Current nanocomposite advances for biomedical and environmental application diversity. *Med Res Rev*. 2024;44:1-53.

doi: 10.1002/med.22082

7. Mamidi N, Zuníga AE, Villela-Castrejón J. Engineering and evaluation of forcespun functionalized carbon nano-onions reinforced poly (ε-caprolactone) composite nanofibers for pH-responsive drug release. *Mater Sci Eng C Mater Biol Appl*. 2020;112:110928.

doi: 10.1016/j.msec.2020.110928

8. Mamidi N, De Silva FF, Vacas AB, *et al*. Multifaceted hydrogel scaffolds: Bridging the gap between biomedical needs and environmental sustainability. *Adv Healthc Mater*. 2024;13(27):e2401195.

doi: 10.1002/adhm.202401195

9. Morris VJ. In: Motarjemi YB, editor. *Food Technologies: Nanotechnology and Food Safety*. Waltham: Academic Press; 2014. p. 208-210.

doi: 10.1016/B978-0-12-378612-8.00277-8

10. Suchomel P, Kvitek L, Prucek R, *et al*. Simple size-controlled synthesis of Au nanoparticles and their size-dependent catalytic activity. *Sci Rep*. 2018;8(1):4589.

doi: 10.1038/s41598-018-22976-5

11. Zhang X, Li P, Barreda Á, *et al*. Size-tunable rhodium nanostructures for wavelength-tunable ultraviolet plasmonics. *Nanoscale Horiz*. 2016;1(1):75-80.

doi: 10.1039/C5NH00062A

12. Baig N, Kammakakam I, Falath W. Nanomaterials: A review of synthesis methods, properties, recent progress, and challenges. *Mater Adv*. 2021;2(6):1821-1871.

doi: 10.1039/D0MA00807A

13. Bedlovičová Z. Green synthesis of silver nanoparticles using actinomycetes. In: Abd-Elsalam KA, Prasad R, editors. *Nanobiotechnology for Plant Protection*. Ch. 21. Netherlands: Elsevier; 2022. p. 47-69.

doi: 10.1016/B978-0-12-824508-8.00001-0

14. Britto-Hurtado R, Cortez-Valadez M. Green synthesis approaches for metallic and carbon nanostructures. In: Shanker U, Hussain CM, Rani M, editors. *Micro and Nano Technologies*. Netherlands: Elsevier; 2022. p. 83-127.

doi: 10.1016/B978-0-12-823137-1.00002-6

15. Tabassum Z, Mohan A, Mamidi N, *et al*. Recent trends in nanocomposite packaging films utilising waste generated biopolymers: Industrial symbiosis and its implication in sustainability. *IET Nanobiotechnol*. 2023;17(3):127-153.

doi: 10.1049/nbt2.12122

16. Saratale RG, Karuppusamy I, Saratale GD, *et al*. A comprehensive review on green nanomaterials using biological systems: Recent perception and their future applications. *Colloids Surf B Biointerfaces*. 2018;170:20-35.

doi: 10.1016/j.colsurfb.2018.05.045

17. Anastas PT, Warner JC. *Green Chemistry: Theory and Practice*. Oxford University Press; 2000.

doi: 10.1093/oso/9780198506980.001.0001

18. Das RK, Pachapur VL, Lonappan L, *et al*. Biological synthesis of metallic nanoparticles: Plants, animals and microbial aspects. *Nanotechnol Environ Eng*. 2017;2(1):18.

doi: 10.1007/s41204-017-0029-4

19. Ahmad F, Ashraf N, Ashraf T, Zhou RB, Yin DC. Biological synthesis of metallic nanoparticles (MNPs) by plants and microbes: Their cellular uptake, biocompatibility, and biomedical applications. *Appl Microbiol Biotechnol*. 2019;103:2913-2935.

doi: 10.1007/s00253-019-09675-5

20. Zhang D, Ma XL, Gu Y, Huang H, Zhang GW. Green synthesis of metallic nanoparticles and their potential applications to treat cancer. *Front Chem*. 2020;8:799.

doi: 10.3389/fchem.2020.00799

21. Sabarees G, Velmurugan V, Tamilarasi GP, Alagarsamy V, Raja Solomon V. Recent advances in silver nanoparticles containing nanofibers for chronic wound management. *Polymers* (*Basel*). 2022;14(19):3994.

doi: 10.3390/polym14193994

22. Gudikandula K, Vadapally P, Singara Charya MA. Biogenic synthesis of silver nanoparticles from white rot fungi: Their characterization and antibacterial studies. *OpenNano*. 2017;2:64-78.

doi: 10.1016/j.onano.2017.07.002

23. Kaabipour S, Hemmati S. A review on the green and sustainable synthesis of silver nanoparticles and one-dimensional silver nanostructures. *Beilstein J Nanotechnol*. 2021;12:102-136.

doi: 10.3762/bjnano.12.9

24. Sana SS, Hou T, Li H, *et al*. Crude polysaccharide produces silver nanoparticles with inherent

antioxidant and antibacterial activity. *ChemistrySelect*. 2023;8(18):e202203658.

doi: 10.1002/slct.202203658

25. Barreto GP, Morales G, Quintanilla MLL. Microwave assisted synthesis of ZnO nanoparticles: Effect of precursor reagents, temperature, irradiation time, and additives on Nano-ZnO morphology development. *J Mater*. 2013;2013(1):478681.

doi: 10.1155/2013/478681

26. Streubel R, Barcikowski S, Gökce B. Continuous multigram nanoparticle synthesis by high-power, high-repetition-rate ultrafast laser ablation in liquids. *Opt Lett*. 2016;41(7):1486-1489.

doi: 10.1364/OL.41.001486

27. Ghiuță I, Cristea D, Croitoru C, *et al*. Characterization and antimicrobial activity of silver nanoparticles, biosynthesized using *Bacillus* species. *Appl Surf Sci*. 2018;438:66-73.

doi: 10.1016/j.apsusc.2017.09.163

28. Rautela A, Rani J, Debnath (Das) M. Green synthesis of silver nanoparticles from *Tectona grandis* seeds extract: Characterization and mechanism of antimicrobial action on different microorganisms. *J Anal Sci Technol*. 2019;10(1):5.

doi: 10.1186/s40543-018-0163-z

29. Ashraf JM, Ansari MA, Khan HM, Alzohairy MA, Choi I. Green synthesis of silver nanoparticles and characterization of their inhibitory effects on AGEs formation using biophysical techniques. *Sci Rep*. 2016;6(1):20414.

doi: 10.1038/srep20414

30. Seku K, Gangapuram BR, Pejjai B, Kadimpati KK, Golla N. Microwave-assisted synthesis of silver nanoparticles and their application in catalytic, antibacterial and antioxidant activities. *J Nanostructure Chem*. 2018;8(2):179-188.

doi: 10.1007/s40097-018-0264-7

31. Mao BH, Chen ZY, Wang YJ, Yan SJ. Silver nanoparticles have lethal and sublethal adverse effects on development and longevity by inducing ROS-mediated stress responses. *Sci Rep*. 2018;8(1):2445.

doi: 10.1038/s41598-018-20728-z

32. Moschini E, Colombo G, Chirico G, Capitani G, Dalle-Donne I, Mantecca P. Biological mechanism of cell oxidative stress and death during short-term exposure to nano CuO. *Sci Rep*. 2023;13(1):2326.

doi: 10.1038/s41598-023-28958-6

33. Niżnik Ł, Noga M, Kobylarz D, *et al*. Gold nanoparticles (AuNPs)-toxicity, safety and green synthesis: A critical review. *Int J Mol Sci*. 2024;25(7):4057.

doi: 10.3390/ijms25074057

34. Nagar V, Singh T, Tiwari Y, *et al*. ZnO Nanoparticles: Exposure, toxicity mechanism and assessment. *Mater Today Proc*. 2022;69:56-63.

doi: 10.1016/j.matpr.2022.09.001

35. O'Gorman J, Humphreys H. Application of copper to prevent and control infection. Where are we now? *J Hosp Infect*. 2012;81(4):217-223.

doi: 10.1016/j.jhin.2012.05.009

36. Ali M, Ijaz M, Ikram M, Ul-Hamid A, Avais M, Anjum AA. Biogenic synthesis, characterization and antibacterial potential evaluation of copper oxide nanoparticles against *Escherichia coli*. *Nanoscale Res Lett*. 2021;16(1):148.

doi: 10.1186/s11671-021-03605-z

37. Usman M, Ahmed A, Yu B, Peng Q, Shen Y, Cong H. Photocatalytic potential of bio-engineered copper nanoparticles synthesized from *Ficus carica* extract for the degradation of toxic organic dye from waste water: Growth mechanism and study of parameter affecting the degradation performance. *Mater Res Bull*. 2019;120:110583.

doi: 10.1016/j.materresbull.2019.110583

38. Xu VW, Nizami MZI, Yin IX, Yu OY, Lung CYK, Chu CH. Application of copper nanoparticles in dentistry. *Nanomaterials* (*Basel*). 2022;12(5):805.

doi: 10.3390/nano12050805

39. Van Hengel IAJ, Tierolf MWAM, Valerio VPM, *et al*. Self-defending additively manufactured bone implants bearing silver and copper nanoparticles. *J Mater Chem B*. 2020;8(8):1589-1602.

doi: 10.1039/C9TB02434D

40. Sandoval C, Ríos G, Sepúlveda N, Salvo J, Souza-Mello V, Farías J. Effectiveness of copper nanoparticles in wound healing process using *in vivo* and *in vitro* studies: A systematic review. *Pharmaceutics*. 2022;14(9):1838.

doi: 10.3390/pharmaceutics14091838

41. Liu R, Zhan D, Wang D, *et al*. Surface plasmon resonance effect of noble metal (Ag and Au) nanoparticles on BiVO4 for photoelectrochemical water splitting. *Inorganics* (*Basel*). 2023;11(5):206.

doi: 10.3390/inorganics11050206

42. Betancourt-Galindo R, Reyes-Rodriguez PY, Puente-Urbina BA, *et al*. Synthesis of copper nanoparticles by thermal decomposition and their antimicrobial properties. *J Nanomater*. 2014;2014:980545.

doi: 10.1155/2014/980545

43. Aguilar MS, Esparza R, Rosas G. Synthesis of Cu nanoparticles by chemical reduction method. *Trans Nonferrous Met Soc China*. 2019;29(7):1510-1515.

doi: 10.1016/S1003-6326(19)65058-2

44. Suri S, Ruan G, Winter J, Schmidt CE. Microparticles and nanoparticles. In: Ratner BD, Hoffman AS, Schoen FJ,

Lemons JE, editors. *Biomaterials Science: An Introduction to Materials*. 3rd ed., Ch. I.2.19. United States: Academic Press; 2013. p. 360-388.

doi: 10.1016/B978-0-08-087780-8.00034-6

45. Mali SC, Dhaka A, Githala CK, Trivedi R. Green synthesis of copper nanoparticles using *Celastrus paniculatus* Willd. leaf extract and their photocatalytic and antifungal properties. *Biotechnol Rep (Amst)*. 2020;27:e00518.

doi: 10.1016/j.btre.2020.e00518

46. Jiménez-Rodríguez A, Sotelo E, Martínez L, *et al*. Green synthesis of starch-capped Cu_2O nanocubes and their application in the direct electrochemical detection of glucose. *RSC Adv*. 2021;11(23):13711-13721.

doi: 10.1039/D0RA10054D

47. Zhou M, Zhang X, Quan Y, Tian Y, Chen J, Li L. Visible light-induced photocatalytic and antibacterial adhesion properties of superhydrophilic TiO_2 nanoparticles. *Sci Rep*. 2024;14(1):7940.

doi: 10.1038/s41598-024-58660-0

48. Oi LE, Yee C, Lee H, Ong HC, Abd Hamid SB, Juan JC. Recent advances of titanium dioxide (TiO_2) for green organic synthesis. *RSC Adv*. 2016;6:108741-54.

doi: 10.1039/C6RA22894A

49. Horváth E, Gabathuler J, Bourdiec G, *et al*. Solar water purification with photocatalytic nanocomposite filter based on TiO_2 nanowires and carbon nanotubes. *NPJ Clean Water*. 2022;5(1):10.

doi: 10.1038/s41545-022-00157-2

50. Gohari G, Mohammadi A, Akbari A, *et al*. Titanium dioxide nanoparticles (TiO2 NPs) promote growth and ameliorate salinity stress effects on essential oil profile and biochemical attributes of *Dracocephalum moldavica*. *Sci Rep*. 2020;10(1):912.

doi: 10.1038/s41598-020-57794-1

51. Ullattil S, Periyat P. *Sol-Gel Synthesis of Titanium Dioxide*. Cham: Springer; 2017. p. 271-283.

doi: 10.1007/978-3-319-50144-4_9

52. Keerthana BGT, Solaiyammal T, Muniyappan S, Murugakoothan P. Hydrothermal synthesis and characterization of TiO_2 nanostructures prepared using different solvents. *Mater Lett*. 2018;220:20-23.

doi: 10.1016/j.matlet.2018.02.119

53. Aravind M, Amalanathan M, Mary MSM. Synthesis of TiO_2 nanoparticles by chemical and green synthesis methods and their multifaceted properties. *SN Appl Sci*. 2021;3(4):409.

doi: 10.1007/s42452-021-04281-5

54. Sethy NK, Arif Z, Mishra PK, Kumar P. Green synthesis of TiO_2 nanoparticles from *Syzygium cumini* extract for photo-catalytic removal of lead (Pb) in explosive industrial wastewater. *Green Process Synth*. 2020;9(1):171-181.

doi: 10.1515/gps-2020-0018

55. Auld DS, Bergman T. Medium-and short-chain dehydrogenase/reductase gene and protein families : The role of zinc for alcohol dehydrogenase structure and function. *Cell Mol Life Sci*. 2008;65(24):3961-3970.

doi: 10.1007/s00018-008-8593-1

56. Lindskog S. Structure and mechanism of carbonic anhydrase. *Pharmacol Ther*. 1997;74(1):1-20.

doi: 10.1016/s0163-7258(96)00198-2

57. Wisz G, Virt I, Sagan P, Potera P, Yavorskyi R. Structural, optical and electrical properties of zinc oxide layers produced by pulsed laser deposition method. *Nanoscale Res Lett*. 2017;12(1):253.

doi: 10.1186/s11671-017-2033-9

58. Hou T, Sankar Sana S, Li H, *et al*. Development of plant protein derived tri angular shaped nano zinc oxide particles with inherent antibacterial and neurotoxicity properties. *Pharmaceutics*. 2022;14(10):2155.

doi: 10.3390/pharmaceutics14102155

59. Siddiqi KS, Ur Rahman A, Tajuddin, Husen A. Properties of zinc oxide nanoparticles and their activity against microbes. *Nanoscale Res Lett*. 2018;13(1):141.

doi: 10.1186/s11671-018-2532-3

60. Malhotra BD, Ali MA. Nanomaterials in biosensors: Fundamentals and applications. In: *Nanomaterials for Biosensors*. Norwich, NY: William Andrew; 2018. p. 1-74.

doi: 10.1016/B978-0-323-44923-6.00001-7

61. Paltusheva ZU, Ashikbayeva Z, Tosi D, Gritsenko LV. Highly sensitive zinc oxide fiber-optic biosensor for the detection of CD44 protein. *Biosensors* (*Basel*). 2022;12(11):1015.

doi: 10.3390/bios12111015

62. Agarwal H, Nakara A, Shanmugam VK. Anti-inflammatory mechanism of various metal and metal oxide nanoparticles synthesized using plant extracts: A review. *Biomed Pharmacother*. 2019;109:2561-2572.

doi: 10.1016/j.biopha.2018.11.116

63. Sharma H, Kumar K, Choudhary C, Mishra PK, Vaidya B. Development and characterization of metal oxide nanoparticles for the delivery of anticancer drug. *Artif Cells Nanomed Biotechnol*. 2016;44(2):672-679.

doi: 10.3109/21691401.2014.978980

64. Hasnidawani JN, Azlina HN, Norita H, Bonnia NN, Ratim S, Ali ES. Synthesis of ZnO nanostructures using Sol-Gel method. *Procedia Chem*. 2016;19:211-216.

doi: 10.1016/j.proche.2016.03.095

65. Sana SS, Vadde R, Kumar R, *et al*. Eco-friendly and facile production of antibacterial zinc oxide nanoparticles from *Grewia flavescens* (*G. flavescens*) leaf extract for biomedical applications. *J Drug Deliv Sci Technol*. 2023;80:104186.

doi: 10.1016/j.jddst.2023.104186

66. Jayachandran A, Aswathy TR, Nair AS. Green synthesis and characterization of zinc oxide nanoparticles using *Cayratia pedata* leaf extract. *Biochem Biophys Rep.* 2021;26:100995.

doi: 10.1016/j.bbrep.2021.100995

67. Gad G, Hegazy M. Optoelectronic properties of gold nanoparticles synthesized by using wet chemical method. *Mater Res Express*. 2019;6:85024.

doi: 10.1088/2053-1591/ab1bb8

68. Zhang J, Mou L, Jiang X. Surface chemistry of gold nanoparticles for health-related applications. *Chem Sci*. 2020;11(4):923-936.

doi: 10.1039/C9SC06497D

69. Srivastava KR, Awasthi S, Mishra PK, Srivastava PK. Biosensors/molecular tools for detection of waterborne pathogens. In: Vara Prasad MN, Grobelak ABT, editors. *Waterborne Pathogen*. United Kingdom: Butterworth-Heinemann; 2020. p. 237-277.

doi: 10.1016/B978-0-12-818783-8.00013-X

70. Nguyen HH, Park J, Kang S, Kim M. Surface plasmon resonance: A versatile technique for biosensor applications. *Sensors* (*Basel*). 2015;15(5):10481-1510.

doi: 10.3390/s150510481

71. Elahi N, Kamali M, Baghersad MH. Recent biomedical applications of gold nanoparticles: A review. *Talanta*. 2018;184:537-556.

doi: 10.1016/j.talanta.2018.02.088

72. Zukauskas S, Rucinskiene A, Ratautaite V, *et al*. Electrochemical biosensor for the determination of specific antibodies against SARS-CoV-2 spike protein. *Int J Mol Sci*. 2023;24(1):718.

doi: 10.3390/ijms24010718

73. Ali MRK, Wu Y, El-Sayed MA. Gold-nanoparticle-assisted plasmonic photothermal therapy advances toward clinical application. *J Physical Chem C*. 2019;123(25):15375-15393.

doi: 10.1021/acs.jpcc.9b01961

74. Turkevich J, Stevenson PC, Hillier J. A study of the nucleation and growth processes in the synthesis of colloidal gold. *Discuss Faraday Soc*. 1951;11(0):55-75.

doi: 10.1039/DF9511100055

75. Frens G. Controlled nucleation for the regulation of the particle size in monodisperse gold suspensions. *Nat Phys Sci*. 1973;241(105):20-22.

doi: 10.1038/physci241020a0

76. Li S, Al-Misned FA, El-Serehy HA, Yang L. Green synthesis of gold nanoparticles using aqueous extract of *Mentha longifolia* leaf and investigation of its anti-human breast carcinoma properties in the *in vitro* condition. *Arab J Chem*. 2021;14(2):102931.

doi: 10.1016/j.arabjc.2020.102931

77. Rajasekar T, Karthika K, Muralitharan G, *et al*. Green synthesis of gold nanoparticles using extracellular metabolites of fish gut microbes and their antimicrobial properties. *Braz J Microbiol*. 2020;51(3):957-967.

doi: 10.1007/s42770-020-00263-8

78. Muddapur UM, Alshehri S, Ghoneim MM, *et al*. Plant-based synthesis of gold nanoparticles and theranostic applications: A review. *Molecules*. 2022;27(4):1391.

doi: 10.3390/molecules27041391

79. Hutchinson N, Wu Y, Wang Y, *et al*. Green synthesis of gold nanoparticles using upland cress and their biochemical characterization and assessment. *Nanomaterials (Basel)*. 2021;12(1):28.

doi: 10.3390/nano12010028

80. Santhosh PB, Genova J, Chamati H. Green synthesis of gold nanoparticles: An eco-friendly approach. *Chemistry* (*Easton*). 2022;4(2):345-369.

doi: 10.3390/chemistry4020026

81. Raheem AA, Thangasamy P, Sathish M, Praveen C. Supercritical water assisted preparation of recyclable gold nanoparticles and their catalytic utility in cross-coupling reactions under sustainable conditions. *Nanoscale Adv* 2019;1(8):3177-3191.

doi: 10.1039/C9NA00240E

82. Haro-González PG, Ramírez-Rico DS, Larios-Durán ER. Synthesis of gold nanoparticles in aqueous solutions by electrochemical reduction using poly(ethylen glicol) as stabilizer. *Int J Electrochem Sci*. 2019;14(10):9704-9710.

doi: 10.20964/2019.10.10

83. Irfan M, Moniruzzaman M, Ahmad T, Mandal PC, Abdullah B, Bhattacharjee S. Growth kinetic study of ionic liquid mediated synthesis of gold nanoparticles using *Elaeis guineensis* (oil palm) kernels extract under microwave irradiation. *Arab J Chem*. 2020;13(1):620-631.

doi: 10.1016/j.arabjc.2017.07.005

84. Koel M. Developments in analytical chemistry initiated from green chemistry. *Sustain Chem Environ.* 2024;5:100078.

doi: 10.1016/j.scenv.2024.100078

85. Gurusamy L, Anandan S, Wu JJ. In: Khan A, Verpoort F, Asiri AM, *et al*., editors. *Nanomaterials Derived from Metal-Organic Frameworks for Energy Storage Supercapacitor Application*. Ch. 18. Netherlands: Elsevier; 2021. p. 441-470.

doi: 10.1016/B978-0-12-822099-3.00018-6

86. Wang Q, Sun Y, Li S, Zhang P, Yao Q. Synthesis and modification of ZIF-8 and its application in drug delivery and tumor therapy. *RSC Adv*. 2020;10(62):37600-37620.

doi: 10.1039/D0RA07950B

87. Chen S, Pang H, Sun J, Li K. Research advances and applications of ZIF-90 metal-organic framework nanoparticles in the biomedical field. *Mater Chem Front*. 2024;8(5):1195-1211.

doi: 10.1039/D3QM01020A

88. Park KS, Ni Z, Côté AP, *et al*. Exceptional chemical and thermal stability of zeolitic imidazolate frameworks. *Proc Natl Acad Sci*. 2006;103(27):10186-10191.

doi: 10.1073/pnas.0602439103

89. Zhang J, Tan Y, Song WJ. Zeolitic imidazolate frameworks for use in electrochemical and optical chemical sensing and biosensing: A review. *Microchimica Acta*. 2020;187:234.

doi: 10.1007/s00604-020-4173-3

90. Kouhdareh J, Karimi-Nami R, Keypour H, *et al*. Synthesis of a Au/Au NPs-PPy/l-CYs/ZIF-8 nanocomposite electrode for voltammetric determination of insulin in human blood. *RSC Adv*. 2023;13(35):24474-24486.

doi: 10.1039/D3RA04064J

91. Tran TV, Nguyen H, Le PHA, *et al*. Microwave-assisted solvothermal fabrication of hybrid zeolitic-imidazolate framework (ZIF-8) for optimizing dyes adsorption efficiency using response surface methodology. *J Environ Chem Eng*. 2020;8(4):104189.

doi: 10.1016/j.jece.2020.104189

92. Saini P, Chakinala N, Surolia PK, Gupta Chakinala A. Ultrasound-assisted enhanced adsorption of textile dyes with metal organic frameworks. *Sep Purif Technol*. 2025;354:128730.

doi: 10.1016/j.seppur.2024.128730

93. Kenyotha K, Chanapattharapol KC, McCloskey S, Jantaharn P. Water based synthesis of ZIF-8 assisted by hydrogen bond acceptors and enhancement of CO_2 uptake by solvent assisted ligand exchange. *Crystals* (*Basel*). 2020;10(7):599.

doi: 10.3390/cryst10070599

94. Lo KH, Anuratha KS, Cheng CC, *et al*. *In situ* synthesis of ZIF-67 thin films using low temperature chemical vapor deposition to fabricate all-solid-state flexible interdigital in-planar microsupercapacitors. *Int J Energy Res*. 2023;2023(1):3754111.

doi: 10.1155/2023/3754111

95. Cai W, Zhang W, Chen Z. Magnetic Fe3O4@ZIF-8 nanoparticles as a drug release vehicle: pH-sensitive release of norfloxacin and its antibacterial activity. *Colloids Surf B Biointerfaces*. 2023;223:113170.

doi: 10.1016/j.colsurfb.2023.113170

96. Wiśniewska P, Haponiuk J, Saeb MR, Rabiee N, Bencherif SA. Mitigating metal-organic framework (MOF) toxicity for biomedical applications. *Chem Eng J*. 2023;471:144400.

doi: 10.1016/j.cej.2023.144400

97. Meng L, Xiao K, Zhang X, Du C, Chen J. A novel signal-off photoelectrochemical biosensor for M.SssI MTase activity assay based on GQDs@ZIF-8 polyhedra as signal quencher. *Biosens Bioelectron*. 2020;150:111861.

doi: 10.1016/j.bios.2019.111861

98. Ren Q, Mou J, Guo Y, *et al*. Simple homogeneous electrochemical target-responsive aptasensor based on aptamer bio-gated and porous carbon nanocontainer derived from ZIF-8. *Biosens Bioelectron*. 2020;166:112448.

doi: 10.1016/j.bios.2020.112448

99. Anderson DE, Balapangu S, Fleischer HNA, *et al*. Investigating the influence of temperature on the kaolinite-base synthesis of zeolite and urease immobilization for the potential fabrication of electrochemical urea biosensors. *Sensors* (*Basel*). 2017;17(8):1831.

doi: 10.3390/s17081831

100. Li W, Yu Z, Zhang Y, *et al*. Scalable multifunctional MOFs-textiles via diazonium chemistry. *Nat Commun*. 2024;15(1):5297.

doi: 10.1038/s41467-024-49636-9

101. Gan N, Sun Q, Peng X, *et al*. MOFs-alginate/polyacrylic acid/poly (ethylene imine) heparin-mimicking beads as a novel hemoadsorbent for bilirubin removal *in vitro* and *vivo* models. *Int J Biol Macromol*. 2023;235:123868.

doi: 10.1016/j.ijbiomac.2023.123868

102. Lu J, Luan J, Li Y, He X, Chen L, Zhang Y. Hydrophilic maltose-modified magnetic metal-organic framework for highly efficient enrichment of N-linked glycopeptides. *J Chromatogr A*. 2020;1615:460754.

doi: 10.1016/j.chroma.2019.460754

103. Iijima S. Helical microtubules of graphitic carbon. *Nature*. 1991;354(6348):56-58.

doi: 10.1038/354056a0

104. Patil TV, Patel DK, Dutta SD, Ganguly K, Randhawa A, Lim KT. Carbon nanotubes-based hydrogels for bacterial eradiation and wound-healing applications. *Appl Sci*. 2021;11(20):9550.

doi: 10.3390/app11209550

105. Mamidi N, Delgadillo RMV, Castrejón JV. Unconventional and facile production of a stimuli-responsive multifunctional system for simultaneous drug delivery and environmental

remediation. *Environ Sci Nano.* 20218(7):2081-2097.

doi: 10.1039/D1EN00354B

106. Mamidi N, Leija HM, Diabb JM, *et al*. Cytotoxicity evaluation of unfunctionalized multiwall carbon nanotubes-ultrahigh molecular weight polyethylene nanocomposites. *J Biomed Mater Res A*. 2017;105(11):3042-3049.

doi: 10.1002/jbm.a.36168

107. Mamidi N. *Cytotoxicity Evaluation of Carbon Nanotubes for Biomedical and Tissue Engineering Applications*. London: IntechOpen; 2019.

doi: 10.5772/intechopen.85899

108. Qian S, Yan Z, Xu Y, *et al*. Carbon nanotubes as electrophysiological building blocks for a bioactive cell scaffold through biological assembly to induce osteogenesis. *RSC Adv*. 2019;9(21):12001-12009.

doi: 10.1039/C9RA00370C

109. Gupta P, Gupta VK, Huseinov A, Rahm CE, Gazica K, Alvarez NT. Highly sensitive non-enzymatic glucose sensor based on carbon nanotube microelectrode set. *Sens Actuators B Chem*. 2021;348:130688.

doi: 10.1016/j.snb.2021.130688

110. Ajayan PM, Ebbesen TW. Nanometre-size tubes of carbon. *Rep Progress Phys*. 1997;60(10):1025.

doi: 10.1088/0034-4885/60/10/001

111. Shi Z, Lian Y, Zhou X, *et al*. Mass-production of single-wall carbon nanotubes by arc discharge method. *Carbon*. 1999;37:1449-1453.

doi: 10.1016/S0008-6223(99)00007-X

112. Chan KF, Maznam NAM, Hazan MA, *et al*. Multi-walled carbon nanotubes growth by chemical vapour deposition: Effect of precursor flowing path and catalyst size. *Carbon Trends*. 2022;6:100142.

doi: 10.1016/j.cartre.2021.100142

113. Ding EX, Liu P, Khan AT, *et al*. Towards the synthesis of semiconducting single-walled carbon nanotubes by floating-catalyst chemical vapor deposition: Challenges of reproducibility. *Carbon N Y*. 2022;195:92-100.

doi: 10.1016/j.carbon.2022.04.020

114. Adeniran B, Mokaya R. Low temperature synthesized carbon nanotube superstructures with superior CO_2 and hydrogen storage capacity. *J Mater Chem A Mater*. 2015;3(9):5148-5161.

doi: 10.1039/C4TA06539E

115. Tripathi N, Pavelyev V, Islam SS. Synthesis of carbon nanotubes using green plant extract as catalyst: Unconventional concept and its realization. *Appl Nanosci*. 2017;7(8):557-566.

doi: 10.1007/s13204-017-0598-3

116. Jiříčková A, Jankovský O, Sofer Z, Sedmidubský D. Synthesis and applications of graphene oxide. *Materials (Basel)*. 2022;15(3):920.

doi: 10.3390/ma15030920

117. Bai RG, Husseini GA. Graphene-based drug delivery systems. In: Unnithan AR, Sasikala ARK, Park CH, Kim CS, editors. *Biomimetic Nanoengineered Materials for Advanced Drug Delivery*. Ch. 11. Netherlands: Elsevier; 2019. p. 149-168.

doi: 10.1016/B978-0-12-814944-7.00011-4

118. Peña-Bahamonde J, Nguyen HN, Fanourakis SK, Rodrigues DF. Recent advances in graphene-based biosensor technology with applications in life sciences. *J Nanobiotechnol*. 2018;16(1):75.

doi: 10.1186/s12951-018-0400-z

119. Mamidi N, Velasco Delgadillo RM, Barrera EV, Ramakrishna S, Annabi N. Carbonaceous nanomaterials incorporated biomaterials: The present and future of the flourishing field. *Compos B Eng*. 2022;243:110150.

doi: 10.1016/j.compositesb.2022.110150

120. Özcan M, Volpato CAM, Hian L, Karahan BD, Cesar PF. Graphene for Zirconia and titanium composites in dental implants: Significance and predictions. *Curr Oral Health Rep*. 2022;9(3):66-74.

doi: 10.1007/s40496-022-00310-3

121. Shams SS, Zhang R. Graphene synthesis: A review. *Mater Sci Poland*. 2015;33:566-578.

doi: 10.1515/msp-2015-0079

122. Xu S, Zhang L, Wang B, Ruoff RS. Chemical vapor deposition of graphene on thin-metal films. *Cell Rep Phys Sci*. 2021;2(3):100372.

doi: 10.1016/j.xcrp.2021.100372

123. Priyadarsini S, Mohanty S, Mukherjee S, Basu S, Mishra M. Graphene and graphene oxide as nanomaterials for medicine and biology application. *J Nanostructure Chem*. 2018;8(2):123-137.

doi: 10.1007/s40097-018-0265-6

124. Gürünlü B, Taşdelen Yücedağ Ç, Bayramoğlu MR. Green synthesis of graphene from graphite in molten salt medium. *J Nanomater*. 2020;2020:7029601.

doi: 10.1155/2020/7029601

125. Bindumadhavan K, Srivastava S, Srivastava I. Green synthesis of graphene. *J Nanosci Nanotechnol*. 2013;13:4320-4324.

doi: 10.1166/jnn.2013.7461

126. Meka Chufa B, Abdisa Gonfa B, Yohannes Anshebo T, Adam Workneh G. A novel and simplest green synthesis method of reduced graphene oxide using methanol extracted *Vernonia amygdalina*: Large-scale production. *Adv Condens Matter*

Phys. 2021;2021:6681710.

doi: 10.1155/2021/6681710

127. Haley B, Frenkel E. Nanoparticles for drug delivery in cancer treatment. *Urol Oncol Semin Orig Investig*. 2008;26(1):57-64.

doi: 10.1016/j.urolonc.2007.03.015

128. Akbarzadeh A, Rezaei-Sadabady R, Davaran S, *et al*. Liposome: classification, preparation, and applications. *Nanoscale Res Lett*. 2013;8(1):102.

doi: 10.1186/1556-276X-8-102

129. Luiz H, Oliveira Pinho J, Gaspar MM. Advancing medicine with lipid-based nanosystems-the successful case of liposomes. *Biomedicines*. 2023;11:435-447.

doi: 10.3390/biomedicines11020435

130. Zhang H. Thin-film hydration followed by extrusion method for liposome preparation. *Methods Mol Biol*. 2017;1522:17-22.

doi: 10.1007/978-1-4939-6591-5_2

131. Istenič K, Cerc Korošec R, Poklar Ulrih N. Encapsulation of (−)-epigallocatechin gallate into liposomes and into alginate or chitosan microparticles reinforced with liposomes. *J Sci Food Agric*. 2016;96(13):4623-4632.

doi: 10.1002/jsfa.7691

132. Charcosset C, Juban A, Valour JP, Urbaniak S, Fessi H. Preparation of liposomes at large scale using the ethanol injection method: Effect of scale-up and injection devices. *Chem Eng Res Design*. 2015;94:508-515.

doi: 10.1016/j.cherd.2014.09.008

133. Hou K, Bao M, Xin C, *et al*. Green synthesis of gold nanoparticles coated doxorubicin liposomes using procyanidins for light-controlled drug release. *Adv Powder Technol.* 2020;31(8):3640-3649.

doi: 10.1016/j.apt.2020.07.012

134. Siyadatpanah A, Norouzi R, Mirzaei F, *et al*. Green synthesis of nano-liposomes containing *Bunium persicum* and *Trachyspermum ammi* essential oils against *Trichomonas vaginalis*. *J Microbiol Immunol Infect.* 2022;56:150-162.

doi: 10.1016/j.jmii.2022.06.006

135. Rabiee N, Bagherzadeh M, Kiani M, *et al*. Biosynthesis of copper oxide nanoparticles with potential biomedical applications. *Int J Nanomed.* 2020;15:3983-3999.

doi: 10.2147/IJN.S255398

136. Faisal S, Jan H, Shah SA, *et al*. Green synthesis of zinc oxide (zno) nanoparticles using aqueous fruit extracts of *Myristica fragrans*: Their characterizations and biological and environmental applications. *ACS Omega* 2021;6(14):9709-9722.

doi: 10.1021/acsomega.1c00310

137. Khalil AT, Ovais M, Ullah I, Ali M, Shinwari ZK, Maaza M. Biosynthesis of iron oxide (Fe2O3) nanoparticles via aqueous extracts of *Sageretia thea* (Osbeck.) and their pharmacognostic properties. *Green Chem Lett Rev*. 2017;10(4):186-201.

doi: 10.1080/17518253.2017.1339831

138. Abbasi A, Mir Mohamad Sadeghi G, Ghasemi I, Shahrousvand M. Shape memory performance of green *in situ* polymerized nanocomposites based on polyurethane/graphene nanoplatelets: Synthesis, properties, and cell behavior. *Polym Compos*. 2018;39(11):4020-4033.

doi: 10.1002/pc.24456

139. Hemlata, Meena PR, Singh AP, Tejavath KK. Biosynthesis of silver nanoparticles using *Cucumis prophetarum* aqueous leaf extract and their antibacterial and antiproliferative activity against cancer cell lines. *ACS Omega*. 2020;5(10):5520-5528.

doi: 10.1021/acsomega.0c00155

140. Ventrella A, Camisasca A, Fontana A, Giordani S. Synthesis of green fluorescent carbon dots from carbon nano-onions and graphene oxide. *RSC Adv*. 2020;10(60):36404-3612.

doi: 10.1039/D0RA06172G

141. Li H, Zhang N, Hao Y, *et al*. Formulation of curcumin delivery with functionalized single-walled carbon nanotubes: Characteristics and anticancer effects *in vitro*. *Drug Deliv*. 2014;21(5):379-387.

doi: 10.3109/10717544.2013.848246

142. Gupta RK, Patel SKS, Lee JK. Novel cofactor regeneration-based magnetic metal-organic framework for cascade enzymatic conversion of biomass-derived bioethanol to acetoin. *Bioresour Technol*. 2024;408:131175.

doi: 10.1016/j.biortech.2024.131175

ACCSCIENCE PUBLISHING

Global Translational Medicine

ORIGINAL RESEARCH ARTICLE

A simple manual neck examination predicts the apnea-hypopnea index obtained from polysomnography

Alan B. Douglass[1,2*] and Mark Kaluzienski[3]

[1]Department of Psychiatry, Faculty of Medicine, University of Ottawa, Ottawa, Ontario, Canada

[2]Department of Sleep Research, University of Ottawa Institute of Mental Health Research, Ottawa, Ontario, Canada

[3]Department of Psychiatry, The Ottawa Hospital, Ottawa, Ontario, Canada

Abstract

While questionnaires are common ways to screen patients suspected of having sleep apnea, the "gold standard" of diagnosis by nocturnal polysomnography is not easily available in many clinical settings. This is particularly true outside of Europe and North America. Even in the latter, there are long waiting lists for assessment and the costs of polysomnography are high. In this study, we created a new screening test based on a simple physical examination that we called the Douglass gagging test (DGT). It involved the clinician pressing lightly on a seated patient's anterior neck above the thyroid cartilage while the patient inspired deeply. Airway breath sounds were rated on a five-point scale. Using this scale with a series of 224 consecutive patients referred to an urban sleep disorders center, we successfully predicted the severity of the apnea-hypopnea index (AHI) as measured by polysomnography. Using multivariate Poisson regression, the DGT was then compared to the ability of other rating scales that are based on physical examination to predict AHI: the Friedman tonsil size scale (rated 0 – 4), and the modified Mallampati scale (classes 1 – 4) which assesses visibility of the soft palate. Other predictors included sex, age, Epworth sleepiness scale (ESS), and body mass index (BMI). The regression coefficients showed strong prediction of AHI by the DGT and weaker prediction by age, sex, and BMI. There was non-significant prediction by the Friedman and Mallampati scales. In conclusion, this simple test, which requires only 30 s to perform, constitutes a viable clinical screening tool for sleep apnea. It might be particularly useful in rural or underdeveloped areas where complex diagnostic equipment such as the polysomnogram is not easily available. Further investigation of the DGT in larger samples and different populations is warranted.

Keywords: Sleep apnea diagnosis; Airway sounds; Mallampati score; Friedman tonsil index; Oropharynx; Tongue base; Polysomnography

***Corresponding author:**
Alan B. Douglass
(adouglas@uottawa.ca)

Citation: Douglass AB, Kaluzienski M. A simple manual neck examination predicts the apnea-hypopnea index obtained from polysomnography. *Global Transl Med*. 2024:3(4):4548. doi: 10.36922/gtm.4548

Received: August 16, 2024
Accepted: October 28, 2024
Published Online: November 14, 2024

1. Introduction

Since the original description of obstructive sleep apnea (OSA) by Guilleminault *et al.* at Stanford University Sleep Disorders Center,[1] where the nocturnal polysomnogram (NPSG) was developed in the late 1970s,[2] this previously unrecognized condition has

been found to occur internationally at the rate of 12% of the general population for all types of sleep-disordered breathing (SDB, minor to severe) and at the rate of 5% for moderate to severe OSA.[3] While these authors noted some racial, ethnic, and geographic differences, they showed that the condition is found in all countries and populations at approximately the same rate, attesting to its biological etiology. In most cases, its etiology is attributed to reversible obstruction of the "soft" airway, that is, the airway superior to the vocal cords. OSA has strong associations with pathological daytime sleepiness, hypertension, type 2 diabetes, and myocardial infarction.[4] The most common and least invasive treatment is continuous positive airway pressure (CPAP) for OSA, but various otolaryngological surgeries that produce various outcomes against SDB have been proposed.[5]

Since 1976, OSA has been reliably identified through an NPSG. Recently, milder forms of SDB such as hypopneas and the even milder respiratory event-related arousals (RERAs) have been identified and found to cause sleep disruption similar to OSA in many patients,[6] although they cause less hypoxia. Due to the diverse definitions of RERAs, we did not assess them in this study.

For many years, the NPSG has been the only definitive way to identify SDB. However, in North America and Europe, despite most major hospitals having a sleep laboratory, it is still a scarce resource in rural and isolated areas. In many other countries, NPSG is essentially unavailable. While NPSG is still regarded as the "gold standard" for diagnosis of SDB, it is also a labor-intensive procedure that presently costs upwards of US$ 1000 per night[7] and even existing sleep disorders centers have long waiting lists.

For this reason, other methods that enable instant and economical identification of SDB have been proposed. In this context, a simple screening test that could easily detect the characteristics of SDB is required so that the patient could be referred for more rigorous diagnosis and treatment. Such screening tests fall into one of four categories: (i) patient self-report questionnaires (see below); (ii) simple physical examination methods;[8,9] (iii) portable "wearable" electronic devices[10,11] that essentially perform some or all of the functions of an NPSG; and (iv) high-technology devices such as skull imaging through computed tomography (CT) scan, magnetic resonance imaging (MRI), cranio-facial X-ray, or ultrasound evaluation of the upper airway, although the latter equipment is not the focus of the present paper.

Numerous questionnaires have been validated against NPSG for the identification of OSA. These include: STOP-Bang,[12] Berlin Questionnaire,[13] SDB subscale of the Sleep Disorders Questionnaire (SDQ)-2,[14] the NoSAS,[15] and the OSA50.[16] There have also been several critical reviews of these and other questionnaires[17-19] focusing on their sensitivity to the presence of SDB and their specificity in excluding other diagnoses. This is usually reported as a receiver operating characteristics (ROC) analysis using the NPSG as the gold standard. In summary, very few questionnaires have a sensitivity over 70% with a simultaneous specificity of over 60%, and therefore, their positive and negative predictive values leave much to be desired, considering the modest fraction of the population who suffer OSA or milder SDB. While questionnaires can be suggestive of SDB, they fall considerably short of a diagnosis on which treatment decisions could be made.

Physical examinations that have been used to predict the presence of SDB include: body weight and body mass index (BMI); neck circumference; and oral cavity examination rating scales such as the modified Mallampati (MM) soft palate position scale (scored 1 – 4) and the Friedman tonsil size (FTS) scale[20] (scored 0 – 4 with "0" indicating that tonsils have been removed). As these two tests have been performed in different ways by different clinicians, Yu and Rosen[21] summarized the accepted way to perform them and also reviewed individual papers and meta-analyses that showed a modest but significant prediction of OSA by both techniques. In brief, the MM palate assessment is performed with the mouth wide open and the tongue protruded, while in the FTS, the tonsil size is rated with the tongue at rest in the open mouth. Yu and Rosen concluded that there was still debate about the utility of these two rating scales due to their relatively modest correlations with polysomnographic OSA diagnosis, higher correlations in men compared to women, and low inter-rater reliability (kappa = 0.36).

Confusion in the literature arises due to a second rating scale proposed by Friedman, the "Friedman tongue position" (FTP) scale, which to simplify, is an MM examination with the tongue in the rest position. The FTP was not employed in the present study. Therefore, in the present paper, MM refers exclusively to assessment of palate position and visibility, while the FTS refers exclusively to tonsil size.

It can be seen from the above discussion that almost all non-NPSG diagnostic methods are essentially observational and correlational in nature. Only modern "wearable" electronics that replicate some or all of the functions of an NPSG are truly diagnostic, yet they come at a significant cost and their results require expert interpretation. Even the gold standard NPSG is only a snapshot of a single night of sleep, which may or may not include supine rapid eye-movement (REM) sleep – where

apneas are usually worse due to the normal REM paralysis of striate muscles. Although assessment of breathing under anesthesia with manual pressure applied on the throat[22] has been proposed, this is virtually the only provocative test available for SDB and is not practical for most patients.

The rationale for the present study was to examine if a rapid, simple, and non-invasive stress test of airway collapse could be devised for use by any physician in the course of a general physical examination. For maximum utility, it was crucial that it should be executed without the use of specialized equipment and with the patient awake. Such a test could potentially produce a graded rating scale to predict airway collapsibility in sleep, perhaps performing better than the above demographic, morphometric, or questionnaire methods. This daytime test would need to be validated against NPSG. Our solution was a simple "gagging test" that uses mild standardized pressure against the anterior neck of the patient while they are seated and performing a moderately deep inspiration.

This study was approved by the Research Ethics Board of the University of Ottawa Institute of Mental Health Research at the Royal Ottawa Hospital (approval no.: 200620).

2. Materials and methods

2.1. Materials

This study included 224 sequential referrals, usually by their general practitioner, to a sleep disorders clinic at a university-affiliated hospital in a large Canadian urban center. The presenting complaint was either disturbed sleep or suspected sleep apnea.

At the consultation visit, patients completed the Epworth Sleepiness Scale (ESS)[23] and had BMI calculated from their measured height and weight. The same examining physician (the first author) assessed all patients, to reduce error variance. At the ear-nose-throat portion of the physical examination, the physician recorded the FTS and MM scales, then filled out a rating of airway sounds – the Douglass gagging test (DGT) – as described in section 2.2. No specialized equipment was used for the examination. Since the DGT and all examination data were collected before the NPSG, this study was double-blind with respect to the apnea-hypopnea index (AHI) measured on the NPSG.

All patients then underwent a standard NPSG using procedures and methods promulgated by the American Academy of Sleep Medicine (AASM),[24] which includes regular assessments of technician inter-rater reliability. The 16-channel NPSG was recorded using the Embla Sandman Elite sleep-diagnostic hardware and software system. Sleep waveforms and SDB were recorded on computer disk (Windows 10 operating system) and scored the next day by Registered Polysomnographic Technicians (RPsgT) using the above published AASM criteria. The NPSG data of interest were the AHI, along with sleep continuity measurements.

2.2. Method 1

Note that the DGT rating scale presupposes relatively normal waking airflow in the collapsible airway. Conditions such as excessive bronchial secretions, allergic reactions, acute asthma, or uncontrollable coughing would invalidate the test. The DGT was performed using the following procedures:

- Patient sits in an upright position, with mouth closed (unless nose is completely obstructed, in which case the mouth can be open a few millimeters). The patient is instructed to begin a moderately deep inspiration. The examiner applies thumb pressure to the patient's neck just after the inspiration commences.
- The "fingerprint" part of the examiner's thumb is applied to the anterior mid-line of the patient's neck, immediately above the thyroid cartilage, with the fingers loosely cupping the patient's neck.
- A thumb press with a force of 3 Newtons is applied to the anterior neck. This force was not measured with any engineering devices; rather, a clinical approximation to the desired 3-Newton force was made as follows: the single examiner (first author) practiced lifting a 300-gram weight with a string tied to his thumb. Subjectively, this force was found to be similar to compressing by 1 cm the side of a 20 cm tall thin-walled single-use water bottle, which was used to practice the maneuver.
- The direction of thumb force starts from the position above the thyroid cartilage but is then angled vertically and posteriorly at about 45 degrees, aiming toward the skull vertex. The intended purpose of the force is to provoke airway collapse between the base of the tongue and the posterior oropharynx.
- Even in a slim normal female, this force causes nil to minimal airway obstruction noise. In contrast, even heavy male sleep apnea patients with thick necks were noted to experience severe to complete airway obstruction (nil breath sounds) during this mild challenge to airway patency.

2.3. Method 2

To assess airway collapsibility, airway sounds while throat pressure is applied during inspiration are rated on the DGT, a 5-point scale (0 – 4):

- 0 = Nil audible airflow;
- 1 = Minimal but discernable sounds of airflow;

- 2 = Loud airflow noise with some tactile fremitus;
- 3 = Continuous fremitus and loud gurgling during the inspiration;
- 4 = Complete airway obstruction (*i.e.*, silence); harsh glottal stop.

2.4. Statistical analysis

The statistical software employed was the "MASS: glm" package of the R Statistical System, version 4.3.3. A cross-tabulation table of sex versus AHI with Chi-squared analysis was used to illustrate sex differences in AHI.

We used Poisson regression with a proportional odds model to predict the AHI from three airway predictor variables (numerical scoring ranges in brackets): MM classes (1 – 4), FTS scale (0 – 4), and DGT (0 – 4). Other predictor variables included age, sex, BMI, and ESS. The regression coefficients were reported in both raw and exponentiated form to facilitate comparisons.

To accommodate this statistical model, the AHI from the NPSG was also quantized into five ordered categories, labeled as follows: 0 = Normal (0 < 5 respiratory events/h); 1 = Mild (5 < 15 events/h); 2 = Moderate (15 < 30 events/h); 3 = Moderately severe (30 < 60 events/h); and 4 = Very severe (60+ events/h).

3. Results

The patient group comprised 124 males and 100 females. Because we required at least 60 min of polysomnographic sleep for the AHI estimate to be reliable, eight males and one female had to be removed from the dataset, leaving a total of 215 subjects. Those patients removed tended to have very severe apnea that disrupted their sleep, which may have reduced the power of the statistical results.

The mean age of the male and female subjects was 47.2 ± 14.2 years and 48.2 ± 15.5 years, respectively. Mean BMI of the males was 29.5 ± 6.4 kg/m^2 and of the females was 30.7 ± 9.4 kg/m^2. Mean sleep efficiency of the males was 58.5 ± 30.4% and of the females was 67.7 ± 26.4%. Total sleep time was 232 ± 136 min for the males and 282 ± 127 min for the females. Mean wake after first sleep onset (WASO) for the males and the females was 59.9 ± 52.9 min and 65.7 ± 64.7 min, respectively. Mean AHI of the males was 30.2 ± 27.0 events/hr and of the females was 20.5 ± 26.1 events/hr. Mean minimum arterial oxygen saturation of the males and the females was 87.8 ± 14.6% and 87.2 ± 16.6%, respectively. The average duration of the longest apnea was 26 ± 20.1 s in the males and 19.6 ± 15.5 s in the females.

Table 1 shows a cross-tabulation by sex and AHI category. There was a significant difference in the pattern of severity, with males having more of the severe SDB and less of the mild SDB than the females (χ^2 = 21.36, df = 4, p = 0.0003). Table 2 shows the results of the multivariable Poisson regression of the variables predicting AHI category. Among these, the DGT significantly predicted the AHI score while the MM, FTS, and ESS scales did not. Also shown are some less significant predictors of AHI category, namely age, sex, and BMI.

Table 1. Cross-tabulation of frequency by sex and AHI category

Gender	AHI category				
	0	1	2	3	4
F	14	38	25	18	4
M	7	21	38	31	19

Note: Males had significantly worse apnea-hypopnea index (AHI) on nocturnal polysomnogram (χ^2=21.36, df=4, P=0.0003). See text for explanation of AHI categories. Numbers in the body of the table are frequency counts.

Table 2. Multivariate Poisson regression model

	Coefficient	Exp (Coeff)	S.E.	Z-value	Pr(>|z|)
(Intercept)	−0.678	0.507	0.281	−2.408	0.016*
Age	0.007	1.007	0.003	2.210	0.027*
Sex (male)	0.301	1.351	0.102	2.953	0.003**
BMI	0.018	1.018	0.006	2.952	0.003**
ESS_level mild	−0.030	0.970	0.118	−0.262	0.793
ESS_level mod	0.052	1.053	0.233	0.225	0.821
ESS_level severe	−0.271	0.762	0.242	−1.121	0.262
DGT	0.140	1.150	0.039	3.541	0.0004***
FTS Tonsils	0.009	1.009	0.053	0.180	0.857
MM Palate	0.015	1.015	0.049	0.307	0.759
Null deviance: 144.583 on 214 degrees of freedom					
Residual deviance: 96.113 on 205 degrees of freedom					
AIC: 646.74					

Notes: This multivariate Poisson regression model used a 5-point apnea-hypopnea index (AHI) scale (see text) as the dependent variable and the three anatomical rating scales (Douglass gagging test [DGT], Friedman tonsil size scale [FTS], modified Mallampati scale [MM]; see text) as well as body mass index (BMI), Epworth sleepiness scale (ESS; reference level "normal"), age, and sex (reference level "female") as predictor variables. The ESS, MM, and FTS scales were not statistically significant and did not successfully predict the AHI. ***P<0.001, **P<0.01, *P<0.05.

Abbreviations: AIC: Akaike information criterion; Coeff: Regression coefficient from the Poisson regression; DGT: Douglass gagging test; Exp (Coeff): Base of the natural logarithms exponentiated by Coeff, which can be interpreted as follows: A one-point increase in DGT, such as from 0 to 1, predicted a 1.15 point increase in the AHI scale; FTS Tonsils: Friedman tonsil size scale; MM Palate: Modified Mallampati soft palate position scale; Pr(>|z|): Statistical significance of Coeff; S.E.: Standard error of Coeff; Z-value: Multivariate Z-score from the regression.

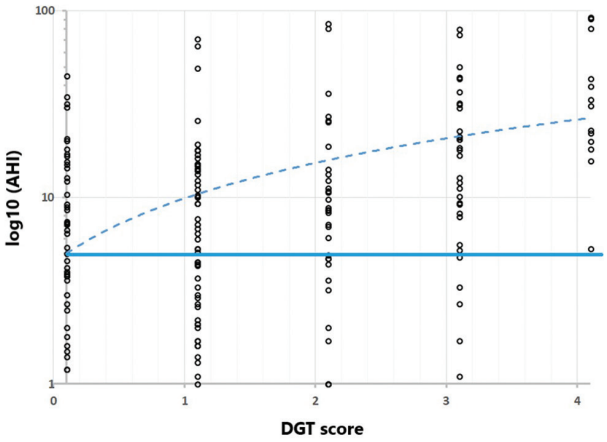

Figure 1. Dot plot of 215 patients who were assessed by the Douglass gagging test, whose 0 – 4 scale is shown on the X-axis. Some dots represent more than one patient. The logarithmic vertical Y-axis shows the distribution of the apnea-hypopnea index (AHI) of these patients as measured on nocturnal polysomnogram. Dotted blue line is a least-squares regression fit for illustrative purposes but see the Poisson regression in Table 2 for accurate regression parameters. Solid blue line indicates AHI = 5 per hour, so all patients below this line have a "normal" AHI.

Figure 1 shows the AHI observed in patients at various levels of the DGT. A horizontal line indicates the AHI level below which a patient is regarded as "normal."

4. Discussion

Creation of the DGT was successful in that it has now been validated against the AHI derived from a polysomnogram on each patient. In other words, the DGT does predict the presence of SDB, as measured by AHI, from a simple 30-second office examination. In the present study, the performance of the DGT in this regard was superior to that of the MM and FTS scales, neither of which succeeded in significantly predicting the AHI, although as noted above they did achieve significant prediction in some previous studies. Interestingly, it has been reported that tonsil size is relatively non-predictive of AHI, and that patients who have had tonsils removed as a child have even a slightly worse AHI than those who did not.[25] BMI has been found to be a predictor of AHI in a previous publication,[26] as was the case in the present study.

One possible reason that the DGT is superior to a rating of palate shape or tonsil size is that DGT is in effect a "stress test" of the complex system of anatomy and muscle tone that maintains a patent airway against the negative pressure of inspiration. In other words, it does not rely on an assessment of static anatomical features such as tonsils, tongue, soft palate, BMI, or neck circumference – although, taken together, these could all possibly contribute to airway collapse in different patients. In contrast, apnea questionnaires focus on self-reported symptoms such as snoring and daytime sleepiness but do not assess the abnormal physiology that treatments such as CPAP are designed to correct.

An important but unanswered question is, "which site of airway obstruction is identified by the DGT?" Although the DGT is initiated at the tongue base/hyoid area, we do not as yet have manometry data to indicate exactly which levels of the airway are affected by the DGT. Given the superior-posterior direction of its force vector, the DGT could possibly be affecting higher levels of the airway. However, there have been several experimental and review papers that have identified the sites of obstruction in various OSA patients.

Katsantonis *et al.*[27] studied 20 OSA patients during NPSG, 19 of whom were male, using a catheter with four pressure transducers placed at posterior nasopharynx, tip of uvula, level of the hyoid bone/base of the tongue, and mid-esophagus. In 14/20 patients, obstruction was confined to the oropharynx; this extended to the base of the tongue in 7/20; another 6/20 had collapse only at the base of the tongue or hypopharynx.

Demin *et al.*[28] used a catheter with five solid state pressure transducers during NPSG on 24 male and six female OSA patients. Transducers were located from the nasal cavity to the esophagus. They found three main sites of obstruction during sleep: 9/30 had obstruction primarily at the soft palate; 15/30 had obstruction both at the soft palate and the tongue base; and 6/30 had obstructions alternating between nasopharynx, soft palate, and tongue base. Pressure abnormalities correlated to AHI ($r = 0.471$) but more robustly with longest duration of apnea ($r = 0.800$).

An extensive review article by Stuck and Maurer[29] reported evidence from a number of airway evaluation methods, including the Mueller maneuver, X-ray cephalometry, CT, MRI, endoscopy during sleep, and pressure manometry at various sites. The clinical Mueller maneuver involves observing three levels of the airway with a flexible endoscope while the awake patient voluntarily inhales with nose and mouth closed. They concluded that the sites of obstruction found by the Mueller maneuver do not reliably reflect the sites that occur during sleep and its reliability is questionable. Combining data from 23 papers, Table 1 of their paper shows a cross-tabulation of sites of obstruction that have been identified using various methods of airway assessment. Overall, the sites of obstruction were found to be palatal (47%), retro lingual (23%), combined (14%), epiglottal (4%), and unknown (12%). Their review of multi-channel pressure recordings concluded that there is high sensitivity and specificity of these techniques with respect to apneas detected on the NPSG and also a high night-to-night reliability.

In summary, it is possible that the DGT only detects OSA obstruction at the base of the tongue; alternatively, it might detect multi-site obstructions as noted above. In any case, it is possible that some sites of obstruction would not be identified by the DGT, thereby producing a false-negative result. The answer to this question will have to await a comparison of the DGT versus sleep manometry of the airway.

One limitation of the present study is that it was performed with patients who were already suspected by their referring doctor of having a sleep disorder, possibly OSA. They were not a random sample of the general population; therefore, the DGT may not achieve the same significant prediction of AHI if used for much wider screening. This will need to be addressed in future large validation studies.

Typically, statistical regressions of the type used in the present study are performed separately for males and females. However, considering the relatively small sample size of this study, it was decided to pool the sexes to get results that were more statistically reliable and instead to enter sex as one of the predictor variables in the regression model. Future validation studies will need to be done separately on males and females.

Another limitation of this study is that it was done on North American patients whose ethnicity was overwhelmingly white-European, so the findings may not be generalizable to other racial, ethnic, or geographic populations.[30] Therefore, research on more diverse populations is necessary to confirm the efficacy and universality of this test; these should include a reasonable proportion of participants who do not have OSA, to provide an adequate "floor" for the statistical distribution. In addition, much larger sample sizes will be required in future studies.

The present findings are encouraging but preliminary. The next step would be to do an ROC analysis of the DGT. This test would be used to define a "cut-off" DGT rating that corresponds to the threshold between normal and abnormal AHI values on the NPSG. To make the analysis clinically relevant, the cutoff point should be chosen so that cases regarded as positive on the DGT would predict levels of AHI that would merit dental or CPAP treatment in a sleep disorders center. This is not to say that milder levels of SDB such as RERAs are clinically irrelevant but the purpose of the DGT is to identify the need for treatment of significant SDB. The ROC would also provide values for the sensitivity, specificity, positive predictive value (PPV), and negative predictive value (NPV) of the DGT. Sensitivity refers to the ability of the DGT to detect SDB if it is present. Specificity refers to the ability of the DGT to specifically exclude SDB if it is not present. NPV and PPV refer to the number of patients who would need to be evaluated by DGT to find one who merited treatment. These values vary depending on the prevalence of SDB in the population studied. Finally, the DGT has not yet been compared to more complex anatomical assessments such as cranio-facial X-ray, CT, MRI, or other *in vivo* tests such as airway sound analysis when asleep, or airway patency under anesthesia. It is possible that further aspects of the DGT could be brought to light by such comparisons.

5. Conclusion

The DGT has been successfully validated against the AHI derived from a night of polysomnography. In addition, its prediction of the AHI proved to be superior to ratings of tonsils or soft palate alone. A DGT is a simple addition to any routine physical examination, requiring minimal preparation by the examiner and requiring only 30 s to perform. In contrast to questionnaires about sleep apnea, it does not rely on the patient's reading ability, language skills, or memory. In other words, the DGT is an objective test. However, in other studies, the FTS scale, MM scale, sex, BMI, and several self-report sleep apnea questionnaires have also shown significant correlations to polysomnographic AHI, which is the gold standard. The DGT appears to be a novel addition to the above anatomical evaluations, perhaps tapping a new source of variance in the evaluation of the airway in OSA. In the absence of a sleep laboratory, a general practitioner could combine all of the above measures to make a rational decision on whether to refer the patient to a specialist, or in an isolated setting, to consider emergent treatment.

Acknowledgments

The authors thank Lisa Kis, Chief Technician of the Royal Ottawa Hospital Sleep Disorders Clinic and her staff of Registered Polysomnographic Technicians for their tireless and accurate work on this project.

Funding

None.

Conflict of interest

The authors declare that they have no competing interests.

Author contributions

Conceptualization: All authors
Formal analysis: All authors
Investigation: All authors
Methodology: Alan Douglass

Writing – original draft: All authors
Writing – review & editing: Alan Douglass

Ethics approval and consent to participate

The Institutional Review Board (REB), University of Ottawa Institute of Mental Health Research at the Royal Ottawa Hospital, granted the approval to carry out this project (approval no.: 200620). While the patients had consented in writing to be clinically evaluated and treated at the Sleep Disorders Clinic, the REB decided that individual consents were not required for their data to be included in this retrospective anonymous chart review.

Consent for publication

The Institutional Review Board, University of Ottawa Institute of Mental Health Research at the Royal Ottawa Hospital, granted approval to publish the data from this project without individual consents from the patients, since their identities were anonymized at the clinical level before data analysis was performed.

Availability of data

Data from this project can be obtained, on reasonable request, from the corresponding author.

References

1. Guilleminault C, Eldridge FL, Dement WC. Human pathology--sleep-induced apneas and cardio-vascular changes. *Bull Physiopathol Respir* (*Nancy*). 1974;10(2):244-247.
2. Guilleminault C, Tilkian A, Dement WC. The sleep apnea syndromes. *Annu Rev Med*. 1976;27:465-484.

   doi: 10.1146/annurev.me.27.020176.002341
3. Benjafield AV, Ayas NT, Eastwood PR, *et al*. Estimation of the global prevalence and burden of obstructive sleep apnoea: A literature-based analysis. *Lancet Respir Med*. 2019;7(8):687-698.

   doi: 10.1016/S2213-2600(19)30198-5
4. Mehra R, Moul DE, Strohl KP. Sleep breathing disorders: Clinical overview. In: Kryger MH, Roth T, Dement WC, editors. *Principles and Practice of Sleep Medicine*. 6th ed. Canada, Toronto: Elsevier; 2017.

   doi: 10.1016/C2012-0-03543-0
5. Quimby A, Salman SO. Surgical evaluation and airway assessment of patients with OSA. In: Salman SO, editor. *Modern Management of Obstructive Sleep Apnea*. Cham: Springer International Publishing; 2019. p. 25-37.

   doi: 10.1007/978-3-030-11443-5_3
6. Tsara V, Amfilochiou A, Papagrigorakis MJ, Georgopoulos D, Liolios E. Guidelines for diagnosis and treatment of sleep-related breathing disorders in adults and children. Definition and classification of sleep related breathing disorders in adults: Different types and indications for sleep studies (Part 1). *Hippokratia*. 2009;13(3):187-191.
7. Masa JF, Corral J, Sanchez de Cos J, *et al*. Effectiveness of three sleep apnea management alternatives. *Sleep*. 2013;36(12):1799-1807.

   doi: 10.5665/sleep.3204
8. Takegami M, Hayashino Y, Chin K, *et al*. Simple four-variable screening tool for identification of patients with sleep-disordered breathing. *Sleep*. 2009;32(7):939-948.
9. Barcelo X, Mirapeix RM, Buges J, Cobos A, Domingo C. Oropharyngeal examination to predict sleep apnea severity. *Arch Otolaryngol Head Neck Surg*. 2011;137:990-996.

   doi: 10.1001/archoto.2011.176
10. Penzel T, Schobel C, Fietze I. New technology to assess sleep apnea: Wearables, smartphones, and accessories. *F1000Res*. 2018;7:413.

    doi: 10.12688/f1000research.13010.1
11. Khor YH, Khung SW, Ruehland WR, *et al*. Portable evaluation of obstructive sleep apnea in adults: A systematic review. *Sleep Med Rev*. 2023;68:101-143.

    doi: 10.1016/j.smrv.2022.101743
12. Chung F, Yegneswaran B, Liao P, *et al*. STOP questionnaire: A tool to screen patients for obstructive sleep apnea. *Anesthesiology*. 2008;108(5):812-821.

    doi: 10.1097/ALN.0b013e31816d83e4
13. Netzer NC, Stoohs RA, Netzer CM, Clark K, Strohl KP. Using the Berlin Questionnaire to identify patients at risk for the sleep apnea syndrome. *Ann Intern Med*. 1999;131(7):485-491.

    doi: 10.7326/0003-4819-131-7-199910050-00002
14. Biard K, De Koninck J, Douglass AB. Creation of a shortened version of the Sleep Disorders Questionnaire (SDQ). *PLoS One*. 2024;19(2):e0288216.

    doi: 10.1371/journal.pone.0288216
15. Marti-Soler H, Hirotsu C, Marques-Vidal P, *et al*. The NoSAS score for screening of sleep-disordered breathing: A derivation and validation study. *Lancet Respir Med*. 2016;4(9):742-748.

    doi: 10.1016/S2213-2600(16)30075-3
16. Chai-Coetzer CL, Antic NA, Rowland LS, *et al*. A simplified model of screening questionnaire and home monitoring for obstructive sleep apnoea in primary care. *Thorax*. 2011;66(3):213-219.

    doi: 10.1136/thx.2010.152801
17. Abrishami A, Khajehdehi A, Chung F. A systematic review of screening questionnaires for obstructive sleep apnea. *Can J Anaesth*. 2010;57(5):423-438.

    doi: 10.1007/s12630-010-9280-x

18. Ramachandran SK, Josephs LA. A meta-analysis of clinical screening tests for obstructive sleep apnea. *Anesthesiology*. 2009;110(4):928-939.

doi: 10.1097/ALN.0b013e31819c47b6

19. Klingman KJ, Jungquist CR, Perlis ML. Questionnaires that screen for multiple sleep disorders. *Sleep Med Rev*. 2017;32:37-44.

doi: 10.1016/j.smrv.2016.02.004

20. Friedman M, Ibrahim H, Bass L. Clinical staging for sleep-disordered breathing. *Otolaryngol Head Neck Surg*. 2002;127(1):13-21.

doi: 10.1067/mhn.2002.126477

21. Yu JL, Rosen I. Utility of the modified Mallampati grade and Friedman tongue position in the assessment of obstructive sleep apnea. *J Clin Sleep Med*. 2020;16(2):303-308.

doi: 10.5664/jcsm.8188

22. Van den Bossche K, Op de Beeck S, Dieltjens M, *et al*. Multimodal phenotypic labelling using drug-induced sleep endoscopy, awake nasendoscopy and computational fluid dynamics for the prediction of mandibular advancement device treatment outcome: A prospective study. *J Sleep Res*. 2022;31(6):e13673.

doi: 10.1111/jsr.13673

23. Johns MW. A new method for measuring daytime sleepiness: The Epworth sleepiness scale. *Sleep.* 1991;14(6):540-545.

doi: 10.1093/sleep/14.6.540

24. Berry RB, Brooks R, Gamaldo CE, *et al*. *The AASM Manual for the Scoring of Sleep and Associated Events: Rules, Terminology and Technical Specifications. Version 2.4*. Darien, IL: American Academy of Sleep Medicine; 2017.

25. Zonato AI, Bittencourt LR, Martinho FL, Júnior JF, Gregório LC, Tufik S. Association of systematic head and neck physical examination with severity of obstructive sleep apnea-hypopnea syndrome. *Laryngoscope*. 2003;113(6):973-980.

doi: 10.1097/00005537-200306000-00011

26. Friedman M, Tanyeri H, La Rosa M, *et al*. Clinical predictors of obstructive sleep apnea. *Laryngoscope*. 1999;109(12):1901-1907.

doi: 10.1097/00005537-199912000-00002

27. Katsantonis GP, Moss K, Miyazaki S, Walsh J. Determining the site of airway collapse in obstructive sleep apnea with airway pressure monitoring. *Laryngoscope*. 1993;103(10):1126-1131.

doi: 10.1288/00005537-199310000-00009

28. Demin H, Jingying Y, Jun W, Qingwen Y, Yuhua L, Jiangyong W. Determining the site of airway obstruction in obstructive sleep apnea with airway pressure measurements during sleep. *Laryngoscope*. 2002;112(11):2081-2085.

doi: 10.1097/00005537-200211000-00032

29. Stuck BA, Maurer JT. Airway evaluation in obstructive sleep apnea. *Sleep Med Rev*. 2008;12:411-436.

doi: 10.1016/j.smrv.2007.08.009

30. Lam B, Ip MSM, Tench E, Ryan CF. Craniofacial profile in Asian and white subjects with obstructive sleep apnoea. *Thorax*. 2005;60(6):504-510.

doi: 10.1136/thx.2004.031591

ACCSCIENCE PUBLISHING

Global Translational Medicine

ORIGINAL RESEARCH ARTICLE

Local anesthesia in 23-gauge vitreoretinal surgery: A comparison of efficacy between retrobulbar and sub-Tenon's injection

Fatemeh Golsoorat Pahlaviani[1], Fardin Yousefshahi[2], Hanieh Niktinat[1], Ramak Roohipourmoallai[3], Samaneh Davoudi[4], Siva S. R. Iyer[5], Samaneh Bourbour[1], and Nazanin Ebrahimiadib[6]*

[1]Department of Ophthalmology, Tehran University of Medical Sciences, Tehran, Iran

[2]Hospital Hôtel-Dieu de Sorel, CISSS de la Montérégie-Est, Quebec, Canada

[3]Department of Ophthalmology, Morsani Hospital, University of South Florida, Florida, United States of America

[4]Department of Ophthalmology, Boston University School of Medicine, Boston, Massachusetts, United States of America

[5]Vitreoretinal Associates, Gainesville, Florida, United States of America

[6]Department of Ophthalmology, University of Florida, Gainesville, Florida, United States of America

Abstract

This study aimed to compare sub-Tenon's and retrobulbar blocks during vitreoretinal surgery in terms of postoperative pain and surgeon experience. This prospective study included 53 patients scheduled for 23-gauge pars plana vitrectomy under local anesthesia. Patients were nonrandomly assigned to receive a xylocaine injection through either the transconjunctival sub-Tenon's or retrobulbar routes, supplemented with intravenous (IV) sedation (midazolam + fentanyl). A sharp needle was used for both techniques. In the sub-Tenon's group, anesthetic injection was initiated through subconjunctival administration after prepping and draping. Pain was assessed immediately postsurgery and the following day using a standardized questionnaire. Patient and surgeon satisfaction levels, along with complications in each group, were recorded. Of the 53 patients, 42 (79%) received the sub-Tenon's block and 11 (21%) received the retrobulbar block. No statistically significant differences in pain scores, patient satisfaction, or surgeon satisfaction were found between the groups. Postoperative pain and surgeon satisfaction were negatively correlated in both groups ($B = -0.465$; $P < 0.001$), and a moderate-to-high correlation was observed between patient and surgeon satisfaction ($B = 0.686$; $P < 0.001$). Overall, sub-Tenon's and retrobulbar blocks showed comparable effectiveness in terms of postoperative pain and patient and surgeon satisfaction in vitreoretinal surgery, with no significant differences in outcomes or complication rates.

Keywords: Retrobulbar block; Sub-Tenon's; Vitreoretinal surgery; Local anesthesia; 23-gauge vitrectomy; Ocular pain questionnaire

***Corresponding author:**
Nazanin Ebrahimiadib
E-mail: nebrahimiadib@ufl.edu

Citation: Pahlaviani FG, Yousefshahi F, Niktinat H, *et al.* Local anesthesia in 23-gauge vitreoretinal surgery: A comparison of efficacy between retrobulbar and sub-Tenon's injection. *Global Transl Med.* 2024:3(4):3900. doi: 10.36922/gtm.3900

Received: June 9, 2024
Accepted: October 21, 2024
Published Online: November 14, 2024

1. Introduction

In ophthalmic surgery, anesthesia not only relieves pain but also facilitates extraocular muscle akinesia.[1] An increasing preference for local anesthesia in ophthalmic surgeries

enables quicker postoperative mobilization and patient discharge.[2-5] Three principal techniques – retrobulbar, peribulbar, and sub-Tenon's block – are available for delivering anesthetic agent around the cranial nerves supplying the eye. The route of administration and the anatomical location of delivering the medication are the main difference, but all aim to numb the nerves supplying the ocular tissue. The difference in delivering medication may influence their efficacy and safety.[6,7]

In retrobulbar and peribulbar anesthesia, a needle delivers anesthetics directly into intraconal and extraconal spaces, respectively. In the retrobulbar technique, the needle enters the intraconal space, located behind the globe within a cone of muscles and connective tissues. Anesthetic injection in this space blocks the optic, oculomotor, trochlear, and abducens nerves, preventing the movement of the extraocular muscles and immobilizing the eye during surgery. The retrobulbar block also numbs the cornea, conjunctiva, uvea, and sclera by blocking the ciliary nerves, providing approximately 45 min of anesthesia – typically sufficient for many ophthalmic procedures. Conversely, the peribulbar technique involves injecting anesthetic into the extraconal space, which is outside the cone of muscles, around the globe. While it offers similar anesthetic effects as retrobulbar anesthesia, peribulbar anesthesia requires a larger volume, has a delayed onset, and often does not achieve akinesia. This technique provides broader anesthesia around the eye, which can be beneficial in certain surgical contexts.

Both techniques, however, carry risks. Although rare, globe perforation is a serious complication of blind needle penetration, particularly in myopic eyes with longer axial lengths and thinner sclera in retrobulbar anesthesia. Peribulbar anesthesia carries similar risks but at a lower rate. Myopic patients with scleral anomalies, such as staphyloma, face an increased risk.[8] Retrobulbar hemorrhage is another potential complication of retrobulbar anesthesia, which may occur if the needle punctures an artery or vein, leading to proptosis, ecchymosis, lid swelling, and elevated intraocular pressure. These conditions are threaten vision. If hemorrhage occurs, emergent lateral canthotomy and cantholysis should be performed, and the planned eye surgery should be postponed. In addition, admission and vision monitoring may be necessary due to the risk of retrobulbar rebleeding. The venous puncture may lead to slower bleeding with eventual chemosis.

Other possible complications of retrobulbar anesthesia include ptosis, chemosis, extraocular muscle injury, central retinal artery occlusion, optic nerve damage, proptosis, and hypertonia. These risks emphasize the need for precision from an experienced ophthalmologist or anesthesiologist and careful monitoring during the administration of retrobulbar anesthesia to minimize risks and ensure patient safety.[5,8-12] Brainstem anesthesia may occur due to retrograde anesthetic flow from the ophthalmic artery to the cerebral or internal carotid artery or due to dural puncture around the optic nerve. This lethal complication, while rare, can manifest as apnea, bradycardia, hypotension, and seizures. Surgical teams must be aware of preventive measures and equip the ophthalmic surgery room with resuscitation equipment.

First described in 1884, the sub-Tenon's capsule block gained popularity for cataract surgery in 1994.[4,13,14] Tenon's capsule, composed of dense elastic and vascular tissue, forms a sleeve-like covering for the extraocular muscles and globe, extending from the limbus to optic nerve. The sub-Tenon's space, between the sclera and Tenon's capsule, contains ciliary nerve endings (Figure 1). Injection of anesthetics into the episcleral area allows the medication to diffuse through the posterior Tenon's capsule into the retrobulbar space without penetrating the orbital space, thus reducing the risk of life-threatening complications. Anesthesia diffuses along the extraocular muscle sheaths and into the eyelid, providing akinesia and analgesia within minutes. Anesthetics may be administered through a conjunctival incision, followed by blunt cannula infusion or by transconjunctival needle penetration into the sub-Tenon's space.[4,15] Subconjunctival hemorrhage, hematoma, chemosis, orbital cellulitis, extraocular muscle paresis, and optic neuropathy have been reported following sub-Tenon's injection.[16,17] There is also an increase likelihood of vomiting following pars plana vitrectomy for the repair of retinal detachment due to eye manipulation and the oculo-emetic and oculo-cardiac reflexes.[18] Regarding the rate of complications with these three techniques,[19] some studies indicate that sub-Tenon's anesthesia has a lower

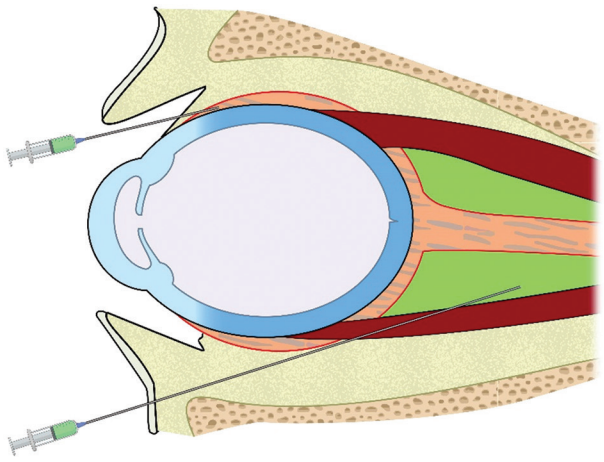

Figure 1. Illustration of injection sites for sub-Tenon's and retrobulbar blocks

complication rate than other techniques[20-23], whereas others report no significant differences.

Although multiple studies have compared these three techniques, results on complication rates and efficacy are inconclusive.[6-8,11,12,20,23-28] Few studies have directly compared retrobulbar and sub-Tenon's anesthesia in vitreoretinal surgeries or assessed postoperative pain, surgeon experience, or satisfaction in vitreoretinal cases.[23,27] As sub-Tenon's anesthesia appears safer, we aimed to assess its potential as an alternative to retrobulbar block. This study aimed to compare sub-Tenon's and retrobulbar techniques in vitreoretinal surgeries, with a focus on postoperative pain, nausea, vomiting, and surgeon experience.

2. Materials and methods

This comparative case series involved consecutive patients who underwent posterior pars plana vitrectomy under local anesthesia, with or without concurrent cataract surgery, at Farabi Eye Hospital. All surgeries included scleral indentation and laser. Participants were nonrandomly assigned to receive either sub-Tenon's or retrobulbar anesthesia, with the technique alternating daily. Exclusion criteria included a history of substance use, chronic pain, major psychiatric disorders, and cerebrovascular or neurologic diseases. The Human Research Ethics Committee of Tehran University of Medical Sciences approved the study protocol (refer to Appendix). This study was in accordance with the principles of the Helsinki Declaration. All patients provided oral and written informed consent.

After transferring the patients to the operating room, sedative medications (0.02 mg/kg midazolam and 1 mg/kg fentanyl) were administered intravenously in both groups for anxiety reduction and cooperation during injection. In the retrobulbar group, we injected 3 – 4 mL of 2% xylocaine (with or without hyaluronidase) in the retrobulbar space from the inferotemporal part of the eyelid using a 23- or 25-gauge needle of 1.5 inches (38 mm) in length before sterile preparation and draping. Ocular massage was performed after injection to distribute the drug effectively. This additional step is crucial in ensuring that the drug is adequately dispersed, providing adequate anesthesia throughout the surgical procedure.

In the sub-Tenon's group, we applied topical anesthetic in the eye. This initial step was intended to provide preliminary numbness of the ocular surface and minimize discomfort before prepping with betadine, followed by careful sterile preparation and draping. We used a 27-gauge needle to puncture the conjunctiva in the inferotemporal and/or superotemporal areas of the sub-Tenon's space to inject 3 – 5 mL of 2% xylocaine. An additional 1 cc of 2% xylocaine was injected subconjunctivally, with 0.5 cc administered on each nasal and temporal side at the site where the sclerotomy incision would be made. Ocular massage at the injection site was performed to promote faster diffusion of the anesthetic.

In both groups, additional sedation was administered and documented if patients experienced discomfort during surgery. Patients were also provided with acetaminophen tablets during the 24-h postoperative period if they reported pain.

A questionnaire designed to assess postoperative pain and comfort levels were administered to each patient twice: once immediately after surgery in the recovery room and again 24 h postsurgery. This dual assessment helped confirm the reliability of evaluations regarding patients' pain and satisfaction levels over time (Appendix). Questions regarding patient pain and comfort levels during surgery and in the recovery room were analyzed as separate items to better assess the overall patient experience in the operating theater. The patient questionnaire, which utilized a Visual Analog Scale, scored responses on a 4-point scale with ratings of excellent (8 – 10), good (6 – 8), fair (3 – 6), and poor (0 – 3). In addition to pain and comfort assessments, occurrences of intraoperative and postoperative nausea, vomiting, and ophthalmic complications were recorded through patient and surgeon feedback. The investigator assessing the patients was blinded to the method of local anesthesia used. Surgeon satisfaction factors included surgery duration, adequate akinesia, hemorrhage occurrence, and patient comfort during the procedure. All surgeries were performed by one expert (N.E.) to ensure consistency in technique and approach. Each surgery involved ocular pathology that required scleral indentation and laser photocoagulation during vitrectomy.

Data were entered into SPSS Statistics for Windows, version 23 (IBM Corp., Armonk, New York) and analyzed using descriptive statistics, including mean and standard deviation for quantitative values and number and percentage for qualitative values. The normality of quantitative data was assessed using the Kolmogorov–Smirnov test. Variables with normal distribution were compared using an independent *t* test, whereas nonparametric variables were analyzed using the Mann–Whitney *U* test. Spearman correlation was used to evaluate variable associations. A p value of <0.05 was considered statistically significant.

3. Results

Fifty-three participants (29 males [55%]) were included in the study, with a mean patient age of 64.84 ± 11.6 years

(*SD*) and a range of 39 – 98 years. The mean participant weight was 70.3 ± 14.8 kg (range, 47 – 120 kg). Eleven patients received retrobulbar anesthesia, and the remaining 42 patients received sub-Tenon's capsule anesthesia.

No patient required additional sedation beyond initial administration. Six patients in the sub-Tenon's group and none in the retrobulbar group reported postoperative nausea and/or vomiting. In our study, one surgery was excluded due to retrobulbar hemorrhage (Figure 2). No statistically significant differences were observed between the two groups regarding demographic factors such as age, sex, and weight. Similarly, no statistically significant differences in reported pain scores, patient or surgeon satisfaction, or patient discomfort during surgery, in the recovery room, or 24 h postsurgery were found between the groups ($P > 0.05$; Table 1).

A negative correlation was found between patient pain scores and surgeon satisfaction in both groups (*B*: −0.465; $P < 0.001$), indicating that increased patient pain was associated with lower surgeon satisfaction. A moderate–high positive correlation was observed between patient and surgeon satisfaction (*B*: 0.686; $P < 0.001$), suggesting that higher patient satisfaction was linked to greater surgeon satisfaction (Figure 3). These findings underscore the interconnected nature of patient and surgeon satisfaction and highlight the influence of patient pain levels on overall satisfaction with the surgical experience.

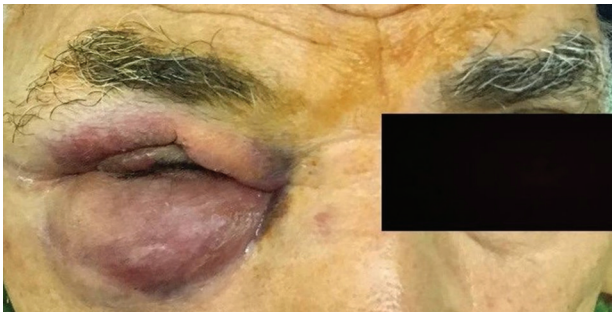

Figure 2. A patient presenting with retrobulbar hemorrhage following retrobulbar anesthesia injection, resulting in rescheduled surgery. Emergent canthotomy and cantholysis were performed immediately. The image shows notable chemosis, total ptosis due to periorbital edema, and ecchymosis of the eyelids.

Table 1. Comparison of patient pain score, patient satisfaction, and surgeon satisfaction among groups

	Sub-Tenon's anesthesia (*n*=42)	Retrobulbar anesthesia (*n*=11)	*P*-value
Pain during surgery	2.74 ± 2.57	3 ± 3.16	0.964
Pain at recovery	1.46 ± 1.92	1.91 ± 2.07	0.511
Pain 24 h after surgery	0.52 ± 1.25	1.09 ± 1.58	0.111
Patient satisfaction	9.74 ± 0.91	9.82 ± 0.60	0.948
Surgeon satisfaction			
Weak	0	0	0.814
Good	3 (7.1)	1 (9.1)	
Very good	7 (16.7)	1 (9.1)	
Excellent	32 (76.2)	8 (81.9)	

4. Discussion

Our study found no significant differences in pain scores, patient satisfaction, and surgeon satisfaction between retrobulbar and sub-Tenon's anesthesia, each supplemented by intravenous (IV) sedation for vitreoretinal surgery. These results suggest that both anesthetic methods provide comparable outcomes for managing intraoperative discomfort and achieving satisfactory surgical results.

Previous studies have reported a higher complication rate, such as retrobulbar hemorrhage, with retrobulbar techniques, but we observed no such difference. However, this may be attributed to the small sample size in our retrobulbar group as well as the lack of data on underlying systemic conditions. Patients scheduled for pars plana vitrectomy often present with systemic conditions requiring anticoagulants, such as hypertension, cardiovascular disorders, and diabetes.[29] Given the higher likelihood of retrobulbar hemorrhage in patients on anticoagulants and a low tendency to discontinue this medication by primary doctors, an anesthetic technique with a lower risk of complications is preferable in these cases.[30]

Given these considerations, evaluating the choice of anesthetic technique within the context of a patient's overall health is crucial. In settings where systemic conditions and the use of anticoagulant medications are common, selecting an anesthetic method with a lower risk of complications is essential.

Two studies assessed the efficacy of sub-Tenon's and retrobulbar anesthesia in vitreoretinal surgery, finding both techniques to be comparably effective.[23,27] Reichstein *et al.*[23] noted that a history of scleral buckle placement influenced the preference for retrobulbar over sub-Tenon's anesthesia. Their study concluded that sub-Tenon's anesthesia is as effective and safe as retrobulbar anesthesia for vitreoretinal surgeries and could potentially replace retrobulbar anesthesia. No complications, such as conjunctival chemosis, retrobulbar hemorrhage, or globe perforation, were observed in either group.[23] In these studies,[23,27] anesthesia was administered following IV sedation and before preoperative sterile preparation. However, in our study, we administered sub-Tenon's block after sterile

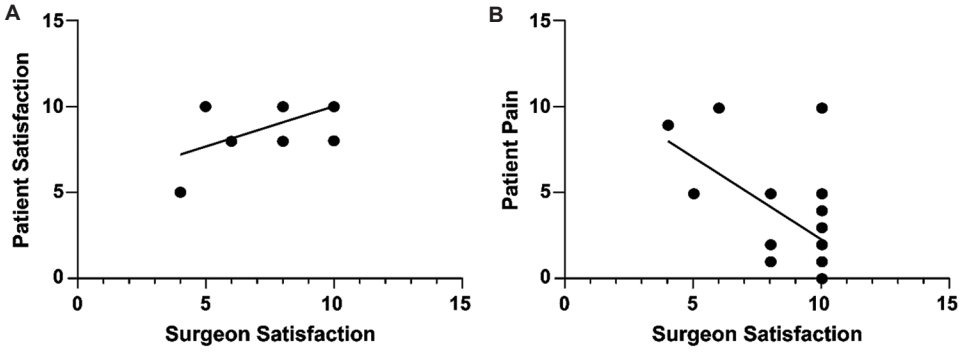

Figure 3. Graphs illustrating the relationship between patient and surgeon satisfaction (A) and between patient pain scores and surgeon satisfaction (B). Identical scores are represented by a single dot in each graph.

preparation after sedation, but the retrobulbar block was administered before sterile preparation. This approach could save preincisional time with sub-Tenon's block, as preoperative preparation can commence immediately after sedation. Future studies should investigate the timing of surgical protocols when using sub-Tenon's anesthesia, which allows the surgeon to scrub and proceed directly to local injection and surgery.

Lai *et al.*[27] reported that patients receiving either sub-Tenon's or retrobulbar anesthesia experience little or no pain during and after vitreoretinal surgery; however, patients in the sub-Tenon's group reported lower pain levels the day after surgery.

Another study compared trans-sub-Tenon's retrobulbar block (TSTRB), sub-Tenon's block (STB), and peribulbar block (PBB) in vitreoretinal surgeries, evaluating analgesia, akinesia, intraoperative pain, and postoperative pain. TSTRB, extending STB into the retrobulbar space, was the most effective in achieving akinesia and prolonging postoperative analgesia. Notably, two patients receiving STB reported moderate postoperative pain, whereas patients in the other groups reported only mild pain. No patients in the TSTRB group required postoperative analgesia. Another notable finding was that the postoperative pain score for patients receiving STB was higher than the other two groups. The study concluded that TSTRB is preferable in both sub-Tenon's and peribulbar anesthesia.[11] However, we did not examine the TSTRB technique in our study.

Alpay *et al.*[31] evaluated sub-Tenon's anesthesia in comparison to retrobulbar anesthesia, concluding that it effectively controls pain during vitreoretinal surgery and could serve as an alternative to retrobulbar anesthesia. However, postoperative pain was not measured in this study.

Franco *et al.*[32] assessed pain levels in patients administered sub-Tenon's anesthesia during vitreoretinal surgery. Patients reported a mean postoperative pain score of 2.4, with seven patients scoring above 3. These findings suggest that sub-Tenon's anesthesia is generally effective and safe, with the potential to become a preferred method for vitreoretinal surgeries in the future. Surgeons reported high satisfaction with sub-Tenon's anesthesia, citing its advantages in terms of patient comfort and surgical experience. In this study, patients' pain levels were assessed only during and immediately after surgery. The study exclusively investigated STB without comparing it with other anesthesia methods, and postoperative pain was not measured.

A detailed study on anesthesia for 25-gauge vitrectomy compared retrobulbar, sub-Tenon's, and medial canthus episcleral anesthesia methods, focusing on intraoperative and postoperative pain levels. Remarkably, none of the patients, regardless of the anesthesia type used, reported any postoperative pain or discomfort. This result indicates that all three anesthesia techniques effectively managed pain throughout the vitrectomy, providing a pain-free postoperative experience for the patients involved.[33]

In a study by Xu *et al.*,[34] patients undergoing pars plana vitrectomy with sub-Tenon's anesthesia reported less pain than those receiving retrobulbar anesthesia during surgery and on the first postoperative day. In addition, sub-Tenon's anesthesia was more effective in inducing akinesia and controlling eye movements compared to retrobulbar anesthesia. However, they did not administer supplemental IV sedation, possibly contributing to increased discomfort in the retrobulbar group. IV sedation, often a combination of opioid and/or benzodiazepine, is typically used to enhance patient comfort and reduce intraoperative stress by inducing retrograde amnesia. This approach can help patients relax, reduce anxiety, and minimize movement during surgery. However, it is not without risks, as it requires an anesthesiologist monitoring of heart rate and blood pressure and preparation for potential complications, including apnea, airway obstruction, allergic reactions,

drowsiness, and disorientation. Without IV sedation, introducing the needle around the eye, particularly in the retrobulbar space, can be very uncomfortable and painful for the patient. Consequently, the results of both this and our study suggest that comparisons between the efficacy of retrobulbar injection and sub-Tenon's technique may be influenced by the presence or absence of IV sedation.[34] Similarly, Haider *et al*.[35] compared topical, sub-Tenon's, and retrobulbar anesthesia for pars plana vitrectomy without supplemental IV sedation, finding that topical anesthesia was the least painful method. Although topical anesthesia showed the lowest pain scores, retrobulbar anesthesia, with a mean perioperative pain score of 10.87 and a postoperative score of 13.73, was deemed the most convenient.

In our sub-Tenon's group, we added a preliminary step involving the subconjunctival injection. The resulting chemosis, although potentially disruptive to surgical procedures, could be alleviated by conjunctival massage, which helped provide more reliable pain relief, particularly during conjunctival manipulation at the start of surgery and during trocar placement. This massage step could fill the time gap needed to achieve complete anesthetic infiltration in the retrobulbar space, thus enhancing patient comfort and allowing surgery to proceed sooner. Alternatively, the time required for this massage could offset the time saved between the retrobulbar block and sterile preparation. Therefore, it is unclear if sub-Tenon's capsule anesthesia is faster than retrobulbar anesthesia. However, like the sub-Tenon's method, the retrobulbar technique also requires massage to disperse the anesthesia and prevent elevated intraocular pressure, especially when hyaluronidase is not used.

We conducted the STB using a sharp 27-gauge needle, a common practice in clinical settings. However, some experts advocate using an angiocatheter due to its superior safety profile, as its design may lower complication risks during the procedure. Nevertheless, a significant drawback of the angiocatheter is that it often requires a conjunctival incision, which could extend the procedure duration and be uncomfortable for the patient.

All our surgeries involved two painful steps—namely, intraoperative indentation and laser photocoagulation—which were well tolerated by patients in both groups. When ocular anesthesia faded during prolonged surgeries, necessitating reinjection, the sub-Tenon's technique was more feasible. In one study comparing sub-Tenon's and retrobulbar anesthesia for trabeculectomy in glaucoma surgery, additional sedation was more frequently required in the retrobulbar group, as was postoperative analgesia. This study also showed that the sub-Tenon's method required a lower volume of local anesthetic.[12] In another study on cataract surgery, STB was associated with lower pain scores.[25] A separate study showed that although the need for resedation was lower with the retrobulbar technique, the sub-Tenon's group reported higher patient satisfaction during surgery.[24]

Although STB is known to be less effective in inducing akinesia compared to other anesthetic techniques, this did not impact surgeon performance in our study. An experienced surgeon can stabilize the globe using probes inserted into the trocars; however, this level of proficiency may be challenging for less experienced trainees. In our study, the factor most affecting surgeon satisfaction was the level of perceived patient discomfort. This patient-reported discomfort had a notable impact on surgeon satisfaction, underscoring the significance of patient comfort in enhancing the overall surgical experience.

One of the limitations of the current study is the selection bias resulting from the nonrandomized allocation of patients into groups. The unequal distribution of patients in the two study groups and the small sample size are significant limitations. We also recognize that the lack of blinding could introduce bias, as evaluators may have known the participants' group assignments. In addition, the duration of the vitreoretinal surgeries per anesthesia group was not recorded, and we did not exclude patients with diabetes or hypertension, which could influence perceived pain levels.

5. Conclusion

Our results suggest that sub-Tenon's anesthesia, combined with subconjunctival injection, has similar efficacy to retrobulbar block in patients undergoing pars plana vitrectomy in our cohort. Sub-Tenon's anesthesia may serve as a suitable alternative to retrobulbar anesthesia in some vitreoretinal surgery patients. Compared with the retrobulbar technique, sub-Tenon's anesthesia is less invasive, involves a shorter learning curve, and has a lower risk of complications and fewer preparatory steps.

Acknowledgments

None.

Funding

None.

Conflict of interest

The authors declare that they have no competing interests.

Author contributions

Conceptualization: Nazanin Ebrahimiadib, Fardin Yousefshahi

Formal analysis: Hanieh Niktinat, Ramak Roohipourmoallai
Investigation: Fatemeh Golsoorat Pahlaviani, Samaneh Bourbour
Methodology: Fatemeh Golsoorat Pahlaviani, Nazanin Ebrahimiadib, Siva S. R. Iyer, Samaneh Davoudi, Hanieh Niktinat
Writing – original draft: Fatemeh Golsoorat Pahlaviani, Nazanin Ebrahimiadib, Hanieh Niktinat,
Writing – review & editing: Nazanin Ebrahimiadib, Fardin Yousefshahi, Hanieh Niktinat, Samaneh Bourbour, Ramak Roohipourmoallai, Samaneh Davoudi, Siva S. R. Iyer

Ethics approval and consent to participate

The questionnaire and methodology for this study were approved by the Human Research Ethics Committee of Tehran University of Medical Sciences. Written informed consent was obtained from each of the subjects to participate in the study.

Consent for publication

Written informed consent was obtained from each of the subjects to publish their data.

Availability of data

Raw data of this study are available on request from the corresponding author.

References

1. Mavrakanas NA, Stathopoulos C, Schutz JS. Are ocular injection anesthetic blocks obsolete? Indications and guidelines. *Curr Opin Ophthalmol*. 2011;22(1):58-63.
   doi: 10.1097/ICU.0b013e328341426f
2. Imarengiaye CO, Adamu SA, Isesele T, Tudjegb SO. Anaesthesia for ophthalmic procedures in a teaching hospital. *Niger J Ophthalmol*. 2008;16(1):1-4.
   doi: 10.4314/njo.v16i1.11948
3. Hodgkins PR, Luff AJ, Morrell AJ, Botchway LT, Featherston TJ, Fielder AR. Current practice of cataract extraction and anaesthesia. *Br J Ophthalmol*. 1992;76(6):323-326.
   doi: 10.1136/bjo.76.6.323
4. Tomanović N. Local anesthesia in ophthalmologic surgery. *Med Arh*. 2003;57(4 Suppl 1):37-40.
5. Hamilton RC, Gimbel HV, Strunin L. Regional anaesthesia for 12,000 cataract extraction and intraocular lens implantation procedures. *Can J Anaesth*. 1988;35(6):615-623.
   doi: 10.1007/BF03020350
6. Ali-Melkkila T, Virkkila M, Leino K, Palve H. Regional anaesthesia for cataract surgery: Comparison of three techniques. *Br J Ophthalmol*. 1993;77(12):771-773.
   doi: 10.1136/bjo.77.12.771
7. Stevens JD. A new local anesthesia technique for cataract extraction by one quadrant sub-Tenon's infiltration. *Br J Ophthalmol*. 1992;76(11):670-674.
   doi: 10.1136/bjo.76.11.670
8. Fahmi A, Bowman R. Administering an eye anaesthetic: Principles, techniques, and complications. *Community Eye Health*. 2008;21(65):14-17.
9. Adekoya BJ, Onakoya AO, Balogun BG, Oworu O. Current practice of ophthalmic anesthesia in Nigeria. *Middle East Afr J Ophthalmol*. 2013;20(4):341-344.
   doi: 10.4103/0974-9233.120022
10. Klein ML, Jampol LM, Condon PI, Rice TA, Serjeant GR. Central retinal artery occlusion without retrobulbar hemorrhage after retrobulbar anesthesia. *Am J Ophthalmol*. 1982;93(5):573-577.
    doi: 10.1016/S0002-9394(14)77371-4
11. Young-Zvasara T, Winder J, Wijetilleka S, Wheeler L, Mcpherson R. Efficacy and safety of a novel blunt cannula trans-sub-Tenon's retrobulbar block for vitreoretinal surgery. *Middle East Afr J Ophthalmol*. 2019;26(3):163-167.
    doi: 10.4103/meajo.MEAJO_151_18
12. Buys YM, Trope GE. Prospective study of sub-Tenon's versus retrobulbar anesthesia for inpatient and day-surgery trabeculectomy. *Ophthalmology*. 1993;100(10):1585-1589.
    doi: 10.1016/S0161-6420(93)31440-5
13. Turnbull CS. The hydrochlorate of cocaine, a judicious opinion of its merits. *Med Surg Rep*. 1884;29:628-629.
14. Guise P. Sub-Tenon's anesthesia: An update. *Local Reg Anesth*. 2012;5:35-46.
    doi: 10.2147/LRA.S16314
15. Athanasiov P, Henderson T. Ocular anaesthesia and the never-ending story. *Br J Ophthalmol*. 2010;94(1):1.
    doi: 10.1136/bjo.2009.168831
16. Kaini KR. Subtenon's anesthesia in extracapsular cataract extraction. *Nepal Med Coll J*. 2003;5(2):69-72.
17. Nouvellon E, L'Hermite J, Chaumeron A, *et al*. Ophthalmic regional anesthesia: Medial canthus episcleral (sub-tenon) single injection block. *Anesthesiology*. 2004;100(2):370-374.
    doi: 10.1097/00000542-200402000-00028
18. Van Den Berg AA, Lambourne A, Clyburn PA. The oculo-emetic reflex. A rationalisation of postophthalmic anaesthesia vomiting. *Anaesthesia*. 1989;44(2):110-117.
    doi: 10.1111/j.1365-2044.1989.tb11157.x
19. Alhassan MB, Kyari F, Ejere HO. Peribulbar versus

retrobulbar anaesthesia for cataract surgery. *Cochrane Database Syst Rev*. 2015;2015(7):CD004083.

doi: 10.1002/14651858.CD004083.pub3

20. Villafranca Barba A, Mouslim S, De la Gala García FA, Reyes Fierro A. Sub-Tenon block for ocular globe anesthesia: A review. *Rev Esp Anestesiol Reanim*. 2011;58(3):167-173.

doi: 10.1016/s0034-9356(11)70025-1

21. Chuang LH, Wu WC, Yang KJ, Tsao YP, Chen TL, Lai CC. Sub-Tenon anesthesia for segmental scleral buckling and assessment of postoperative pain. *Chang Gung Med J*. 2002;25(1):16-22.

22. Eke T, Thompson JR. Serious complications of local anaesthesia for cataract surgery: A 1 year national survey in the United Kingdom. *Br J Ophthalmol*. 2007;91(4):470-475.

doi: 10.1136/bjo.2006.106005

23. Reichstein DA, Warren CC, Han DP, Wirostko WJ. Local anesthesia with blunt sub-Tenon's cannula versus sharp retrobulbar needle for vitreoretinal surgery: A retrospective, comparative study. *Ophthalmic Surg Lasers Imaging Retina*. 2016;47(1):55-59.

doi: 10.3928/23258160-20151214-08

24. Ryu JH, Kim M, Bahk JH, Do SH, Cheong IY, Kim YC. A comparison of retrobulbar block, sub-Tenon block, and topical anesthesia during cataract surgery. *Eur J Ophthalmol*. 2009;19(2):240-246.

doi: 10.1177/112067210901900211

25. Khoo BK, Lim TH, Yong V. Sub-Tenon's versus retrobulbar anesthesia for cataract surgery. *Ophthalmic Surg Lasers*. 1996;27(9):773-777.

26. Tokuda Y, Oshika T, Amano S, Inouye J, Yoshitomi F. Analgesic effects of sub-Tenon's versus retrobulbar anesthesia in planned extracapsular cataract extraction. *Graefes Arch Clin Exp Ophthalmol*. 2000;238(3):228-231.

doi: 10.1007/s004170050348

27. Lai M, Lai J, Lee W, *et al*. Comparison of retrobulbar and sub-Tenon's capsule injection of local anesthetic in vitreoretinal surgery. *Ophthalmology*. 2005;112(4):574-579.

doi: 10.1016/j.ophtha.2004.10.043

28. Sohn HJ, Moon HS, Nam DH, Paik HJ. Effect of volume used in sub-Tenon's anesthesia on efficacy and intraocular pressure in vitreoretinal surgery. *Ophthalmologica*. 2008;222(6):414-421.

doi: 10.1159/000161556

29. Shaikh N, Srishti R, Khanum A, *et al*. Vitreous hemorrhage - Causes, diagnosis, and management. *Indian J Ophthalmol*. 2023;71(1):28-38.

doi: 10.4103/ijo.IJO_928_22

30. He X, Chen AF, Nirwan RS, Sridhar J, Kuriyan AE. Perioperative management of anticoagulants in ocular surgeries. *Int Ophthalmol Clin*. 2020;60(3):3-15.

doi: 10.1097/IIO.0000000000000316

31. Alpay A, Güney T. Evaluating the effectiveness of localized sub-Tenon's anesthesia in 23-gauge vitreoretinal surgery. *Int Ophthalmol*. 2021;41(1):195-201.

doi: 10.1007/s10792-020-01566-3

32. Franco F, Vicchio L, Barbera GR, Virgili G, Giansanti F. Patient and surgeon comfort in vitreoretinal surgery performed with sub-Tenon's anaesthesia. *Rom J Ophthalmol*. 2021;65(2):136-140.

doi: 10.22336/rjo.2021.28

33. Roman-Pognuz D, Scarpa G, Virgili G, Roman-Pognuz E, Paluzzano G, Cavarzeran F. Comparison of retrobulbar, sub-Tenon anesthesia and medial canthus episcleral anesthesia for 25-gauge posterior vitrectomy. *Retina*. 2022;42(1):19-26.

doi: 10.1097/IAE.0000000000003260

34. Xu Q, Ren M, Guan J, Shi G, Ni Y, Luan J. Efficacy and safety of trans-sub-Tenon's retrobulbar anesthesia for pars plana vitrectomy: A randomized trial. *BMC Ophthalmol*. 2022;22(1):289.

doi: 10.1186/s12886-022-02507-7

35. Haider MA, Sattar U, Mehak F, Ahmed I, Sagheer S. Comparison of pain in topical, sub-Tenon and retrobulbar anesthesia for 23g pars plana vitrectomy. *Pak J Med Health Sci*. 2020;14(1):622-625.

Appendix

PRE OP QUESTIONNAIRE

Patient Number	
Patient Name	
Age	
Gender	
Education Level	
Height	
Weight	
Anesthesia Method	
Duration of Surgery	

Medical History:

Diabetes	
Hypertension	
Joint and Muscle Pain	
Low Back Pain	
Migraine and Headache	
Major Depressive Disorder	
Contact Lens Use	

Medications Used for Sedation:

Midazolam	
Fentanyl	
Lidocaine	
Other Medications	

Please rate your pain by circling the number that best describes your pain immediately after surgery.

0 1 2 3 4 5 6 7 8 9 10

No Pain — Pain As Bad As You Can Imagine

Please rate your pain by circling the number that best describes your pain in the recovery room.

0 1 2 3 4 5 6 7 8 9 10

No Pain — Pain As Bad As You Can Imagine

Please rate your nausea and vomiting by circling the number that best describes your nausea and vomiting in the recovery room.

0 1 2 3 4 5 6 7 8 9 10

No Nausea and Vomiting — Severe Nausea and Vomiting

Please rate your satisfaction by circling the number that best describes your satisfaction.

	Dissatisfaction Satisfaction									Great
Patient Satisfaction Immediately After Surgery	0	1	2	3	4	5	6	7	8	9	10
Patient Satisfaction In The Recovery Room.	0	1	2	3	4	5	6	7	8	9	10
Surgeon Satisfaction	0	1	2	3	4	5	6	7	8	9	10

POST OP QUESTIONNAIRE (24 hours after surgery)

Please rate your pain by circling the number that best describes your pain at its **worst** in the last 24 hours.

0 1 2 3 4 5 6 7 8 9 10

No Pain — Pain As Bad As You Can Imagine

Please rate your pain by circling the number that best describes your pain at its **least** in the last 24 hours.

0 1 2 3 4 5 6 7 8 9 10

No Pain — Pain As Bad As You Can Imagine

How many hours after the operation did the pain start?

ACCSCIENCE PUBLISHING

Global Translational Medicine

ORIGINAL RESEARCH ARTICLE

Blood laboratory parameters can predict relapse-free survival of patients with advanced squamous cell lung cancer and adenocarcinoma

Anatoli D. Tahanovich[1]*, Mikalai M. Kauhanka[1], Alexander V. Kolb[1], Oxana V. Gotko[2], and Violetta I. Prokharova[2]

[1]Department of Biochemistry, Educational Institution "Belarusian State Medical University", Minsk, Belarus

[2]Department of Laboratory Methods of Diagnostics, N.N. Alexandrov National Cancer Center of Belarus, a.g. Lesnoy, Belarus

Abstract

The aim of the work was to study the relationship between the concentration of cells and proteins in the blood of patients with Stage III squamous cell lung cancer (SCLC) and adenocarcinoma (AC) before surgical treatment and the duration of the relapse-free period after tumor resection to develop prognostic models for relapse-free survival in these diseases. Using logistic regression equations, the models incorporated variables included cytokeratin 19 fragment antigen 21-1 (CYFRA 21-1) concentration, the proportion of lymphocytes expressing the C-X-C motif chemokine receptor 1 (CXCR1), and monocytes expressing the C-X-C motif chemokine receptor 2 for SCLC. For AC, the models included the CYFRA 21-1 concentration, lymphocytes expressing the CXCR1 receptor, and the eosinophil-to-monocyte ratio. These models can predict the probability of tumor recurrence based on measurements of blood parameters in the pre-operative period, with a prediction efficiency of 87.7% for SCLC and 89.0% for AC.

Keywords: Squamous cell lung cancer; Adenocarcinoma; Relapse; Prognosis; CYFRA 21-1; CXCR1; CXCR2; Stage III

***Corresponding author:**
Anatoli D. Tahanovich] (taganovich@bsmu.by)

Citation: Tahanovich AD, Kauhanka MM, Kolb AV, Gotko OV, Prokharova VI. Blood laboratory parameters can predict relapse-free survival of patients with advanced squamous cell lung cancer and adenocarcinoma. *Global Transl Med*. 2024:3(4):4865. doi: 10.36922/gtm.4865

Received: September 16, 2024
Accepted: November 26, 2024
Published Online: December 13, 2024

1. Introduction

Lung cancer (LC) is one of the most common forms of malignant tumors. According to the histological structure, 80 – 85% of LC cases are classified as non-small cell LC (NSCLC).[1] Within the NSCLC category, two main histological types are distinguished: adenocarcinoma (AC) and squamous cell LC (SCLC).[2]

In most patients, NSCLC is diagnosed at an advanced stage, often with disease metastases present. About 30% of all NSCLC cases are patients with Stage III disease.[1,2] According to the TNM classification,[3] Stage III NSCLC is a heterogeneous group of tumors that differ in size, the presence of invasion into surrounding mediastinal structures, and damage to the mediastinal lymph nodes. These are categorized as stage IIIA (T1-2N2, T3N1, T4N0-1), Stage IIIB (T1-2N3, T3-4N2), and Stage IIIC (T3-4N3), each of which determines the particular treatment regimen. Surgical treatment is

typically performed for stage IIIA and some stage IIIB cases, often supplemented with neoadjuvant and/or adjuvant chemotherapy, sometimes in combination with radiation therapy.[2]

Different treatment regimens are aimed at preventing disease recurrence. Despite this, the prognosis in patients with Stage III NSCLC remains poor. For patients with T1-4N0-2, the overall 5-year survival rate after treatment varies from 36% to 82%.[1-3] The median survival rate for stage III NSCLC generally does not exceed 20 months, with no more than 20% of patients surpassing the 5-year survival barrier.[2,3] At the same time, patients with the same TNM stage may have different outcomes and the likelihood of relapse. One of the approaches to optimizing the effectiveness of treatment in this category of patients is the ability to predict those at high risk of disease relapse. They have a high risk of retaining hidden metastases after surgical removal of the tumor, which significantly contributes to disease recurrence, referred to as "relapse."

Early prediction of rapid relapse after treatment would allow for the timely and targeted implementation of neoadjuvant and adjuvant therapy, in addition to surgical treatment. Therapeutic treatments are associated with various side effects, but when targeted, they can provide maximum benefit,[2] thereby increasing the survival of patients with Stage III NSCLC. Therefore, predicting the risk of tumor recurrence in patients with Stage III (T1-4N0-2) NSCLC before treatment is highly relevant.

There is considerable evidence supporting the relationship between systemic inflammation and cancer.[4] On one hand, the inflammatory reaction creates conditions for the development of cancer, and on the other hand, it is a consequence of metabolic changes in tumor cells.[5] Inflammation in the tumor microenvironment plays a role in the proliferation and survival of malignant tumor cells, angiogenesis in tumor tissue, and metastasis.[6] Signs of tumor-associated inflammation are the presence of cells and inflammatory mediators (chemokines, cytokines) in tumor tissue, similar to those observed in chronic inflammation and reparation.

During transformation, many cells of epithelial or mesenchymal origin begin to express chemokine receptors, thereby utilizing these factors for migration and survival at sites distant from the primary tumor. In particular, the proinflammatory C-X-C motif chemokine ligand 8 (CXCL8) exerts its effects by signaling through two seven-transmembrane-segment receptors, C-X-C motif chemokine receptor 1 (CXCR1) and receptor 2 (CXCR2). Activation of the CXCL8-CXCR1/2 signaling pathway in the tumor microenvironment of numerous cancers enhances tumor progression by promoting proliferation, angiogenesis, migration, invasion, cell survival, and involvement in organ-specific metastasis.[6] Another chemokine that binds to the CXCR2 receptor is C-X-C motif chemokine ligand 5 (CXCL5), which serves as an attractant for granulocytes. The CXCL5/CXCR2 axis has been shown to be important in the development of many human cancers. The serum CXCL5 protein concentration was significantly increased in NSCLC compared to healthy volunteers. CXCL5 expression correlated with tumor size and stage of NSCLC, lymph node metastases, and decreased patient survival.[7] Our previous studies also showed changes in the levels of these proteins in the blood of NSCLC patients.[8-10] Their relationship with tumor process descriptors was established, and the diagnostic efficiency of their determination in this disease was calculated, which in some cases exceeded that of classical markers.

An aggressive, rapidly growing tumor with multiple metastases produces and secretes a large number of these proteins into the blood serum, which indicates a poor prognosis.[11] Therefore, blood, being a minimally invasive and the most accessible material, plays a crucial role in the search for oncobiomarkers, including in patients with NSCLC. Tumor cell components, or molecules involved in the development of tumor tissue, circulating in the bloodstream, have been studied as candidates for malignant growth markers. These include the well-established cytokeratin 19 fragment antigen 21-1 (CYFRA 21-1), squamous cell carcinoma (SCC) antigen, and cancer embryonic antigen (CEA).[11] Subsequent studies have shown that CEA and CYFRA 21-1, in addition to their diagnostic value, also hold prognostic significance in NSCLC.[12-17] However, determining the level of each of these markers separately in blood serum has not demonstrated sufficient specificity and sensitivity.

Researchers are increasingly focusing on other systemic inflammatory markers in the blood, such as lymphocytes (L),[18] neutrophils (N), platelets (P),[19] C-reactive protein (CRP), and albumin,[20] as well as their ratios,[21-23] as prognostic markers in cancer. Interest in such indicators is understandable, given that the quantitative and semi-quantitative assessment of blood cells is a routine and relatively inexpensive test, which is usually carried out for every patient admitted to a clinic. Evaluating these results to predict patient survival is a critical issue. For these same purposes, the calculation of the systemic immune-inflammatory index (SII), which has proven effective in determining treatment strategies for a wide variety of cancers,[24] and the inflammatory prognostic index (IPI),[25] have been proposed. The advantage of these laboratory indicators lies not only in their low cost but also in the stability and reproducibility of the results. However, the data obtained often contradict each other, and the

correspondence between their concentration in the blood and the tumor response in NSCLC is only 40 – 70%.[26]

To increase the diagnostic and prognostic efficiency of these markers, there have been attempts to create multianalytical panels incorporating these and other indicators of tumor tissue metabolism.[27] However, to date, there is still no informative single biomarker or combination of biomarkers that can help in predicting the recurrence of LC after diagnosis and before treatment initiation. This is believed due to the lack of a standardized study designs, patient stratification criteria, and the low diagnostic sensitivity and/or specificity of the markers.[27]

As histological subtypes of NSCLC, AC and SCLC differ in etiology and course.[28] Thus, SCLC develops significantly more often in smoking patients, while AC is more associated with obesity. Compared to AC, SCLC is more prevalent in men, whereas AC is more frequently seen in women.

Both subtypes are characterized by symptoms, including hemoptysis, dyspnea, chest pain, cough, and general weakness. Changes in the level of some laboratory parameters in the blood of patients, such as CRP, fibrinogen, and haptoglobin, also show similar patterns in both subtypes.[29] In both cases, the disease often proceeds without any clinical manifestations for extended periods, leading to a late diagnosis (stage III or IV) in 45% of patients with AC and SCLC.[30]

Compared with SCLC, AC is slightly more often detected in patients with early-stage disease (I or II).[31] In patients with Stage I SCLC, the 5-year survival rate is 47%, while for AC, this figure is almost twice as high (79%).[28] For Stage II AC and SCLC, the prognosis of the disease worsens significantly. During this period, the 5-year survival rate for patients with SCLC (32%) is also significantly lower than for those with AC (50%). In patients with Stage IV SCLC and AC, this figure drops to only 2% and 6%, respectively.[28]

In SCLC, serum levels of CYFRA 21-1 and CEA have been reported to associate with overall and relapse-free survival.[12] However, these studies were also conducted only in patients with early-stage disease (I–II). Patients with Stage III were examined only in a mixed group with early stages.[32] Information on the role of blood laboratory parameters in predicting relapse-free survival in patients with Stage III SCLC, as well as with Stage III AC, was lacking.

Therefore, the aim of this study was to investigate the potential use of pre-operative levels several indicators, which characterize the cellular composition and metabolism in the blood of patients with Stage III AC and SCLC, to predict their relapse-free survival and make a decision on the therapeutic strategy. A key condition for selecting these indicators was to compare their prognostic value with known marker, including CYFRA 21-1, SCC antigen, and tissue polypeptide antigen (TPA).

2. Materials and methods

2.1. Study population

To substantiate the risk groups for tumor recurrence in patients with operable Stage III (T1-4N0-2) SCLC, a retrospective study was initially undertaken using information from the Belarusian Cancer Registry database. The study included 416 patients with newly diagnosed SCLC (Table 1) and 451 patients with Stage III (T1-4N0-2) AC (Table 2), between January 1, 2015, and December 31, 2021. The period of relapse development after treatment was analyzed based on the results of 1-year observation, due to the majority of NSCLC relapses develop within the first year following treatment.[33]

The investigation of laboratory parameters was carried out in a "study group" of 73 patients with newly diagnosed SCLC (Table 1) and 77 patients with Stage III (T1-4N0-2) AC (Table 2), who were admitted to the thoracic oncology department of the N.N. Alexandrov Republican Scientific and Practical Center for OMR between January 1, 2022, and December 31, 2023. Inclusion criteria included a newly diagnosed stage IIIA or IIIB SCLC, while exclusion criteria were the presence of metachronous or secondary cancer, and patient refusal to participate in the study. No patient dropped out during the first year of observation. Patients with T1N2M0, T2N2M0, T3N1M0, and T3N2M0 underwent surgical tumor resection (surgical volume - R0) followed by 4 courses of adjuvant polychemotherapy, consisting of a combination of vinorelbine (V) at 25 – 30 mg/m^2 and cisplatin (C) at 80 mg/m^2. Meanwhile, in patients with T4N0M0, T4N1M0, and T4N2M0, two courses of neoadjuvant chemotherapy, consisting of a combination of V+C were administered, followed by surgical tumor resection and two additional courses of adjuvant polychemotherapy of V+C.

2.2. Ethical approval and consent

All patients provided written informed consent. The study was performed according to the ethical regulations in Belarus and approved by the Ethics Committee at Belarusian State Medical University, protocol №2 from April 10, 2021.

2.3. Sample collection and analysis

Blood samples were collected from patients of the "study group" before treatment (39 patients with SCLC and 40 patients with AC). Blood cell concentrations were determined on a Sysmex XE-5000 hematology analyzer (Sysmex Group, Japan). Albumin and CRP levels

Table 1. Characteristics of patients with SCLC

Parameter	Retrospective group (%)	Study group (%)	*P*-value
Number of patients, total	416	73	
Age, years (M±σ)	58±29	59±27	0.379
<40	17 (4.1)	2 (2.7)	
41 – 50	72 (17.3)	13 (17.8)	
51 – 60	197 (47.4)	33 (45.2)	
61 – 70	98 (23.6)	20 (27.64)	
>70	32 (7.7)	5 (6.8)	
Gender			0.435
Male	297 (71.4)	56 (76.7)	
Female	119 (28.6)	17 (23.3)	
Smoking status, male			0.286
Former	18 (6.1)	7 (12.5)	
Current	267 (89.9)	46 (82.1)	
Never	12 (4.0)	3 (5.4)	
Smoking status, female			0.315
Former	20 (16.8)	2 (11.8)	
Current	93 (78.2)	14 (82.4)	
Never	6 (5.0)	1 (5.9)	
Stage III (based on 8th edition of TNM staging of lung cancer)			0.421
T1N2M0	46 (11.1)	7 (9.6)	
T2N2M0	69 (16.6)	15 (20.5)	
T3N1M0	66 (15.9)	10 (13.7)	
T4N0M0	48 (11.5)	9 (12.3)	
T4N1M0	50 (12.0)	9 (12.3)	
T3N2M0	76 (18.3)	12 (16.4)	
T4N2M0	61 (14.7)	11 (15.1)	
Degree of tumor differentiation			0.127
G I	150 (36.1)	23 (31.5)	
G II	166 (39.9)	37 (50.71)	
G III	100 (24.0)	13 (17.8)	
Localization			0.519
Right lung	215 (51.7)	41 (56.2)	
Left lung	201 (48.3)	32 (43.8)	

Abbreviation: SCLC: Squamous cell lung cancer.

Table 2. Characteristics of patients with AC

Parameter	Retrospective group (%)	Study group (%)	*P*-value
Number of patients, total	451	77	
Age, years (M ± σ)	59±26	58±28	0.258
<40	14 (3.1)	3 (3.9)	
41 – 50	75 (16.6)	13 (16.9)	
51 – 60	201 (44.6)	38 (49.4)	
61 – 70	107 (23.7)	20 (26.0)	
>70	54 (12.0)	3 (3.9)	
Gender			0.315
Male	329 (72.9)	58 (75.3)	
Female	122 (27.1)	19 (24.7)	
Smoking status, male			0.193
Former	21 (6.4)	7 (12.5)	
Current	285 (86.6)	48 (85.7)	
Never	23 (7.0)	3 (5.4)	
Smoking status, female			0.143
Former	27 (22.1)	5 (26.3)	
Current	86 (70.5)	12 (63.2)	
Never	9 (7.4)	2 (10.5)	
Stage III (based on 8th edition of TNM staging of lung cancer)			0.329
T1N2M0	50 (11.1)	7 (9.1)	
T2N2M0	72 (16.0)	16 (20.8)	
T3N1M0	72 (16.0)	9 (11.7)	
T4N0M0	53 (11.8)	10 (13.0)	
T4N1M0	55 (12.2)	11 (14.3)	
T3N2M0	84 (18.6)	13 (16.9)	
T4N2M0	65 (14.4)	11 (14.3)	
Degree of tumor differentiation			0.724
G I	168 (37.3)	25 (32.5)	
G II	184 (40.8)	39 (50.6)	
G III	99 (21.9)	13 (16.9)	
Localization			0.357
Right lung	249 (55.2)	40 (51.9)	
Left lung	201 (44.8)	37 (48.1)	

Abbreviation: AC: Adenocarcinoma.

were determined using a biochemical analyzer AU680 (Beckman Coulter, USA) with original reagent kits. The SII was calculated using the equation P × N/L, where P, N, and L are platelets, neutrophils, and lymphocytes, respectively. The IPI was calculated as ([CRP] × N)/(L × [albumin]), while the systemic inflammatory response index (SIRI) was calculated using the equation N × M/L, where M represents monocytes.

The concentrations of CYFRA 21-1 and SCC were determined using an automatic Cobas e411 analyzer (Rosche Diagnostics GmbH, Germany), based on the principle of electrochemiluminescence.[11]

The concentrations of CXCL5, CXCL8, TPA, HIF -1α, TuM2 PK, and hyaluronic acid were measured on a Brio automatic ELISA analyzer (Seac, Italy) with ELISA kits (FineTest, China).[12]

Blood cell receptors CXCR1, CXCR2, and CD44v6 were determined using a Navios flow cytometer (Beckman Coulter, USA).[13]

2.4. Statistical analysis

The dependence of the relapse-free period duration on the observation time was assessed using Kaplan-Meier graphs. Single and multivariate Cox proportional hazard models were used to analyze the relationship between the determined laboratory parameters and survival. Comparison of groups with different risks of NSCLC relapse was performed using the Log-Rank test. The data analysis included non-parametric statistics methods (MedCalc Software, Belgium). Differences in the values of the determined parameters between groups of patients were evaluated using Mann–Whitney U-test. The overall prognostic value of the laboratory tests was assessed by constructing receiver operating characteristic (ROC) curves, followed by calculating the area under the ROC curve (AUC).[34] Statistical significance was defined as $P < 0.05$.

3. Results

Kaplan-Meier graphs show that the relapse-free survival of patients with tumor descriptors T4N1M0 and T4N2M0 in SCLC (Figure 1A) and AC (Figure 1C) differs significantly from patients with other TNM descriptors (T1N2M0, T3N1M0, T2N2M0, T4N0M0, and T3N2M0). In patients with T4N1M0 (stage IIIA AC), the relapse-free survival after treatment is lower than in patients with other T and N variants of Stage IIIA. In addition, patients with T3N2M0 (stage IIIB) experience slower disease relapses than the other T and N variants within the same stage. According to the Kaplan-Meier graph (Figure 1A and C), the relapse-free survival of patients 1 year after treatment can be divided into two groups. One is characterized by a relatively high survival rate, includes patients with T1N2M0, T3N1M0, T2N2M0, T4N0M0, and T3N2M0. The other group typically with a shorter relapse-free period includes patients with T4N1M0 and T4N2M0. The difference in survival between these groups is statistically significant, as indicated by the results of the Log-Rank test (Figure 1B and D). The χ^2 value for differences in relapse-free survival between risk groups based on TNM stratification for patients with operable Stage III SCLC is 10.25 ($P = 0.017$), and for patients with AC, it is 10.31 ($P = 0.025$).

We compared several blood laboratory parameters between the two risk groups of relapse-free survival for Stage III SCLC patients (Table 3). Only the proportion of lymphocytes with the CXCR1 receptor, monocytes with the CXCR2 receptor, and the CYFRA 21-1 level showed

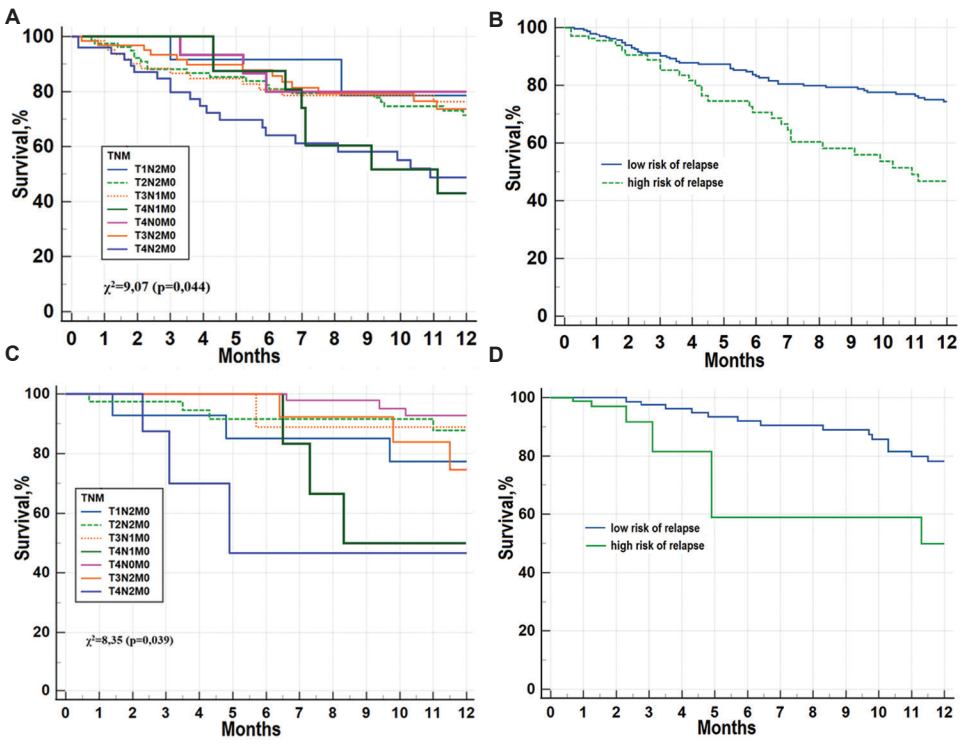

Figure 1. Relapse-free survival of patients with Stage III squamous cell lung cancer (A and B) and adenocarcinoma (C and D), stratified by the TNM classifications over the course of 12 months after the treatment.

Table 3. Level of laboratory parameters in patients (stage III SCLC, study group) with low and high risk of relapse

Indicator	Low risk	High risk	*P*-value
Neutrophilic leukocytes, $\times10^9$/L	5.13 (3.66; 6.57)	5.17 (3.81; 7.14)	0.844
Monocytes, $\times10^9$/L	0.87 (0.68; 1.03)	1.03 (0.86; 1.23)	0.121
Lymphocytes, $\times10^9$/L	2.38 (2.13; 3.07)	2.48 (2.09; 3.29)	0.728
Basophilic leukocytes, $\times10^9$/L	0.03 (0.02; 0.04)	0.04 (0.03; 0.07)	0.260
Eosinophilic leukocytes, $\times10^9$/L	0.14 (0.08; 0.23)	0.22 (0.17; 0.38)	0.298
Platelets, $\times10^9$/L	307.3 (257.8; 387.3)	313.8 (247.3; 391.5)	0.954
Neutrophilic leukocytes/Lymphocytes	1.99 (1.48; 3.28)	1.98 (1.35; 2.81)	0.789
Platelets/Lymphocytes	128.4 (84.5; 201.3)	120.3 (101.2; 137.2)	0.678
Lymphocytes/Monocytes	2.81 (2.01; 3.81)	2.69 (2.17; 3.12)	0.465
Eosinophilic leukocytes/Monocytes	0.177 (0.092; 0.263)	0.291 (0.137; 0.414)	0.297
CXCR1, granulocytes, %	94.6 (92.5; 97.5)	94.6 (93.7; 96.9)	0.825
CXCR1, granulocytes, MFI	32.0 (28.5; 51.5)	32.9 (28.5; 53.0)	0.645
CXCR1, lymphocytes, %	0.90 (0.65; 1.65)	3.55 (2.85; 3.70)	*0.001
CXCR1, lymphocytes, MFI	12.84 (3.50; 15.85)	12.85 (7.06; 14.85)	0.872
CXCR1, monocytes, %	0.61 (0.45; 19.65)	0.85 (0.40; 17.40)	0.316
CXCR1, monocytes, MFI	31.7 (3.6; 41.8)	33.5 (17.9; 35.5)	0.591
CXCR2, granulocytes, %	91.8 (63.1; 95.2)	92.5 (72.9; 95.5)	0.993
CXCR2, granulocytes, MFI	66.4 (68.5; 98.7)	65.5 (51.6; 79.5)	*0.029
CXCR2, lymphocytes, %	15.2 (10.5; 21.5)	15.0 (13.6; 18.5)	1.005
CXCR2, lymphocytes, MFI	12.9 (11.3; 15.5)	13.5 (11.5; 14.5)	0.933
CXCR2, monocytes, %	1.42 (0.60; 2.35)	2.55 (1.90; 3.70)	0.044
CXCR2, monocytes, MFI	62.3 (27.5; 75.5)	63.9 (37.9; 70.5)	0.581
CD44v6, granulocytes, %	2.22 (1.65; 4.15)	2.60 (1.75; 5.05)	0.745
CD44v6, granulocytes, MFI	2.70 (2.45; 3.50)	2.65 (2.10; 6.15)	0.849
CD44v6, lymphocytes, %	0.90 (0.25; 1.45)	1.05 (0.35; 1.75)	0.462
CD44v6, lymphocytes, MFI	3.85 (2.05; 6.50)	4.15 (1.85; 6.50)	0.323
CD44v6, monocytes, %	1.45 (0.25; 3.15)	1.40 (0.15; 1.85)	0.444
CD44v6, monocytes, MFI	3.95 (3.60; 35.45)	4.30 (2.45; 37.20)	0.483
Albumin, g/L	41.3 (38.9; 45.5)	42.5 (41.1; 44.75)	0.518
CRP, mg/dL	1.42 (0.39; 6.05)	1.67 (1.24; 4.85)	0.784
C-RB/Albumin	0.032 (0.01; 0.17)	0.036 (0.03; 0.13)	0.770
CXCL5, pg/mL	914.5 (679.8; 1542.7)	983.6 (753.9; 1713.8)	0.856
CXCL8, pg/mL	111.8 (101.1; 220.5)	118.1 (75.8; 267.3)	0.540
Hyaluronic acid, ng/mL	22.7 (20.8; 35.9)	24.5 (21.8; 25.2)	0.531
HIF-1a, pg/mL	3.17 (2.75; 3.95)	3.47 (2.71; 4.74)	0.922
SCC, ng/mL	2.76 (1.64; 5.37)	2.99 (2.04; 6.05)	0.591
TPA, pg/mL	953.0 (767.9; 1108.7)	1027.3 (805.0; 1229.3)	0.652
TuM2-PK, pg/mL	1830.0 (1493.7; 2173.3)	1829.0 (1428.5; 2329.6)	0.962
CYFRA 21-1, ng/mL	5.06 (3.22; 5.987)	7.53 (5.37; 18.15)	*0.020
IPI	0.057 (0.012; 0.207)	0.092 (0.031; 0.229)	0.679
SII	673.3 (362.6; 1221.3)	597.6 (366.2; 1017.7)	0.641
SIRI	1.57 (1.04; 3.08)	1.84 (1.45; 3.15)	0.554

Note: * $P<0.05$ indicates the value is statistically significant.
Abbreviations: MFI: Mean fluorescence intensity; CXCR1: C-X-C motif chemokine receptor 1; CD44v6: CD44 variant isoform v6; CXCR2: C-X-C motif chemokine receptor 2; CRP: C-reactive protein; CXCL5: C-X-C motif chemokine ligand 5; CXCL8: C-X-C motif chemokine ligand 8; HIF-1a: Hypoxia-inducible factor 1-alpha; SCC: Squamous cell carcinoma antigen; TPA: Tissue polypeptide antigen; TuM2-PK: Tumor type M2 pyruvate kinase; CYFRA 21-1: Cytokeratin 19 fragment antigen 21-1; IPI: Inflammatory prognostic index; SII: Systemic immune-inflammatory index; SIRI: systemic inflammatory response index.

significant differences between patients with a high and low risk of relapse-free survival.

The results of the Cox proportional hazards model analysis confirm the relationship of all 3 parameters with relapse-free survival in both the univariate and multivariate models ($P < 0.05$, Table 4).

In the high-risk group of AC recurrence, only the absolute values of the concentration of monocytes, eosinophilic leukocytes, the ratio between them, the proportion of lymphocytes with the CXCR1 receptor and the CYFRA 21-1 level were significantly higher than in the low-risk group (Table 5). The remaining parameters (SII, IPI, SIRI indices, HIF-1α, CXCL5, CXCL8, TuM2 PK, CXCR1, etc.) did not demonstrate any significant differences between the high- and low-risk groups of patients. Only these five parameters were included in the Cox proportional hazards models, where they were found to significantly affect patient survival (Table 6).

The results of ROC analysis show the prognostic characteristics of the selected indicators for the duration of relapse-free survival in Stage III SCLC (Table 7). The proportion of blood lymphocytes expressing the CXCR1 receptor demonstrated the highest prognostic efficiency (76.7%). The prognostic efficiency was 71.2% and 74.0% for CXCR2-positive monocytes and CYFRA 21-1, respectively. To improve the accuracy of the results, the values of these parameters were subjected to logistic regression analysis. The resulting Equation I includes a combination of these indicators. The prognostic accuracy for the calculated threshold value (> 0.417) was 87.7% (Table 7).

$$Y = \frac{\exp(-5.315 + 0.116 * [CYFRA] + 1.901 * [CXCR1] + 0.279 * [CXCR2])}{1 + \exp(-5.315 + 0.116 * [CYFRA] + 1.901 * [CXCR1] + 0.279 * [CXCR2])} \quad (I)$$

Logistic regression equation for predicting relapse-free survival in patients with Stage III SCLC.

Note: [CYFRA] – the concentration (ng/ml) of the CYFRA 21-1 antigen in the blood serum; [CXCR1] – the relative amount (percentage) of the CXCR1 receptor in lymphocytes; [CXCR2] – the relative amount (percentage) of the CXCR2 receptor in monocytes; "Y" is the result of the regression equation.

According to the AUC expert scale, the prognostic model is classified as "very good" quality with an AUC of 0.831.[14] The optimal threshold value for distinguishing low- and high-risk groups for tumor recurrence is 0.417, with a sensitivity of 84.9%, and specificity of 89.0% (Table 7). Specifically, if the Y value is >0.417, the probability that the patient has a high risk of tumor recurrence is 90.4%. Conversely, if the Y value is ≤0.417, the probability that the patient has a low risk of tumor recurrence is 84.9%.

The performance of the proposed regression model is demonstrated by the Kaplan-Meier graph, which shows relapse-free survival in patients with Stage III SCLC (Figure 2).

The 1-year follow-up shows the distribution of high and low relapse-free survival of patients with Stage III SCLC according to the results of the regression equation Y (Figure 2), which corresponds to TNM stratification (Figure 1B). By the end of the 1st year, the survival rate for the low-risk group was 74% according to TNM stratification, and 76% according to the regression equation of blood parameters. For patients with a high risk, survival after treatment was 47% and 45%, according to TNM stratification and regression equation of blood parameters, respectively. Besides, there is a clear difference between high and low survival of patients based on the regression equation as early as the first month after the treatment, with this difference increasing over time. In contrast, the curve difference in high and low relapse-free survival based on TNM stratification becomes visible only two months after the treatment.

According to the results of ROC analysis for selected parameters in Stage III AC, the highest specificity (84.4%) was found for the relative number of lymphocytes expressing the CXCR1, while its diagnostic sensitivity did not exceed 66.2% (Table 8). The values of other selected indicators showed comparable figures, with sensitivity

Table 4. Cox proportional hazards models for SCLC patients

Indicator	Univariate model			Multivariate model		
	HR	95% CI	*P*-value	HR	95% CI	*P*-value
CXCR1, lymphocytes, %	1.122	1.003 – 1.241	*0.007	1.091	1.001 – 1.181	*0.021
CXCR2, monocytes, %	1.023	1.002 – 1.044	*0.023	1.013	1.001 – 1.025	*0.043
CYFRA 21-1, ng/ml	1.102	1.009 – 1.195	*0.027	1.073	1.009 – 1.137	*0.022

Note: *: $P<0.05$ indicates the value is statistically significant.
Abbreviations: HR: Hazards ratio; 95% CI: 95% Confidence interval; CXCR1: C-X-C motif chemokine receptor 1; CXCR2: C-X-C motif chemokine receptor 2; CYFRA 21-1: Cytokeratin 19 fragment antigen 21-1.

Table 5. Level of laboratory parameters in patients (stage III AC, study group) with low and high risk of relapse

Indicator	Low risk	High risk	*P*-value
Neutrophilic leukocytes, $\times10^9$/L	4.95 (3.56; 6.38)	5.01 (3.71; 6.92)	0.816
Monocytes, $\times10^9$/L	0.62 (0.51; 0.72)	0.93 (0.68; 1.19)	0.032
Lymphocytes, $\times10^9$/L	2.32 (2.08; 2.99)	2.42 (2.02; 3.18)	0.705
Basophilic leukocytes, $\times10^9$/L	0.03 (0.02; 0.04)	0.04 (0.03; 0.06)	0.251
Eosinophilic leukocytes, $\times10^9$/L	0.12 (0.06; 0.21)	0.36 (0.30; 0.45)	0.006
Platelets, $\times10^9$/L	298.1 (248.1; 379.5)	303.7 (244.7; 382.7)	0.923
Neutrophilic leukocytes/Lymphocytes	1.93 (1.43; 3.19)	1.93 (1.34; 2.74)	0.764
Platelets/Lymphocytes	120.6 (82.2; 198.3)	114.9 (99.1; 140.8)	0.656
Lymphocytes/Monocytes	2.75 (1.97; 3.69)	2.57 (2.11; 2.92)	0.449
Eosinophilic leukocytes/Monocytes	0.158 (0.088; 0.287)	0.453 (0.288; 0.682)	*0.022
CXCR1, granulocytes, %	91.6 (89.8; 94.1)	91.7 (89.9; 94.0)	0.798
CXCR1, granulocytes, MFI	31.1 (27.1; 49.6)	30.8 (26.6; 51.4)	0.624
CXCR1, lymphocytes, %	1.60 (0.70; 2.30)	3.56 (3.40; 4.80)	*0.016
CXCR1, lymphocytes, MFI	12.22 (3.44; 15.33)	12.39 (6.85; 14.36)	0.845
CXCR1, monocytes, %	0.59 (0.41; 19.03)	0.79 (0.39; 16.93)	0.306
CXCR1, monocytes, MFI	30.45 (3.51; 39.60)	32.78 (17.39; 33.95)	0.572
CXCR2, granulocytes, %	88.7 (62.2; 93.3)	84.3 (70.7; 92.3)	0.961
CXCR2, granulocytes, MFI	64.5 (66.6; 95.7)	62.8 (50.1; 76.9)	*0.028
CXCR2, lymphocytes, %	14.71 (10.19; 21.02)	15.12 (13.14; 18.09)	0.973
CXCR2, lymphocytes, MFI	12.53 (10.93; 14.52)	12.63 (11.16; 14.16)	0.903
CXCR2, monocytes, %	1.38 (0.58; 2.25)	2.51 (1.84; 3.64)	*0.043
CXCR2, monocytes, MFI	60.5 (26.8; 73.4)	61.7 (36.8; 68.7)	0.562
CD44v6, granulocytes, %	2.12 (1.60; 3.98)	2.49 (1.70; 4.85)	0.720
CD44v6, granulocytes, MFI	2.61 (2.33; 3.44)	2.39 (2.04; 5.92)	0.821
CD44v6, lymphocytes, %	0.88 (0.19; 1.44)	1.03 (0.34; 1.70)	0.448
CD44v6, lymphocytes, MFI	3.67 (1.94; 6.26)	3.93 (1.79; 6.35)	0.313
CD44v6, monocytes, %	1.35 (0.22; 3.07)	1.42 (0.15; 1.75)	0.430
CD44v6, monocytes, MFI	3.79 (3.49; 34.41)	4.25 (2.38; 36.13)	0.468
Albumin, g/L	40.7 (37.7; 43.9)	41.7 (39.8; 43.4)	0.501
CRP, mg/dL	1.37 (0.38; 5.90)	1.62 (1.20; 4.74)	0.758
C-RB/Albumin	0.032 (0.010; 0.146)	0.036 (0.029; 0.116)	0.746
CXCL5, pg/mL	883.4 (655.5; 1506.1)	937.0 (731.2; 1704.1)	0.828
CXCL8, pg/mL	105.6 (99.0; 212.9)	114.6 (73.4; 270.2)	0.522
Hyaluronic acid, ng/mL	23.7 (20.1; 33.9)	23.9 (21.1; 25.4)	0.515
HIF-1a, pg/mL	3.26 (2.68; 3.80)	3.39 (2.63; 4.58)	0.892
SCC, ng/mL	2.67 (1.64; 5.22)	2.89 (1.98; 5.85)	0.572
TPA, pg/mL	941.0 (747.7; 1069.7)	1017.2 (781.8; 1194.5)	0.631
TuM2-PK, pg/mL	1781.3 (1451.8; 2112.3)	1783.7 (1453.6; 2284.0)	0.931
CYFRA 21-1, ng/mL	3.97 (2.22; 4.24)	7.39 (3.60; 12.31)	*0.032
IPI	0.05 (0.01; 0.20)	0.09 (0.03; 0.22)	0.657
SII	669.73 (352.71; 1180.76)	583.49 (367.80; 991.07)	0.620
SIRI	1.54 (1.01; 2.98)	1.77 (1.41; 3.02)	0.536

Note: *: $P<0.05$ indicates the value is statistically significant.
Abbreviations: MFI: Mean fluorescence intensity; CXCR1: C-X-C motif chemokine receptor 1; CD44v6: CD44 variant isoform v6; CXCR2: C-X-C motif chemokine receptor 2; CRP: C-reactive protein; CXCL5: C-X-C motif chemokine ligand 5; CXCL8: C-X-C motif chemokine ligand 8; HIF-1a: Hypoxia-inducible factor 1-alpha; SCC: Squamous cell carcinoma antigen; TPA: Tissue polypeptide antigen; TuM2-PK: Tumor type M2 pyruvate kinase; CYFRA 21-1: Cytokeratin 19 fragment antigen 21-1; IPI: Inflammatory prognostic index; SII: Systemic immune-inflammatory index; SIRI: systemic inflammatory response index.

Table 6. Cox proportional hazards models for selected laboratory parameters in III-stage AC patients

Indicator	Univariate model			Multivariate model		
	HR	95% CI	*P*-value	HR	95% CI	*p*-value
CXCR1, lymphocytes, %	1.137	1.005 – 1.275	0.012*	1.114	1.003 – 1.222	0.017*
CYFRA 21-1, ng/mL	1.215	1.009 – 1.419	0.016*	1.182	1.007 – 1.413	0.016*
Monocytes, $\times 10^9$/L	1.189	1.093 – 1.289	0.022*	1.162	1.074 – 1.254	0.024*
Eosinophilic leukocytes, $\times 10^9$/L	11.337	1.205 – 14.248	0.027*	10.121	1.181 – 13.325	0.031*
Eosinophilic leukocytes/Monocytes	12.153	1.511 – 22.799	0.019*	11.371	1.409 – 21.335	0.021*

Note: $P<0.05$ indicates the value is statistically significant.
Abbreviations: CXCR1: HR: Hazards ratio; 95% CI: 95% Confidence interval; CXCR1: C-X-C motif chemokine receptor 1; CYFRA 21-1: Cytokeratin 19 fragment antigen 21-1.

Table 7. Significance of determining laboratory parameters in blood for predicting low and high risk of recurrence in patients with stage III SCLC (ROC analysis data)

Indicator	TV	SE	SP	PPV	NPV	AUC	ACC
CXCR1, lymphocytes, %	>2.25	75.3	79.5	79.5	76.3	0.729	76.7
CXCR2, monocytes, %	>2.05	69.9	74.0	72.6	71.2	0.687	71.2
CYFRA 21-1, ng/mL	>6.02	80.8	68.5	72.6	76.7	0.711	74.0
Y	>0.417	84.9	89.0	90.4	84.9	0.831	87.7

Abbreviations: TV: Threshold value; SE: Sensitivity; SP: Specificity; PPV: Positive predictive value; NPV: Negative predictive value; AUC: Area under ROC-curve; ACC: Accuracy; CXCR1: C-X-C motif chemokine receptor 1; CXCR2: C-X-C motif chemokine receptor 2; CYFRA 21-1: Cytokeratin 19 fragment antigen 21-1.

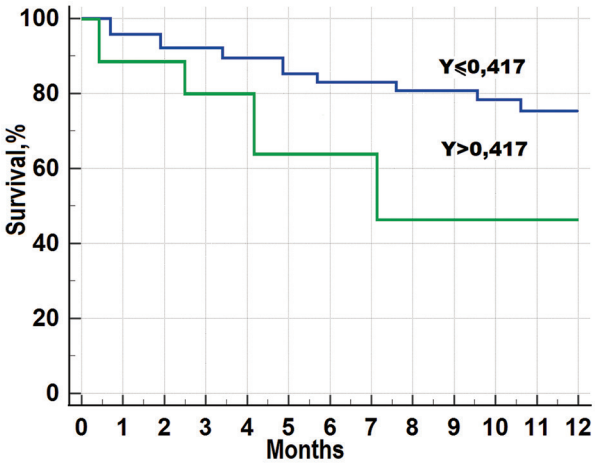

Figure 2. Relapse-free survival of patients with Stage III squamous cell lung cancer according to the results of the regression equation Y.

ranging from 62.3% to 76.6%. As a result, the diagnostic efficiency for predicting relapse-free survival was the lowest for monocyte concentration (64.9%), and the highest for CXCR1-positive lymphocytes (75.3%).

CYFRA 21-1, CXCR1-positive lymphocytes, and eosinophilic leukocytes/monocytes (E/M) ratio were included in the regression analysis. The reliability of the regression equation (2), which uses a combination of these markers to predict the risk of tumor recurrence, is also evidenced by the results of the ROC analysis. The AUC of 0.841 indicates a "very good" quality of the prognostic model.[14] The optimal TV for distinguishing the low- and high-risk groups of tumor recurrence is 0.597 (Table 8). Specifically, if the value of Z > 0.597, the probability that the patient has a high risk of tumor recurrence is 89.6%. Conversely, if the value of Z ≤ 0.597, the probability that the patient has a low risk of tumor recurrence is 84.4%.

$$Z = \frac{\exp(-14.022 + 0.539 * [CYFRA] + 1.294 * [CXCR1] + 12.035 * [E/M])}{1 + \exp(-14.022 + 0.539 * [CYFRA] + 1.294 * [CXCR1] + 12.035 * [E/M])} \quad \text{(II)}$$

Logistic regression equation for predicting of relapse-free survival in patients with Stage III AC.

Note: [CYFRA] – the concentration (ng/ml) of the CYFRA 21-1 antigen in blood serum; [CXCR1] – the relative amount (percentage) of the CXCR1 receptor in lymphocytes; [E/M] – Eosinophilic leukocytes to monocytes ratio; "Z" is the result of the regression equation.

The diagnostic efficiency of predicting the probability of low or high risk of tumor recurrence using the results of the logistic equation increased significantly, reaching 89.0% (sensitivity: 85.7%, specificity: 94.8%) (Table 6). The performance of the proposed regression model, based on

Table 8. Diagnostic significance of determining low and high risk of recurrence of AC (ROC analysis data)

Indicator	TV	SE	SP	PPV	NPV	AUC	ACC
CXCR1, lymphocytes, %	>2.55	66.2	84.4	81.8	70.1	0.715	75.3
CYFRA 21-1, ng/mL	>4.16	71.4	74.0	75.3	70.1	0.709	72.7
Monocytes, $\times 10^9$/L	>0.77	66.2	63.6	66.2	63.6	0.627	64.9
Eosinophilic leukocytes, $\times 10^9$/L	>0.24	62.3	74.0	72.7	63.6	0.651	67.5
Eosinophilic leukocytes/Monocytes	>0.313	76.6	63.6	70.1	70.1	0.673	70.1
Z	>0.597	85.7	94.8	89.6	84.4	0.841	89.0

Abbreviations: TV: Threshold value; SE: Sensitivity; SP: Specificity; PPV: Positive predictive value; NPV: Negative predictive value; AUC: Area under ROC-curve; ACC: Accuracy; CXCR1: C-X-C motif chemokine receptor 1; CYFRA 21-1: Cytokeratin 19 fragment antigen 21-1.

the obtained threshold value Z = 0.597, is demonstrated by the Kaplan-Meier graph of the survival of patients with Stage III AC before progression (Figure 3).

The analysis of the quality of the logistic regression equation (2) shows that all the selected indicators make a significant contribution. This is demonstrated by the significant decrease in the negative doubled value of the logarithm of the likelihood function ($\Delta = 35.1$, $P < 0.05$), indicating the good quality of the proposed model. This is also evidenced by the Hosmer–Lemeshev goodness-of-fit criterion, which was calculated to be 12.1 ($P = 0.158$). The $P > 0.05$ confirms the consistency of the regression equation in classifying patients as having low or high risks of tumor occurrence in AC.

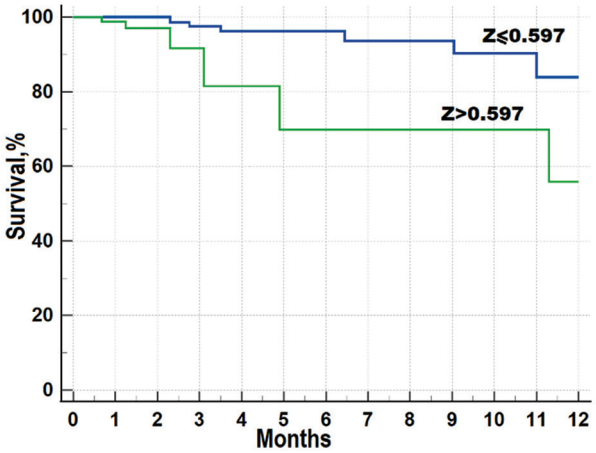

Figure 3. Relapse-free survival of patients with Stage III adenocarcinoma according to the results of the regression equation Z.

4. Discussion

The prognosis for patients with Stage III (T1-4N0-2) NSCLC remains poor, with their overall five-year survival after treatment varying and the median not exceeding 20 months.[1-3] It is vital to anticipate disease progression, not only to save time but also to reduce treatment expenditures by switching to alternative therapeutic strategies.[2,15] One of the approaches to optimizing the effectiveness of treatment in this category of patients is the ability to predict those at high risk of relapse. Despite the relevance and motivation of researchers, prognostic markers of NSCLC remain controversial. As has been demonstrated, the impacts of these prognostic markers are influenced by the histological type of the tumor, the disease stage, and the treatment regimen employed.[17-19,22] However, there is no information regarding the use of prognostic markers for patients with Stage III NSCLC, specifically for the two main histological types: AC and SCLC.

Nevertheless, most researchers have observed a correlation between the concentration of CYFRA 21-1 in blood serum and both relapse-free and overall survival in patients with advanced stages of NSCLC. However, these studies analyzed a mixed cohorts in terms of the disease stage, including patients at early stages of the disease.[3,9,10] It is evident that to obtain such information, cohort studies focusing on patients with relatively homogeneous characteristics and individual histological subtypes of NSCLC are required. The scarcity of information on biomarkers prompted us to conduct our own retrospective and prospective study involving patients with Stage III (T1-4N0-2) SCLC and AC. Based on the pathogenesis of these tumors, we decided to investigate blood cells parameters and proteins, including the CXCR1 and CXCR2 receptors, as well as their ligands, the proinflammatory cytokines CXCL5 and CXCL8.

First, Kaplan-Meier survival analysis of the results from one year of retrospective observation showed a significant difference in relapse-free survival between patients with tumor descriptors T4N1M0 and T4N2M0 in SCLC and AC (high risk of recurrence) and those with other combination of TNM descriptors (T1N2M0, T3N1M0, T2N2M0, T4N0M0, and T3N2M0) (low risk of recurrence).

Then, the results of the TNM stratification were used in the study group to compare the levels of 42 detectable laboratory parameters between patients with high and low

risk of relapse. It has been previously shown that cellular ratios such as N/L, P/L, and L/M, as well as the level of CRP, were known as indicators of the inflammatory reaction associated with tumor development.[15] At the same time, elevated levels of CRP, N/L, and P/L ratios, along with a decreased L/M ratio, have been associated with a poor prognosis in NSCLC. The prognostic value of the N/L ratio was higher compared to P/L ratio.[16] Conversely, findings from other studies suggest that the prognosis of NSCLC is associated with the cellular ratio of P/L rather than the N/L ratio.[17,18] Similar inconsistency of results has also been found in the assessment of the prognostic value of CRP.[19]

The findings of our investigation demonstrated that in Stage III SCLC, only the proportion of lymphocytes expressing the CXCR1 receptor, monocytes expressing the CXCR2 receptor, and the CYFRA 21-1 level showed significant differences between patients with high and low risk of relapse-free survival. For the high-risk group of AC recurrence, the absolute concentrations of monocytes, eosinophilic leukocytes, eosinophilic-to-monocyte ratio, the proportion of lymphocytes expressing the CXCR1 receptor, and the CYFRA 21-1 level, are significantly higher than in the low-risk group. In contrast, other parameters, including SII, IPI, and SIRI indices, the levels of HIF-1α, CXCL5, CXCL8, TuM2 PK, and CXCR1, did not demonstrate significant differences between the high- and low-risk groups of patients.

Therefore, only different parameters were used in the Cox proportional hazards models, which show their equal significance for patient survival. Besides, the results of the multivariate analysis confirmed the results of the univariate analysis, establishing a connection between the selected set of parameters and relapse-free survival. This approach validated the identification of the selected parameters as prognostic markers and assessed their influence on prognosis in terms of odds ratios.

However, the generally accepted criteria for the diagnostic and prognostic value of a specific marker include threshold value, diagnostic sensitivity, specificity, efficiency, etc.[34] The results of the ROC analysis for the selected indicators showed that the proportion of blood lymphocytes expressing the CXCR1 receptor demonstrated the highest prognostic efficiency (75.3%) for predicting relapse-free survival in patients with stage III SCLC. For Stage III AC, the highest specificity (84.4%) was observed for the relative proportion of lymphocytes expressing the CXCR1, while the diagnostic sensitivity of this indicator did not exceed 66.2%. The diagnostic sensitivity values of other selected indicators were in the range of 62.3% to 76.6%. As a result, the diagnostic efficiency in predicting relapse-free survival was the lowest for the concentration of monocytes (64.9%), and the highest for lymphocytes expressing CXCR1 receptor (75.3%).

Three parameters in patients with SCLC (proportions of lymphocytes expressing the CXCR1 receptor, monocytes expressing the CXCR2 receptor, and CYFRA 21-1 level) and three parameters in patients with AC (CYFRA 21-1 level, lymphocytes expressing the CXCR1 receptor, and the E/M ratio) were included in the regression analysis to construct the equation. The resulting equations were expected to exhibit higher sensitivity and specificity in stratifying patients with Stage III AC based on the duration of relapse-free survival. Utilizing a combination of parameters or markers is a common technique for improving prognostic accuracy.[25-30] The convenience of the regression equation lies in its ability to combine several markers into a single numerical value, streamlining prognostic analysis.

All the prognostic characteristics (sensitivity, specificity etc.) were much higher than when using each indicator separately for a similar prognostic purpose. For Stage III SCLC, the prognostic accuracy in predicting relapse-free survival ($Y > 0.417$) was 87.7%.

For patients with Stage III AC, the optimal threshold value for distinguishing between low- and high-risk groups of tumor recurrence was 0.597. Specifically, if the value of $Z > 0.597$, the patient has an 89.6% probability of high tumor recurrence, while for value of $Z \leq 0.597$, 84.4% of patients are correctly predicted to have a low risk of tumor recurrence. The use of the logistic equation significantly improved the probability in accurately predicting a low or high risk of tumor recurrence, reaching an overall accuracy of 89.0% (with sensitivity of 85.7%, and specificity of 94.8%). As illustrated, all these indicators were notably higher than those achieved when using individual parameters for the same prognostic purpose.

The distribution of relapse-free survival into relatively high and low, according to the results of logistic equation, aligns to the results of TNM stratification. In patients with Stage III SCLC, the relapse-free survival at the end of the first year for those at low risk of tumor recurrence is 79% according to TNM stratification and 77% when selected blood parameters are included in the regression equation. For patients with a high risk of tumor recurrence, survival at the end of the 1st year after treatment is 49% and 48%, respectively. Another notable observation is that a clear difference between the high and low survival curves occurs as early as the 1st month after the treatment, with this difference subsequently increasing. In contrast, the differences in the high and low relapse-free survival curves constructed based on TNM appear only two months after the treatment. In subsequent studies, further verification of the proposed prognostic model is needed, not only to

predict the development of the tumor recurrence but also to evaluate the effectiveness of the therapy.

5. Conclusion

A regression equation has been developed to predict the probability of tumor recurrence in patients with Stage III SCLC based on measurements of CYFRA 21-1 concentration, the proportion of lymphocytes expressing the CXCR1 receptor, and blood monocytes expressing the CXCR2 receptor in the pre-operative period. If the result of the equation exceeds 0.417, the risk of relapse is high, and additional treatment measures are required to reduce it. The model's PPV is 90.4%, NPV is 84.9%, sensitivity is 84.9%, and specificity is 89.0%. Meanwhile, for the patients with Stage III AC, a different set of laboratory parameters (CYFRA 21-1 level, lymphocytes expressing the CXCR1 receptor, and the E/M ratio) can be incorporated into the logistic equation to improve the prognosis of relapse-free survival. If the result exceeds 0.597, the risk of relapse after the treatment is high. The model's PPV is 89.6%, NPV is 84.4%, sensitivity is 85.7%, and specificity is 94.8%.

Acknowledgments

We appreciate Professor Victor T. Malkevich, the head of the Laboratory of Thoracic Oncopathology at N.N. Alexandrov National Cancer Center of Belarus, for his kind and fruitful cooperation and discussion on the study design.

Funding

The work was carried out with financial support from the Ministry of Health of the Republic of Belarus, grant 2.17/20220385.

Conflict of interest

The authors declare that they have no competing interests.

Author contributions

Conceptualization: Anatoli D. Tahanovich, Mikalai M. Kauhanka

Investigation: Anatoli D. Tahanovich, Mikalai M. Kauhanka, Alexander V. Kolb, Oxana V. Gotko

Methodology: Anatoli D. Tahanovich, Mikalai M. Kauhanka, Violetta I. Prokhorova

Writing–original draft: Anatoli D. Tahanovich, Mikalai M. Kauhanka, Violetta I. Prokhorova

Writing–review & editing: Anatoli D. Tahanovich, Mikalai M. Kauhanka

Ethics approval and consent to participate

All patients gave written voluntary consent to participate in the study. The study was approved by the decision of the Biomedical Ethics Committee of the educational institution "Belarusian State Medical University" (protocol of the Committee meeting №2 dated 10/04/2021).

Consent for publication

Not applicable.

Availability of data

Data used in this work can be made available to the readers by contacting the corresponding author.

References

1. Siegel RL, Miller KD, Wagle NS, Jemal A. Cancer statistics. *CA Cancer J Clin*. 2023;73(1):17-48.

   doi: 10.3322/caac.21763

2. Araghi M, Mannani R, Heidarnejad MA, *et al*. Recent advances in non-small cell lung cancer targeted therapy; an update review. *Cancer Cell Int*. 2023;23(1):162.

   doi: 10.1186/s12935-023-02990-y

3. Lababede O, Meziane MA. The eighth edition of TNM staging of lung cancer: Reference chart and diagrams. *Oncologist*. 2018;23(7):844-848.

   doi: 10.1634/theoncologist.2017-0659

4. Wu G, Pan B, Shi H, *et al*. Neutrophils' dual role in cancer: From tumor progression to immunotherapeutic potential. *Int Immunopharmacol*. 2024;140:112788.

   doi: 10.1016/j.intimp.2024.112788

5. Carvalho S, Troost EG, Bons J, Menheere P, Lambin P, Oberije C. Prognostic value of blood-biomarkers related to hypoxia, inflammation, immune response and tumour load in non-small cell lung cancer - a survival model with external validation. *Radiother Oncol*. 2016;119(3):487-494.

   doi: 10.1016/j.radonc.2016.04.024

6. Ha H, Debnath B, Neamati N. Role of the CXCL8-CXCR1/2 axis in cancer and inflammatory diseases. *Theranostics*. 2017;7(6):1543-1588.

   doi: 10.7150/thno.15625

7. Wu K, Yu S, Liu Q, Bai X, Zheng X, Wu K. The clinical significance of CXCL5 in non-small cell lung cancer. *Onco Targets Ther*. 2017;10:5561-5573.

   doi: 10.2147/OTT.S148772

8. Tahanovich AD, Kauhanka NN, Prohorova VI, Murashka DI, Gotko OV. Determination of the risk of tumor progression in patients with early stages of adenocarcinoma and squamous cell lung carcinoma based on laboratory parameters. *Biochem Moscow Suppl Ser B*. 2022;16:154-163.

   doi: 10.1134/S1990750822020081

9. Tahanovich AD, Kauhanka NN, Kolb AV, *et al*. Prediction of

relapse-free survival of patients with stage III non-small cell lung cancer after treatment. The role of the concentration of blood cells. *Lab Diagn Vost Eur.* 2022;2:148-162. in Russian.

doi: 10.34883/PI.2022.11.2.013

10. Tahanovich AD, Kauhanka NN, Murashka DI, *et al.* Preoperative blood markers for prediction of recurrence-free survival after surgical treatment of patients with stage III lung adenocarcinoma. *Rus Clin Lab Diagn.* 2022;67(11):640-646. in Russian.

doi: 10.51620/0869-2084-2022-67-11-640-646

11. Duffy MJ, O'Byrne K. Tissue and blood biomarkers in lung cancer: A review. *Adv Clin Chem*. 2018;86:1-21.

doi: 10.1016/bs.acc.2018.05.001

12. Muley T, Rolny V, He Y, *et al*. The combination of the blood based tumor biomarkers cytokeratin 19 fragments (CYFRA 21-1) and carcinoembryonic antigen (CEA) as a potential predictor of benefit from adjuvant chemotherapy in early stage squamous cell carcinoma of the lung (SCC). *Lung Cancer*. 2018;120:46-53.

doi: 10.1016/j.lungcan.2018.03.015

13. Niklinski J, Furman M, Burzykowski T, *et al*. Preoperative CYFRA 21-1 level as a prognostic indicator in resected primary squamous cell lung cancer. *Br J Cancer.* 1996;74(6):956-960.

doi: 10.1038/bjc.1996.464

14. Holdenrieder S, Wehnl B, Hettwer K, Simon K, Uhlig S, Dayyani F. Carcinoembryonic antigen and cytokeratin-19 fragments for assessment of therapy response in non-small cell lung cancer: A systematic review and meta-analysis. *Br J Cancer.* 2017;116(8):1037-1045.

doi: 10.1038/bjc.2017.45

15. Svaton M, Blazek J, Krakorova G, *et al*. Prognostic role for CYFRA 21-1 in patients with advanced-stage NSCLC treated with bevacizumab plus chemotherapy. *Anticancer Res*. 2021;41(4):2053-2058.

doi: 10.21873/anticanres.14974

16. Baek AR, Seo HJ, Lee JH, *et al.* Prognostic value of baseline carcinoembryonic antigen and cytokeratin 19 fragment levels in advanced non-small cell lung cancer. *Cancer Biomark*. 2018;22(1):55-62.

doi: 10.3233/CBM-170885

17. Vodicka J, Skala M, Sebek J, *et al*. The role of serum tumor markers in follow-up after surgical treatment of malignant lung tumors. *Anticancer Res*. 2021;41(10):5117-5122.

doi: 10.21873/anticanres.15328

18. Zhang J, Huang SH, Li H, *et al.* Preoperative lymphocyte count is a favorable prognostic factor of disease-free survival in non-small-cell lung cancer. *J Med Oncol*. 2013;30(1):352-357.

doi: 10.1007/s12032-012-0352-3

19. Song X, Chen D, Yuan M, Wang H, Wang Z. Total lymphocyte count, neutrophil-lymphocyte ratio, and platelet-lymphocyte ratio as prognostic factors in advanced non-small cell lung cancer with chemoradiotherapy. *Cancer Manag Res.* 2018;10:6677-6683.

doi: 10.2147/CMAR.S188578

20. Agassandian M, Shurin GV, Ma Y, Shurin MR. C-reactive protein and lung diseases. *Int J Biochem Cell Biol.* 2014;53:77-88.

doi: 10.1016/j.biocel.2014.05.016

21. Huang Q, Diao P, Li CL, *et al*. Preoperative platelet-lymphocyte ratio is a superior prognostic biomarker to other systemic inflammatory response markers in non-small cell lung cancer. *Medicine (Baltimore).* 2020;99(4):e18607.

doi: 10.1097/MD.0000000000018607

22. Li X, Qin S, Sun X, *et al*. Prognostic significance of albumin-globulin score in patients with operable non-small-cell lung cancer. *Ann Surg Oncol.* 2018;25(12):3647-3659.

doi: 10.1245/s10434-018-6715-z

23. Okugawa Y, Toiyama Y, Yamamoto A, *et al.* Lymphocyte-C-reactive protein ratio as promising new marker for predicting surgical and oncological outcomes in colorectal cancer. *Ann. Surg.* 2020;272(2):342-351.

doi: 10.1097/SLA.0000000000003239

24. Yang R, Chang Q, Meng X, Gao N, Wang W. Prognostic value of systemic immune-inflammation index in cancer: A meta-analysis. *J Cancer.* 2018;9(18):3295-3302.

doi: 10.7150/jca.25691

25. Dirican N, Dirican A, Anar C, *et al.* New inflammatory prognostic index, based on C-reactive protein, the neutrophil to lymphocyte ratio and serum albumin is useful for predicting prognosis in non-small cell lung cancer cases. *Asian Pac J Cancer Prev.* 2016;17(12):5101-5106.

doi: 10.22034/APJCP.2016.17.12.5101

26. Wang Y, Hu X, Xu W, Wang H, Huang Y, Che G. Prognostic value of a novel scoring system using inflammatory response biomarkers in non-small cell lung cancer: A retrospective study. *Thorac Cancer*. 2019;10(6):1402-1411.

doi: 10.1111/1759-7714.13085

27. van den Heuvel M, Holdenrieder S, Schuurbiers M, *et al.* Serum tumor markers for response prediction and monitoring of advanced lung cancer: A review focusing on immunotherapy and targeted therapies. *Tumour Biol.* 2024;46(S1):S233-S268.

doi: 10.3233/TUB-220039

28. Wang BY, Huang JY, Chen HC, *et al*. The comparison between adenocarcinoma and squamous cell carcinoma in lung cancer patients. *J Cancer Res Clin Oncol*. 2020;146(1):43-52.

doi: 10.1007/s00432-019-03079-8

29. Lu J, Wang Y, Yan M, *et al*. High serum haptoglobin level is associated with tumor progression and predicts poor prognosis in non-small cell lung cancer. *Oncotarget*. 2016;7(27):41758-41766.

doi: 10.18632/oncotarget.9676

30. Burki TK. Late detection of lung cancer. *Lancet Oncol*. 2014;15(13):e590.

doi: 10.1016/S1470-2045(14)70371-7

31. Maeda R, Yoshida J, Ishii G, Hishida T, Nishimura M, Nagai K. Risk factors for tumor recurrence in patients with early-stage (stage I and II) non-small cell lung cancer: Patient selection criteria for adjuvant chemotherapy according to the seventh edition TNM classification. *Chest*. 2011;140(6):1494-1502.

doi: 10.1378/chest.10-3279

32. Berghmans T, Paesmans M, Sculier JP. Prognostic factors in stage III non-small cell lung cancer: A review of conventional, metabolic and new biological variables. *Ther Adv Med Oncol*. 2011;3(3):127-138.

doi: 10.1177/1758834011401951

33. Yun JK, Lee GD, Choi S, *et al*. Various recurrence dynamics for non-small cell lung cancer depending on pathological stage and histology after surgical resection. *Transl Lung Cancer Res*. 2022;11(7):1327-1336.

doi: 10.21037/tlcr-21-1028

34. Hosmer DW, Lemeshow S, Sturdivant RX. *Applied Logistic Regression*. 3rd ed. Hoboken, NJ: John Wiley & Sons; 2013.

doi: 10.1002/9781118548387

ACCSCIENCE PUBLISHING

Global Translational Medicine

ORIGINAL RESEARCH ARTICLE

Prediction of in-stent restenosis based on systematic and retrospective analyses

Alina M. Enikeeva[1,2], Liutsiia Yu. Gazizova[2], Igor V. Buzaev[1], Irina E. Nikolaeva[1,2], Irina A. Lakman[3], Haibo Jia[4], Tagir Aminov[1,2], Elena A. Badykova[1], and Naufal Sh. Zagidullin[1]*

[1]Department of Internal Diseases, Bashkir State Medical University, Ufa, Republic of Bashkortostan, Russia

[2]Department of Cardiology, Republic Cardiological Centre, Ufa, Republic of Bashkortostan, Russia

[3]Laboratory for the Study of Socio-Economic Problems of the Regions, Ufa University of Science and Technology, Ufa, Republic of Bashkortostan, Russia

[4]National Key Laboratory of Frigid Zone Cardiovascular Diseases, The Second Affiliated Hospital of Harbin Medical University, Harbin, Heilongjiang, China

(This article belongs to the *Special Issue: Special Issue of Global Translational Medicine in the Fourth RCCCDT-2024*)

Abstract

Coronary restenosis is a pressing challenge in cardiovascular diseases with an annual incidence of 3 – 4%. The aim of the study was to assess the influence of known risk factors in predicting coronary restenosis in a systematic analysis and an original retrospective survey. In the first stage, we performed a systematic review of restenosis risk factors using the Preferred Reporting Items for Systematic Reviews and Meta-Analyses (PRISMA) protocol. In the second stage, we searched for the restenosis risk factors in 15,000 patients who had undergone coronary angiography, considering risk factors identified during the first stage. From the second stage, we identified 516 patients with restenosis versus 282 patients without restenosis. Coronary risk factors included male sex (hazard ratio [HR] = 2.194; confidence interval [CI]: 1.5 – 3.22) and history of myocardial infarction (HR = 1.098; CI: 1.05 – 1.15). Moderate-diameter stenosis (2.75 – 3.5 mm) exhibited a protective effect on restenosis (HR = 0.713; CI: 0.58 – 0.87), whereas small-diameter stenosis did not. Drug-eluting stents reduced the risk of restenosis (HR = 0.554; CI: 0.41 – 0.75). The risk factors for coronary restenosis included male sex, history of myocardial infarction, small-diameter stent, and the use of bare-metal stents.

Keywords: Coronary heart disease; Coronary restenosis; Risk factors; Drug-eluting stent; Bare metal stent

***Corresponding author:**
Naufal Sh. Zagidullin
(znaufal@mail.ru)

Citation: Enikeeva AM, Gazizova LY, Buzaev IV, *et al.* Prediction of in-stent restenosis based on systematic and retrospective analyses. *Global Transl Med.* 2024:3(4):4957. doi: 10.36922/gtm.4957

Received: September 26, 2024

Accepted: November 22, 2024

Published Online: December 26, 2024

1. Introduction

Annually, cardiovascular diseases (CVD) claim millions of lives worldwide and have remained the leading cause of mortality for decades.[1] In Europe, over 60 million potential years of life are lost annually due to CVD.[2] According to the Russian Statistical Yearbook 2021,[3] almost half of all deaths result from CVD, with over 80% of them being caused by coronary heart disease (CHD). The number of CVD-related deaths per total population

represents the standardized mortality rate and remains high in the Russian Federation (590.9 in men and 576.3 in women). For comparison, the standardized mortality rate for cancer was 397.4 in 2021.[4] However, over the past 20 years in Russia, CVD mortality has decreased by 30% since 2003.[5] The availability of high-tech interventions continues to grow, with the number of percutaneous coronary interventions, including primary procedures, increased more than 20 times, contributing to a decrease in CVD mortality. It is also crucial to address the risk factors, which can be classified as non-modifiable (male sex, age, and burdened family history) and modifiable. Risk factors, such as obesity, diabetes mellitus (DM), hypertension, dyslipidemia, alcohol abuse, and smoking, are well-studied and modifiable.[6] However, current knowledge of risk factors allows for the prediction of CHD in only 50% of cases.[7] Likewise, even when these risk factors are addressed, the disease often progresses, and acute CHD continues to develop and relapse.

In addition, successful surgical treatment and adequate medical therapy do not guarantee protection from acute CHD recurrence, as one in five patients with acute coronary syndrome develops a recurrent event within 3 years of the intervention.[8]

Since the introduction of coronary angioplasty some 40 years ago, late stent thrombosis, in-stent restenosis, and *de novo* neo-atherosclerosis have been recognized as major causes of disease recurrence in long-term prognosis. In almost 50% of cases, re-stenosis of a previously implanted stent results in unstable angina pectoris, with 18.7% of patients developing non-ST-elevation myocardial infarction (NSTEMI) and 8.5% of patients developing ST-elevation myocardial infarction (STEMI).[9]

In-stent restenosis is defined as the re-narrowing of a vessel lumen diameter after percutaneous coronary intervention. Angiographically, it is identified as recurrent diameter stenosis >50% at the stent segment or its edges (5-mm segments adjacent to the stent).[10] Restenosis results from vascular injury due to balloon inflation and stent implantation. Inflammation that occurs in response to mechanical stretch, endothelial exposure, and subintimal hemorrhage plays a key role by triggering a cascade of proliferative processes.[11,12] In-stent restenosis significantly aggravates the CHD prognosis. Hence, identifying the predictors of coronary restenosis is essential for adjusting treatments and improving treatment outcomes.

The aim of the study was to assess the influence of known risk factors in predicting coronary restenosis in high-risk patients via two stages: (i) systematic analysis and (ii) retrospective analysis.

2. Methods

2.1. Systematic analysis

In the first stage, we performed a systematic analysis of available sources to identify restenosis predictors using data from Russian and foreign publications. The search criteria included scientific papers published not earlier than 2002 that covered analysis of risk factors for coronary in-stent restenosis, as well as long-term outcomes, endpoints, and survival rates of patients after stenting, based on the type of stent coating (bare metal stent [BMS] or drug-eluting stent [DES]). A mandatory selection criterion was the availability of literature information on the risk ratio of in-stent restenosis or data for calculating the corresponding risk ratio. We used PubMed and eLibrary to search for the articles. The keywords included "in-stent restenosis," "clinical presentation," "outcome," "bare metal stent," "drug-eluting stent," "target lesion revascularization," "myocardial infarction," and "percutaneous coronary intervention." The search used OR and AND operators. The meta-analysis included cohort and case–control studies, both prospective and retrospective. These studies evaluated predictors of restenosis, such as smoking, DM, arterial hypertension, dyslipidemia, chronic kidney disease (CKD), dialysis, previous myocardial infarction, chronic heart failure, respiratory failure, cerebrovascular disease, and Leriche syndrome. In addition, clinical manifestations of in-stent restenosis were evaluated (stable angina, unstable angina, and myocardial infarction), and endpoints were assessed depending on stent coating. The endpoints were hospitalization, repeat revascularization, myocardial infarction, stent thrombosis, and death. The Preferred Reporting Items for Systematic Reviews and Meta-Analyses (PRISMA) protocol was used for the search procedure.

2.2. Retrospective analysis

In the second stage, we analyzed 15,000 medical records of stented patients from 2015 to 2020 (Figure 1) in a single center (Republican Cardiological Center, Ufa, Russia). Survival status and the occurrence of coronary restenosis were recorded using the remote data capture system, Program for Medical Cases Monitoring (ProMed), which is used in all the medical institutions in the region.

The inclusion criteria were primary or scheduled percutaneous coronary intervention, namely coronary artery stenting. The exclusion criteria were: (i) Patients younger than 18 years of age; (ii) early restenosis or stent thrombosis (up to 30 days of percutaneous coronary intervention); (iii) transplanted heart; (iv) severe renal or hepatic insufficiency; (v) severe connective tissue diseases

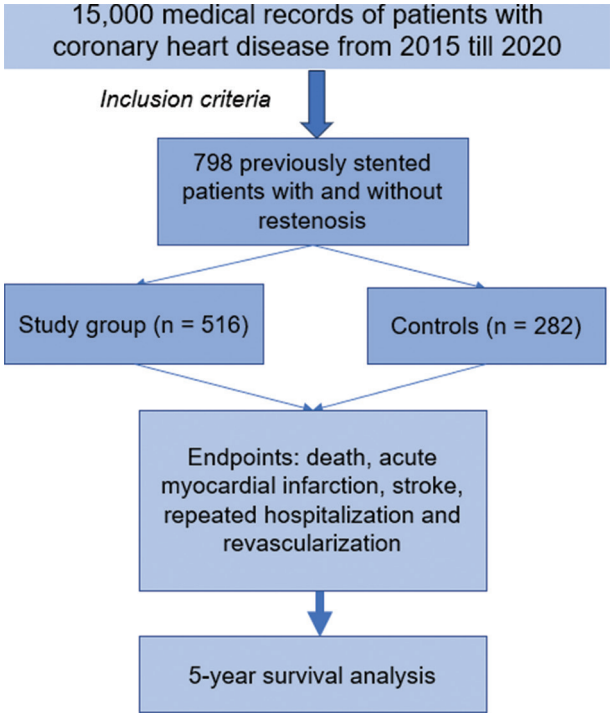

Figure 1. Retrospective analysis design

requiring continuous glucocorticosteroids and another controller therapy; (vi) familial hypercholesterolemia; and (vii) cancer that required chemotherapy and radiation therapy after percutaneous coronary intervention.

2.3. Statistical analysis

Patients were divided into two groups based on the absence (control group) or presence (restenosis group) of re-stenosis requiring repeat percutaneous coronary intervention. The restenosis group included 516 patients, while the control group included patients without hemodynamically significant restenosis. The endpoints (death, acute myocardial infarction, acute cerebrovascular accident, repeat hospitalization, and repeat revascularization) were determined for all patients within 5 years. R Studio was used in packages ("survival," "survMisc," and "survminer"). Single- and multivariate survival analyses (e.g., Cox regressions) and Kaplan-Meier analysis were performed. The latter was used to estimate the differences in function *S(t)* before the development or absence of restenosis in different stent types:

$$S(t) \qquad [\frac{(n \quad j)}{(n-j+\ )}] \tag{I}$$

where n is the total number of observations; d_j is equal to 1 if the event occurred during the considered observation period or 0 – if the event was censored.

To illustrate the results of the evaluation, Kaplan-Meier curves were plotted on the survival function graph (with restenosis as the endpoint), where the x-axis is the observation period (before the development or absence of restenosis; defined in months). The log-rank test was used to compare the time intervals before restenosis in groups with or without a certain variable (e.g., stent type [DES vs. BMS]), with the null hypothesis stating no differences between the groups. The significance level for rejecting the null hypothesis was $P < 0.05$.

To confirm the influence of potential risk predictors identified in the first stage of the study on restenosis development, we performed survival analysis using Cox regression with multiple variables:

$$\lambda_i(t) = \lambda_0(t) \cdot \exp(\beta_1 x_{1i} + \ldots + \beta_k x_{ki} + \beta_0) \tag{II}$$

where $\lambda_i(t)$ is the risk of restenosis in the i-th patient during the observation period t; $\lambda_0(t)$ is the baseline risk of restenosis in each patient by default; $x_{1i}, \ldots x_{ki}$ is the potential risk factor(s) of restenosis; $\beta_1, \ldots \beta_k$ is the coefficient(s) of the regressors identified in the first stage of the study and evaluated using the partial likelihood method; and β_0 is the intercept. The coefficients of the regressors in the Cox model were estimated using the maximum partial likelihood method with the partial likelihood function according to the Efron and the Breslow formulas. For both formulas (Equations I and II), the Akaike and Schwartz information criteria values (AIC and BIC) were calculated. The model was estimated using the Efron partial likelihood method, as it yielded lower Akaike and Schwartz information criteria values compared to the Breslow method (for Breslow: AIC=3282.33, BIC=3313.58; for Efron AIC=3280.96, BIC=3312.21). The form of the partial likelihood function was selected based on the smallest information criteria values.

Statistical significance of risk predictors was tested according to the Wald test at a significance level of $p < 0.05$; the null hypothesis was the assumption that the regressor coefficient = 0, that is, there was no impact of the investigated factor on the risk of restenosis. The Wald statistic (Z_w) was calculated as follows:

$$Z_W = \hat{\beta} \Big/ SE(\hat{\beta}) \tag{III}$$

where $SE(\hat{\beta})$ is the estimated standard error $\hat{\beta}$.

To assess the quality of the Cox model, the likelihood ratio (LR) test was performed with the null hypothesis of no significance in the general model. The hypothesis was rejected in favor of the alternative at $P < 0.05$. Harrell's

concordance (C)-index (CIH), the measure of explained randomness (R^2_{mer}), and the measure of explained deviation (R^2_{mev}) were considered as the quality metrics of the Cox model parameterization. The measures are defined as follows:

$$R^2_{mer} = 1 - \exp\left(\frac{2}{n}(\bar{l} - l)\right) \quad \text{(IV)}$$

$$R^2_{mev} = \frac{R^2_{mer}}{\left(R^2_{mer} + \pi / 6 \cdot (1 - R^2_{mer})\right)} \quad \text{(V)}$$

where l is the logarithm of the partial likelihood function, $\bar{l}$ is the logarithm of the restricted (0 for all regressors) partial likelihood function, and n is the number of patients. It was believed that the explanatory power of the Cox model is higher if the quality metrics are close to 1.

Simulation results were interpreted based on the calculation using estimated hazard ratio (HR) regression coefficients:

$$HR(x_i) = \frac{\lambda(t \mid x_i)}{\lambda_0(t)} = \exp\left(x_i \beta\right) \quad \text{(VI)}$$

In addition, we assumed that the baseline risk function $\lambda_i(t)$ depends on time t, but the risk factors were not independent of the time t. The 95% confidence interval (CI) was calculated using the Greenwood formula:

$$D\left(\hat{S}(t)\right) \sim \left(\hat{S}(t)\right)^2 \sum_{j:t_j \le t} \frac{d_j}{n_j\left(n_j - d_j\right)} \quad \text{(VII)}$$

3. Results

3.1. Systematic analysis results

In the first stage, we analyzed publications in the PubMed and eLibrary databases. A total of 13,775 full-text articles were identified using the keyword "coronary in-stent restenosis" (PubMed: 11,950; eLibrary: 1,825). At the primary screening stage, 997 articles remained after excluding duplicates and articles that did not correspond to the topic. After a detailed review of the abstracts, 61 full-text publications were selected for further analysis. The aim of the systematic analysis was to identify potential risk factors for coronary restenosis. In the final selection, only six full-text articles remained (Table 1), enabling the identification of 12 restenosis variables. A detailed analysis of publications matching the search criteria is presented in Figure 2.

3.2. Retrospective analysis results

In the second stage, we analyzed the identified risk factors for coronary restenosis from the systematic review. We collected all data required based on the retrospective analysis from 2015 to 2020 (5-year sample). After excluding incomplete and low-quality data, the total sample size was 798 patients and nine risk factors (variables). The number of risk factors was reduced from 12 to 9, as three manuscripts lack qualitative information for quantitative analysis. Potential risk predictors were selected based on the scientific articles reviewed. In 516 cases, restenosis developed within 5 years (60 months) after stent implantation. In 282 cases, no hemodynamically significant restenosis was reported. Table 2 presents the comparison of two groups (patients with vs. without restenosis) based on the frequency of coronary restenosis risk factors. The median (*Me*), as well as the first (Q_i) and third quartiles (*Q3*), were calculated for continuous attributes, while the incidence (%) and relative frequency (%) were calculated for frequency attributes. The *P*-level for frequency attributes was calculated based on X^2 (the criterion with likelihood correction for continuous attributes) using the Wald-Wolfowitz runs test.

Group comparisons indicated that the following predictors are statistically significant ($P < 0.05$): male sex, history of myocardial infarction, nominal stent diameter, and the presence of stent coating.

Figure 3 displays the survival curves (before restenosis) of patients with DES/BMS. The graph illustrates that the type of stent significantly affects restenosis development. BMS in the first few months leads to a dramatic increase in the incidence of restenosis, and the likelihood of no adverse events occurring within 60 months is drastically reduced. This is confirmed by the log-rank test, which rejects the null hypothesis of no difference in the likelihood of restenosis at 60 months after BMS/DES stenting ($P < 0.001$).

In 2016, Buccheri *et al.*[13] performed a systematic review of multiple studies, evaluating risk factors, survival, and the frequency of adverse events in patients who underwent implantation of different stents. Our results are consistent with the findings of this review.

Using the selected risk factors as potential predictors for coronary restenosis, a Cox model was plotted. The model was estimated using the Efron partial likelihood method, as it yielded lower Akaike and Schwartz information criteria values compared to the Breslow method. Table 3 presents Cox regression coefficient values for each predictor, calculated based on the HR, the 95% CI limits (determined using Greenwood's formula), and the corresponding *p*-level of error for rejecting the null hypothesis (i.e., model coefficient estimate = 0). Model quality is relatively high: CIH (Harrell's C-index) = 0.615; R^2_{mer} = 0.71; R^2_{mev} = 0.74. Moreover, the LR test confirmed the significance of the overall Cox model equation (LR = 15.84; $P < 0.001$).

Table 1. Systematic analysis of studies related to coronary stenosis predictors

Study topic	Number of patients	Number of restenosis cases	Analysis tool	Restenosis predictors identified
Predictors of restenosis after DES implantation in one or more coronary arteries	1,795	125	Multivariate analysis	Lesion length, stent length, minimum lumen diameter after intervention, minimum lumen diameter before intervention, reference artery size, complex lesions, and use of the paclitaxel-eluting stent
Occurrence and predictive factors of restenosis in CHD patients with sirolimus-eluting stent implantation	398	37	Multivariate analysis	Demographic characteristics (age), cardiovascular risk factors (hypertension and hyperuricemia), biochemical indexes (fasting blood glucose, total cholesterol, LDL-C, and HsCRP), cardiac function index (cardiac troponin I), lesion features (multivessel artery lesions, target lesion at left circumflex artery (LCX), two target lesions, length of target lesion, and operation procedure (length of stent) correlated with higher restenosis risk; age, hypertension, diabetes mellitus, LDL-C, HsCRP, and target lesion at LCX were independent predictive factors for increased restenosis risk
Predictors of restenosis after implantation of 2.5-mm diameter stents in small coronary arteries	134	55	Univariate and multivariate analysis	Diabetes mellitus, acute coronary syndrome, lesion length, bifurcation lesion, lower LVEF, stent strut, stent/artery ratio, and stent length were identified as predictors of restenosis by univariate analysis; subsequent multivariate analysis revealed that lower LVEF (OR: 3.37; P=0.01), bifurcation lesion (OR: 2.47; P=0.04), thicker stent strut (OR: 2.30; P=0.04), and longer stent length (OR: 1.05; P=0.02) were significant predictors of restenosis
Relationship between the level of circulating CD45+platelets and development of restenosis after implantation of DES in patients with CHD	126	42	Logistic regression; ROC analysis	Five significant risk factors of restenosis were identified by binary comparisons of different variables: level of CD45-positive platelets, diabetes mellitus, small vessel of stent, number of simultaneously implanted stents in one patient, and lesion length demonstrates ISR risk (OR: 22.8; P<0.001); ROC analysis demonstrated a high prognostic value of the logit model (AUC: 0.87; P<0.001)
CHA_2DS_2-Vasc and CHA_2DS_2-Vasc-HS scores are poor predictors of ISR in patients with coronary DES	358	98	Multivariate logistic regression analysis	Compared with the non-ISR group, more patients in the ISR group had diabetes mellitus and received stents with smaller diameters but longer lengths; multivariate logistic regression analyses demonstrated that stent diameter, follow-up duration, and glycosylated hemoglobin were independent risk factors for ISR
Use of NLR for prediction of ISR in bifurcation lesions	181	47	ROC analysis	NLR (before stenting; P<0.001) was significantly higher in the group with restenosis; NLRΔ was found to be a significant independent predictor of ISR from the multivariate logistic regression analysis; NLRΔ level>0.58 mg/dL had 81.8% sensitivity and 93.5% specificity for the prediction of ISR; NLR level (after stenting) >3.43 mg/dL predicted ISR with 45.5% sensitivity and 95.8% specificity; NLRΔ was the strongest independent predictor of ISR (P=0.001).

Abbreviations: DES: Drug-eluting stent; CHD: Coronary heart disease; HsCRP: High-sensitivity C-reactive protein; ISR: In-stent restenosis; LDL-C: Low-density lipoprotein; LVEF: Left ventricular ejection fraction; NLR: Neutrophil-to-lymphocyte ratio; OR: Odds ratio; AUC: Area under the curve; ISR: In-stent restenosis.

Table 2. Comparison of two groups based on the frequency of coronary restenosis risk factors

Restenosis risk predictors	Patients without restenosis (*n*=282)	Patients with restenosis (*n*=516)	*P*
Smoking	14 (25.9%)	57 (15.3%)	0.476
Sex (male/female)	202/80	402/113	0.001**
Family history	2 (9%)	39 (10.48%)	0.993
Atrial fibrillation	35 (12.41%)	47 (9.49%)	0.176
Prior myocardial infarction	178 (63.12%)	368 (73.9%)	0.033*
Arterial hypertension	257 (91.46%)	465 (93.56%)	0.065
Nominal stent diameter (<2.5 mm)	3 (2.75; 3.5)	3 (2.75; 3.5)	<0.001***
Patient's age at the first stenting, years	61.68 (55.09; 67.05)	59.53 (54.29; 66.19)	0.123
Stent type (BMS%)	90 (31.25%)	68 (17.66%)	0.001**

Note: Data presented as *Me* (Q_1; Q_3) or frequency (%); *P<0.05; **P<0.01; ***P<0.001.
Abbreviations: BMS: Bare metal stent; *Me*: Median; Q_1: First quartile; Q_3: Third quartile.

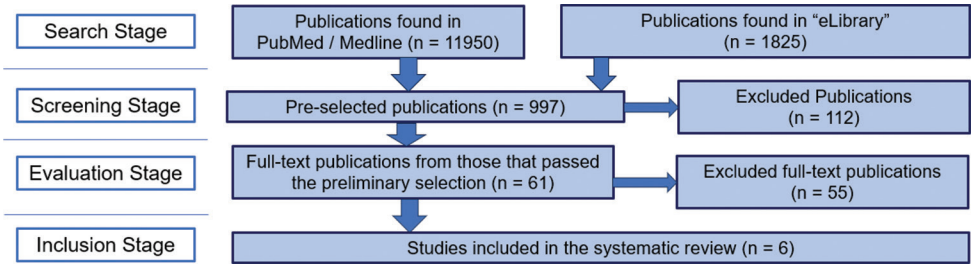

Figure 2. Publication selection process

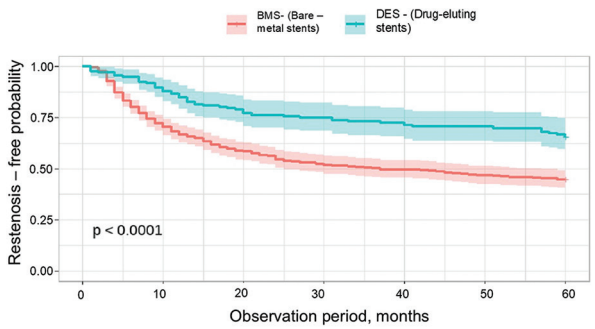

Figure 3. Kaplan-Meier curves to evaluate function before restenosis depending on the presence or absence of stent coating.

The simulation results led to the following observations:

(i) Male sex almost doubles the likelihood of restenosis risk (HR = 2.194; 95% CI: 1.5 – 3.22);
(ii) Myocardial infarction increases the risk of restenosis by 1.1-fold, i.e., by almost 10% (HR = 1.098; 95% CI: 1.05 – 1.15);
(iii) Moderate-diameter stenosis (2.75 – 3.5 mm) reduces the risk of restenosis (HR = 0.713; 95% CI: 0.58 – 0.87), whereas small-diameter occlusion increases the risk of restenosis;
(iv) DES reduces the risk of coronary restenosis by almost 50% compared to BMS (HR = 0.554; 95% CI: 0.41 – 0.75).

4. Discussion

Percutaneous coronary intervention has dramatically reduced mortality and other adverse outcomes in patients with CHD. Percutaneous coronary interventions cause mechanical injury and vascular inflammation. The presence of a foreign body and the proinflammatory effects of the polymer and the drug eluted by the stent stimulate complex processes involving endothelial cells, smooth muscle cells, platelets, and inflammatory cells.[14] Locally, vascular injury caused by stenting triggers a cascade of events that include endothelial denudation, exposure of prothrombotic intima and inflammation, the release of growth factors and cytokines, platelet activation, and SMC proliferation and migration. The result of these processes may be healing or pathological processes, such as excessive neointimal hyperplasia (in 6 – 12 months) or neoatherogenesis (>12 months after intervention), which cause restenosis.[15]

After percutaneous interventions, the most common cause of long-term failure is in-stent restenosis. It has been reported to occur at a frequency as high as 25 – 50% in BMS, though its rate has become significantly lower with the introduction of DES.[16] DES failure remains a problem that affects up to 20% of the devices implanted, depending on several factors.[17] Beyond the implications for the treatment of these events, percutaneous treatment of in-stent

Table 3. Cox regression evaluation of the impact of risk factors for coronary restenosis

Risk factor	Coefficient	HR	95% CI	*P*
Male sex	0.785	2.194	1.5 – 3.22	<0.001***
Prior myocardial infarction	0.0934	1.098	1.05 – 1.15	0.045*
Nominal stent diameter (<2.5 mm)	−0.338	0.713	0.58 – 0.87	0.0011**
Stent type (BMS)	−0.591	0.554	0.41 – 0.75	0.0001***

Note: *P<0.05; **P<0.01; ***P<0.001.
Abbreviations: BMS: Bare metal stent; HR: Hazard ratio; CI: Confidence interval.

restenosis is also associated with a much higher rate of failure than revascularization treatment of native vessels. Consequently, DES significantly reduces the incidence of in-stent restenosis; however, the problem remains relevant. The currently known risk factors for in-stent restenosis can be classified into three groups: patient-related, vessel-related, and procedure-related.[18] Patient-related risk factors include patient age, comorbidities (e.g., DM), genetic disorders, and systemic inflammation, with DM being the most important risk factor in this group that may trigger in-stent restenosis. According to the Swedish Coronary Angiography and Angioplasty Registry (SCAAR), which includes information about 35,000 stented patients, after 2 years of follow-up, restenosis in patients with DM was twice as frequent with the zotarolimus-eluting stent.[19] This is due to metabolic disorders that trigger endothelial dysfunction, accelerate neointimal proliferation, and induce a prothrombotic state by increasing platelet aggregation and thrombogenicity.[20,21]

Several papers demonstrate the role of genetic abnormalities, such as polymorphisms of genes encoding haptoglobin 2/2.25, interleukin-8 (IL-8), angiotensin-converting enzyme, and glycoprotein receptor IIIaPLA1/2, in the development of stent restenosis in most of these patients.[22-24]

Multiple studies have been conducted to identify inflammation markers and correlate their levels with coronary restenosis. Plasma C-reactive protein (CRP) level has long been proven to be a CVD predictor and is now being investigated for its predictive value for restenosis. One study found that CRP levels strongly correlated with the angiographic signs of restenosis.[25,26] The number of macrophages in tissue samples and restenosis have been found to strongly correlate.[27] Circulating matrix metalloproteinases (MMPs), namely, MMP-2 and MMP-9, have recently been identified as potentially useful markers for identifying patients at high risk of restenosis after stent implantation.[28]

The vascular-related risk factors of coronary restenosis include complex calcified, long vessel lesions, atherosclerotic plaques in the Ostia, and bifurcations of coronary arteries, as well as small vessel diameter and multivessel disease.[29] For example, Coughlan *et al.*[30] presented a novel clinical score (the ISAR score) to predict the risk of repeat percutaneous coronary intervention for recurrent DES-in-stent restenosis (DES-ISR). They retrospectively analyzed 1,986 consecutive patients with DES-ISR (2,392 in-stent restenosis lesions) from two centers. Patients were randomly divided (3:1 ratio) into training (1,471 patients, 1,778 lesions) and validation (515 patients, 614 lesions) cohorts to develop and validate the predictive model. The median duration of clinical follow-up after DES-ISR treatment was 7.4 years. Four clinical variables were associated with repeat percutaneous coronary intervention for recurrent DES-ISR after 1 year: (i) A non-focal in-stent restenosis pattern, (ii) time interval to in-stent restenosis <6 months, (iii) in-stent restenosis in the left circumflex coronary artery, and (iv) in-stent restenosis in a calcified vessel. In addition, the numerical four-item ISAR score (one point for each variable) proved clinically useful to readily predict percutaneous coronary intervention for recurrent DES-ISR.

Percutaneous coronary intervention-related risk factors include stent deployment failure, excessive stent dilatation, stent fracture, and polymer damage. These cases occur most frequently when stenting complex lesions or markedly calcified vessels, resulting in neointimal hyperplasia and impaired delivery of the drug coating the stent.[31] Some investigators proposed new biomarkers, such as the triglyceride-glucose index[32] and epicardial fat thickness.[33]

Coronary restenosis remains a common complication following coronary revascularization and stenting. The technical reasons for in-stent restenosis are well elucidated. Multiple studies indicated that adequate stent deployment, complete inflation, and optimal stent diameter play key roles in preventing restenosis. In addition, the complexity of the procedure due to multivessel disease, bifurcation lesions, small-diameter vessel lesions, and pronounced calcification is another important risk factor.

Our study analyzed known predictors of coronary restenosis in a large sample of stented patients who developed hemodynamically significant restenosis, requiring repeat revascularization within 60 months of the first stenting. The roles of sex and history of myocardial infarction have been demonstrated for restenosis formation and the rate of its development. Moreover, DES is significantly superior to BMS in terms of adverse event incidence and rate. These results are consistent with

the meta-analysis by Zhang *et al.*,[34] in which the use of DES and drug-coated balloons was the only choice for *de novo* CAD, chronic coronary disease,[35] and myocardial infarction.[36] The smaller the diameter of the revascularized vessel, the higher the risk of restenosis. Coronary stent < 3 mm was also identified by Zhang *et al.*[37] as a risk factor for coronary restenosis. In this study, 350 patients with CHD after percutaneous coronary intervention were divided into a stent stenosis group and a stent non-stenosis group based on coronary angiography results performed 2 years after percutaneous coronary intervention. Of the 350 patients with CHD, 138 (39.43%) had stent restenosis, while 212 did not. Multivariate logistic regression analysis revealed that family history of CHD, history of Type 2 diabetes, hypertension, smoking, and drinking, aspirin withdrawal, use of conventional doses of statins, calcified lesions, ≥3 implanted stents, stent length ≥30 mm, stent diameter <3 mm, and tandem stenting were risk factors for in-stent restenosis within 2 years after percutaneous coronary intervention. A family history of CHD, history of Type 2 diabetes, hypertension, smoking, and drinking, discontinuation of aspirin, use of conventional dose statins, calcified lesions, ≥3 stent implantations, stent length ≥30 mm, stent diameter <3 mm, and tandem stenting are risk factors for ISR within 2 years after percutaneous coronary intervention in patients with CHD.

However, prior myocardial infarction and male sex were less frequently identified as risk factors. Although DES reduced the occurrence of stent restenosis compared with BMS, managing DES-restenosis is more challenging and results in poorer long-term clinical and angiographic outcomes than BMS-associated restenosis.[38] At present, both new-generation DES and drug-coated balloons are recommended by the European guidelines on coronary revascularization for the treatment of patients presenting with in-stent restenosis.[39]

In-stent restenosis significantly aggravates CHD prognosis. The 5-year survival rate of such patients is reduced when treated with conservative therapy alone. These factors determine unfavorable prognosis, the need for repeat revascularizations, and the progression of heart failure. Consequently, the identification of restenosis predictors is increasingly important, despite limited existing knowledge. This could enable the development of personalized treatment regimens, informed decisions on revascularization methods, material selection, and stenting techniques.

Our study had several limitations. Despite the large sample size, the study was based on a single center, thus limiting its findings to a specific region within the unique. The study was not controlled, and no measures were implemented to address selection bias. In addition, some patients were probably lost to follow-up after leaving the region, rendering them unavailable in the medical recording system.

5. Conclusion

Our systematic review analyzed the risk factors for coronary restenosis, their influence on the frequency and rate of adverse events, and the corresponding favorable outcomes. The retrospective analysis revealed that the stent type and stented artery diameter significantly affect the duration of stent function and the likelihood of restenosis. Developing a mathematical model for predicting risk factors and identifying new predictors of restenosis will improve the prognosis in patients with recurrent coronary restenosis.

Acknowledgments

The authors are grateful to all CHD patients for their participation in this study, as well as the clinicians and hospital staff of the Republic Cardiological Centre (Russia) who contributed to this study.

Funding

None.

Conflict of interest

Naufal Sh. Zagidullin is the Editorial Board Member of this journal and Guest Editor of this special issue but was not in any way involved in the editorial and peer-review process conducted for this paper, directly or indirectly. Separately, other authors declared that they have no known competing financial interests or personal relationships that could have influenced the work reported in this paper.

Author contributions

Conceptualization: Haibo Jia
Methodology: Igor Buzaev, Irina Lakman, Naufal Zagidullin
Investigation: Alina Enikeeva, Liutsiia Gazizova
Resources: Irina Nikolaeva
Writing – original draft: Alina Enikeeva, Liutsiia Gazizova
Writing – review & editing: Igor Buzaev, Tagir Aminov, Elena Badykova

Ethics approval and consent to participate

The study was approved by the Ethics Committee of Bashkir State Medical University, Russia (Ufa, Protocol No 9; November 17, 2021). The systematic review conducted in this study was in accordance with the PRISMA protocol statement. The protocol was registered in (registration platform, PROSPERO) under the ID (registration number 622760). All procedures carried out in the study involving patient participation complied with the ethical standards

of the institutional and/or national Research Ethics Committee and the 1964 Helsinki Declaration and its subsequent changes or comparable standards of ethics. Informed voluntary consent was obtained from each of the participants in the study.

Consent for publication

Written informed consent for the publication of any associated data was obtained from each participant in the study.

Availability of data

The datasets generated and/or analyzed during the current study are available from the corresponding author on reasonable request.

References

1. GBD 2017 Causes of Death Collaborators. Global, regional, and national age-sex-specific mortality for 282 causes of death in 195 countries and territories, 1980-2017: A systematic analysis for the Global Burden of Disease Study 2017. *Lancet*. 2018;392(10159):1736-1788.

   doi: 10.1016/S0140-6736(18)32203-7

2. Townsend N, Kazakiewicz D, Wright FL, *et al*. Epidemiology of cardiovascular disease in Europe. *Nat Rev Cardiol*. 2022;19(2):133-143.

   doi: 10.1038/s41569-021-00607-3

3. *Russian Statistical Yearbook 2021*. Russia: Federal State Statistics Service; 2021. p. 692.

4. Karpin AD, Starvinsky VV, Shakhzadova AO, Lisichnikova IV. *Malignant Neoplasms in Russia in 2021 (Morbidity and Mortality)*. Russia: Federal State Statistics Service; 2022. p. 233.

5. *The Demographic Yearbook of Russia 2021*. Russia: Federal State Statistics Service; 2021. p. 256.

6. Alekyan BG, Grigoryan AM, Staferov AV, Karapetyan NG. X-ray endovascular diagnostics and treatment of heart and vascular diseases in the Russian Federation. *Endovasc Surg J*. 2021;8:233.

7. Kalinina AM, Ipatov PV, Kushunina DV, *et al*. Results of circulatory disease detection during prophylactic medical examination of the adult population: The first two years' experience. *Terapevticheskii Arkhiv*. 2016;88(1):46-52.

8. Stone G, Maehara A, Lansky A, *et al*. A prospective natural - history study of coronary atherosclerosis. *N Engl J Med*. 2011;364(3):226-235.

   doi: 10.1056/NEJMoa1002358

9. Ullrich H, Olschewski M, Münzel T, Gori T. Coronary in-stent restenosis: Predictors and treatment. *Dtsch Arztebl Int*. 2021;118(38):637-644.

   doi: 10.3238/arztebl.m2021.0254

10. Alfonso F, Byrne RA, Rivero F, Kastrati A. Current treatment of in-stent restenosis. *J Am Coll Cardiol*. 2014;63(24):2659-2673.

    doi: 10.1016/j.jacc.2014.02.545

11. Hamon M, Bauters C, McFadden EP, *et al*. Restenosis after coronary angioplasty. *Eur Heart J*. 1995;16(Suppl I):33-48.

    doi: 10.1093/eurheartj/16.suppl_i.33

12. Jukema JW, Verschuren JJ, Ahmed TA, Quax PH. Restenosis after PCI. Part 1: pathophysiology and risk factors. *Nat Rev Cardiol*. 2011;9:53-62.

    doi: 10.1038/nrcardio.2011.132

13. Buccheri D, Cimino G. Drug-eluting stent restenosis treatment: An "old" stent, a "new" balloon or a "newer" scaffold? *J Thorac Dis*. 2016;8(12):3478-3483.

    doi: 10.21037/jtd.2016.12.21

14. Gori T. Restenosis after coronary stent implantation: Cellular mechanisms and potential of endothelial progenitor cells (a short guide for the interventional cardiologist). *Cells*. 2022;11(13):2094.

    doi: 10.3390/cells11132094

15. Neubauer K, Zieger B. Endothelial cells and coagulation. *Cell Tissue Res*. 2022;387:391-398.

    doi: 10.1007/s00441-021-03471-2

16. Timmis A, Townsend N, Gale C, *et al*. European society of cardiology: Cardiovascular disease statistics 2017. *Eur Heart J*. 2018;39:508-579.

    doi: 10.1093/eurheartj/ehx628

17. Moses JW, Leon MB, Popma JJ, *et al*. Sirolimus-eluting stents versus standard stents in patients with stenosis in a native coronary artery. *N Engl J Med*. 2003;349:1315-1323.

    doi: 10.1056/NEJMoa035071

18. Shumakov DV, Shekhyan GG, Zybin DI, Yalymov AA, Vedenikin TY, Popov MA. In-stent restenosis: Symptoms, hemodynamic signs, pathogenesis and treatment. *Russ Cardiol Bull*. 2021;16(1):20-27.

    doi: 10.17116/cardiobulletin20211601120

19. Fröbert O, Lagerqvist B, Carlsson J, Lindbäck J, Stenestrand U, James SK. Differences in restenosis rate with different drug-eluting stents in patients with and without diabetes mellitus: A report from the SCAAR (Swedish Angiography and Angioplasty Registry). *J Am Coll Cardiol*. 2009;53(18):1660-1667.

    doi: 10.1016/j.jacc.2009.01.054

20. MacRury SM, Lowe GD. Blood rheology in diabetes mellitus. *Diabet Med*. 1990;7(4):285-291.

    doi: 10.1111/j.1464-5491.1990.tb01391.x37

21. Ostermann H, van de Loo J. Factors of the hemostatic

system in diabetic patients. A survey of controlled studies. *Haemostasis*. 1986;16(6):386-416.

doi: 10.1159/000215317

22. Ribichini F, Steffenino G, Dellavalle A, *et al*. Plasma activity and insertion/dele-tion polymorphism of angiotensin I-converting enzyme: A major risk factor and a marker of risk for coronary stent restenosis. *Circulation*. 1998;97(2):147-154.

doi: 10.1161/01.cir.97.2.14741

23. Vogiatzi K, Apostolakis S, Voudris V, Thomopoulou S, Kochiadakis GE, Spandidos DA. Interleukin 8 gene polymorphisms and susceptibility to rest-enosis after percutaneous coronary intervention. *J Thromb Thrombolysis*. 2010;29(1):134-140.

doi: 10.1007/s11239-009-0338-y42

24. Richardson A, Kaye SB. Drug resistance in ovarian cancer: the emerging im-portance of gene transcription and spatio-temporal regulation of resistance. *Drug Resist Updates*. 2005;8(5):311-321.

doi: 10.1016/j.drup.2005.09.001

25. Iijima R, Byrne RA, Ndrepepa G, *et al*. Pre-procedural C-reactive protein levels and clinical out-comes after percutaneous coronary interventions with and without ABCIX-IMAB: Pooled analysis of four ISAR trials. *Heart*. 2009;95(2):107-112.

doi: 10.1136/hrt.2008.15363547

26. Dibra A, Mehilli J, Braun S, *et al*. Inflammatory response after intervention assessed by serial C-reactive protein measurements correlates with rest-enosis in patients treated with coronary stenting. *Am Heart J*. 2005;150(2):344-350.

doi: 10.1016/j.ahj.2004.09.030

27. Moreno PR, Bernardi VH, López-Cuéllar J, *et al*. Macrophage infiltration predicts rest-enosis after coronary intervention in patients with unstable angina. *Circulation*. 1996;94(12):3098-3102.

doi: 10.1161/01.cir.94.12.3098

28. Katsaros KM, Wiesbauer F, Speidl WS, *et al*. High soluble Fas and soluble Fas ligand serum levels before stent implantation are protective against restenosis. *Thromb Haemostasis*. 2011;105(5):883-891.

doi: 10.1160/TH10-09-0566

29. Fujii K, Mintz GS, Kobayashi Y, *et al*. Contribution of stent underexpansion to recurrence after sirolimus-eluting stent implantation for in-stent restenosis. *Circulation*. 2004;109(9):1085-1088.

doi: 10.1161/01.CIR.0000121327.67756.19

30. Coughlan JJ, Aytekin A, Lahu S, *et al*. Derivation and validation of the ISAR score to predict the risk of repeat percutaneous coronary interventions for recurrent drug-eluting stent restenosis. *EuroIntervention*. 2023;18:e1328-e1338.

doi: 10.4244/EIJ-D-22-00860

31. Takebayashi H, Mintz GS, Carlier SG, *et al*. Nonuniform strut distribution correlates with more neointimal hyperplasia after sirolimus-eluting stent implantation. *Circulation*. 2004;110(22):3430-3434.

doi: 10.1161/01.CIR.0000148371.53174.05

32. Guo X, Shen R, Yan S, Su Y, Ma L. Triglyceride-glucose index for predicting repeat revascularization and in-stent restenosis in patients with chronic coronary syndrome undergoing percutaneous coronary intervention. *Cardiovasc Diabetol*. 2023;22(1):43.

doi: 10.1186/s12933-023-01779-7

33. Cabrera-Rego JO, Escobar-Torres RA, Parra-Jiménez JD, Valiente-Mustelier J. Epicardial fat thickness correlates with coronary in-stent restenosis in patients with acute myocardial infarction. *Clin Investig Arterioscler*. 2019;31(2):49-55.

doi: 10.1016/j.arteri.2018.11.002

34. Zhang W, Zhang M, Tian J, Zhang M, Zhou Y, Song X. Drug-coated balloon-only strategy for *de novo* coronary artery disease: A meta-analysis of randomized clinical trials. *Cardiovasc Ther*. 2023;8:3121601.

doi: 10.1155/2023/3121601

35. Kokkinidis DG, Waldo SW, Armstrong EJ. Treatment of coronary artery in-stent restenosis. *Expert Rev Cardiovasc Ther*. 2017;15(3):191-202.

doi: 10.1080/14779072.2017.1284588

36. Scheller B, Ohlow MA, Ewen S, *et al*. Bare metal or drug-eluting stent versus drug-coated balloon in non-ST-elevation myocardial infarction: the randomised PEPCAD NSTEMI trial. *Eurointervention*. 2020;15(17):1527-1533.

doi: 10.4244/EIJ-D-19-00723

37. Zhang J, Zhang Q, Zhao K, Bian YJ, Liu Y, Xue YT. Risk factors for in-stent restenosis after coronary stent implantation in patients with coronary artery disease: A retrospective observational study. *Medicine (Baltimore)*. 2022;101(47):e31707.

doi: 10.1097/MD.0000000000031707

38. Giacoppo D, Alfonso F, Xu B, *et al*. Paclitaxel-coated balloon angioplasty vs. drug-eluting stenting for the treatment of coronary in-stent restenosis: A comprehensive, collaborative, individual patient data meta-analysis of 10 randomized clinical trials (DAEDALUS study). *Eur Heart J*. 2020;41:3715-3728.

doi: 10.1093/eurheartj/ehz594

39. Neumann FJ, Sousa-Uva M, Ahlsson A, *et al*. 2018 ESC/EACTS Guidelines on myocardial revascularization. *EuroIntervention*. 2019;14:1435-1534.

doi: 10.4244/EIJY19M01_01

ACCSCIENCE PUBLISHING

Global Translational Medicine

BRIEF REPORT

Influence of neodymium-doped yttrium aluminum garnet laser exposure time on cytokine secretion in lipopolysaccharide-challenged rat peripheral blood mononuclear cells

Sarah M. Vargas[1], Michael A. Washington[2], Megan E. Bunting[3], Rachel J. Duval[4], Claudia P. Millan[3], Kimberly Ann Inouye[3], Adam R. Lincicum[3], Brian W. Stancoven[3], and Thomas M. Johnson[3]*

[1]Department of Periodontics, Army Postgraduate Dental School, Postgraduate Dental College, Uniformed Services University, Fort Liberty, NC, United States of America

[2]Department of Clinical Investigation, Dwight David Eisenhower Army Medical Center, Fort Eisenhower, GA, United States of America

[3]Department of Periodontics, Army Postgraduate Dental School, Postgraduate Dental College, Uniformed Services University, Fort Eisenhower, GA, United States of America

[4]Department of Periodontics, United States Army Dental Activity, Fort Liberty, NC, United States of America

(This article belongs to the *Special Issue: Soft and Hard Tissues Reconstruction in Dentistry*)

Abstract

Multiple investigators have suggested that infrared laser energy facilitates hard and soft tissue wound healing through various mechanisms, including the suppression of inflammation. This study investigated the influence of neodymium-doped yttrium aluminum garnet (Nd:YAG) laser exposure time on pro-inflammatory cytokine/chemokine concentrations in lipopolysaccharide (LPS)-stimulated rat peripheral blood mononuclear cells (PBMCs). Cultured rat PBMCs were stimulated with various LPS concentrations (0, 10, 100, or 1000 ng/mL) and treated with Nd:YAG laser irradiation for 0 (control), 30, 45, or 60 s. For these experiments, the average power, pulse duration, and repetition rate remained constant at 5 W, 100 μs, and 20 Hz, respectively. Luminex magnetic microsphere immunoassays were used to compare the secretion of 27 inflammatory mediators from LPS-stimulated PBMCs in laser-irradiated versus control groups. Two-way analysis of variance was used to compare the main effects of laser exposure time and LPS concentration on cytokine/chemokine concentrations and evaluate the potential interaction between these factors. Four pro-inflammatory cytokines – tumor necrosis factor-α, macrophage inflammatory protein (MIP)-1α, MIP-2, and interferon gamma-induced protein-10 – exhibited a trend of reduced secretion in laser-irradiated cultures. The effect appeared more pronounced at longer exposure times (45 and 60 s). However, none of the 27 inflammatory mediators exhibited statistically significant reductions in concentrations in laser-irradiated cultures versus control cultures. These observations do not support a robust anti-inflammatory effect of Nd:YAG laser irradiation. Further studies should explore the potential impact of Nd:YAG laser irradiation on cytotoxicity and cellular growth kinetics and extend across a range of irradiation parameters and cell types.

Keywords: Lasers; Leukocytes; Mononuclear; Inflammation; Cytokines; Low-level light therapy; Lipopolysaccharide

***Corresponding author:**
Thomas M. Johnson
(thomas.m.johnson34.mil@health.mil)

Citation: Vargas SM, Washington AM, Bunting ME, *et al*. Influence of neodymium-doped yttrium aluminum garnet laser exposure time on cytokine secretion in lipopolysaccharide-challenged rat peripheral blood mononuclear cells. *Global Transl Med*. 2024:3(4):4433. doi: 10.36922/gtm.4433

Received: August 3, 2024
Accepted: October 23, 2024
Published Online: November 15, 2024

1. Introduction

The concept of utilizing light for medical purposes originated long ago. Ancient Egyptian, Greek, Roman, and Arab physicians used sunlight to treat various human ailments, beginning as early as 1400 B.C.[1] However, modern phototherapy began to take form around the turn of the 20th century. In 1903, Niels Ryberg Finsen received a Nobel Prize for his work demonstrating the bactericidal and tissue-stimulating effects of concentrated light.[2] In 1960, Theodore Maiman introduced the first laser,[3] and by the end of the same decade, Dr. Endre Mester demonstrated the improvement of a biological process (hair growth) in mice irradiated with a ruby laser.[4] Since then, researchers have associated laser irradiation with pain relief,[5-11] improved wound healing,[5,12-16] bone[17-21] and nerve regeneration,[22-26] and reduced inflammation.[5,27-38]

After Mester's early experiments, investigators quickly realized that progressively large laser exposures or "doses" did not always result in concomitant increases in the recorded biological outcome.[6] In fact, laser irradiation may produce either stimulatory or inhibitory responses, depending on the applied laser parameters.[2] Of principal importance is the wavelength of the laser light, which determines the absorption profile within the tissue.[39] Fluence (J/cm^2) and irradiance (W/cm^2) are also major determinants of the biological response.[40] Other relevant and interrelated parameters include the average power, peak power, pulse duration, pulse repetition rate, exposure time, spot size, target cell type, pulse energy, total energy applied, number of laser applications, and interval between laser applications.[41,42]

Mester referred to the effect he observed as "laser biostimulation,"[4] and low-level laser/light therapy is another commonly used term for the phenomenon.[2] In 2014, the North American Association for Photobiomodulation (PBM) Therapy and the World Association for Laser Therapy (WALT) jointly affirmed "photobiomodulation" as the most appropriate term. WALT defines PBM as the induction of non-thermal photophysical and photochemical events in target cells or tissues, resulting in physiological changes at various biological scales.[43] PBM responses are produced through non-thermal mechanisms and are distinguishable from the effects that result from simply heating the tissue.[2] Typical fluence values used in PBM range from 1 to 20 J/cm^2,[40] above which thermal effects may predominate or partially account for the observed responses.

Modulation of the inflammatory response is one of the most consistent observations in PBM research, and this effect may account for some of the clinical benefits associated with laser therapy.[28] Various researchers have reported a reduction in the secretion of pro-inflammatory cytokines such as interleukin (IL)-1β and tumor necrosis factor (TNF)-α using infrared lasers.[37,38,44] Infrared laser irradiation also appears to decrease cyclooxygenase (COX)-2 mRNA levels and prostaglandin synthesis in some cell types.[33] Considering the number of laser parameters potentially influencing cell/tissue effects and the complexity of the immune response, additional studies are required to clarify the underlying mechanisms of PBM and optimize therapeutic protocols. Although clinical investigations have suggested that laser irradiation improves wound healing in various contexts, narrowly focused *in vitro* studies contribute to the body of evidence highlighting the underlying mechanisms. The primary purpose of this study was to explore the influence of a specific laser parameter (exposure time) on cytokine secretion in stimulated peripheral blood mononuclear cell (PBMC) cultures irradiated with a neodymium-doped yttrium aluminum garnet (Nd:YAG) laser.

2. Materials and methods

2.1. Materials

2.1.1. Target cells and culture conditions

Sprague–Dawley rat PBMCs were obtained from IQ Biosciences (Berkeley, California, USA) and maintained in liquid nitrogen before culturing. Cells were initially resuspended in Hank's balanced salt solution without calcium or magnesium supplemented with 10% fetal bovine serum (FBS). They were then pelleted and resuspended in RPMI 1640 medium supplemented with 10% FBS (Thermofisher Scientific, Waltham, MA, USA). Approximately 1×10^6 cells were seeded into T-75 culture flasks (Fisher Scientific, Hampton, NH, USA) for expansion. The cells were grown at 37°C in a 5% CO_2 atmosphere with ambient humidity. The medium was replaced every 3 days and as required. The cells were evaluated through microscopy during each media change, and they were found to remain morphologically consistent, structurally intact, and free of debris throughout the course of the study.

2.1.2. Laser system

An Nd:YAG laser (1064 nm, Lightwalker AT, Fotona, Dallas, Texas, USA) was used to irradiate the cultures according to the manufacturer's operating instructions.

2.2. Lipopolysaccharide (LPS) stimulation

Near-confluent rat PBMC cultures (consisting of 1×10^6 cells each) were exposed to one of four LPS concentrations of 0, 10, 100, or 1000 ng/mL for 1 h in the cell culture media. The cells were then transferred

Table 1. Experimental design.

	Group 1 (Unexposed controls)	Group 2	Group 3	Group 4	Group 5
Pulse duration	Not applicable	100 μs	100 μs	100 μs	100 μs
Pulse repetition rate	Not applicable	20 Hz	20 Hz	20 Hz	20 Hz
Average power	Not applicable	5 W	5 W	5 W	3 W
Exposure time	Not applicable	30 s	45 s	60 s	60 s

Note: Each experiment included three wells per group, completed in duplicate.

to 96-well plates (2.0×10^4 cells/well; Fisher Scientific, Hampton, NH) for laser irradiation.

2.3. Laser application

Laser irradiation was performed immediately after the 1-h incubation with LPS. A 300-micron optical fiber directed the laser beam perpendicularly to the plated cells from a distance of 1.8 cm, and a standardized support reliably reproduced the laser position. Plate covers were removed before irradiation to avoid reflection and diffusion of the laser light. The cultures stimulated at each LPS concentration received Nd:YAG laser irradiation (5 W average power) at one of four exposure times, *viz.*, 0 (control), 30, 45, or 60 s (Table 1). The pulse duration and repetition rate remained constant at 100 μs and 20 Hz, respectively. After irradiation, the cells were incubated for 1 h at 37°C before analysis. Each experiment (LPS concentration and laser treatment combination) was completed with three wells per condition in two independent experiments, yielding a total of six wells per condition. For comparison with cultures irradiated at 5 W, three wells in each experiment were irradiated at a lower average power (3 W) for 60 s.

2.4. Evaluation of cytokine levels

For each condition tested, the concentrations of 27 cytokines were analyzed simultaneously using a Luminex cytokine assay (Thermofisher Scientific) (Table 2). The immunoassay kit included magnetic microspheres tagged with fluorescent dyes covalently coupled to antibodies specific for cytokines of interest (capture antibodies). After incubating the microspheres for 2 h with 200 μL of culture media from each condition, a secondary antibody (detection antibody) labeled with a streptavidin–phycoerythrin conjugate was introduced. A light-emitting diode was used to excite the conjugate, and the fluorescence from each microsphere was detected using a charge-coupled device camera. The median fluorescence intensities provided the basis for sample analysis. Images were processed using the analysis software (Luminex MAGPIX System, Thermofisher Scientific), and the cytokine/chemokine concentrations were determined in pg/mL using standard curves.

Table 2. Analytes evaluated through magnetic microsphere immunoassay

Tumor necrosis factor-α
Macrophage inflammatory protein-1α
Macrophage inflammatory protein-2
Interferon gamma-induced protein 10
Granulocyte colony-stimulating factor
Eotaxin
Granulocyte-macrophage colony-stimulating factor
Interleukin-1α
Leptin
Interleukin-4
Interleukin-1β
Interleukin-2
Interleukin-6
Epidermal growth factor
Interleukin-13
Interleukin-10
Interleukin-12p70
Interferon
Interleukin-5
Interleukin-17α
Interleukin-18
Monocyte chemoattractant protein-1
Growth-regulated oncogene/keratinocyte chemoattractant
Vascular epithelial growth factor
RANTES (CCL-5)
Fractalkine
Liposaccharide-induced CXC chemokine

2.5. Statistical analysis

A two-way analysis of variance was used to compare the main effects of laser exposure time and LPS concentration on cytokine/chemokine concentrations and evaluate the potential interaction between these factors. Statistical significance was determined at an alpha level of 0.05. Normalized cytokine concentrations are expressed as mean ± standard error of mean (SE).

3. Results

TNF-α, macrophage inflammatory protein (MIP)-1α, MIP-2, and interferon gamma-induced protein-10 (IP-10) showed a trend toward reduced concentrations in the laser-irradiated cultures. This effect was more pronounced at longer exposure times (45 and 60 s) (Figure 1). However, none of the 27 inflammatory mediators that were evaluated in this study showed statistically significant reductions in concentration in the laser-irradiated versus control cultures. As anticipated, we observed LPS dose-dependent increases in cytokine concentrations in the control groups (Figure 2).

4. Discussion

This study aimed to explore the effect of Nd:YAG laser exposure time on the secretion of 27 inflammatory mediators in LPS-stimulated rat PBMCs. Because a general reduction in inflammation is a consistent finding in PBM studies,[28] extensive effects on a large proportion of the evaluated proteins may have been anticipated. In contrast, we detected no statistically significant reductions in the concentrations of the pro-inflammatory cytokines.

The ability to modulate inflammation is relevant for clinical and patient-oriented outcomes in dental implant therapy, hard and soft tissue augmentation procedures, and the treatment of periodontal disease. In fact, periodontitis – which involves inflammatory destruction of the alveolar bone and periodontal attachment – is the most common non-communicable chronic inflammatory disease affecting humans.[45] The microbial etiology of this disease is complex, and the emerging concept of dysbiosis remains incomplete.[46,47] Nevertheless, one mode by which dysbiosis can manifest involves the expansion of pathobionts within the microbial ecosystem.[46] Multiple putative periodontal pathogens are gram-negative anaerobes that contain LPS within their outer membranes.[48] LPS is a virulence factor and a potent inflammatory stimulus, which may cause bone resorption and loss of attachment.[48,49] Nd:YAG lasers are used clinically in the treatment of periodontitis and in alveolar ridge preservation procedures;[41,50] however, the effect of laser periodontal therapy (LPT) on the local immune response has not been established.

The results of this study should be interpreted with caution due to multiple limitations. Notably, our experiments were incapable of optimizing the exposure parameters to minimize the levels of pro-inflammatory cytokines. Numerous PBM outcomes of interest exhibit biphasic responses.[40] Hence, a lower fluence value (J/cm^2) may have affected the investigated inflammatory mediators more broadly and to a greater degree. The power levels applied may have exceeded the ideal for exerting anti-inflammatory effects. Clinically, an average power of 4 W is typical for intraoral applications,[50] which can be increased to 6 W for extraoral PBM. The average power applied in these experiments was within this range. It is difficult to

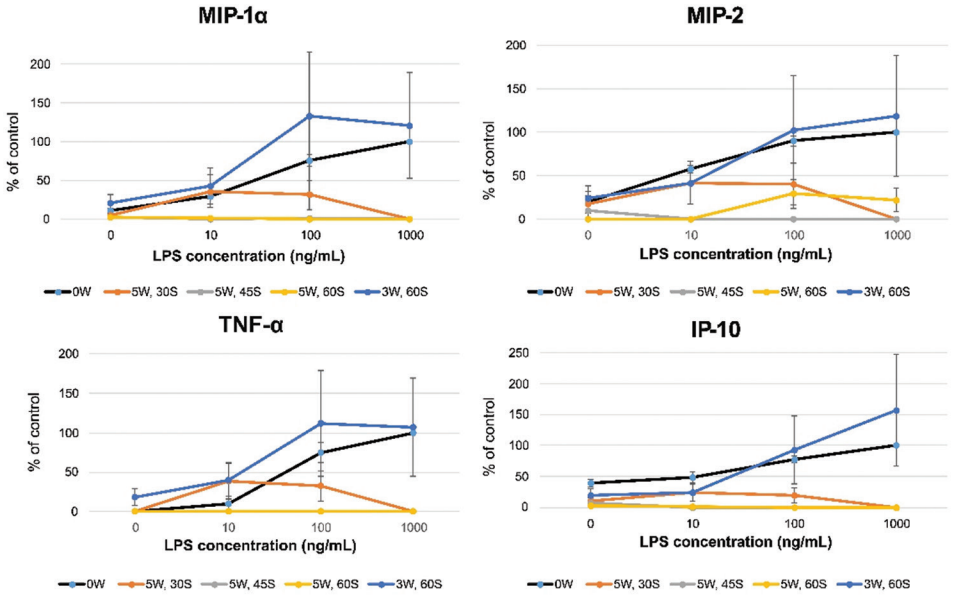

Figure 1. Normalized mean concentrations of cytokines trending toward reduced concentrations in laser-exposed cell cultures
Abbreviations: IP-10: Interferon gamma-induced protein 10; LPS: lipopolysaccharide; MIP-1α: Macrophage inflammatory protein-1α; MIP-2: Macrophage inflammatory protein-2; TNF-α: Tumor necrosis factor-α.

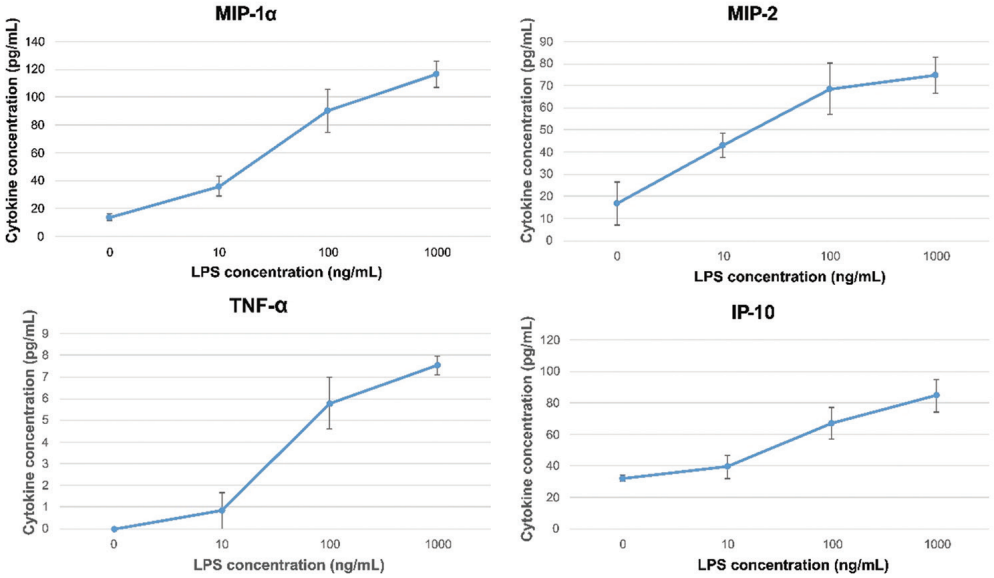

Figure 2. Results from control cultures. Cytokine and lipopolysaccharide (LPS) concentrations were correlated appropriately
Abbreviations: IP-10: Interferon gamma-induced protein 10; LPS: lipopolysaccharide; MIP-1α: Macrophage inflammatory protein-1α; MIP-2: Macrophage inflammatory protein-2; TNF-α: Tumor necrosis factor-α.

place the exposure times evaluated in this study into the clinical context. A typical LPT procedure may require ≥2 h, with multiple laser applications at different irradiation parameters interrupted by mechanical debridement of the tooth roots.[50] Alveolar ridge preservation at a single tooth extraction socket may involve laser application for several minutes.[41] The distance between the optical fiber and target cells/tissues is another factor potentially affecting the observed response. In distinct clinical situations, the distance between the optical fiber and the target tissue varies from direct contact to several centimeters. Changing the standardized distance used in this study (1.8 cm) would probably affect the results. An excessively small distance may damage cells directly aligned with the fiber, whereas an excessively large distance could result in laser exposure affecting the cells in adjacent wells. In this study, cell viability was not confirmed before the evaluation of cytokine levels. Therefore, the observed reductions in some cytokine levels may have reflected cell death rather than PBM.

5. Conclusion

Under the experimental conditions of this study, the observations do not support the reduced secretion of pro-inflammatory cytokines in PBMC cultures receiving Nd:YAG laser irradiation. Modifying the irradiation parameters may alter the observed cytokine secretion profiles. Further studies should extend experiments across a range of laser irradiation parameters and cell types and include evaluations of cytotoxicity and cellular growth kinetics.

Acknowledgments

None.

Funding

The Defense Health Agency (United States) funded this research entirely. The authors received no extramural funding.

Conflict of interest

The authors declare that they have no competing interests.

Author contributions

Conceptualization: Sarah M. Vargas, Brian Stancoven, Adam Lincicum, Kimberly Ann Inouye
Formal analysis: Thomas Johnson, Michael A. Washington
Investigation: Sarah M. Vargas, Megan E. Bunting, Rachel J. Duval, Michael A. Washington
Methodology: Sarah M. Vargas, Michael A. Washington, Thomas M. Johnson
Writing–original draft: Sarah M. Vargas, Thomas M. Johnson
Writing–review & editing: Michael A. Washington, Brian Stancoven, Kimberly Ann Inouye, Claudia P. Millan, Adam Lincicum, Rachel J. Duval, Megan E. Bunting

Ethics approval and consent to participate

Not applicable. This research involved the use of a commercially available animal cell line.

Consent for publication

Not applicable.

Availability of data

The Dwight David Eisenhower Army Medical Center Human Research Protections Office has not approved data sharing for this investigation.

References

1. Gusain P, Paliwal R, Joga R, Gupta N, Singh V. Ancient light therapies: A boon to medical science. *Sci Cult*. 2016;82:231-236.
2. Anders JJ, Lanzafame RJ, Arany PR. Low-level light/laser therapy versus photobiomodulation therapy. *Photomed Laser Surg*. 2015;33:183-184.

   doi: 10.1089/pho.2015.9848
3. Townes CH. The first laser. In: *A Century of Nature: Twenty-One Discoveries that Changed Science and the World*. London: University of Chicago Press; 2010. p. 107.
4. Mester E, Szende B, Gartner P. The effect of laser beams on the growth of hair in mice. *Radiobiol Radiother* (*Berl*). 1968;9:621-626.
5. Carroll JD, Milward MR, Cooper PR, Hadis M, Palin WM. Developments in low level light therapy (LLLT) for dentistry. *Dent Mater*. 2014;30:465-475.

   doi: 10.1016/j.dental.2014.02.006
6. Enwemeka CS. Laser biostimulation of healing wounds: Specific effects and mechanisms of action. *J Orthop Sports Phys Ther*. 1988;9:333-338.

   doi: 10.2519/jospt.1988.9.10.333
7. Suter VG, Sjölund S, Bornstein MM. Effect of laser on pain relief and wound healing of recurrent aphthous stomatitis: A systematic review. *Lasers Med Sci*. 2017;32:953-963.

   doi: 10.1007/s10103-017-2184-z
8. Qamruddin I, Alam MK, Mahroof V, Fida M, Khamis MF, Husein A. Effects of low-level laser irradiation on the rate of orthodontic tooth movement and associated pain with self-ligating brackets. *Am J Orthod Dentofacial Orthop*. 2017;152:622-630.

   doi: 10.1016/j.ajodo.2017.03.023
9. Jang H, Lee H. Meta-analysis of pain relief effects by laser irradiation on joint areas. *Photomed Laser Surg*. 2012;30:405-417.

   doi: 10.1089/pho.2012.3240
10. Chow RT, Johnson MI, Lopes-Martins RA, Bjordal JM. Efficacy of low-level laser therapy in the management of neck pain: A systematic review and meta-analysis of randomised placebo or active-treatment controlled trials. *Lancet*. 2009;374:1897-1908.

    doi: 10.1016/S0140-6736(09)61522-1
11. Bjordal JM, Lopes-Martins RA, Joensen J, *et al.* A systematic review with procedural assessments and meta-analysis of low level laser therapy in lateral elbow tendinopathy (tennis elbow). *BMC Musculoskelet Disord*. 2008,;9:75.

    doi: 10.1186/1471-2474-9-75
12. Mester E, Nagylucskay S, Doklen A, Tisza S. Laser stimulation of wound healing. *Acta Chir Acad Sci Hung*. 1976;17:49-55.
13. Suzuki R, Takakuda K. Wound healing efficacy of a 660-nm diode laser in a rat incisional wound model. *Lasers Med Sci*. 2016;31:1683-1689.

    doi: 10.1007/s10103-016-2038-0
14. Solmaz H, Ulgen Y, Gulsoy M. Photobiomodulation of wound healing via visible and infrared laser irradiation. *Lasers Med Sci*. 2017;32:903-910.

    doi: 10.1007/s10103-017-2191-0
15. Yu W, Naim JO, Lanzafame RJ. Effects of photostimulation on wound healing in diabetic mice. *Lasers Surg Med*. 1997;20:56-63.

    doi: 10.1002/(sici)1096-9101(1997)20:1<56::aid-lsm9>3.0.co;2-y
16. Bryant GL, Davidson JM, Ossoff RH, Garrett CG, Reinisch L. Histologic study of oral mucosa wound healing: A comparison of a 6.0-to 6.8-micrometer pulsed laser and a carbon dioxide laser. *Laryngoscope*. 1998;108:13-17.

    doi: 10.1097/00005537-199801000-00003
17. Fujimoto K, Kiyosaki T, Mitsui N, *et al.* Low-intensity laser irradiation stimulates mineralization via increased BMPs in MC_3T_3-E1 cells. *Lasers Surg Med*. 2010;42:519-526.

    doi: 10.1002/lsm.20880
18. Ueda Y, Shimizu N. Effects of pulse frequency of low-level laser therapy (LLLT) on bone nodule formation in rat calvarial cells. *J Clin Laser Med Surg*. 2003;21:271-277.

    doi: 10.1089/104454703322564479
19. Karoussis IK, Kyriakidou K, Psarros C, Lang NP, Vrotsos IA. Nd:YAG laser radiation (1.064 nm) accelerates differentiation of osteoblasts to osteocytes on smooth and rough titanium surfaces *in vitro*. *Clin Oral Implants Res*. 2017;28:785-790.

    doi: 10.1111/clr.12882
20. Arisu HD, Türköz E, Bala O. Effects of Nd:YAG laser irradiation on osteoblast cell cultures. *Lasers Med Sci*. 2006;21:175-180.

    doi: 10.1007/s10103-006-0398-6
21. Aleksic V, Aoki A, Iwasaki K, *et al.* Low-level Er: YAG laser irradiation enhances osteoblast proliferation through activation of MAPK/ERK. *Lasers Med Sci*. 2010;25:559-569.

doi: 10.1007/s10103-010-0761-5

22. Rochkind S. Stimulation effect of laser energy on the regeneration of traumatically injured peripheral nerves. *Morphogen Regen*. 1978;83:25-27.

23. Gigo-Benato D, Geuna S, de Castro Rodrigues A, *et al.* Low-power laser biostimulation enhances nerve repair after end-to-side neurorrhaphy: A double-blind randomized study in the rat median nerve model. *Lasers Med Sci*. 2004;19:57-65.

doi: 10.1007/s10103-004-0300-3

24. Matsushita HI, Kakami KA, Ito A, *et al.* Effect on the action potential of the low power Nd: YAG laser as irradiated directly to the nerve. *Aichi Gakuin Dent Sci*. 1989;2:19-28.

25. Orchardson R, Peacock JM, John Whitters C. Effect of pulsed Nd:YAG laser radiation on action potential conduction in isolated mammalian spinal nerves. *Lasers Surg Med*. 1997;21:142-148.

doi: 10.1002/(sici)1096-9101(1997)21:2<142::aid-lsm5>3.0.co;2-q

26. Midamba ED, Haanaes HR. Low reactive-level 830 NM GaAlAs diode laser therapy (LLLT) successfully accelerates regeneration of peripheral nerves in human. *Laser Ther*. 1993;5:125-129.

doi: 10.5978/islsm.93-OR-14

27. Giannelli M, Bani D, Tani A, *et al. In vitro* evaluation of the effects of low-intensity Nd:YAG laser irradiation on the inflammatory reaction elicited by bacterial lipopolysaccharide adherent to titanium dental implants. *J Periodontol*. 2009;80:977-984.

doi: 10.1902/jop.2009.080648

28. Hamblin MR. Mechanisms and applications of the anti-inflammatory effects of photobiomodulation. *AIMS Biophys*. 2017;4:337-361.

doi: 10.3934/biophy.2017.3.337

29. Yamaura M, Yao M, Yaroslavsky I, *et al.* Low level light effects on inflammatory cytokine production by rheumatoid arthritis synoviocytes. *Lasers Surg Med*. 2009;41:282-290.

doi: 10.1002/lsm.20766

30. Hwang MH, Shin JH, Kim KS, *et al.* Low level light therapy modulates inflammatory mediators secreted by human annulus fibrosus cells during intervertebral disc degeneration *in vitro*. *Photochem Photobiol*. 2015;91:403-410.

doi: 10.1111/php.12415

31. Lim W, Choi H, Kim J, *et al.* Anti-inflammatory effect of 635 nm irradiations on *in vitro* direct/indirect irradiation model. *J Oral Pathol Med*. 2015;44:94-102.

doi: 10.1111/jop.12204

32. Choi H, Lim W, Kim I, *et al.* Inflammatory cytokines are suppressed by light-emitting diode irradiation of P. gingivalis LPS-treated human gingival fibroblasts: Inflammatory cytokine changes by LED irradiation. *Lasers Med Sci*. 2012;27:459-467.

doi: 10.1007/s10103-011-0971-5

33. Sakurai Y, Yamaguchi M, Abiko Y. Inhibitory effect of low-level laser irradiation on LPS-stimulated prostaglandin E2 production and cyclooxygenase-2 in human gingival fibroblasts. *Eur J Oral Sci*. 2000;108:29-34.

doi: 10.1034/j.1600-0722.2000.00783.x

34. Nomura K, Yamaguchi M, Abiko Y. Inhibition of interleukin-1beta production and gene expression in human gingival fibroblasts by low-energy laser irradiation. *Lasers Med Sci*. 2001;16:218-223.

doi: 10.1007/pl00011358

35. Funk JO, Kruse A, Kirchner H. Cytokine production after helium-neon laser irradiation in cultures of human peripheral blood mononuclear cells. *J Photochem Photobiol B*. 1992;16:347-355.

doi: 10.1016/1011-1344(92)80022-n

36. Pourzarandian A, Watanabe H, Ruwanpura SMP, Aoki A, Noguchi K, Ishikawa I. Er: YAG laser irradiation increases prostaglandin E production via the induction of cyclooxygenase-2 mRNA in human gingival fibroblasts. *J Periodontal Res*. 2005;40:182-186.

doi: 10.1111/j.1600-0765.2005.00789.x

37. Eltas A, Orbak R. Effect of 1,064-nm Nd: YAG laser therapy on GCF IL-1beta and MMP-8 levels in patients with chronic periodontitis. *Lasers Med Sci*. 2012;27:543-550.

doi: 10.1007/s10103-011-0939-5

38. Gomez C, Dominguez A, Garcia-Kass AI, Garcia-Nunez JA. Adjunctive Nd: YAG laser application in chronic periodontitis: Clinical, immunological, and microbiological aspects. *Lasers Med Sci*. 2011;26:453-463.

doi: 10.1007/s10103-010-0795-8

39. Coluzzi DJ, Convissar RA, Roshkind DM. Laser fundamentals. In: *Principles and Practice of Laser Dentistry*. 2nd ed. Amsterdam: Elsevier; 2015. p. 12-26.

40. Huang YY, Chen ACH, Carroll JD, Hamblin MR. Biphasic dose response in low level light therapy. *Dose Response*. 2009;7:358-383.

doi: 10.2203/dose-response.09-027.Hamblin

41. Choi AY, Reddy CM, McGary RT, *et al.* Adjunctive Nd:YAG laser irradiation for ridge preservation and immediate implant procedures: A consecutive case series. *Clin Adv Periodontics*. 2019;9:125-134.

doi: 10.1002/cap.10059

42. Johnson TM, Jusino MA. Management of an immediate implant horizontal defect using freeze-dried bone allograft

and a neodymium: Yttrium-aluminum-garnet laser. *Clin Adv Periodontics*. 2017;7:175-181.

doi: 10.1902/cap.2017.160093

43. Robijns J, Lodewijckx J, Mebis J. Photobiomodulation therapy for acute radiodermatitis. *Curr Opin Oncol*. 2019;31:291-298.

doi: 10.1097/CCO.0000000000000511

44. Aoki A, Mizutani K, Schwarz F, *et al.* Periodontal and peri-implant wound healing following laser therapy. *Periodontol 2000*. 2015;68:217-269.

doi: 10.1111/prd.12080

45. Kassebaum NJ, Smith AGC, Bernabé E, *et al.* Global, regional, and national prevalence, incidence, and disability-adjusted life years for oral conditions for 195 countries, 1990-2015: A systematic analysis for the global burden of diseases, injuries, and risk factors. *J Dent Res*. 2017;96:380-387.

doi: 10.1177/0022034517693566

46. Kumar PS. Microbial dysbiosis: The root cause of periodontal disease. *J Periodontol*. 2021;92:1079-1087.

doi: 10.1002/JPER.21-0245

47. Scannapieco FA, Dongari-Bagtzoglou A. Dysbiosis revisited: Understanding the role of the oral microbiome in the pathogenesis of gingivitis and periodontitis: A critical assessment. *J Periodontol*. 2021;92:1071-1078.

doi: 10.1002/JPER.21-0120

48. Dixon DR, Bainbridge BW, Darveau RP. Modulation of the innate immune response within the periodontium. *Periodontol 2000*. 2004;35:53-74.

doi: 10.1111/j.0906-6713.2004.003556.x

49. Xu W, Zhou W, Wang H, Liang S. Roles of *Porphyromonas gingivalis* and its virulence factors in periodontitis. *Adv Protein Chem Struct Biol*. 2020;120:45-84.

doi: 10.1016/bs.apcsb.2019.12.001

50. Yu YH, Nevins ML. Tooth retention and clinical and radiographic long-term results among patients treated with the full-mouth laser-assisted new attachment procedure (LANAP): A case series. *Int J Periodontics Restorative Dent*. 2023;43:181-191a.

doi: 10.11607/prd.6418

ACCSCIENCE PUBLISHING

Global Translational Medicine

BRIEF REPORT

Capability of questionnaires to screen for sleep apnea in patients with tachyarrhythmias

Yuliya Dmitrievna Weissman[1,2†*], Azamat Maratovich Baymukanov[1†], Irina Andreevna Bulavina[1], Maria Vladimirovna Yunayeva[1], Artem Anatolievich Evmenenko[1], Ilya Leonidovich Ilyich[1], and Sergey Arturovich Termosesov[1]

[1]Department of Electrophysiology and Cardiac Pacing, Moscow City Clinical Hospital after V.M. Buyanov, Moscow, Russian Federation

[2]World-Class Research Center "Digital Biodesign and Personalized Healthcare", Sechenov First Moscow State Medical University, Moscow, Russian Federation

(This article belongs to the *Special Issue: Special Issue of Global Translational Medicine in the Fourth RCCCDT-2024*)

Abstract

Early screening for sleep apnea in patients with tachyarrhythmia is particularly relevant for managing their treatment. Herein, we aimed to assess the screening capabilities of the Berlin Questionnaire, STOP-BANG Sleep Apnea Risk Scale, and Epworth Sleepiness Scale in patients with atrial fibrillation (AF) and atrial flutter. This study included 207 patients with tachyarrhythmia. The patients were asked to fill the three questionnaires. Respiratory monitoring was performed, and the cohort was divided into two groups: those with sleep apnea (Group I) and those without sleep apnea (Group II). Sleep apnea was identified in 155 patients. The remaining 52 patients did not have sleep apnea. Patients in Group I were older (64 vs. 57 years; $P = 0.001$) and had a higher body mass index (34 vs. 31.65 kg/m^2; $P = 0.027$), waist circumference (114 vs. 108 cm; $P = 0.001$), and neck circumference (43 cm vs. 41 cm; $P = 0.001$) than patients in Group II. Type-2 diabetes (59 vs. 8; $P = 0.004$), heart failure (OR 0.797 [95% CI:0.683–0.929]; $P = 0.004$), and AF (OR 1.252 [95% CI:1.088–1.441]; $P = 0.013$) were more common in Group I than in Group II. Eighty-seven patients exhibited paroxysmal AF. The Berlin (area under the curve [AUC] 0.709; sensitivity 80%; specificity 54%) and STOP-BANG (AUC 0.708; sensitivity 79%; specificity 46%) Questionnaires effectively identified sleep apnea. The Epworth Sleepiness Scale had a low predictive ability for sleep apnea (sensitivity 15%; specificity 87%; AUC 0.543). Thus, the Berlin Questionnaire and STOP-BANG Scale may be used to assess the risk of sleep apnea in patients with AF.

Keywords: Sleep apnea syndromes; Mass screening; Atrial fibrillation; Radiofrequency ablation

1. Introduction

According to the EPOCH-CHF study, the prevalence of atrial fibrillation (AF) in the European part of the Russian Federation is 2.04% or 2,040 patients per 100,000

[†]These authors contributed equally to this work.

***Corresponding author:**
Yuliya Dmitrievna Weissman
(judy50@mail.ru)

Citation: Weissman YD, Baymukanov AM, Bulavina IA, *et al*. Capability of questionnaires to screen for sleep apnea in patients with tachyarrhythmias. *Global Transl Med*. 2024:3(4):5059. doi: 10.36922/gtm.5059

Received: October 7, 2024

Accepted: December 10, 2024

Published Online: December 27, 2024

population.[1] The prevalence of AF increases with age, reaching a maximum at 80 – 89 years of age (9.6%). Moreover, AF is associated with a high risk of cardiovascular complications, such as acute cerebrovascular accidents or transient ischemic attacks, heart failure, cognitive decline, depression, frequent hospitalization, and mortality.[2]

AF often coexists with other conditions, particularly obstructive sleep apnea (OSA).[3] This coexistence is attributed to common risk factors such as age, hypertension, and other cardiovascular diseases CVS, which increase the independent attributable risk to 21% (odds ratio [OR] 1.12 – 1.31).[4,5] A dose-dependent relationship exists between AF risk and OSA severity.[6] Therefore, the effectiveness of AF management may depend on the OSA severity. Furthermore, a moderate and severe OSA increases AF recurrence after radiofrequency catheter ablation and electrical cardioversion.[7-10]

The arrhythmogenic mechanism of OSA involves a transient obstruction of the upper airway that leads to chronic transient hypoxia, contributing to atrial remodeling through local and systemic inflammatory responses and oxidative stress.[3] In combination with high-frequency deoxygenation episodes, the negative intrathoracic pressure fluctuations during inspiration and upper airway obstruction in OSA cause myocardial stretch and changes in transmural pressure gradients.[11,12] Obstructive respiratory events increase venous return, which increases the right atrial and right ventricular preload.[13,14] The subsequent right ventricular and right atrial stretch impairs left ventricular filling, further increasing left atrial volume load and causing left atrial dilation.[11,12]

At present, several methods are available for identifying sleep apnea, such as polysomnography, portable respiratory monitoring (RM), and overnight pulse oximetry. These studies require specialized equipment, appropriate infrastructure, and trained medical staff. Early and accessible screening for suspected sleep apnea is particularly relevant for patients with arrhythmias. Various questionnaires including the Berlin Questionnaire,[15] STOP-BANG Sleep Apnea Risk Scale,[16] and Epworth Sleepiness Scale[17] are used for OSA screening. However, the sensitivity and specificity of these questionnaires for patients with tachyarrhythmia (AF and flutter) remain debatable.[18-23] Therefore, herein, we aimed to assess the screening capabilities of the Berlin Questionnaire, STOP-BANG Sleep Apnea Risk Scale, and Epworth Sleepiness Scale in patients with tachyarrhythmia.

2. Materials and methods

This study included 207 patients with tachyarrhythmia who were hospitalized for a possible surgical intervention in the Department of Electrophysiology and Cardiac Pacing at the Moscow City Clinical Hospital named after V.M. Buyanov between July 2022 and March 2024. The study was conducted in accordance with the Helsinki Declaration's principles and approved by the Institutional Ethics Committee (No: 115/5; June 09, 2022).

The clinical and demographic characteristics of the patients are presented in Table 1. The mean age of the patients was 63 years (interquartile range [IQR]: 55 – 68). No differences were observed in sex, height, weight, or body surface area. The study included 83 (40.1%) men and 126 (60.8%) women. Of the included patients, 23 (11.1%) had atrial flutter, 163 (78.7%) had AF, and 25 (12.1%) had a combination of atrial flutter and AF.

The following were the inclusion criteria: Age >18 years, presence of tachyarrhythmias, and signed informed consent form.

The following were the exclusion criteria: moderate or severe cognitive decline, inability to sign informed consent, and presence of bradyarrhythmias (sick sinus syndrome, 2nd-and 3rddegree atrioventricular block, and AF with atrioventricular conduction disturbances) with or without pacemaker.

After obtaining consent, patients were asked to complete the Berlin Questionnaire, STOP-BANG Sleep Apnea Risk Scale, and the Epworth Sleepiness Scale for OSA screening. In addition, anxiety and depression were assessed using the hospital anxiety and depression scale (HADS).

2.1. Description of the questionnaires

(i) The Berlin Questionnaire comprises 11 questions in three sections. A positive score (≥2 points) in 2 – 3 sections is considered a high risk for OSA.

(ii) The STOP-BANG Sleep Apnea Risk Scale comprises two parts: STOP and BANG. A score of 3 – 4 points (number of "yes" answers) and 5 – 8 points is considered moderate and high risk of OSA, respectively. The following conditions are also considered high risk for OSA: Two or more "yes" answers in the STOP part + male sex; two or more "yes" answers in the STOP part + Body mass index (BMI) of at least 35 kg/m^2; or two or more "yes" answers in the STOP part + neck circumference of ≥40 cm.

(iii) The Epworth Sleepiness Scale includes eight situations from daily life that are assessed for causing sleepiness. Scores range from 0 ("would never doze off") to 3 ("high chance of dozing"). After the total score is calculated, a score of 0 – 10, 11 – 12, 13 – 15, and 16 – 24 is considered normal, mild daytime sleepiness, moderate daytime sleepiness, and severe daytime

Table 1. Characteristics of the study population

Characteristics	Group I (*n*=155) (%)	Group II (*n*=52) (%)	*P*-value
Age (years), mean (IQR)	64 (58 – 69)	57 (52 – 66)	0.001
Sex, *n* (%)			0.156
Female	58 (28.02)	25 (12.08)	
Male	97 (46.86)	27 (13.04)	
Height (cm), mean (IQR)	174 (166 – 179)	174.5 (164.5 – 181)	0.999
Weight (kg), mean (IQR)	100 (89 – 115)	95.5 (85 – 110)	0.092
BMI (kg/m^2), mean (IQR)	34 (30.4 – 38)	31.65 (27.95 – 35.72)	0.027
BSA (m^2), mean (IQR)	2.182 (2.05 – 2.34)	2.133 (2.01 – 2.31)	0.173
Waist circumference (cm), mean (IQR)	114 (107 – 124.5)	108 (100.5 – 115.5)	0.001
Neck circumference (cm), mean (IQR)	43 (40.85 – 46)	41 (39 – 43)	0.001
Risk of CVD as assessed by SCORE2 (patients age 40 – 69 years) or SCORE-OP (patients age >70) (%), mean (IQR)	13 (7 – 18)	10 (7 – 15)	0.254
Hypertension, *n* (%)	137 (66.18)	43 (20.77)	0.448
Type-2 diabetes, *n* (%)	59 (28.51)	8 (3.86)	0.003
Heart failure, *n* (%)	79 (38.16)	14 (6.76)	0.004
NYHA Class I,	12 (5.79)	1 (0.48)	0.33
NYHA Class II,	51 (24.64)	12 (5.79)	0.249
NYHA Class III,	16 (7.73)	1 (0.48)	0.06
Previous myocardial infarction, *n* (%)	11 (5.32)	1 (0.48)	0.17
Previous ischemic stroke or TIA, *n* (%)	3 (1.45)	4 (1.93)	0.045
Hospital anxiety and depression scale (HADS) score (Part I), mean (IQR)	4 (2 – 7)	5 (3 – 8)	0.065
Borderline anxiety, *n* (%)	17 (8.22)	9 (4.35)	0.093
Anxiety, *n* (%)	5 (2.43)	2 (0.97)	0.684
Hospital anxiety and depression scale (HADS) score (Part II), mean (IQR)	4 (2 – 7)	4 (2 – 6)	0.757
Borderline depression, *n* (%)	12 (5.79)	3 (1.45)	0.82
Depression, *n* (%)	6 (2.89)	4 (1.93)	0.164

Abbreviations: BMI: Body mass index; BSA: Body surface area; CVD: Cardiovascular disease; IQR: Interquartile range; NYHA: New York Heart Association; TIA: Transient ischemic attack.

sleepiness, respectively. One of the most common symptoms of OSA is daytime tiredness.

(iv) The HADS was used to assess anxiety and depression. A score of 0 – 7, 8 – 10, and 11 is considered normal, borderline anxiety or depression, and clinically significant anxiety or depression, respectively.

After the screening questionnaires were completed, RM was performed using a respiratory polygraph (SOMNOtouch™ RESP eco; SOMNOmedics AG, Randersacker, Germany).

2.2. Diagnosis of OSA

OSA severity was assessed according to the guidelines of the Russian Society of Sleep Medicine,[24] which is based on the apnea-hypopnea index (AHI). The AHI represents the average number of episodes (apnea) per hour of sleep or study. Mild, moderate, and severe OSA is defined as 5 – 15, 15 – 30, and >30 episodes/h, respectively. The cohort was divided into patients with OSA (Group I) and those without OSA (Group II).

2.3. Statistical analysis

Data were analyzed using SPSS Statistics (version 26.0; IBM, Armonk, New York, United States). Normality of distribution was determined using the Kolmogorov–Smirnov test. Quantitative variables are presented as medians and IQRs due to the asymmetric distribution. Differences between the two groups were assessed using the Mann–Whitney U-test. Qualitative variables are presented as absolute (n) and relative (%) values. In addition, receiver operating characteristic (ROC) curve analysis was performed using curve construction. The AUC was used to quantify test significance. Spearman correlation was used

to analyze the correlation between the questionnaire scores and AHI. A $P < 0.05$ was considered statistically significant.

3. Results

According to the RM results, 155 patients had OSA (Group I) and 52 patients did not have OSA (Group II). Patients in Group I were older than those in Group II (64 vs. 57 years; $P = 0.001$). Both groups exhibited high and very high risk for CVS according to the SCORE-2 and SCORE-OP scales, respectively. The SCORE-2 scale is designed to calculate the total risk of fatal and non-fatal CVS and assess the 10-year risk of fatal and non-fatal cardiovascular events (e.g., myocardial infarction and stroke) in people 40–69 years of age with risk factors. The SCORE2-OP scale complements the SCORE-2 scale and estimates the 5-and 10-year risk of fatal and non-fatal cardiovascular events, adjusted for competing risks, in people aged > 70 years.

Patients in Group I had a higher BMI (34 vs. 31.65 kg/m^2; $P = 0.027$), waist circumference (114 vs. 108 cm; $P = 0.001$), and neck circumference (43 vs. 41 cm; $P = 0.001$) than those in Group II.

Type 2 diabetes (59 vs. 8; $P = 0.004$) and heart failure (79 vs. 14; [OR] 0.797 [95% confidence interval {CI}: 0.683 – 0.929]; $P = 0.004$) were more common in Group I than in Group II. AF was significantly more common in Group I than in Group II (113 vs. 46; OR 1.252 [95% CI: 1.088 – 1.441]; $P = 0.013$), particularly the paroxysmal form (84 vs. 37; OR 1.238 [95% CI: 1.06 – 1.447]; $P = 0.007$) (Table 2). Transient ischemic attacks were slightly more common in Group II than in Group I (4 vs. 3; OR 1.779 [95% CI: 0.754 – 4.201]; $P = 0.045$).

Borderline anxiety (HADS scale) was more common in Group I than in Group II (17 vs. 9; OR 1.235 [95% CI: 0.92 – 1.659]; $P = 0.093$); however, this was not statistically significant.

Pulmonary vein radiofrequency isolation (67 vs. 29; OR 1.263 [95% CI: 1.034 – 1.543]; $P = 0.038$) and cavotricuspid isthmus radiofrequency ablation (17 vs. 1; OR 0.678 [95% CI: 0.578 – 0.794]; $P = 0.001$) were performed more frequently in Group I than in Group II (Table 3).

3.1. RM

Key RM parameters are presented in Table 4. Sleep efficiency was high in both groups (>85%). Among the 155 patients in Group I, 59 (28.5%) had mild, 50 (24.2%) had moderate, and 46 (22.3%) had severe disease.

3.2. Screening capabilities of the questionnaires

The Epworth Sleepiness Scale exhibited a low risk of OSA (OR 1.897; 95% CI: 0.406 – 8.851; $P = 0.408$), with only 11 patients (5%) being identified as having OSA. By contrast, the STOP-BANG (OR 3.022; 95% CI: 1.549 – 5.897; $P = 0.001$) and Berlin (OR 3.480; 95% CI: 1.429 – 8.472; $P = 0.004$) Questionnaires identified a higher risk of OSA.

According to the ROC analysis, the Epworth Sleepiness Scale exhibited a low predictive ability for OSA (sensitivity 15%; specificity 87%; AUC 0.543) (Figure 1).

The STOP-BANG Sleep Apnea Risk Scale accurately identified patients with OSA (AUC 0.708; sensitivity 79%; specificity 46%) (Table 5). The Berlin Questionnaire had the highest predictive ability (AUC 0.709; sensitivity 80%; specificity 54%).

Table 2. Prevalence of tachyarrhythmias in the study cohort

Tachyarrhythmias	Group I (*n*=155)	Group II (*n*=52) (%)	*P*-value
Atrial fibrillation, *n* (%)	113 (54.59)	46 (22.23)	0.013
Typical atrial flutter, *n* (z)	18 (8.69)	2 (0.97)	0.102
Atypical atrial flutter, *n* (%)	2 (0.97)	1 (0.48)	0.742
Atrial fibrillation with typical atrial flutter, *n* (%)	22 (10.63)	3 (1.45)	0.108
Paroxysmal, *n* (%)	84 (40.58)	37 (17.87)	0.007
Persistent, *n* (%)	58 (28.02)	14 (6.76)	0.189
Permanent, *n* (%)	13 (6.28)	1 (0.48)	0.113
Impact of the symptoms on daily activities during the episodes of AF (the EHRA scale)			
EHRA class I, *n* (%)	32 (15.46)	11 (5.32)	0.746
EHRA class II, *n* (%)	92 (44.45)	31 (14.97)	0.541
EHRA class III, *n* (%)	31 (14.97)	10 (4.83)	0.902
The CHA2DS2-VASc Score, mean (IQR)	2 (1 – 3)	2 (1 – 3)	0.183

Abbreviations: EHRA: European heart rhythm association; IQR: Interquartile range.

Table 3. Interventions performed in the study population

Interventions	Group I (*n*=155) (%)	Group II (*n*=52) (%)	*P*-value
Radiofrequency PVI, *n* (%)	67 (32.37)	29 (14.01)	0.038
Radiofrequency CTIA, *n* (%)	27 (13.04)	1 (0.48)	0.001
Cryoballoon PVI, *n* (%)	13 (6.28)	6 (2.89)	0.497
PVI+CTIA, *n* (%)	5 (2.43)	5 (2.43)	0.106
Electrical cardioversion, *n* (%)	49 (23.67)	11 (5.32)	0.67

Abbreviations: CTIA: Cavotricuspid isthmus ablation; PVI: Pulmonary vein isolation.

Table 4. Respiratory monitoring data of the study participants

Respiratory monitoring data	Group I (*n*=155)	Group II (*n*=52)
Sleep efficiency (%), mean (IQR)	92.7 (84.9 – 95.6)	90.75 (86.8 – 96.1)
AHI (episodes per hour), mean (IQR)	18.4 (10.2 – 32.75)	2.3 (1.5 – 3.1)
Obstructive sleep apnea index, mean (IQR)	7.4 (3.85 – 15.85)	0.5 (0.2 – 1.05)
Mixed apnea index, mean (IQR)	0 (0 – 1)	0 (0 – 0)
Central apnea index, mean (IQR)	0.3 (0 – 2.3)	0 (0 – 0.25)
Maximum duration of apnea (seconds), mean (IQR)	40 (26.5 – 60)	19 (12.5 – 23.5)
Average duration of apnea (seconds), mean (IQR)	19.1 (15.2 – 24.25)	12.8 (11.3 – 15)
Desaturation index, mean (IQR)	17.2 (9.7 – 32.05)	3.05 (1.65 – 5.05)
Average SpO_2 (%), mean (IQR)	94 (92 – 95)	95 (94 – 96)
Average minimum SpO_2 (%), mean (IQR)	90 (88 – 92)	92 (90.5 – 93)
Minimum SpO_2 (%), mean (IQR)	81 (75 – 86)	86.5 (84 – 91)
Basal SpO2 (%), mean (IQR)	94 (93 – 96)	95 (94 – 96)
Snoring episodes, mean (IQR)	607 (218 – 1272)	400 (137 – 791)
All desaturations sum (min), mean (IQR)	43 (21.5 – 73)	28 (14 – 72)

Abbreviations: AHI: Apnea-hypopnea index; IQR: Interquartile range; SpO_2: Oxygen saturation.

A moderate positive correlation was observed between the Berlin Questionnaire and AHI (Spearman's correlation coefficient 0.353; $P < 0.0001$), which was similar to the correlation between the STOP-BANG Questionnaire and AHI (Spearman's correlation coefficient 0.358; $P < 0.0001$). The Epworth Sleepiness Scale had a weak correlation with AHI (Spearman's correlation coefficient = 0.113).

Table 5. ROC analysis of the STOP-BANG sleep apnea risk scale, Berlin questionnaire, and Epworth sleepiness scale

Parameters	STOP-BANG sleep apnea risk scale	Berlin questionnaire	Epworth sleepiness scale
Area under the curve	0.708	0.709	0.543
95% confidence interval	0.619 – 0.797	0.619 – 0.799	0.446 – 0.64
P-value	0.0001	0.0001	0.417
Sensitivity	79%	80%	15%
Specificity	46%	54%	87%

Abbreviation: ROC: Receiver operating characteristic.

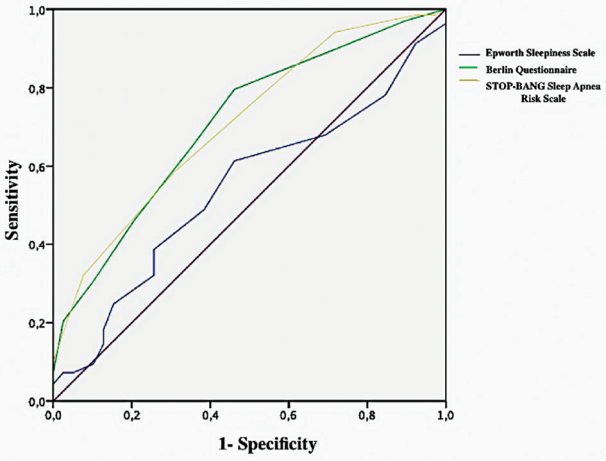

Figure 1. ROC analysis of the questionnaires
Abbreviation: ROC: Receiver operating characteristic.

4. Discussion

Herein, we analyzed the ability of three questionnaires (Berlin Questionnaire, STOP-BANG Sleep Apnea Risk Scale, and Epworth Sleepiness Scale) to predict OSA among patients with tachyarrhythmias. The STOP-BANG scale identified OSA more frequently than the other questionnaires, which is consistent with the findings of Abumuamar *et al.* (AUC 0.74; sensitivity 89%; specificity 36%; $P = 0.004$).[25] However, the specificity was low in the above study.

In Mohammadieh *et al.*, the STOP-BANG Scale exhibited high sensitivity and low specificity for detecting any sleep apnea in patients with AF (AUC 0.58; sensitivity 77.6%; specificity 38.5%).[26] Furthermore, the Berlin Questionnaire (AUC 0.664; sensitivity 56.3%; specificity 76.5%) and Epworth Sleepiness Scale (AUC 0.608; sensitivity 88%; specificity 91.2%) exhibited lower predictive ability than the STOP-BANG scale. However, Betz *et al.* demonstrated

that the STOP-BANG Questionnaire was ineffective as a screening tool for moderate to severe OSA (AUC 0.654, 95% CI 0.580–0.728).[27]

In a meta-analysis by Ramachandran and Josephs a comparison of the accuracy of various predictive models and questionnaires for sleep apnea using diagnostic OR demonstrated that the Berlin Questionnaire (OR 2.28 [95% CI: 7.46 – 69.66]) exhibited a better predictive value for severe OSA than the other questionnaires (STOP-BANG OR 6.59 [95% CI: 3.22 – 13.49]).[28] The meta-analysis included studies with patients with CVS who were undergoing orthopedic surgeries.

Delesie *et al*. found that in patients with AF, the sensitivity and specificity of the Epworth Sleepiness Scale (score > 11), Berlin Questionnaire (high risk), and STOP-BANG Sleep Apnea Risk Scale (high risk) were 30.4% and 74.2%, 50.7% and 80.6%, 59.4% and 61.3%, respectively.[29] Moreover, the AUCs of the Epworth Sleepiness Scale, Berlin Questionnaire, and STOP-BANG Questionnaire were 0.532 (0.411 – 0.654; k = 0.034), 0.704 (0.592 – 0.817; k = 0.251), and 0.673 (0.553 – 0.794; k = 0.181), respectively.

Lin *et al*. also reported similar results after evaluating the risk factors and STOP-BANG Questionnaire in patients with AF.[30] The AUC was 0.705 (95% CI: 0.519 – 0.892), and the sensitivity and specificity were 94.2% and 45.5%, respectively. Spearman's correlation analysis revealed a strong positive correlation between the STOP-BANG scores and AHI (r = 0.449; $P < 0.0001$). Multiple linear regression with AHI as the dependent variable and the STOP-BANG score as the predictor was also significant (t = 4.286; $P < 0.0001$).

Rogel *et al*. demonstrated that the standard use of the STOP-BANG questionnaire can contribute to a more effective identification and treatment referral of patients with OSA.[31]

The study had the following limitations:

(i) This was a single-center study with a small sample size
(ii) The patients had significant pre-existing comorbid conditions (e.g., heart failure, diabetes mellitus, and history of stroke)
(iii) This study included patients referred to the hospital for pulmonary vein radiofrequency catheter or cryoballoon isolation, cavotricuspid isthmus radiofrequency catheter ablation, or electrical cardioversion
(iv) All patients underwent RM rather than polysomnography. Polysomnography was not performed because of the lack of specialized equipment. Thus, the authors decided to use RM for primary diagnosis.

5. Conclusion

The prevalence of OSA among patients with AF and atrial flutter is quite high, which considerably affects their course. However, the current diagnostic capabilities of OSA are limited because of the small number of hospitals where it can be primarily diagnosed. Screening methods such as the STOP-BANG Sleep Apnea Risk Scale and Berlin Questionnaire demonstrated high sensitivity. Thus, all patients with AF and flutter can be screened using these questionnaires. The study of additional screening tools or the combination of questionnaires with objective measurements (polysomnography) in clinical settings may validate our findings.

Acknowledgment

None.

Funding

This research was funded by a grant from the Moscow Government for the implementation of a scientific and practical project in medicine No. 0702-2.

Conflict of interest

The authors declare that there are no conflicts of interest with any financial organization regarding the work discussed in this manuscript.

Author contributions

Conceptualization: Azamat Maratovich Baymukanov
Data curation: Irina Andreevna Bulavina, Maria Vladimirovna Yunayeva
Formal analysis: Yuliya Dmitrievna Weissman
Investigation: Irina Andreevna Bulavina, Maria Vladimirovna Yunayeva, Yuliya Dmitrievna Weissman
Methodology: Azamat Maratovich Baymukanov
Writing-original draft: Yuliya Dmitrievna Weissman
Writing-review & editing: Azamat Maratovich Baymukanov, Ilya Leonidovich Ilyich, Sergey Arturovich Termosesov, Artem Anatolievich Evmenenko

Ethics approval and consent to participate

The study was conducted in accordance with the Helsinki Declaration and approved by the Ethics Committee of Moscow City Clinical Hospital after V.M. Buyanov (protocol code 115/5 from 9 June 2022).

Consent for publication

During patient recruitment, informed consent of patients was obtained. Any personal information was excluded from the study.

Availability of data

Data are available from the corresponding author on reasonable request.

Further disclosure

Part of the findings has been presented in several congresses:

(i) Baymukanov A.M. *et al*. OSA in patients with atrial fibrillation. XI Saint Petersburg School of Arrhythmology 2023;

(ii) Weissman Yu. D. *et al*. Prevalence and possibilities for timely diagnosis of sleep apnea in patients with AF. KHRS 2024 The 16th Annual Scientific Session of The Korean Heart Rhythm Society;

(iii) Baymukanov A.M. *et al*. Sleep disorders breathing in patients with tachyarrhythmias. V St. Petersburg Forum of Arrhythmology 2024;

(iv) Baymukanov A.M. *et al*. Sleep apnea and AF: Clinical features and screening capabilities. 12th All-Russian Conference "Contradictions of Modern Cardiology: Controversial and unresolved issues." Collection of abstracts. Russian Journal of Cardiology. 2023;28(8S):1-174. (In Russ.) https://doi.org/10.15829/1560-4071-2023-8S

References

1. Mareev YV, Polyakov DS, Vinogradova NG, *et al*. Epidemiology of atrial fibrillation in a representative sample of the European part of the Russian Federation. Analysis of EPOCH-CHF study. *Kardiologiia*. 2022;62(4):12-19.

   doi: 10.18087/cardio.2022.4.n1997

2. Hindricks G, Potpara T, Dagres N, *et al*. 2020 ESC Guidelines for the diagnosis and management of atrial fibrillation developed in collaboration with the European Association for Cardio-Thoracic Surgery (EACTS): The Task Force for the diagnosis and management of atrial fibrillation of the European Society of Cardiology (ESC) Developed with the special contribution of the European Heart Rhythm Association (EHRA) of the ESC. *Eur Heart J*. 2021;42(5):373-498.

   doi: 10.1093/eurheartj/ehaa612. Erratum in: *Eur Heart J*. 2021;42(5):507.

   doi: 10.1093/eurheartj/ehaa798. Erratum in: *Eur Heart J*. 2021;42(5):546-547.

   doi: 10.1093/eurheartj/ehaa945. Erratum in: *Eur Heart J*. 2021;42(40):4194.

   doi: 10.1093/eurheartj/ehab648

3. Saleeb-Mousa J, Nathanael D, Coney AM, Kalla M, Brain KL, Holmes AP. Mechanisms of atrial fibrillation in obstructive sleep apnoea. *Cells*. 2023;12(12):1661.

   doi: 10.3390/cells12121661

4. Gami AS, Pressman G, Caples SM, *et al*. Association of atrial fibrillation and obstructive sleep apnea. *Circulation*. 2004;110(4):364-367.

   doi: 10.1161/01.CIR.0000136587.68725.8E

5. Chen W, Cai X, Yan H, Pan Y. Causal effect of obstructive sleep apnea on atrial fibrillation: A Mendelian randomization study. *J Am Heart Assoc*. 2021;10(23):e022560.

   doi: 10.1161/JAHA.121.022560

6. Cadby G, McArdle N, Briffa T, *et al*. Severity of OSA is an independent predictor of incident atrial fibrillation hospitalization in a large sleep-clinic cohort. *Chest*. 2015;148(4):945-952.

   doi: 10.1378/chest.15-0229

7. Deng F, Raza A, Guo J. Treating obstructive sleep apnea with continuous positive airway pressure reduces risk of recurrent atrial fibrillation after catheter ablation: A meta-analysis. *Sleep Med*. 2018;46:5-11.

   doi: 10.1016/j.sleep.2018.02.013

8. Ng CY, Liu T, Shehata M, Stevens S, Chugh SS, Wang X. Meta-analysis of obstructive sleep apnea as predictor of atrial fibrillation recurrence after catheter ablation. *Am J Cardiol*. 2011;108(1):47-51.

   doi: 10.1016/j.amjcard.2011.02.343

9. Zhou Y, Yan M, Yuan J, Wang Y, Qiao S. Continuous positive airway pressure treatment decreases the risk of atrial fibrillation recurrence in patients with obstructive sleep apnea after radiofrequency ablation. *Int Heart J*. 2022;63(4):716-721.

   doi: 10.1536/ihj.22-129

10. Kanagala R, Murali NS, Friedman PA, *et al*. Obstructive sleep apnea and the recurrence of atrial fibrillation. *Circulation*. 2003;107(20):2589-2594.

    doi: 10.1161/01.CIR.0000068337.25994.21

11. Linz D, Woehrle H, Bitter T, *et al*. The importance of sleep-disordered breathing in cardiovascular disease. *Clin Res Cardiol*. 2015;104(9):705-718.

    doi: 10.1007/s00392-015-0859-7

12. Kasai T, Bradley TD. Obstructive sleep apnea and heart failure: Pathophysiologic and therapeutic implications. *J Am Coll Cardiol*. 2011;57(2):119-127.

    doi: 10.1016/j.jacc.2010.08.627

13. Pressman GS, Orban M, Leinveber P, *et al*. Effects of the Mueller maneuver on functional mitral regurgitation and implications for obstructive sleep apnea. *Am J Cardiol*. 2015;115(11):1563-1567.

    doi: 10.1016/j.amjcard.2015.02.061

14. Orban M, Bruce CJ, Pressman GS, *et al*. Dynamic changes of

left ventricular performance and left atrial volume induced by the Mueller maneuver in healthy young adults and implications for obstructive sleep apnea, atrial fibrillation, and heart failure. *Am J Cardiol*. 2008;102(11):1557-1561.

doi: 10.1016/j.amjcard.2008.07.050

15. Andrechuk CRS, Netzer N, Zancanella E, Almeida AR, Ceolim MF. Cultural adaptation and evaluation of the measurement properties of the Berlin Questionnaire for Brazil. *Sleep Med*. 2019;60:182-187.

doi: 10.1016/j.sleep.2019.03.022

16. Duarte RLM, Magalhães-da-Silveira FJ, Gozal D. Screening for sleep apnea: When and how? *Curr Sleep Med Rep.* 2018;4:221-230.

doi: 10.1007/s40675-018-0120-9

17. Bertolazi AN, Fagondes SC, Hoff LS, *et al*. Portuguese-language version of the Epworth sleepiness scale: Validation for use in Brazil. *J Bras Pneumol*. 2009;35(9):877-883.

doi: 10.1590/s1806-37132009000900009

18. Chiu HY, Chen PY, Chuang LP, *et al*. Diagnostic accuracy of the Berlin questionnaire, STOP-BANG, STOP, and Epworth sleepiness scale in detecting obstructive sleep apnea: A bivariate meta-analysis. *Sleep Med Rev*. 2017;36:57-70.

doi: 10.1016/j.smrv.2016.10.004

19. Khaledi-Paveh B, Khazaie H, Nasouri M, Ghadami MR, Tahmasian M. Evaluation of Berlin questionnaire validity for sleep apnea risk in sleep clinic populations. *Basic Clin Neurosci*. 2016;7(1):43-48.

20. Nagappa M, Liao P, Wong J, *et al*. Validation of the STOP-Bang Questionnaire as a screening tool for obstructive sleep apnea among different populations: A systematic review and meta-analysis. *PLoS One*. 2015;10(12):e0143697.

doi: 10.1371/journal.pone.0143697

21. Nagappa M, Wong J, Singh M, Wong DT, Chung F. An update on the various practical applications of the STOP-Bang questionnaire in anesthesia, surgery, and perioperative medicine. *Curr Opin Anaesthesiol*. 2017;30(1):118-125.

doi: 10.1097/ACO.0000000000000426

22. Netzer NC, Stoohs RA, Netzer CM, Clark K, Strohl KP. Using the Berlin Questionnaire to identify patients at risk for the sleep apnea syndrome. *Ann Intern Med*. 1999;131(7): 485-491.

doi: 10.7326/0003-4819-131-7-199910050-00002

23. Sharma A, Molano J, Moseley BD. The STOP-BANG questionnaire improves the detection of epilepsy patients at risk for obstructive sleep apnea. *Epilepsy Res*. 2017;129:37-40.

doi: 10.1016/j.eplepsyres.2016.11.009

24. Buzunov RV, Palman AD, Melnikov AY, Averbukh VM, Madaeva IM, Kulikov AN. Diagnosis and treatment of obstructive sleep apnea in adults. Recommendations of the Russian Society of Somnologists. *Effect Pharmacother*. 2018;35:34-45.

25. Abumuamar AM, Dorian P, Newman D, Shapiro CM. The STOP-BANG questionnaire shows an insufficient specificity for detecting obstructive sleep apnea in patients with atrial fibrillation. *J Sleep Res*. 2018;27(6):e12702.

doi: 10.1111/jsr.12702

26. Mohammadieh AM, Sutherland K, Kanagaratnam LB, Whalley DW, Gillett MJ, Cistulli PA. Clinical screening tools for obstructive sleep apnea in a population with atrial fibrillation: A diagnostic accuracy trial. *J Clin Sleep Med*. 2021;17(5):1015-1024.

doi: 10.5664/jcsm.9098

27. Betz K, Verhaert DVM, Gawalko M, *et al.* Atrial fibrillation-specific refinement of the STOP-Bang sleep apnoea screening questionnaire: Insights from the Virtual-SAFARI study. *Clin Res Cardiol*. 2023;112(6):834-845.

doi: 10.1007/s00392-023-02157-9

28. Ramachandran SK, Josephs LA. A meta-analysis of clinical screening tests for obstructive sleep apnea. *Anesthesiology*. 2009;110(4):928-939.

doi: 10.1097/ALN.0b013e31819c47b6

29. Delesie M, Knaepen L, Hendrickx B, *et al*. The value of screening questionnaires/scoring scales for obstructive sleep apnoea in patients with atrial fibrillation. *Arch Cardiovasc Dis*. 2021;114(11):737-747.

doi: 10.1016/j.acvd.2021.08.002

30. Lin W, Wei H, Jiang F, Zhu P. Application of the STOP-BANG questionnaire for screening obstructive sleep apnea syndrome in patients with atrial fibrillation. *Panminerva Med*. 2023.

doi: 10.23736/S0031-0808.23.04886-3

31. Rogel M, Iverson L, Hall A. Identifying obstructive sleep apnea risk using the STOP-BANG Questionnaire in a cardiology clinic. *J Healthc Qual.* 2024;46(1):51-57.

doi: 10.1097/JHQ.0000000000000408

Our Journals

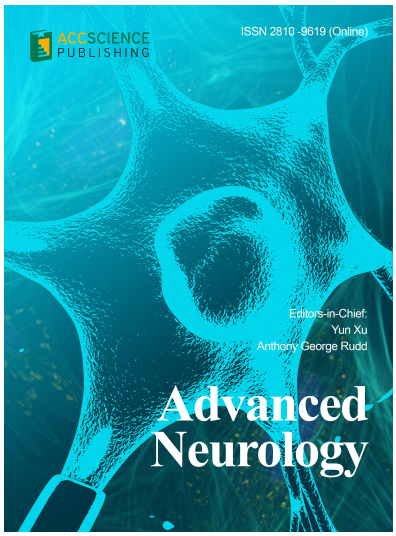

Advanced Neurology is a peer-reviewed and open-access journal that aims to publish and disseminate novel research in the breadth of neurology and neuroscience. The journal aims to advance our understanding in the nervous system and provide a platform to neuroscientists and physicians to showcase their findings in original fundamental and clinical research as well as to present new ideas that highlight the changes in the neurological clinical practice.

Advanced Neurology covers subject areas, including but not limited to the following:

- Neurological disorders
- Neurodegenerative disease
- Cerebrovascular disease
- Epilepsy and movement disorders
- Neuroimmune disease
- Neurological infections
- Muscle disease
- Molecular and cellular neuroscience
- Systems neuroscience
- Cognitive neuroscience
- Computational modeling of nervous system

Gene & Protein in Disease publishes rigorously peer-reviewed and high quality original articles and authoritative reviews that focus on the latest development in multidisciplinary areas in biology and biomedicine, with an emphasis on gene and protein research. The journal has worldwide authorship, and a broad scope in basic and translational biomedical research of genetics, biochemistry, biophysics, oncology, immunology, cell biology, molecular biology, developmental biology, microbiology, neuroscience, stem cell, protein science, structural biology, regenerative medicine and translational medicine.

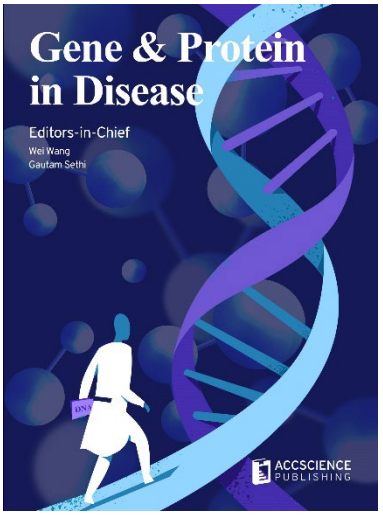

Start a new journal

Write to us via email if you are interested to start a new journal with AccScience Publishing. Please attach your CV, professional profile page and a brief pitch proposal in your email. We shall inform you of our decision whether we are interested to collaborate in starting a new journal.

Contact: info@accscience.com

https://accscience.com/journal/GTM

Contact
www.accscience.com
8 Burn Road, #15-03 Trivex, Singapore 369977
Email: editorial@accscience.com
Phone: +65 8182 1586